INFORMATION TO USERS

This material was produced from a microfilm copy of the original document. While the most advanced technological means to photograph and reproduce this document have been used, the quality is heavily dependent upon the quality of the original submitted.

The following explanation of techniques is provided to help you understand markings or patterns which may appear on this reproduction.

1. The sign or "target" for pages apparently lacking from the document photographed is "Missing Page(s)". If it was possible to obtain the missing page(s) or section, they are spliced into the film along with adjacent pages. This may have necessitated cutting thru an image and duplicating adjacent pages to insure you complete continuity.

2. When an image on the film is obliterated with a large round black mark, it is an indication that the photographer suspected that the copy may have moved during exposure and thus cause a blurred image. You will find a good image of the page in the adjacent frame.

3. When a map, drawing or chart, etc., was part of the material being photographed the photographer followed a definite method in "sectioning" the material. It is customary to begin photoing at the upper left hand corner of a large sheet and to continue photoing from left to right in equal sections with a small overlap. If necessary, sectioning is continued again — beginning below the first row and continuing on until complete.

4. The majority of users indicate that the textual content is of greatest value, however, a somewhat higher quality reproduction could be made from "photographs" if essential to the understanding of the dissertation. Silver prints of "photographs" may be ordered at additional charge by writing the Order Department, giving the catalog number, title, author and specific pages you wish reproduced.

5. PLEASE NOTE: Some pages may have indistinct print. Filmed as received.

Xerox University Microfilms
300 North Zeeb Road
Ann Arbor, Michigan 48106

Reproduced with permission of the copyright owner. Further reproduction prohibited without permission.

74-26,400

SUMARTOJO, Jojok, 1937-
A STUDY OF THE MINERALOGY AND GEOCHEMISTRY OF THE TINDELPINA SHALE (UPPER PROTEROZOIC) ADELAIDE GEOSYNCLINE, SOUTH AUSTRALIA.

University of Cincinnati, Ph.D., 1974
Geology

University Microfilms, A XEROX Company, Ann Arbor, Michigan

THIS DISSERTATION HAS BEEN MICROFILMED EXACTLY AS RECEIVED.

Reproduced with permission of the copyright owner. Further reproduction prohibited without permission.

A STUDY OF THE MINERALOGY AND GEOCHEMISTRY OF THE TINDELPINA SHALE (UPPER PROTEROZOIC) ADELAIDE GEOSYNCLINE, SOUTH AUSTRALIA

A dissertation submitted to the

Division of Graduate Studies
of the University of Cincinnati

in partial fulfillment of the
requirements for the degree of

DOCTOR OF PHILOSOPHY

in the Department of Geology
of the Graduate School of Arts and Sciences

1974

BY

Jojok Sumartojo

Sarjana Institut Teknologi Bandung, 1961
M.S. University of Kentucky, 1966

Reproduced with permission of the copyright owner. Further reproduction prohibited without permission.

UNIVERSITY OF CINCINNATI

January 18th 19 74

I hereby recommend that the thesis prepared under my supervision by JOJOK SUMARTOJO

entitled A STUDY OF THE MINERALOGY AND GEOCHEMISTRY OF THE TINDELPINA SHALE (UPPER PROTEROZOIC), ADELAIDE GEOSYNCLINE, SOUTH AUSTRALIA

be accepted as fulfilling this part of the requirements for the degree of DOCTOR OF PHILOSOPHY

Approved by:

William Fjenks

Form 668—Grad. School—1M—12-69

Reproduced with permission of the copyright owner. Further reproduction prohibited without permission.

TABLE OF CONTENTS

Reproduced with permission of the copyright owner. Further reproduction prohibited without permission.

Reproduced with permission of the copyright owner. Further reproduction prohibited without permission.

LIST OF FIGURES

Reproduced with permission of the copyright owner. Further reproduction prohibited without permission.

Figure

14a Magnesium plus iron in dioctahedral illites and montmorillonites as a function of d_{060} (Maxwell and Hower, 1967)

14b Frequency histograms of b_0 values of pre-Alpine (muscovites) and Alpine (phengites) potassic white micas (Sassi, 1972)

14c Frequency histogram of b_0 values ($6 \times d_{060}$) of the Tindelpina Shale muscovite

15 Conversion graph for the Weaver sharpness ratio and the Kubler index, constructed by Kubler (1968, p. 393), based on his 700 measurements of the Kubler indices. Philips diffractometer chart speed 1,600mm/hour; goniometer 2^{o}/minute

16 Gallium-rubidium-boron ratios of the Sturt Tillite following a method by Degens et al. (1957, 1958).

17 Gallium-rubidium-boron ratios of the Tindelpina Shale following a method by Degens et al. (1957, 1958)

18 Plots of the rubidium/strontium ratio against the rubidium concentration of the Sturt Tillite and the Tindelpina Shale, after a method by Reimer (1972)

19 Plots of the rubidium/strontium ratio against the rubidium concentration of the Tindelpina Shale after a method by Reimer (1972)

20 Histograms of major oxides and quartz in the Tindelpina Shale

21a Ca_2O - Na_2O - K_2O triangular diagram for the Sturt Tillite and its overlying Tindelpina Shale

21b Plots of the major oxides composing the Sturt Tillite and its overlying Tindelpina Shale on the diagram by Ronov and Khlebnikova (1957)

22 Ca_2O - Na_2O - K_2O plots of the Tindelpina Shale

23a Plots of the major oxides composing the Tindelpina Shale on a diagram by Ronov and Khlebnikova (1957)

23b Plots of normalized silicon contents (Si = 100 - Al - Fe) against Al/Fe ratios of the Tindelpina Shale after a method of Dennen and Moore (1971)

Reproduced with permission of the copyright owner. Further reproduction prohibited without permission.

Figure

Reproduced with permission of the copyright owner. Further reproduction prohibited without permission.

LIST OF TABLES

Reproduced with permission of the copyright owner. Further reproduction prohibited without permission.

Reproduced with permission of the copyright owner. Further reproduction prohibited without permission.

Reproduced with permission of the copyright owner. Further reproduction prohibited without permission.

ACKNOWLEDGMENT

The work and preparation of this thesis was completed at the University of Adelaide, Adelaide, South Australia, while the author assumed a position as a full-time Demonstrator in Geology. To the many people who have helped with this thesis, the author wishes to express his gratitude.

Professors R.W.R. Rutland and L.H. Lattman, Heads of the Geology Departments at Adelaide and Cincinnati respectively gave their permission to the author to work in South Australia, under the supervision of Dr. J.B. Jones, Reader in Geology and Mineralogy at the University of Adelaide. This permission was also given by Drs. F.L. Koucky, W.F. Jenks, and W.D. Huff, all of Cincinnati, who acted as major advisers while the author did his graduate course work studies at Cincinnati. They were joined by Dr. J.B. Maynard to form the thesis committee. Their constructive criticism and advice were essential to the completion of this thesis.

The author also wishes to express his gratitude to Professor Rutland who gave privileges, facilities, and financial support from beginning to end of this thesis. The University of Cincinnati has deferred a portion of expenses through the General Funds Account.

Dr. V.A. Gostin of Adelaide, supervised the field collecting and has advised and encouraged the author in completing this study. Dr. R.W. Nesbitt has given his advice on X-ray fluorescence techniques. Bull sessions on the measurement of mass-absorption coefficients with Herb Mastins is also much appreciated. Dr. K. Norrish of the CSIRO

Reproduced with permission of the copyright owner. Further reproduction prohibited without permission.

(Commonwealth Scientific and Industrial Research Organization) Division of Soils gave his permission to use the optical spectrograph at the CSIRO.

Being a newcomer in the game of computer uses, the author has received help from Mike Fitzgerald and David Bruce who have patiently explained what FORTRAN is all about. The author has benefited from discussion on factor analysis with Dr. L.A. Frakes, formerly of the Geology Department, the Florida State University.

Grateful acknowledgment is extended to Burton Murrell, a fellow demonstrator, who has helped with sampling from the hard-to-get places and who has given his time to discuss the geology. Mr. David Holmes of the Occidental Minerals Corporation helped to collect samples from the Copley and Parachilna map-sheet areas during the hot summer week of February, 1971.

Miss E.M. McBriar, Senior Demonstrator, gave her encouragement and help during the last stages of this thesis preparation. Messrs. O. Stanley and J. Trzicky made the logistics during the analytical work run smoothly.

Miss Ann Boos ably and patiently typed the entire thesis. Richard Barrett gave some assistance with the photographic work.

It is with good reason that the author wishes to end this acknowledgment with the mention of his wife, Esther. To her he wishes to acknowledge his debt of gratitude.

Reproduced with permission of the copyright owner. Further reproduction prohibited without permission.

ABSTRACT

The Precambrian rocks in the Adelaide Geosyncline, South Australia are characterized by thick sequences of detrital sediments. One of the rock units is the Tindelpina Shale of Late Proterozoic age. This shale which is an extensively distributed black shale, is the object of a regional mineralogical and geochemical study.

The mineralogical study includes the identification of mineral assemblage, measurements of the basal and d_{060} spacings, and determination of crystallinity of muscovite. Chemical analyses of major oxides and 14 trace elements (Ga, Rb, Sr, As, Ba, B, Cr, Cu, Li, Ni, Pb, V, Zn, and Zr) were carried out on rock samples collected over the greater part of the geosyncline. For comparison, samples of the underlying formation, the Sturt Tillite, were analyzed for their concentrations of the major oxides, Ga, Rb, Sr, and B.

X-ray diffraction indicates that the mineralogy of the Tindelpina Shale is very simple, consisting mainly of quartz, muscovite, and chlorite. Feldspars, calcite, iron oxides, and pyrite also occur in minor amounts. The basal spacings of muscovite indicates the low paragonite content of muscovite. The d_{060} spacing (and b_0 parameter) suggests the phengitic nature of muscovite. All these mineralogical analyses indicate the low grade metamorphic nature (the low greenschist facies) of the Tindelpina Shale. Crystallinity of muscovite expressed

Reproduced with permission of the copyright owner. Further reproduction prohibited without permission.

in terms of the Kubler-index and the Weaver sharpness-ratio substantiates this conclusion.

The concentrations of the 14 trace elements analyzed in about 120 samples of the Tindelpina Shale gave the following results for their average in ppm (standard deviation is in parenthesis): Ga: 19 (4), Rb: 146 (39), Sr: 160 (178), As: 14 (10), Ba: 858 (192), B: 184 (71), Cr: 83 (37), Cu: 30 (18), Li: 22 (9), Ni: 40 (17), Pb: 21 (12), V: 191 (55), Zn: 62 (28), Zr: 225 (33).

Based on the contents of B, Ga-B-Rb ratios and K/Rb ratios, it is suggested that the Sturt Tillite is of marine glacial origin, whereas the Tindelpina Shale is of shallow marine origin. This suggestion is substantiated by the Fe/Mn ratios of those two rock units.

Chemical analyses of about 150 samples of the Tindelpina Shale result in the following percentages (standard deviation is between brackets): SiO_2: 59.77 (7.88), Al_2O_3: 13.65 (2.49), Fe_2O_3: 5.45 (2.85), MgO: 3.75 (1.72), CaO: 4.01 (5.44), Na_2O: 1.17 (0.65), K_2O: 3.35 (0.85), TiO_2: 0.95 (0.19), P_2O_5: 0.18 (0.07), MnO: 0.07 (0.10), Loss on ignition 7.31 (4.67), Free quartz: 40.40 (8.64).

Out of these, 22 samples were compared to the 25 analyses of the underlying Sturt Tillite which has average percentages of: SiO_2: 68.79 (3.14), Al_2O_3: 13.54 (1.96), Fe_2O_3: 5.18 (0.91), MgO: 2.60 (0.92), CaO: 0.62 (0.93), Na_2O: 1.23 (0.44), K_2O: 3.76 (0.68), TiO_2: 0.89 (0.13), P_2O_5: 0.13 (0.04), MnO: 0.03 (0.03), Loss on ignition: 3.31 (1.04), Free quartz: 46.08 (8.62).

Reproduced with permission of the copyright owner. Further reproduction prohibited without permission.

There is essentially no difference in the chemistry of the Tindelpina Shale and the Sturt Tillite, with the exception of lime, magnesia, and silica concentrations. Their compositions suggest the granitic nature of the parent rocks.

Trend surface analysis based on the Niggli parameters (si, al, fm, alk and k), K_2O/Na_2O, Vogt-index, quartz, zircon, adjusted boron, and copper suggest the source material for the Tindelpina Shale lay to the west of the Adelaide Geosyncline, in the Gawler Block. A minor source contribution came from the northeast, the Willyama Block. The general trends for the variables used in trend surface analysis conform with the main north-south elongate shape of the Adelaide Geosyncline.

A correlation matrix of 25 variables (Si, Al, Fe, Mg, Ca, Na, K, Ti, P, Mn, Ga, Rb, Sr, As, Ba, B, Cr, Cu, Li, Ni, Pb, V, Zn, Zr, and quartz) indicates the associations of most of the trace elements with the main phyllosilicate fraction (muscovite). Factor analysis of the 25 variables result in six factors which account for most of the data variance. Those factors are: provenance/sorting, Eh-pH, biogenic activity, salinity, diagenesis, and proximity to source rock. An additional six variables (X-Y coordinates, contents of muscovite and chlorite, the Kubler index and the Weaver sharpness-ratio) result in an additional factor related to regional metamorphism. This metamorphism progressively increases towards the east and towards the south.

Reproduced with permission of the copyright owner. Further reproduction prohibited without permission.

I. INTRODUCTION

The Precambrian sedimentary succession in the Adelaide Geosyncline, South Australia, is characterized by a thick accumulation of detrital sediments. One of the rock units of the succession is the Tindelpina Shale of Upper Proterozoic age, which is the focus of the present study. Recently much attention has been given to this rock unit by numerous exploration companies in search of stratiform copper mineralization. The Tindelpina Shale, which is about 60 meters thick and a good stratigraphic marker, is extensively distributed throughout the Adelaide Geosyncline. It may be identified with relative ease by the presence of a conspicuous underlying tillite unit, the Sturt Tillite.

The Tindelpina Shale type-section was defined by Coats (1964) as a black shale, located near a small abandoned shack called Tindelpina Hut, about 500 kilometers northeast of Adelaide. Like most of the Upper Proterozoic rocks in the Adelaide Geosyncline, the Tindelpina Shale as well as the Sturt Tillite have been subjected to low-grade regional metamorphism.

To date, there has been virtually no published work on the geochemistry or mineralogy of the fine-grained sediments in the Adelaide Geosyncline, although it is known that hundreds of geochemical analyses for base metals, many from the Tindelpina Shale, have been carried out by various exploration companies.

The original purpose of the present work was to study the occurrence of sedimentary sulfides in the Tindelpina Shale. However, field collecting indicated that the sulfides are mainly pyrite which occurs only sporadically. For this reason, it was decided that a regional study of the clay mineralogy and geochemistry of the major oxides, as well as of selected trace elements occurring in the Tindelpina Shale, would yield results of real value in deter-

Reproduced with permission of the copyright owner. Further reproduction prohibited without permission.

mining the depositional, diagenetic, and metamorphic history of this stratigraphic unit.

Regional distribution of selected major and trace elements was plotted in an attempt to show the geographic location of source rocks. The main factors which affect the geochemical variations are also sought.

Major and selected trace-element concentrations are a basis for comparing the geochemistry of the Sturt Tillite with that of the Tindelpina Shale to determine their geochemical relationship and the environment of deposition of the tillite and the shale.

About 150 rock samples were collected from the base of the Tindelpina Shale throughout a major part of the Adelaide Geosyncline. X-ray diffraction was carried out on this collection to determine the mineral assemblage of the minus two-micron fraction, the concentration of quartz, the basal and d_{060} spacings of muscovite, and the crystallinity of muscovite. Chemical analyses by means of X-ray fluorescence, atomic absorption spectrometery, optical spectrography and flame photometry were carried out to determine the concentrations of the major elements and 14 trace elements (As, Ba, B, Cu, Cr, Ga, Li, Pb, Ni, Rb, Sr, V, Zn, and Zr). Microscopic examination was used only for descriptive purpose. Twenty five samples of Sturt Tillite were collected and analyzed for their major elements and Ga, Rb, Sr, and B contents.

In order to carry out the work accurately and efficiently, appropriate analytical techniques had to be developed. These are described in some detail. The data obtained from these analyses were statistically treated using mainly trend surface and factor analyses, so that the data could be quantitatively interpreted.

Reproduced with permission of the copyright owner. Further reproduction prohibited without permission.

II. GEOLOGIC SETTING

II.1. General Geology

The earliest published account on the geology of South Australia was presented by Howchin (1918) who wrote two textbooks, the first dealing with general geological principles, and the second dealing with the geological history of Australia with particular emphasis on South Australia. The latter was revised in 1929. Much later, a publication on the geology of South Australia was presented, edited by Glaessner and Parkin (1958). A book entitled "Handbook of South Australian Geology" was published in 1969 and edited by Parkin, presenting most of the geological work carried out up to that time. A very concise outline of the geology of South Australia has been published by Ludbrook and Johns (1970).

The state of South Australia may physiographically be divided into geologic provinces representing major geologic sequences: areas of Precambrian basement-blocks, the Adelaide Geosyncline and the Kanmantoo Trough, and sedimentary basins such as the Great Artesian Basin and the younger basins containing Mesozoic and Tertiary sediments (Fig. 1). Only the first two provinces are relevant to the present study, and they are summarized below.

The Precambrian basement-blocks. The principal basement blocks which form part of the Australian Precambrian shield exposed in South Australia are the Gawler Block on the Eyre and Yorke peninsulas, the Willyama Block extending from Olary in South Australia into New

Reproduced with permission of the copyright owner. Further reproduction prohibited without permission.

Figure 1

Major geologic provinces of South Australia, redrafted and slightly modified from Talbot and Nesbitt (1968).

Reproduced with permission of the copyright owner. Further reproduction prohibited without permission.

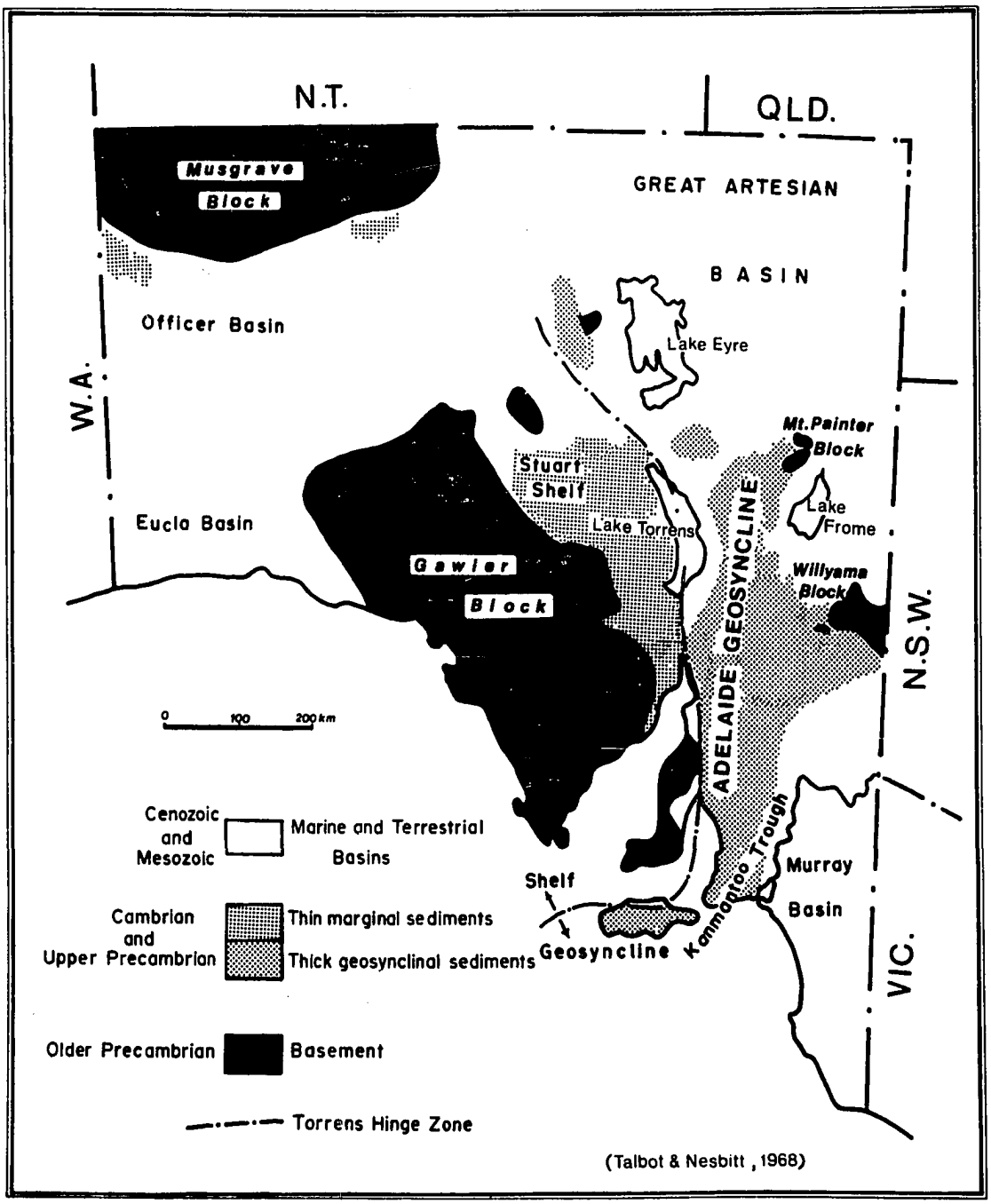

Reproduced with permission of the copyright owner. Further reproduction prohibited without permission.

South Wales, the Mount Painter Block in the Northeastern part of the Flinders Ranges, and the Musgrave Block in the far northwest of the state. Smaller basement exposures occur in the Mount Lofty Ranges and in the Peake and Dennison Ranges.

Geographically, it would seem that all of these blocks, with the exception of the Musgrave, act as the provenance of the sediments deposited in the Adelaide Geosyncline and the Kanmantoo Trough. These sediments in the Adelaide Geosyncline have been generally metamorphosed into the greenschist facies, whereas the Kanmantoo Trough sediments have been metamorphosed into much higher grade staurolite-andalusite-schist facies (Offler and Fleming, 1968).

The Gawler Block is mainly composed of metasediments such as gneisses, a variety of schists, with minor jaspillite. These metasediments are called the Cleve Metamorphics and include the Flinders Gneiss and the mica-schists of the Hutchison Group (Johns, 1961). In places these gneisses and schists have been intruded by granites. The metamorphism and granitic intrusion are thought to have taken place during the Carpentarian. During the final stages of this orogeny, great flows of acidic lavas formed the Gawler Range Volcanics. High-grade iron ore deposits occur in this block.

The Willyama Block exposed in the eastern part of the state extends from Olary into New South Wales and is of greater economic importance than the other blocks. This complex consists of a variety of gneisses and mica-schists intruded by granitic and pegmatitic rocks.

Reproduced with permission of the copyright owner. Further reproduction prohibited without permission.

The intrusions probably occurred during the same period as the formation of the Gawler Block. The famous Broken Hill silver-lead-zinc deposits and the Radium Hill uranium deposit occur in this block.

The Mount Painter Block exposed in the northeastern part of the Flinders Ranges occurs as a basement inlier. It consists mainly of metasediments in the form of schists, porphyry, quartzites, and a suite of granite which intrudes the metasediments. Intrusions of younger granite into the Mount Painter complex and the overlying sediments add to the complexity of the area (Coats and Blissett, 1971).

Smaller exposures of the basement block occur in the core of the Mount Lofty Ranges in the areas of Yankalilla, Mount Compass, Aldgate, Houghton, and the Barossa Valley. These are composed of a complex of schists, gneisses, and pegmatites.

The Adelaide Geosyncline. The geological history of the Adelaide Geosyncline is the most important geological history of South Australia. The present topographic feature is a broad arc of mountain ranges, the Mount Lofty and the Flinders Ranges, which disappears northwesterly towards the Musgrave Ranges at the far northwest of the state.

The geosyncline is characterised by the very thick, about 27,000 meters (80,000 feet), accumulation of sediments. They are thought to have been deposited in generally shallow water during the Upper Proterozoic and part of the Cambrian (Sprigg, 1952). The Upper Proterozoic of the Adelaide Geosyncline, also referred to as the Adelaidean System (Figs. 2 and 3a), is subdivided further into the

Reproduced with permission of the copyright owner. Further reproduction prohibited without permission.

Figure 2

Comparison of selected Precambrian classification (James, 1972).

Reproduced with permission of the copyright owner. Further reproduction prohibited without permission.

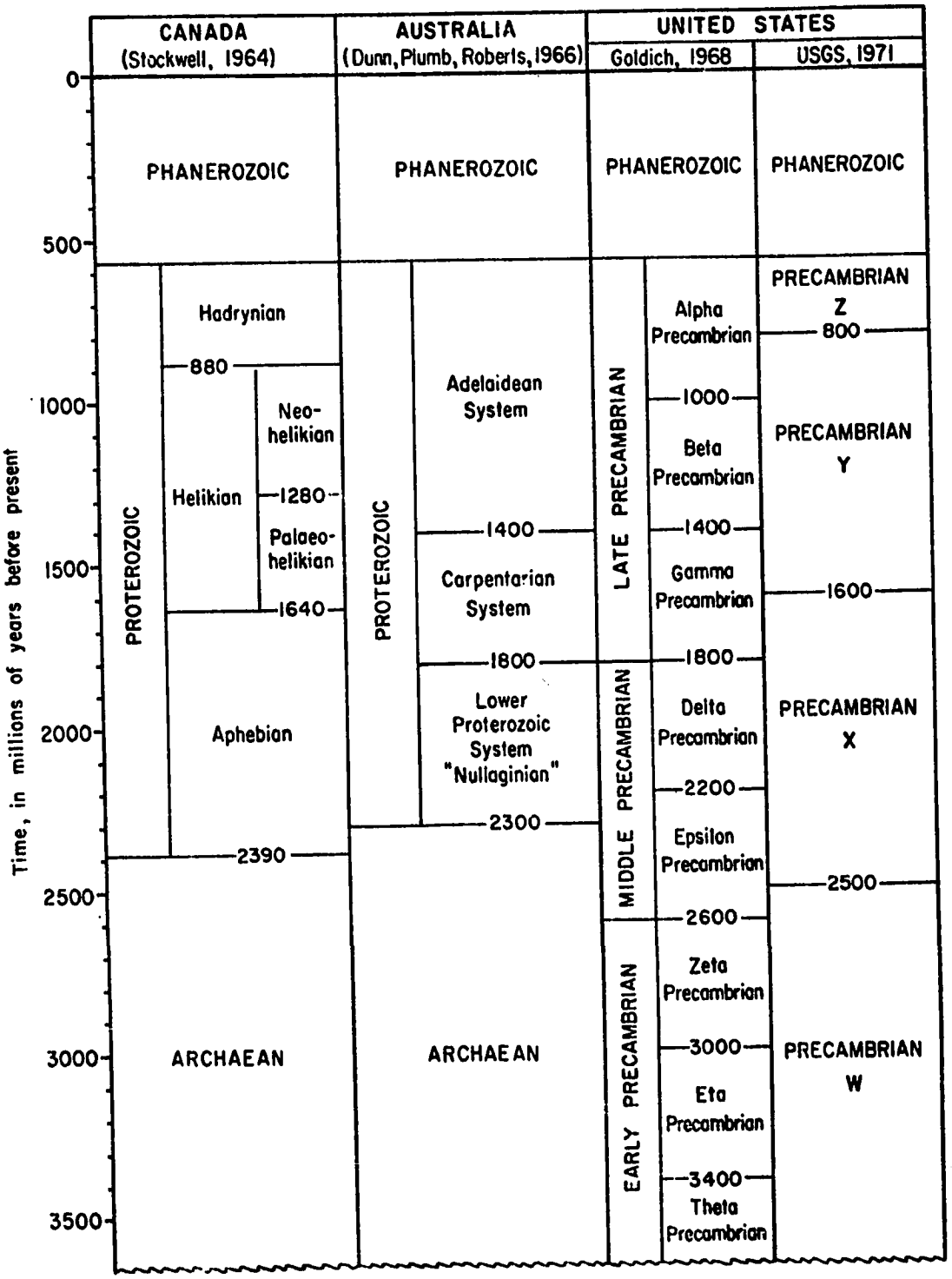

Reproduced with permission of the copyright owner. Further reproduction prohibited without permission.

Reproduced with permission of the copyright owner. Further reproduction prohibited without permission.

Figure 3a

Time and rock terms used in the Adelaide Geosyncline (Thomson, 1969). Arrow indicates the position of Tapley Hill Formation.

Figure 3b

Stratigraphic relationships of Sturt Tillite, Tindelpina Shale and Tapley Hill Formation.

Reproduced with permission of the copyright owner. Further reproduction prohibited without permission.

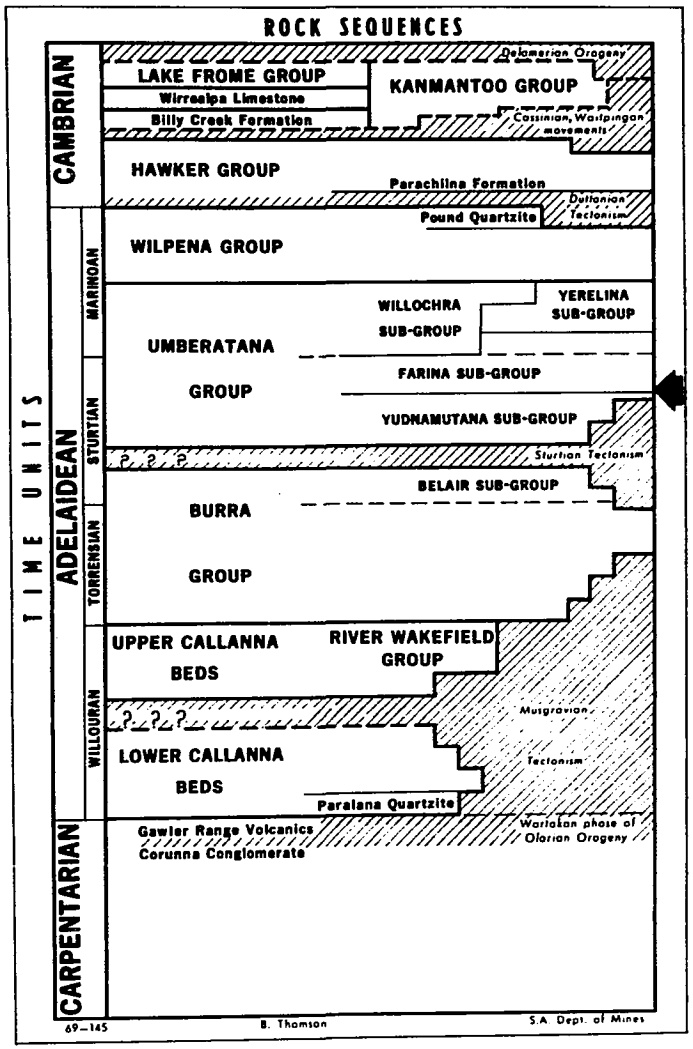

a

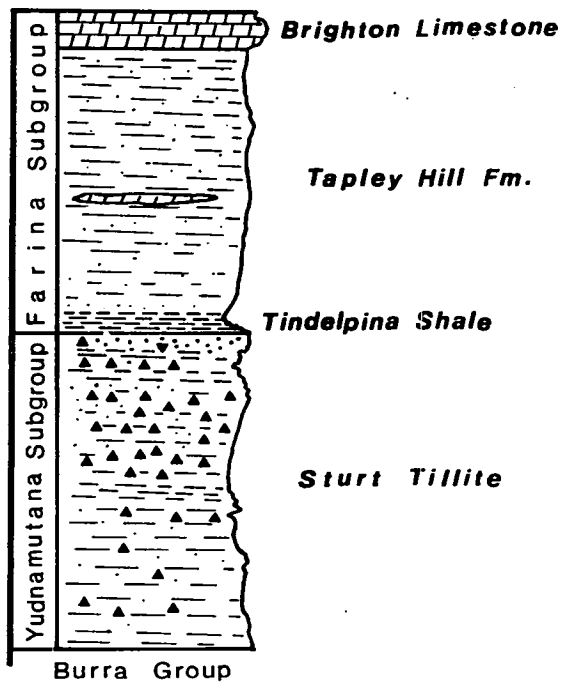

b

Willouran, Torrensian, Sturtian, and the Marinoan. Rocks deposited during these periods are respectively called the Callana Beds (including the River Wakefield Group), the Burra Group, the Umberatana Group, and the Wilpena Group.

The Umberatana Group, which is relevant to this thesis, includes two periods of glaciation (the Yudnamutana and the Yerelina Subgroups) and an interglacial period (the Farina Subgroup). During the first glaciation period and the interglacial period, about 6,000 meters of glacigene and fine-grained detrital sediments were deposited together with lenses of carbonates (dolomite) (Campana, 1958). The glacigenes which form the Sturt Tillite or its stratigraphic equivalent underlie the Tapley Hill Formation of which the Tindelpina Shale is the basal member. This formation, deposited during the interglacial period, constitutes part of the vast mass of detrital sediments deposited in the Adelaide Geosyncline.

It is the mineralogy and geochemistry of the Tindelpina Shale with which this study is concerned. Therefore the stratigraphic position of this shale unit should be described in relation to its upper and lower boundaries (Fig. 3b).

II.2. Stratigraphy

Sturt Tillite

The type section of this tillite is located at Sturt Gorge, very near to the type section of the Tapley Hill Formation. The lithology of the tillite has been adequately described by Howchin (1929, p. 42):

Reproduced with permission of the copyright owner. Further reproduction prohibited without permission.

> "The greater portion of the beds consists of a typical glacial till, in the form of an unstratified gritty mudstone, carrying numerous erratics up to 10 feet in diameter, which are promiscuously distributed throughout the fine material. The ground-mass carries a characteristic appearance in all localities. The stone, when split, exhibits more or less a populose surface, caused by the included small stones standing in relief covered with a shaly film; and, usually, small angular cavities occur where the softer or more soluble inclusions have been removed by weathering. The tillite is somewhat irregularly indurated, being at times highly siliceous, and in other cases, friable and readily weathers. Included in the boulder clay are irregular masses of coarse grits and pockets of stones, and at times stratified slates that are wholly, or nearly, free from boulders, as well as thin, gritty, and siliceous limestones. The beds share in the general cleavage plane of the country, but the cleavage is coarse, and attended by a flaky exfoliation. The cleavage planes cause the rock to weather into sharp and serrated edges . . .."

Figures 4a, 4b, and 4c are photographs of the Sturt Tillite which Howchin classically described.

Locally within the Flinders Ranges, several other formational names have been used for the stratigraphic equivalent of the Sturt Tillite. These are all included in the Yudnamutana Subgroup (Thomson, 1969). For instance, in the area of the Orroroo map sheet, the stratigraphic equivalent of the Sturt Tillite was defined by Mirams (1964) as the Appila Tillite after its type section in Appila Gorge, consisting of boulder tillite, quartzite, and siltstone. Various lithologic units can be distinguished in the tillite unit so that it may be subdivided further into several members when more detailed mapping has been conducted (Binks, 1971). The tillite contains erratics of varying lithology, such as gneiss, schist, granite, volcanic rocks, jaspillite, dolomite, siltstone, and quartzite which is the dominant

Reproduced with permission of the copyright owner. Further reproduction prohibited without permission.

Figure 4. Sturt Tillite

a. Type section of the Sturt Tillite at Sturt Gorge, near Adelaide, South Australia, estimated by Sprigg (1946) to be about 1200 feet thick.

b. A close-up of Sturt Tillite with erratics, Sturt Gorge.

c. A siltstone unit in the tillite, Sturt Gorge. Note the cross-bedding.

Reproduced with permission of the copyright owner. Further reproduction prohibited without permission.

Reproduced with permission of the copyright owner. Further reproduction prohibited without permission.

rock. This quartzite has a similar lithology to that of the upper part of the Burra Group rocks. The erratics of igneous and metamorphic origin, which are foreign to the area, are similar to the basement rocks west of the Torrens Hinge Zone (Fig. 1). It has been suggested that the provenance of the glacigenes is in the west (Binks, 1971).

It should be noted that the Sturt Tillite is a formational name. However, only a fraction of this glacigene consists of diamictite which is true tillite.

Tapley Hill Formation

This formation was originally named by Howchin (1904) as the Tapley's Hill Slates. He (1929, p. 29) described this formation as:

> "The rock is a very fine-grained ribbon-slate, the banded character of the stone being more strongly developed by weathering. It possesses a coarse cleavage, splitting at a high angle, and is a valuable building stone. At its base is an impure dolomitic limestone, about four or five feet in thickness, which rests on the tillite. The beds are more or less, calcareous throughout, which gives rise to a thin mantle of travertine. It is a very persistent horizon in its extension northwards, and can be easily recognized by its characteristic features, but, excepting in the Adelaide district, it generally takes the form of a finely laminated shale, and splits on the bedding plane, ..."

In the type locality at Darlington, near Adelaide, the Tapley Hill Formation is composed of laminated, varve-like, black, calcareous, slaty siltstone and has a thickness of about 1,700 meters (5,000 feet) (Figs. 5a and 5b). Throughout the area under study, this rock unit is remarkably uniform, and is easily recognizable by its typical ribbon-like feature. Segnit (1939) subdivided the Tapley Hill Formation into the lower, middle, and upper group based on its lithologic character.

Reproduced with permission of the copyright owner. Further reproduction prohibited without permission.

Figure 5. Tapley Hill Formation

a. Contact of Sturt Tillite and the overlying Tapley Hill Formation, Flinders University Campus.

b. Type section of Tapley Hill Formation, at a quarry, Darlington.

c. Characteristic ribbon-like texture of Tindelpina Shale, Paddock Creek, Quorn. Diameter of coin is 19 mm.

d. Weathered surface of Tindelpina Shale, showing typical colorful laminations, Horrock's Pass.

e. Authigenic pyrite encrustration on bedding plane, Spring Creek, Wilmington.

f. Tindelpina Shale outcrop, near Copley.

Reproduced with permission of the copyright owner. Further reproduction prohibited without permission.

Reproduced with permission of the copyright owner. Further reproduction prohibited without permission.

Howchin (1929, p. 30) pointed out further that

> "These finely laminated shales must have been laid down under somewhat exceptional circumstances. The laminae are often so finely divided to show twelve distinct layers to the inch, interbedded with other layers, of greater thickness, but with extraordinary parallelism often over long distances. The idea of these being varve shales is out of the question, partly on account of their very great lateral extent; and, also, in that they show no alternating deposits of finer and coarser material, which is the chief characteristic of varve deposits laid down in water in front of a glacier regulated by the annual change of seasons. The clay particles of which the rock is composed are excessively fine, and must have been laid down in water that was entirely free from wave action. The deposit may have been formed from a redeposition of the finer portion of the glacier mud, by land wash, after the disappearance of the ice, but its greatness and extent, together with the absence of any residuals of the heavier material of the boulder clay, as erratics, etc., appear to be opposed to this view . . . ."

Campana (1958) is of the opinion that the Tapley Hill Formation is of aqueo-glacial origin.

Tindelpina Shale Member. The basal member of the Tapley Hill Formation is called the Tindelpina Shale. This name was introduced by Coats (1964) for the type section occurring near Tindelpina Hut (30° 06' 28"S, 139° 18' 28"E.), about 500 kilometers (350 miles) northeast of Adelaide. He describes this rock unit, at the type locality, as a finely laminated, black carbonaceous, pyritic shale approximately 60 meters thick. Black, gritty limestone, sandstone, and grit occur within the unit. At other places, a thin, yellowish-brown dolomite may occur at or near the base of this horizon. A subsidiary type section occurs at Sturt Gorge, where the type section of the underlying Sturt Tillite

Reproduced with permission of the copyright owner. Further reproduction prohibited without permission.

is also defined (Coats, 1971, pers. comm.). The upper boundary of the Tindelpina Shale with the Tapley Hill Formation is not readily recognizable especially when the outcrops have been weathered. In most cases, this boundary is transitional.

Throughout the Adelaide Geosyncline, the Tindelpina Shale overlies the Sturt Tillite. The shale horizon usually forms areas of poor outcrop and low relief as compared to the prominent outcrops of the tillite (Fig. 5f). In the area of the Orroroo map sheet, and probably also in the entire Adelaide Geosyncline, the Tindelpina Shale is considered to be the best marker bed (Binks, 1971).

Field recognition of the Tindelpina Shale was based on the presence of the underlying tillite. The characteristic varve-like texture which is typical of the Tapley Hill Formation is also a characteristic feature of the Tindelpina Shale and was used as a distinctive marker for recognizing the shale. Many of the outcrops have been weathered, causing a colorful banding of green and reddish laminae to stand out strikingly on the weathered surface (Figs. 5c and 5d). On this weathered surface, iron-oxide cubes, pseudomorphous after pyrite and of microscopic size up to an average of three millimeters, often appear as streaks along the lamina boundaries (Fig. 5e). On fresh surfaces pyrite often occurs as streaks following the lamination. Some samples show the rotation of pyrite crystals, probably resulting from the metamorphic effect on the rock.

In the author's opinion, the distinction of this black shale horizon from the Tapley Hill Formation is overemphasized. From field

Reproduced with permission of the copyright owner. Further reproduction prohibited without permission.

collecting and microscopic examination, the Tindelpina Shale has been found to be not always a black shale, to contain more quartz than clay minerals, to be generally silty rather than shaly, and to have a gradational boundary with the overlying Tapley Hill Formation.

Reproduced with permission of the copyright owner. Further reproduction prohibited without permission.

III. MINERALOGY

III.1. Diagenetic-Metamorphic Indicator

Mineral Assemblage

It is generally known that the response of argillaceous sediments to diagenesis or low-grade metamorphism may be reflected in the characteristics of the clay-mineral assemblage. Controversies exist as to the meaning of diagenesis and its boundary with metamorphism. The processes involved in the transformation of sediments, especially pelitic sediments, have been reviewed by Keller (1963), Kossovskaya and Shutov (1970), and Dunoyer de Segonzac (1970), and Weaver and Beck (1971).

Coombs (1954) pointed out that the mineralogy of sediments may be altered by burial metamorphism. He established that the lithologic zonality of the volcanogenic greywackes of the Triassic of New Zealand is due to burial metamorphism.

Burst (1959) found that there is a change in the mineralogy of the Wilcox Formation (Eocene) in the Gulf Coast, U.S.A., with increasing depth. He found that montmorillonite is common in the outcrops, but less common in the bore holes. At a depth between 3,000 and 4,000 feet, montmorillonite occurs as a mixed-layer illite-montmorillonite, and at a depth below 14,000 feet montmorillonite disappears. Chlorite appears at all stratigraphic levels but is apparently more dominant with depth. He attributed this change to the increase of chlorite crystallinity or to the conversion of other clay minerals into chlorite. Muffler and White (1969) came to the same general conclusions with their material obtained from deep drilling in the Salton Sea geothermal field.

Reproduced with permission of the copyright owner. Further reproduction prohibited without permission.

Burst (1969) re-examined his previous results and concluded that the composition of montmorillonite is not changed by burial and that thermal dehydration involving one water layer is responsible for the observed structural changes in the illite-motmorillonite. He proposed an explanation in which the change in illite-montmorillonite is a benefaction of degraded and fragmental lattices by gradual fixation of potassium and magnesium to form illite and chlorite respectively. Recent work on burial diagenesis was done by Perry and Hower (1970), and they formed the same conclusions as Burst (1969).

Maxwell and Hower (1967) in their study of the Belt Series (Proterozoic) argillites in western Montana and northern Idaho found that there is a transformation of 1Md to 2M polymorph of illites, which they attributed to increasing temperature and pressure conditions which accompany deep burial, aided by the geothermal gradient related to the batholithic intrusion. They concluded that the Belt Series argillites have undergone high-grade diagenesis to low-grade metamorphism. Butler (1965) made the generalization that the compositional variation of micas is related to the variation in metamorphic grade, bulk composition, and mineral paragenesis of the rocks.

Crystal Parameter

The effect of metamorphism on the micas may also be reflected by the change in their crystal parameters. Using this principle, Guidotti (1963, 1966) and Guidotti and Crawford (1968), showed that the basal spacing of muscovite can be used as an index of metamorphic

Reproduced with permission of the copyright owner. Further reproduction prohibited without permission.

grade. In their study of metamorphic rocks in southeastern Pennsylvania, U.S.A., Guidotti and Crawford (op. cit.) found that the values of muscovite basal spacings vary from 9.980 to 9.939 Angstroms in the subgarnet zone and 9.963 to 9.991 Angstroms in the sillimanite zone. Furthermore, they deduced on the basis of this basal-spacing variation that the composition of muscovite can be related to its paragonite content.

Sassi (1972) working in the Alps indicated that the b_0 parameter of potassic white mica may be used as a measure of the degree of metamorphism in the low greenschist facies. One important prerequisite required is that the rocks should be of essentially isochemical composition. However, the relationship of pressure-temperature condition to the b_0 parameter in the potassic white micas has not been clearly defined. Sassi pointed out that b_0 increases with phengite content. The analysis of Cipriani, Sassi, and Scolari (1971) cited by Sassi (op. cit.) indicates that other conditions being equal (temperature and bulk chemical composition), the phengite content of potassic white micas decreases with decreasing pressure.

Crystallinity of Illite

When rocks are devoid of the characteristic minerals which appear as a result of metamorphic changes, then other means of recognizing this change should be utilized. It has been found that the degree of crystallinity of the common mica (illite), occurring in sediments which have undergone transitional processes from diagenesis to metamorphism, depends on the stage of the transition. This basic idea,

Reproduced with permission of the copyright owner. Further reproduction prohibited without permission.

which was recognized by Weaver (1960), indicates that with increasing diagenesis and metamorphism, the crystallinity of illite also increases. This concept has been further developed by French workers and has been used to study the effect of metamorphism on various sediments (Kubler, 1964, 1968; Esquevin, 1969).

Weaver (1960) defined crystallinity as the "sharpness ratio", which is the ratio of the peak height at 10 Angstrom (001 plane) to the peak height at 10.5 Angstroms, on X-ray diffractograms of illite (Fig. 6). With increasing digenesis and metamorphism, the first basal reflection of illite becomes sharper, and the ratio becomes larger. In his study in the Ouachita Mountains in Oklahoma, Weaver obtained the following ratios for the different stages of metamorphism:

Unmetamorphosed Atoka Formation	1.8
Unmetamorphosed Stanley Formation	2.3
Incipient metamorphism	2.3
Incipient to very weak metamorphism	4.5
Very weak to weak metamorphism	6.3
Low-grade metamorphism	12.1

His data indicates the suppression of interstratification, the regularization of lattices, and the increase of crystal size of illite during the first stages of metamorphism.

On the other hand, Kubler (1964) defined the crystallinity of illite on the X-ray diffractogram as the width in millimeters, at the half-peak height of the 10 Angstrom reflection. Small values of the "Kubler index" indicate high crystallinity, whereas large values indicate low crystallinity. Using this method, Kubler (1968) can

Reproduced with permission of the copyright owner. Further reproduction prohibited without permission.

Figure 6. Crystallinity of Illite

a. Weaver sharpness ratio $\frac{h_1}{h}$ Kubler index: w (in mm).

b. Fithian Illite, Illinois, U.S.A.

c. Muscovite from Hart Ranges, N.T., Australia.

Reproduced with permission of the copyright owner. Further reproduction prohibited without permission.

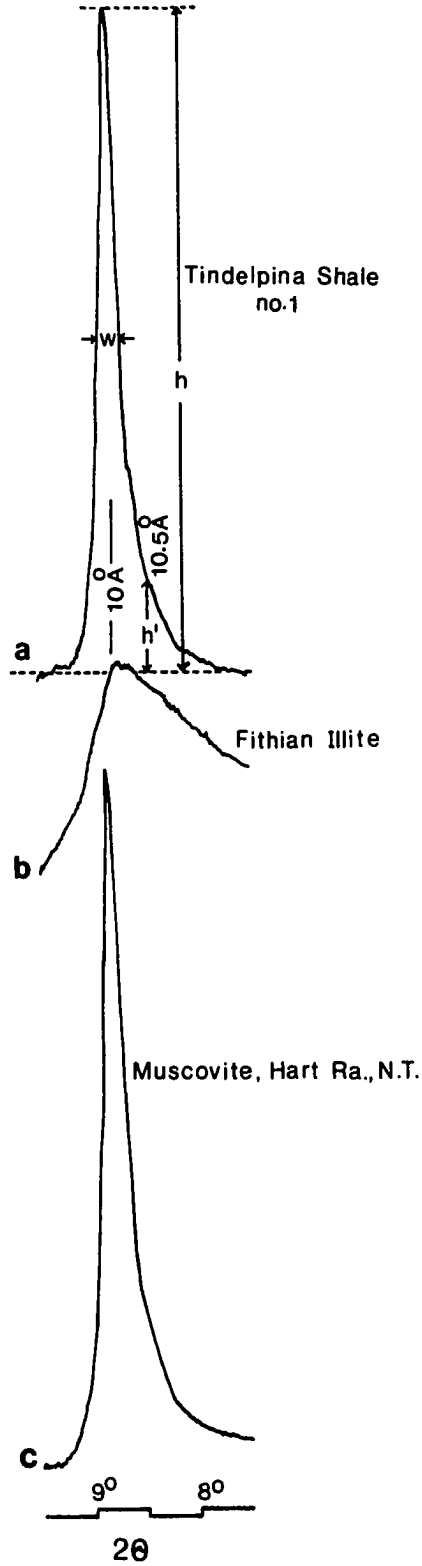

Reproduced with permission of the copyright owner. Further reproduction prohibited without permission.

differentiate anchimetamorphism, which ranges from diagenesis to epimetamorphism (the beginning of metamorphism), into the following intervals based on the Kubler index of illite:

Unmetamorphosed illite (diagenesis)	more than 8.5 mm
Initial metamorphism	8.5 to 6.5 mm
Initial up to very weak metamorphism	6.5 to 6.1 mm
Very weak up to weak metamorphism	6.1 to about 5 mm
Epimetamorphism	less than 5 mm

Kubler's data was obtained by using a Philips X-ray goniometer at a speed of 2^{o}/minute and a chart speed of 160 cm/hour. The shortcoming of his method is that interlaboratory comparison of the results is not possible. This is due to the fact that it is not possible to obtain exactly similar operating conditions of X-ray machines of similar models, let alone x-ray equipment of different make. However, in the author's opinion, this short-coming can be eliminated by using a reference illite (or muscovite) and normalizing the values obtained to that of this reference mineral. Various investigators have used Kubler's method with success (Frey, 1969; van Biljon and Bensch,1970; Weber, 1972a, 1972b).

III.2. Scope and Purpose of this Study

The mineral assemblages of Tindelpina Shale were determined from about 90 of the freshest samples collected. For muscovite present, the basal and $d_{(060)}$-spacings were determined on 50 and 70 samples, respectively, and crystallinity, expressed in terms of the Kubler index and the Weaver sharpness ratio, was measured from 85 samples.

Reproduced with permission of the copyright owner. Further reproduction prohibited without permission.

These mineralogical analyses were carried out for two reasons: firstly, to describe the mineralogical composition of this rock unit on which there was little published information; and secondly, in an attempt to determine whether the effect of the low-stage regional metamorphism occurring in the Adelaide Geosyncline is reflected in the mineral assemblage and the variables of muscovite mentioned above.

Reproduced with permission of the copyright owner. Further reproduction prohibited without permission.

IV. GEOCHEMISTRY

IV.1. Trace Elements as Environmental Indicators

It has been established by various authors that trace elements occurring in sediments may be used as indicators of the environment during deposition (Keith and Degens, 1959; Johns, 1963; Potter et al., 1963; Shimp et al., 1969; Harder, 1963, 1970). The basis of this concept is that certain trace elements such as boron, chlorine, lithium, sulphur, vanadium, and others, are concentrated more in sediments of marine origin than in those of fresh-water origin. This applies especially to sediments of an argillaceous nature. However, the validity of this concept was recently questioned by Cody (1970) as a result of his finding of anomalously high boron content in a fresh-water sediment. While he admitted that this was an exceptional case, he suggested that lack of knowledge about the factors affecting the concentration of trace elements in recent sediments is the reason for some uncertainty in the use of trace elements as environmental indicators.

Most of the studies which have been conducted are empirical, although some investigators have attempted to explain how trace elements occur in sediments and why some are concentrated more in argillaceous rocks of marine origin (Levinson and Ludwick, 1966; Fleet, 1965; Harder, 1970). Cody (1971) stated that, to be a good environmental indicator, the concentration of the trace element occurring in sediments should be affected principally by one environmental parameter, such as salinity,

Reproduced with permission of the copyright owner. Further reproduction prohibited without permission.

and only slightly affected by other parameters such as pH, temperature, or water depth, and also that later postdepositional changes should not appreciably affect the original concentration of the element. Potter et al. (1963) stated that there are essentially no significant differences in trace-element concentrations between ancient and modern argillaceous sediments. This implies that the concentration of trace elements in ancient shales is not significantly altered by postdepositional processes.

Shaw (1954) studied the effect of postdiagenetic processes namely, metamorphism, on the concentrations of trace elements in the pelitic schists of the Littleton Formation (Devonian) in New York, U.S.A. He concluded that metamorphism does not significantly alter the distribution of the trace elements. However, he found that lithium and lead concentrations increase slightly with metamorphism; he explained this as a process of "metasomatism in trace-element scale". Engel (1958) suggested that only the volatiles in the Littleton Formation may have been lost during metamorphism. Goldschmidt (1954) mentioned that boron may reveal the sedimentary or igneous origin of highly metamorphosed rocks.

It can be inferred from these studies that the distribution of trace elements in argillaceous sediments may indicate the environment during deposition of the sediments. An example is boron which is one of the more frequently studied trace elements occurring in argillaceous sediments especially of recent age.

Reproduced with permission of the copyright owner. Further reproduction prohibited without permission.

Work on boron geochemistry was initiated by Goldschmidt and Peters (1932) who found that the boron content is much higher in marine clays than in those of continental origin. They stated that the actual boron content in the sea decreases with younger sediments. Thus, recent sediments tend to have lower total boron content than those of Paleozoic age. This was explained by them as being due to the adsorption or fixation by sediments. Later, Landergren (1945) pointed out that the boron content of recent argillaceous sediments is directly proportional to the salinity of the water in which the sediments occur, and that, in general, shales contain more boron than other sedimentary rocks. He also stated that the ratio of the boron content to the salinity of sea water has remained unchanged since Cambrian, and probably long before that time. This means that boron may be used as an index of paleosalinity, and probably, as other authors have claimed, even as a paleotemperature indicator (Harder, 1959, 1961, and 1970).

Since Landergren's findings, many investigators have studied the geochemistry of boron occurring in sediments, particularly in pelitic rocks (Degens, Williams, and Keith, 1957, 1958; Keith and Degens, 1959; Frederickson and Reynolds, 1960; Harder, 1961; Potter et al., 1963). Levinson and Ludwick (1966) proposed an explanation of the common findings that boron is relatively more concentrated in the marine than in fresh-water argillaceous sediments. They stated that boron present in river water is adsorbed by clay-size particles occurring abundantly in the zone where river and sea water mix. The

Reproduced with permission of the copyright owner. Further reproduction prohibited without permission.

degree of adsorption of boron by the clays depends on the size of the clay particles. The finest particles, irrespective of particular composition, will adsorb the most boron and will be deposited the farthest away in the sea. This results in a linear relationship of boron concentration in argillaceous sediments with the salinity of the water in which the sediments are deposited. This theory was later substantiated by Shimp et al. (1969) who added that, for a given clay content, the total boron content is correlated with the amount of material of less than 2 micron size.

During weathering of parental rock boron may go into solution as boric acid and soluble borates, and eventually moves in streams to the sea. Boron is a part of the buffer solution, second in importance to the carbonate system. In sea water, boron occurs mainly as amphoteric acid H_3BO_3 or $B(OH)_3$ and has an average concentration of 5 parts per million.

It is not clearly understood how boric acid is held by clays. The study of Zachariasen (1934), which was quoted by Ataman (1967), showed that boric acid has a sheet structure which can be held in the interlayer space of clay minerals. Through strong ionization, ionic boron (B^+ or B^{3+}) may diffuse into the octahedral or tetrahedral site, or be held on the clay interlayer-surface.

From researches to date, the occurrence of boron in sediments may be summed up as follows:

1. There is a linear relationship between the boron content and the salinity of the sea water in which the sediments occur; this has been well established in recent sediments.

Reproduced with permission of the copyright owner. Further reproduction prohibited without permission.

2. The concentration depends on the adsorption capacity of the clay minerals present and the amount of relict or recycled boron in the sediments.

3. As illite is the principal clay mineral present in shales, boron is found principally in this constituent.

4. Within a single formation, the actual boron content may be used as an indicator of palaeosalinity. The amount of boron carried by detrital minerals in the argillaceous sediments (such as tourmaline and micas) is assumed to be relatively insignificant.

Work on other trace elements used as environmental indicators has been reviewed by Krejci-Graf (1964), Ernst (1970), and Wedepohl (1971). The general conclusion is that the distribution and concentration of trace elements in sediments, argillaceous sediments, in particular, may indicate the conditions in which they were deposited.

IV.2. Major Elements

Trends and Coherence

The geochemical trends and coherence of the major elements in sedimentary rocks are less well understood than in igneous and metamorphic rocks. The complexity arises because of the added physical and chemical factors which are involved in the weathering processes, transport, and deposition of the sediments. Chemical disequilibria during surficial weathering and later diagenetic changes, as well as other factors such as waves, currents, climatic conditions, salinity, redox potential, and provenance combine in various ways and add to this complexity at different times and places.

Reproduced with permission of the copyright owner. Further reproduction prohibited without permission.

Green and Poldervaart (1958) pointed out that attempts to derive a general sedimentary trend from chemical data would be futile. They showed, for example, that the plots of some major elements (Al, total Fe, Mg, Ca, and combined alkalis) do not produce meaningful trends. However, others maintain that plots showing relationships among major oxides in arenaceous sediments may represent significant trends which may be related to depositional environment. In an investigation of the Moine and Torridonian rocks of the Scottish Highlands, Kennedy (1951) showed that there is a unilateral trend of sedimentary differentiation of the arenaceous sediments across the Caledonian geosyncline. He plotted the concentration of SiO_2 against Al_2O_3, Na_2O, and K_2O, and found that there is a definite difference between the rocks of the eastern and western facies. He defined <u>sedimentary differentiation</u> as:

> ". . . a progressive change in chemical composition within a well-defined formational unit, the change being in the direction of increasing residual character . . .."

Middleton (1960) demonstrated that histograms of the seven major oxides of sandstones (SiO_2, Al_2O_3, total Fe_2O_3, MgO, CaO, Na_2O, and K_2O) and variation diagrams of K_2O/Na_2O against alkalies/Al_2O_3 indicate a significant relationship between the geosynclinal environment of deposition and the tectonic setting of the sandstones.

The coherence of the major elements may be shown by plotting the combined alkalies. Garrels and Mackenzie (1971) showed that there are three distinct groupings for sandstones, shales, and limestones.

Reproduced with permission of the copyright owner. Further reproduction prohibited without permission.

Moore and Dennen (1970) found evidence of a definite relationship between silicon-aluminum-iron ratios and clastic-sediment types. They suggested that plots of silicon-aluminum-iron ratios may assist to clarify the ambiguity of sandstone classification in current usage.

Blatt et al. (1972) pointed out that it is very difficult to interpret chemical trends in terms of source, environment, tectonics, and other factors involved in the deposition of pelitic sediments. While much study has been done on the size distribution, mineralogy, and texture of the coarser fractions, little is known about the finer fractions of detrital sediments. In spite of the difficulty involved in the interpretation of chemical data related to the depositional environment of finer fractions, a study based on the chemical approach seems most appropriate.

Environmental Indicators

The Russian workers have made by far the greatest number of attempts to show the significance of the chemical composition of mudrocks. Ronov et al. (1966) suggested that the content of the alkalies in mudrocks generally increases with the distance from the source rock, and that the K_2O/Na_2O ratio decreases with distance from the provenance. The chemical compositions of marine clays and of the various mudrocks of continental origin found on the Russian platforms have been studied extensively by Vinogradov and Ronov (1956), Ronov and Khlebnikova (1957), Ronov et al. (1966), and Ronov and Migdisov (1971).

The study by Ronov and Khlebnikova (op. cit.) showed that the chemical compositions of continental clays strongly depend on the

Reproduced with permission of the copyright owner. Further reproduction prohibited without permission.

climatic condition during which such clays were formed. The compositions of clays formed in cold to temperate climates are similar to the average composition of igneous rocks when the ultrabasic rocks are excluded. The humid and tropical climate zones produce clays with higher alumina concentrations than those of marine origin. Marine clays have alumina contents similar to those found in continental clays of cold climates; however, marine clays show a wider compositional range which is due mainly to the introduction of carbonates.

The causes of chemical variation among continental clays from different climatic conditions are due to the different affects of the weathering processes on the parent materials. Mudrocks from cold climates are the products of the initial weathering of the stable landmass, during which the most mobile elements (Na, Ca, and Mg) are partially removed. In the humid and tropical climate zones, more extensive physical and chemical weathering takes place. Not only will the mobile elements move away, the less mobile ones such as Fe, K, and even Si will be partially removed. In the weathering products (the clays), enrichment of the least mobile elements (Al and Ti) may occur.

Ronov and Khlebnikova (op. cit.) pointed out that it is not possible, however, to differentiate the chemistry of the major elements of marine clays from that of continental clays from cold to temperate regions.

Chemical Maturity

As early as 1927, Vogt introduced the concept of chemical maturity as applied to detrital sediments. In his geochemical study

Reproduced with permission of the copyright owner. Further reproduction prohibited without permission.

of rocks in the Sulitjelma region of Norway, he introduced the following numerical index, which is the molecular ratio of basic oxides, excluding iron oxides. This index is considered to be a measure of chemical maturity of detrital sediments.

$$\text{Vogt index} = \frac{Al_2O_3 + K_2O}{MgO + CaO + Na_2O}$$

Vogt considered clay sediments to be the washed residual product of the weathering process, with alumina, as the least soluble oxide, tending to be concentrated in the rocks with the most residual character. However, this enrichment of alumina might be obscured by the presence of free quartz. To neutralize the effect of this silica, Vogt recalculated the molecular proportions of the oxides so that they would add up to 100, excluding SiO_2 and TiO_2. He found that the concentrations of MgO, CaO and Na_2O decrease gradually and regularly with increasing residual character, whereas the concentrations of K_2O, SiO_2, and TiO_2 increase with increasing residual character. The concentration of iron was found to be constant over a large range of compositions. For this reason, Vogt left FeO and Fe_2O_3 out of his index. The result of Vogt's study shows that his rocks have indices varying from 0.74 to 3.84.

Low values for Vogt indices result from "immature" sediments, i.e., sediments which are composed mainly of finely ground rock flour and which are practically unaltered or only slightly altered by the weathering process. The main components of such sediments are those

Reproduced with permission of the copyright owner. Further reproduction prohibited without permission.

minerals which are easily decomposed by the weathering process, such as plagioclase and ferromagnesian minerals. On the other hand, high values for Vogt indices indicate "mature" sediments having a high degree of residual character. Such sediments usually have a high content of phyllosilicates and/or quartz, and a low content of basic plagioclase and ferromagnesian minerals. Sediments composed almost exclusively of kaolinite and/or dioctahedral illite will give the highest Vogt index (Roaldset, 1973, pers. comm.). These characteristics of the Vogt index were found to be true by other workers who have studied the geochemistry of fine-grained detrital sediments in Norway (Bjørlykke, 1965; Roaldset, 1972).

IV.3. Scope and Purpose of This Study

Trace Elements

Out of 150 rock samples, at least 117 were analyzed for 14 trace elements (Ga, Rb, Sr, As, Ba, B, Cr, Cu, Li, Ni, Pb, V. Zn, and Zr). The remaining 33 samples have been only partially analysed.

The purposes of choosing and analyzing these 14 trace elements are as follows:

1. As previously mentioned, trace elements may, to a certain extent, indicate the environment of deposition of sediments. The author intends to determine whether the regional distribution and abundance of these trace elements, or some combination of them, in the Tindelpina Shale, would indicate the depositional environment of this sedimentary unit.

Reproduced with permission of the copyright owner. Further reproduction prohibited without permission.

2. As yet, the only published work on the trace elements of the Proterozoic detrital sediments in the Adelaide Geosyncline is very scanty. It is felt by the author that these 14 trace-element analyses would make an initial contribution to the geochemistry of the Adelaide Geosyncline sediments.

Major Elements

A total of about 200 samples (50 of which were duplicates included for the purpose of examining the reproducibility of the analyses) were chemically analyzed for their major oxide contents (SiO_2, Al_2O_3, total Fe_2O_3, MgO, CaO, Na_2O, K_2O, TiO_2, P_2O_5, MnO, and loss on ignition), and their quartz content. In addition, 25 Sturt Tillite samples (matrix material) were analyzed for their major oxide contents.

The purposes of carrying out these analyses are as follows:

1. To provide basic information on the chemistry of the Tindelpina Shale and Sturt Tillite, both of which are extensively distributed throughout the Adelaide Geosyncline.

2. To construct directional patterns out of the regional distributions of the major oxides and detrital quartz, using trend surface analysis.

3. To interrelate the major elements with the 14 trace elements, the mineralogy, and the metamorphic indicators, by means of factor analysis.

Reproduced with permission of the copyright owner. Further reproduction prohibited without permission.

V. SAMPLING, PREPARATION, AND ANALYTICAL TECHNIQUES

V.1. Sampling

Shale represents almost two thirds of the stratigraphic record, and yet this rock is the least understood of sedimentary rocks. Because of their subtle lithologic variation and fine-grained nature, practical difficulty in sampling and examining shales may arise. The result of analysis of one rock sample may not necessarily be representative of the entire outcrop at one particular locality. For example, two samples collected at one sampling locality may give different analytical results. In a regional study such as this, it should be emphasized that the data obtained can only be meaningful if it represents analytical results from a single sedimentary horizon. So that reasonable control in sampling might be maintained, the Tindelpina Shale samples were collected at points as close as possible to the base of this unit, just above the Sturt Tillite or its stratigraphic equivalent. In two cases cores obtained from exploration companies were added to the collection.

About 150 samples were randomly collected on a regional scale throughout the Adelaide Geosyncline (Figs. 7 and 8). From each sampling point, three or four rock fragments of approximately 15 cm by 10 cm by 5 cm were collected and considered as one sample. An attempt was made to collect samples which were as fresh as possible. In addition, twenty-five samples of the Sturt Tillite (matrix material) were collected. This was done so that the chemical compositions of the shale and the tillite could be compared.

Reproduced with permission of the copyright owner. Further reproduction prohibited without permission.

Figure 7

Sample locations and outcrops of the Tindelpina Shale based on geologic maps of 1:250,000 scale, published by the South Australia Department of Mines.

Reproduced with permission of the copyright owner. Further reproduction prohibited without permission.

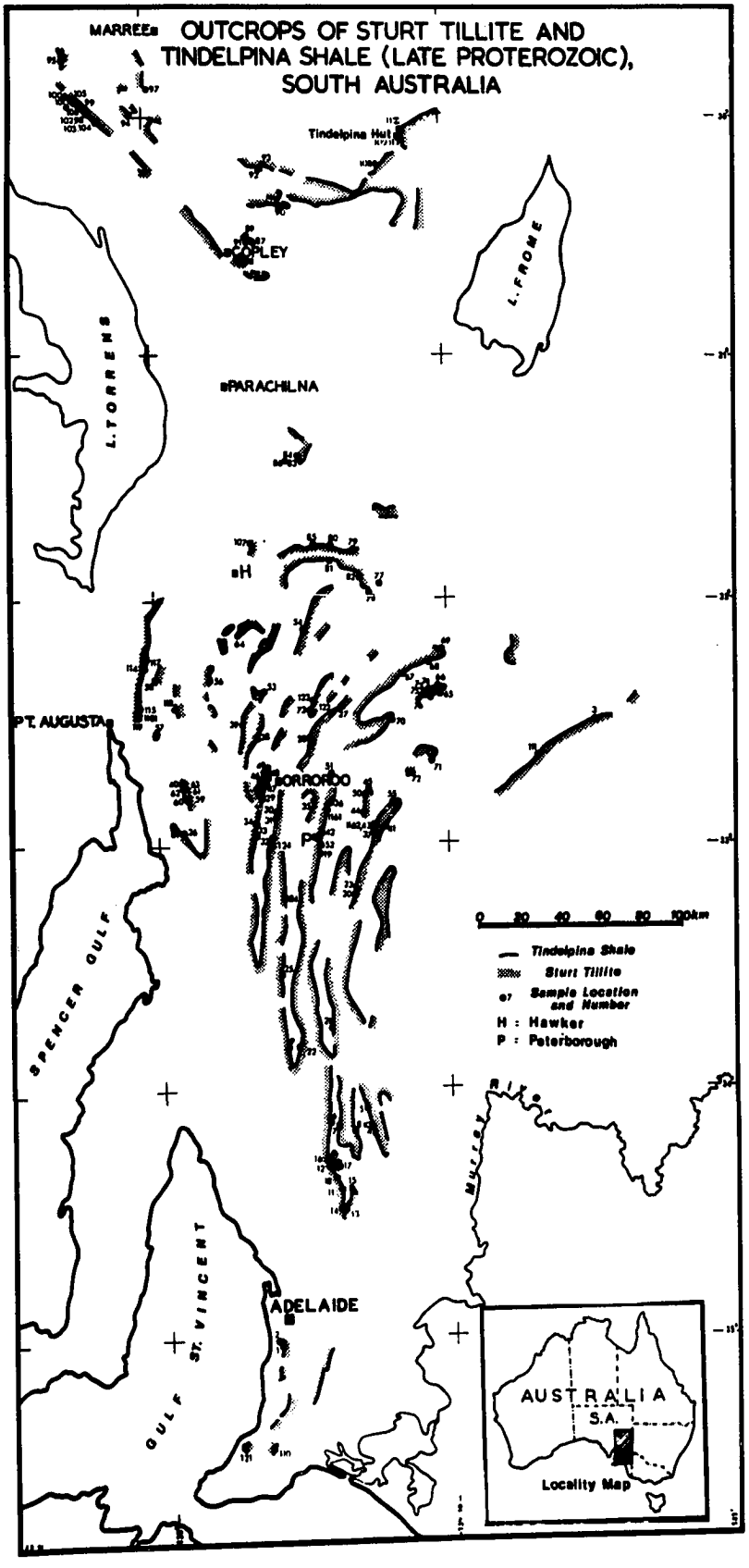

Reproduced with permission of the copyright owner. Further reproduction prohibited without permission.

Figure 8

Sample locations and outcrops of the Sturt Tillite or its stratigraphic equivalents.

Reproduced with permission of the copyright owner. Further reproduction prohibited without permission.

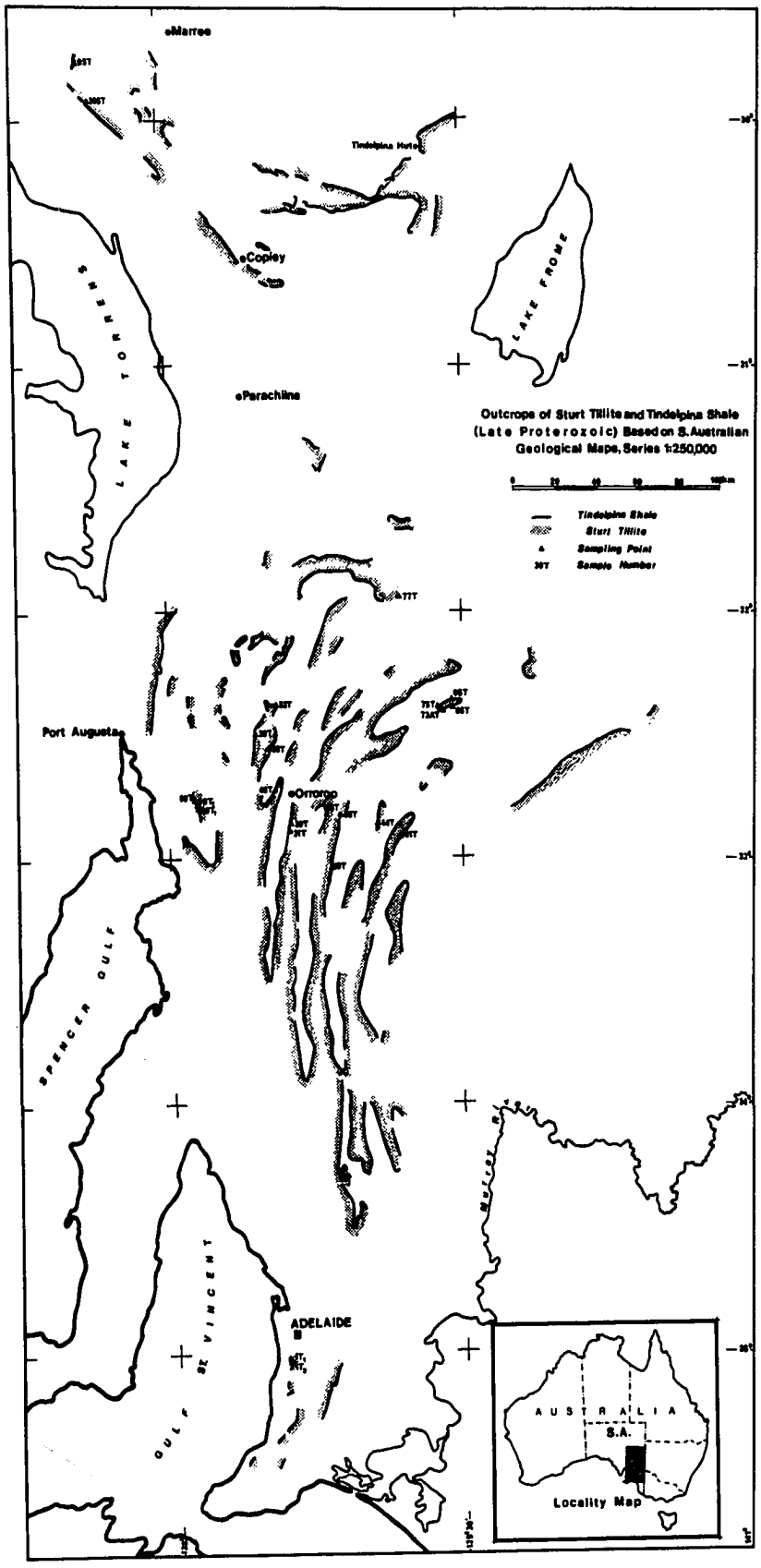

Reproduced with permission of the copyright owner. Further reproduction prohibited without permission.

The distribution of the Tindelpina Shale has been mapped by the South Australia Department of Mines as a part of their general mapping program using scales of 1:250,000 and 1:63,360. With the aid of these maps, the Tindelpina Shale was easily located in the field.

V.2. Preparation

Bulk samples were crushed in a jaw crusher and sieved. The minus $\frac{1}{4}$ mesh (BSS) freshly broken rock chips were retained and crushed further in a small teflon-lined jaw crusher. The crushed rock was then quartered and sieved, and about 100 millimeters of less than 12-mesh size was retained and pulverized in a chrome-steel vibrating disc-mill at a high speed for four minutes. From this stage, preparation of samples varied according to the analytical methods to be used.

V.3. Analytical Techniques

X-ray Diffraction

Identification of minerals. Two types of powder mounts were prepared. An unoriented mount was made for some of the samples by packing the finely powdered rock into a glass holder. An oriented clay slide was prepared for each sample by settling a clay-water slurry containing the less than 2μ-size fraction of the rock powder on a 2 inch by 1 inch frosted glass slide. This size fraction was obtained by drawing the rock-powder-water mixture into a pipette from a beaker glass at a specific time and depth according to Stokes' law. The packed-powder preparations were included so that it could be known whether there was a significant difference in the mineral assemblages of the bulk sample and the clay fraction.

Reproduced with permission of the copyright owner. Further reproduction prohibited without permission.

An X-ray diffraction trace (on PHILIPS PW 1010, see Appendix 1) with a chart speed of 1 cm/minute and a goniometer speed of 1^{o}/minute, was run on each packed powder and clay slide. Each clay slide was then treated in glycol vapor overnight and rerun on the diffractometer. The slides were run a third time on the diffractometer after being heated at 550^{o}C for two hours.

Chlorite, muscovite, quartz, feldspars, biotite, and calcite were identified following the common schemes (Brown, 1961; Warshaw and Roy, 1961; Carroll, 1970). In those cases where septechlorite and kaolinite might be present and could not be convincingly differentiated, new slides were made from samples which had been treated in 6N HCl overnight on a water bath. This treatment preferentially dissolved chlorite.

Quantitative estimation of minerals. The quantitative determination of clay minerals by X-ray diffraction is known to be notoriously difficult because there are very many factors affecting the intensities of X-rays diffracted by a clay mineral assemblage. Van der Marel (1966) has reviewed the various factors which make the quantitative determination of clay minerals a complex problem; he included such factors as crystallinity, particle orientation, chemical composition, and grain size. Investigators have used various methods of determining the clay mineral contents of sediments, without mutually agreeing on the choice of the best method.

Johns et al. (1954), for example, quantitatively estimated the content of different clay minerals present in the Recent sediments of the

Reproduced with permission of the copyright owner. Further reproduction prohibited without permission.

Gulf Coast, U.S.A. They assigned a 1:4 ratio for the integrated (001) peak areas for equal amounts of oriented aggregates of illite and montmorillonite, both treated with glycol. Weaver (1958) assumed that the integrated (001) peak area of untreated montmorillonite is three times that of illite (001) for equal amounts of these two minerals. Others have used different measures to quantitatively determine the amount of clay minerals (Schultz, 1964; Biscaye, 1965; Bayliss and Levinson, 1970).

In this thesis, the peak heights of different minerals were used directly as measures of their relative proportions in the Tindelpina Shale for the minus 2 micron fraction. The respective peaks were $14\mathring{A}$ (chlorite), $10\mathring{A}$ (muscovite), $4.26\mathring{A}$ (quartz), $3.2\mathring{A}$ (feldspar), and $3.03\mathring{A}$ (calcite). The result is only a semiquantitative estimate of minerals.

Measurement of muscovite basal and $d_{(060)}$-spacing. The basal spacing of muscovite was determined by measuring its $d_{(004)}$-spacing, using quartz reflection at 2θ-angle of 20.85° ($CuK\alpha$) as a reference. Muscovite basal reflection on (004)-plane occurs at 2θ-angle of about 17.7°. Since all samples contained quartz, additional quartz was generally not needed. The measurement was done twice for the minus-2μ size of the oriented clay slides, on the diffraction trace run at a goniometer speed of $\frac{1}{4}^{\circ}$/minute and a chart speed of 1cm/minute. The center of the peak on the diffractogram was located on a horizontal line, about two thirds of the distance from the base line. The

Reproduced with permission of the copyright owner. Further reproduction prohibited without permission.

standard deviation of measurement was determined by scanning sample TH-1 ten times. The mean $d_{(004)}$ was 5.006Å, whereas the standard deviation was 0.001Å, which, for the purpose of this study, was sufficiently precise.

The $d_{(060)}$-spacing was measured on a powder photograph of a spindle made from the minus-2 μ size particles which had been treated overnight in 6N HCl warmed on a water bath. This acid treatment was meant to prevent chlorite from causing interference on muscovite (060) reflection. Quartz, which was already present in all samples, was used as an internal standard and showed a reflection at 2θ-angle of 60.03°.

Quantitative determination of quartz. Because of the fine-grained nature of the Tindelpina Shale, the quantitative determination of quartz using a petrographic microscope is not feasible. A chemical method such as of Trostel and Wyne (1940) by pyrosulphate fusion, dissolution of the fusion by alkalies, and gravimetric determination of silica, is somewhat time consuming; it may require a monopoly of laboratory space and equipment, particularly platinum crucibles, and great care must be exercised throughout the procedure. For this reason, an X-ray diffraction technique was adopted. Various investigators have used X-ray diffraction techniques to quantitatively determine quartz (Bristol, 1968; Till and Spears, 1969). In this thesis, the method as described by Norrish and Taylor (1962), in which no added internal standard is required, was followed.

Reproduced with permission of the copyright owner. Further reproduction prohibited without permission.

The intensity of a quartz line (4.26 Å) on the diffractogram of the sample run at $\frac{1}{2}^{o}$/minute was compared to the same quartz line of a known artificial standard. The strongest quartz line of 3.34 Å was not used due to a mica interference line. The standard was made by mixing a known amount of quartz powder and a pure chlorite (from Port Elliott, South Australia, University of Adelaide Geology Museum No. 3445). The intensity of the 4.26 Å line of both standard and sample was then corrected by their mass-absorption coefficient (μ) due to the CuKα radiation (see Appendix 3), as shown in the following equation:

$$\% \text{ quartz in sample} = \frac{\text{Intens. 4.26 Å sample}}{\text{Intens. 4.26 Å std.}} \times \frac{\mu_{\text{sample}}}{\mu_{\text{std.}}} \times \%\text{quartz}_{\text{std.}}$$

The intensity of the quartz line was determined by multiplying the height of the peak by the width of half-peak height on the diffractogram.

X-ray Fluorescence

The theory and practice of element analysis by means of X-ray fluorescence spectrometry have been well developed and described by various authors (Liebhafsky et al., 1960; Adler, 1966; Jenkins and De Vries, 1967; Norrish and Chappell, 1967). For a more complete description of the X-ray fluorescence methods the reader should refer to these authors.

Trace elements. The concentrations of As, Ba, Cu, Ga, Rb, Sr, Pb, Ni, Zn, and Zr in the Tindelpina Shale were determined using X-ray fluorescence spectrometry. The general principles and practice of this technique applied to trace elements have been described by,

Reproduced with permission of the copyright owner. Further reproduction prohibited without permission.

among others, Hower (1959), Norrish and Chappell (op. cit.), Fabbi and Espos, 1972), Parker (1969), and Banno and Chappell (1969).

Methods of sample preparation for analysis vary from author to author although in principle they are similar. The Tindelpina Shale samples were prepared by pressing of about 2 g undiluted rock powder backed with boric acid in a die-and-mould piston; this yielded pellets of 3 cm in diameter and 1 cm thick. Because of the argillaceous nature of the rock samples, no binding material (such as cellulose) was needed to facilitate pressing. Furthermore, undiluted rock powder gives high X-ray fluorescence intensity, and consequently the detection limits are generally low.

Artificial standards were made for each of the above-mentioned elements by mixing their pure oxides* with acid-washed quartz powder. The U.S. National Bureau of Standards NBS-70A feldspar was used as the Rb-Sr standard. Several U.S. Geological Survey reference rocks were also analyzed to check the accuracy of the method being used.

The concentration of a trace element in each sample was determined following this equation:

$$ppm_{sample} = \frac{I_{sample}}{I_{std.}} \times \frac{\mu_{sample}}{\mu_{std.}} \times ppm_{std.}$$

*"Spec pure" oxides, Johnson, Matthey & Co., Ltd., 73/83 Hatton Garden, London, E.C. 1.

Reproduced with permission of the copyright owner. Further reproduction prohibited without permission.

where (I) stands for the X-ray fluorescence intensity of the element sought, and (μ) is the mass-absorption coefficient. The above equation is only valid of the X-ray wave length of the element sought is shorter than the K-absorption edge wave length of the heaviest matrix element, namely iron (Hower, op. cit., Reynolds, 1963).

The intensities of the fluorescent X-rays of the sample and standard (I_{sample} and $I_{std.}$) could be directly read on the X-ray recording instrument and then corrected for background intensity. The concentration of the trace element in the standard material ($ppm_{std.}$) was known; the remaining unknown factors for determining (ppm_{sample}) were the mass-absorption coefficients of the sample and the standard (μ_{sample} and $\mu_{std.}$).

The operating conditions of this method are presented in Appendix 2, and the method of determining the mass-absorption coefficients is described in Appendix 3.

Major Elements. X-ray fluorescence techniques for silicate rock analysis have been described by several investigators (Kodama, et al., 1967; Norrish and Hutton, 1969; Gabis and Sichère, 1970; Stern, 1972). In the present study, the methods as described by Norrish and Hutton (op. cit.), including the preparation of the glass discs made from the samples, have been followed throughout.

The percentage of each major element present, with the exception of sodium, was determined from the following equation:

$$S_x = \frac{C_x}{C_s} \cdot S_s$$

Reproduced with permission of the copyright owner. Further reproduction prohibited without permission.

where C_x, C_s = counts in preset time for the sample and standard, corrected by dead time.

S_s = predetermined value of the standard, called FS_{11} factor (see Norrish and Hutton, 1969, p. 443, and CSIRO Division of Soils Technical Memorandum 13/67).

S_x = percentage of the oxide sought, called: nominal percentage.

A rock standard called "FS_{11}" obtained from Dr. K. Norrish* was used throughout the entire analyses. To check the accuracy of the technique, several U.S. Geological Survey rock standards were also analyzed. The nominal percentage obtained was then corrected by the matrix effects. This correction was applied by using a computer (CDC 6400) with a program called SILIAN also made available by Dr. Norrish. Operating conditions are shown in Appendix 4.

Flame Photometry

The concentration of sodium was determined by means of a flame photometer using about 20 to 40 mg of sample material in a 100 ml solution. The solution was obtained by dissolving the amount of rock sample in 5 ml concentrated reagent grade HF and 1 ml $HClO_4$ in a platinum crucible heated overnight on a sandbath. The following morning, 1 ml $HClO_4$ was added to the dried sample which was again heated to dryness and then diluted to 100 ml in a volumetric flask. This solution was then aspirated in a flame photometer (Evans Electroselenium Ltd.). The concentration of sodium was determined from a calibration curve made from a series of standard solutions.

---

*CSIRO Division of Soils, Glen Osmond, S. Australia.

Reproduced with permission of the copyright owner. Further reproduction prohibited without permission.

As a check, the potassium concentration was also determined on the flame photometer. The result was generally lower than that obtained from X-ray fluorescence analysis.

Loss on Ignition Determination

Loss on ignition was determined by heating the samples in silica crucibles; first in an oven (110° C) overnight, then in an electric furnace (1000° C) for four hours. Loss during ignition which may include water, carbonates, sulfides, and organic matter, was expressed in weight per cent of the oven-dried samples.

Atomic Absorption Spectrometry

Cr, Li, and V were analyzed by means of an atomic absorption spectrometer. The general procedures have been described by various authors, among which are Angino and Billings (1967), and Abbey (1967). The preparation of the samples prior to the actual analysis involved leaching a 0.5 g sample in 5 ml of a mixture composed of 85% concentrated perchloric acid ($HClO_4$) and 15% concentrated orthophosphoric acid (H_3PO_4) in test tubes which have been calibrated to 20 ml. The mixtures in the test tubes were heated on a sandbath at 280°C for about 72 hours. At the end of this period, X-ray diffraction run on the samples showed that all phyllosilicates, feldspars, and carbonaceous materials in the samples were destroyed. Quartz was not attacked by this dissolution. Each test tube was made up to volume (20 ml) then aspirated in the atomic absorption spectrometer (Table 1); the concentration of each element was determined from a calibration curve which was constructed from a series of standard solutions.

Reproduced with permission of the copyright owner. Further reproduction prohibited without permission.

Table 1. Operating Condition

	Line (Å)	Slit (μ)	Current (mA)	Gas
Cr	3579	50	20	Air/Acetylene
Li	6708	25	10	Air/Acetylene
V	3184	100	20	N_2O/Acetylene (rich)

Emission Optical Spectrography

Boron was analysed using a Hilger large-quartz emission spectrograph equipped with a stepped-sector, following a technique used at the C.S.I.R.O. (Oertel, 1961)*. The preparation involved handmixing of about 300 mg each of rock powder and graphite powder in an agate mortar. A small portion of this mixture was packed into the graphite anode (spectrographic-pure Ringsdorff "Spektralkohlen") in triplicate, and arced in a direct current at 200 V and 15 A to completion (approximately 40 seconds).

The spectral lines were recorded on a 10 inch x 4 inch Ilford N-50 half-tone photographic plate, developed in Ilford ID-13 (caustic hydroquinone) for 3 minutes at 20°C. The wave length range of the lines recorded on the plate was 2600 to 3600 Ångstroms.

The intensity of the boron line at 2497.73 Ångstroms was compared on a densitometer against the intensity of spiked standards. These standards were made out of one of the samples (Sample No. 1) spiked with boron of known concentration. The concentration of boron in each sample was calculated from a working calibration curve.

*Supervised by Mr. R.M. McKenzie, CSIRO, Division of Soils.

Reproduced with permission of the copyright owner. Further reproduction prohibited without permission.

VI. STATISTICS

In this thesis statistical techniques are used as a tool for data interpretation. Mathematical derivations of the techniques have been described by various authors; for this reason, only the basic principles are described.

VI.1. Trend Surface Analysis

General Principles

Trend surface analysis has been used by various investigators to show the regional variation of selected geologic parameters. The early literature on trend surface analysis includes the papers by Oldham and Sutherland (1955) and Grant (1957) on the use of trend surface in the interpretation of geophysical data. Papers by Krumbein (1956), Miller (1956), and Whitten (1959) discuss the application of trend surface analysis to geologic problems. The general method for constructing contour-type maps with irregular control-point spacing has been described by Krumbein (1959), and the reliability of trend surface contours compared to geologic contour maps has been discussed by Chayes and Susuki (1963). Krumbein (1963) described the method of calculating the confidence levels of the low-order polynominal trend surfaces, and the reliability and significance of the polynominal trend surfaces were discussed by Agterberg (1964), Howarth (1967), and Tinkler (1969).

Grant (op. cit.) defined trend as a function of two independent variables establishing the sample locations (x-y coordinates) which describes

Reproduced with permission of the copyright owner. Further reproduction prohibited without permission.

the behavior of a dependent variable, namely the geologic data. He described the least-squares method whereby the function z(x,y) is estimated from observations Z_i. The difference in the values of function (z) from the observed values Z at each data point is called the residual which has an expected value over all observations of zero. Miller (1956) and Harbaugh and Merriam (1968) have also discussed clearly the principles involved in the calculation and construction of trend surface by means of the least-squares method.

Physically, trend surfaces are planes or gently curving surfaces which are commonly represented by power-series polynomials fitted by the least-squares method (Figs. 9a and 9b). Coefficients of terms in the equation of trend surface depend on the actual data values. The locations of the geologic parameters (x-y coordinates) are expressed with reference to orthogonal x-y axes on a regular grid system. This regular grid generally produces a better goodness-of-fit of a known surface by a polynomial than that produced by an irregular grid of uneven density (Miller and Kahn, 1962). However, in many cases, geologic sampling on the regular grid may not be possible, as in this study.

Trend surface analysis is not an "objective" contouring method and tends to subdue the local variability in the raw data, and reveal the regional trend which might be hidden by local variation or "noise". Local effects, if above the noise level, can be emphasized by removing the regional trends and may be more readily seen by giving the contours of the residuals (Whitten, 1959; Read and Merriam, 1966).

Reproduced with permission of the copyright owner. Further reproduction prohibited without permission.

Figure 9. Trend Surface Analysis

a. Trend surfaces for first, second, and third degree.

b. Polynomials for first, second, and third degree surfaces.

Harbaugh and Merriam (1968).

Reproduced with permission of the copyright owner. Further reproduction prohibited without permission.

Reproduced with permission of the copyright owner. Further reproduction prohibited without permission.

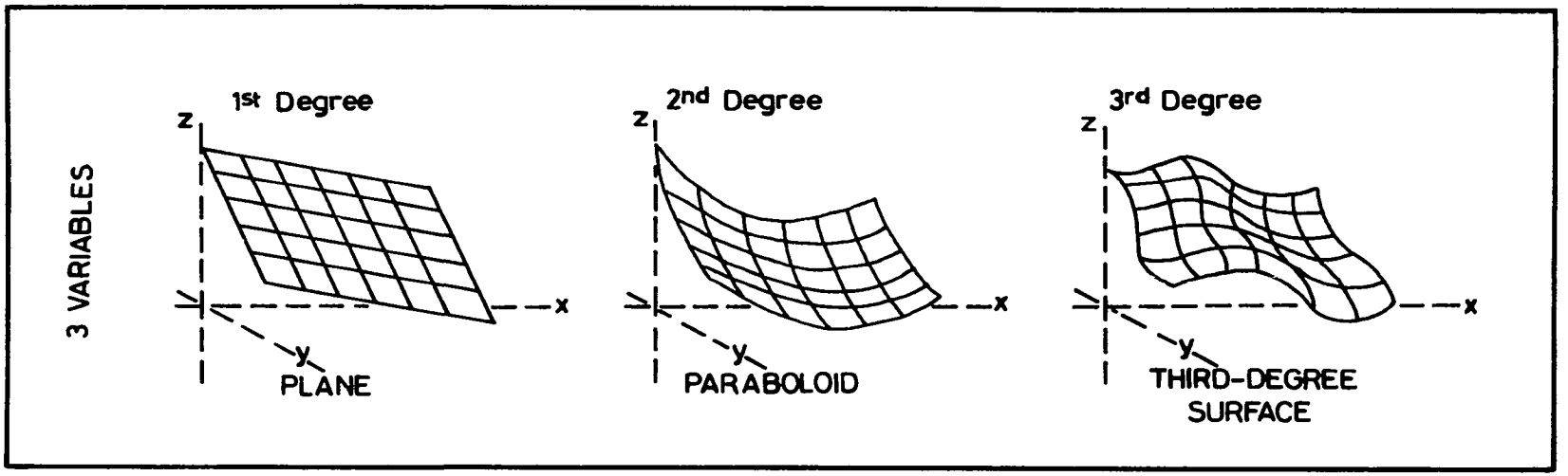

a

Trend-Surface Classification	Dependent Variable	Linear Component	Quadratic Component	Cubic Component
PLANE	$z =$	$A + Bx + Cy$		
PARABOLOID	$z =$	$A + Bx + Cy +$	$Dx^2 + Exy + Fy^2$	
3rd DEGREE SURFACE	$z =$	$A + Bx + Cy +$	$Dx^2 + Exy + Fy^2 +$	$Gx^3 + Hx^2y + Ixy^2 + Jy^3$

b

With the increasing popularity of high-speed computer uses in geology, many investigators have, in recent years, applied the trend surface methods to solve their geologic problems. The more recent literature on this type of analysis was listed by Krumbein and Graybill (1965), Koch and Link (1970) and Whitten (1973). In the study of sediments the trend surface technique has been used to show areal trend of sedimentary parameters (Krumbein, 1959; Read and Merriam, op. cit.; Doveton, 1970). Although the technique has been used extensively in geochemical exploration work (Connor and Miesch, 1964; Nackowski et al., 1967; Armour-Brown and Nichol, 1970), only recently has it been used to show the geochemical variation of detrital sediments (Ondrick and Griffiths, 1969).

Computer programs for trend surface analysis have been written by Harbaugh (1963), Good (1964), O'Leary et al. (1966), and Cole(1969).

Procedure

The purpose of using trend surface analysis in this thesis is to show only the regional trend of certain chemical variables. Surfaces up to third degree were constructed. No residual map was constructed although the residuals were computed. A computer program by Cole (1969) which is adapted to the CDC 6400 computer was made available to the author by John Barry of the Economic Geology Department at the University of Adelaide. The analysis of variance subprogram was written by Phil Leppard of the Statistics Department.

All values of (z) were logarithmically transformed to approach the normal distribution (Garrett, 1968). The coordinate of each sample point was determined in reference to x-y axes on the geological maps of

Reproduced with permission of the copyright owner. Further reproduction prohibited without permission.

the scale 1:250,000. The y-axis is parallel to the western edge of the Orroroo sheet, 11 inches to the west of this edge. The x-axis is perpendicular to y and 12 inches to the south of the southern edge of the Adelaide sheet.

VI.2. Factor Analysis

General Principles

The application of factor analysis was introduced by Spearman (1904) who made a study of a theory of human intelligence. Subsequently, factor analysis has been used exclusively by psychologists, to the point that it is commonly considered to be a theory in psychology rather than a statistical methodology. The fallacy of this point of view can be seen in the fact that this technique has been used in many other fields. Rummel (1970) has comprehensively and elegantly explained the application of factor analysis in political science and allied fields.

The factor analysis technique has been described by many other authors, mostly psychologists, in their books and papers (Cattell, 1965; Harman, 1967; Cooley and Lohnes, 1971). Child (1970), a psychologist, concisely and clearly explained the essentials of factor analysis, while Imbrie and van Andel (1964) and Harbaugh and Merriam (1968) described the principles of factor analysis application in geology. This technique of analysis has been applied by numerous authors to interpret the geologic data obtained from studies of modern as well as ancient sediments (Miller and Weller, 1952; Spencer, 1966b; Cronan, 1969; Hirst and Kaye, 1971; Summerhayes, 1972; Cosgrove, 1973).

Reproduced with permission of the copyright owner. Further reproduction prohibited without permission.

The initial assumption of factor analysis is that the samples have been randomly collected from a homogeneous population in which several variables can be measured. Furthermore, it is assumed that these variables can be transformed and reduced into a smaller number of meaningful factors. It is the interest of the particular user of factor analysis which determines what the various factors represent. That is, the interpretation is not implicit in the factor model, but it is imposed on it by the investigator.

The factors are most commonly thought to represent the underlying causative variates which produce the observed variables (Cattell, 1965). Those who use factor analysis for the first time are, therefore, led to believe that here at last is a method of obtaining cause and effect relationships among, for example, geologic variates (Matalas and Reiher, 1967). Wallis (1968) pointed out that:

> ". . . in view of the fervor shown by its advocates, as well as by its detractors, it is suggested that factor analysis might be better classified as a religion."

The author, being a newcomer, takes an agnostic view.

Mathematically factor analysis attempts to fit the model:

$$z_{ij} = a_{i1}F_{1j} + a_{i2}F_{2j} + a_{i3}F_{3j} + \ldots + a_{im}F_{mj} + a_{i}U_{ij}$$

in which:

z_{ij} = the value of the i^{th} variable in the j^{th} sample

F's = a series of $\underline{m}$ common factors (factors which are common to two or more of the variables under study)

U = a specific factor for a particular variable

Reproduced with permission of the copyright owner. Further reproduction prohibited without permission.

a's = factor weights (called loadings) which are necessary to express the original data in terms of the new factors.

A matrix of a's for all variables and all factors is called a factor pattern, and a matrix of F's, the new factors, is called a matrix of factor scores.

There are essentially three steps involved in factor analysis:

1. The calculation of a matrix of correlation coefficients among the variables.
2. The extraction of the eigen values and eigen vectors of the correlation matrix giving a principal factor solution.
3. The rotation of the principal factors to obtain "simple structure".

Figure 10a shows the plot of six variables, A, B, C, D, E, and F as vectors within a two-sample space. The values of the variables have been standardized so that OA=OB, OC, OD etc. The cosine of the angle between any two variables represent their correlation coefficient. A, B, and C form a cluster of highly correlated variables showing low correlation with the second cluster of D, E, and F.

The principal component solution involves the repositioning of the reference axes, so that the first axis or factor explains most of the variance in the data. Such an axis is shown by PF_1; PF_2, the second factor, would be positioned so that it explains the greatest possible proportion of the remaining variance. The proportion of the

Reproduced with permission of the copyright owner. Further reproduction prohibited without permission.

Figure 10. Factor Analysis

a. Principal factor solution for six variables in a two-sample space.

b. Oblique factors, after rotation.

Reproduced with permission of the copyright owner. Further reproduction prohibited without permission.

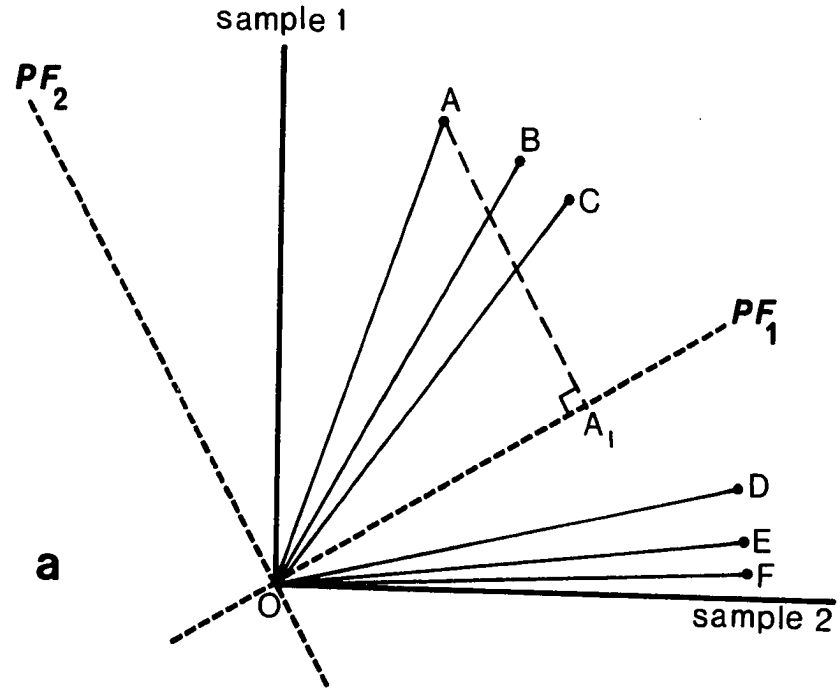

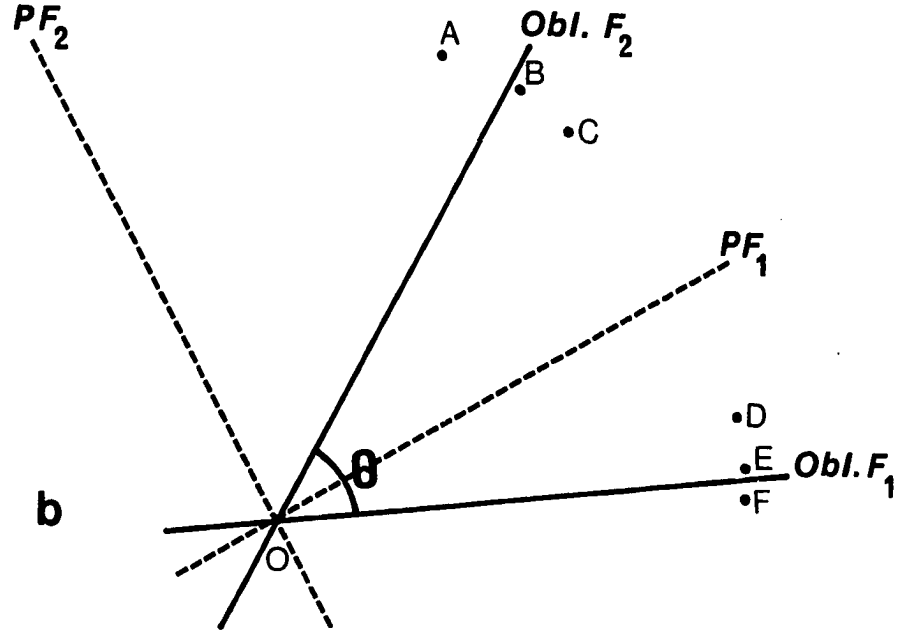

Reproduced with permission of the copyright owner. Further reproduction prohibited without permission.

variance of variable A, which is explained by factor 1, is represented by OA_1. If all samples have been considered (so that the variables would be plotted in 3, 4, 5, . . ., n sample space) and the six variables still remain essentially in the same plane, then it means that only two principal factors are required to account for the total variance of the data. These two factors are the new variables that are simply the linear combinations of the six old variables.

In geology, this (orthogonal) principal solution implies that the factors are independent of each other; this, however, is a most unlikely situation. For this reason, further rotation of the principal factors and altering the orthogonal axes into oblique axes may be carried out to simplify and amplify the factor relationships (Fig. 10b). At this point, the degree of obliqueness depends on how much personal preference the user wishes to impose on the factors. Some workers, such as Spencer (1966a), Hirst and Kaye (1971), and Mather (1972), have a definite basis controlling the choice of the obliqueness of the rotation. However, no mutual agreement has been achieved on the merit of obliquely rotating the factors (Harbaugh and Merriam, 1968, p. 191).

The two most common methods of factor analysis used in geology are the R and the Q-modes. The R-mode is based on the measurement of two variables from a single individual and requires a large number of individuals (such as rock samples). The second method (Q-mode), involves correlation of two individuals based on the variables, thus requiring a large number of variables.

Reproduced with permission of the copyright owner. Further reproduction prohibited without permission.

In general terms, the present application of the R-mode analysis groups together the related variables or geochemically coherent constituents into a smaller number of factors. These factors may be related in terms of the various processes which affect the final mineralogical and geochemical compositions of the rocks under study; in this case, the Tindelpina Shale.

The distribution of elements in sedimentary rocks is largely determined by the following factors:

1. The composition of parent rocks.
2. The environmental conditions at the site of weathering and at the depositional site, such as Eh, pH, and diagenetic processes.
3. Rate of deposition and sorting during transport.
4. Tectonic and volcanic events during the weathering-transport-deposition cycle.
5. The biogenic activities at the depositional site.

These above factors are obvious and all have been discussed and used by various authors to explain the distribution of elements. It seems that the only independent factors are the nature of the parent rocks and the climate. However, these two factors are interrelated with the rest, thus justifying the use of the oblique rotation.

Procedure

Computer programs for R-mode factor analysis used in geology have been written by various authors such as Cameron (1967), Sampson

Reproduced with permission of the copyright owner. Further reproduction prohibited without permission.

(1968), Ondrick and Srivasta (1970), whereas for general usage, programs such as BMDX 72 (Dixon, 1970) and the SPSS (Statistical Package for the Social Sciences) by Nie, et al. (1970) are generally available in university computing centers.

In this thesis, the SPSS program, which is very versatile, adapted for the CDC Computer Series 6000 by the Vogelback Computing Center of the Northwestern University, Evanston, Illinois, was used to process the geochemical and mineralogical data. This program (SPSS 100, Version 5.0) adapted for the CDC 6400 computer at the University of Adelaide, was made available to the author by Mr. W.D. Gould of the Psychology Department of the same university.

The write up for the computer program is presented in detail by Nie et al. (op. cit.). The input for the present study was in the form of raw data representing 31 variables grouped into five classes and processed simultaneously:

1. X and Y coordinates relative to an arbitrarily positioned orthogonal axes.
2. Concentrations of major oxides, converted into concentrations of their respective elements, in per cent.
3. Concentrations of trace elements, in parts per million.
4. Concentration of quartz and estimated proportions of chlorite and muscovite, in per cent.
5. A measure of muscovite crystallinity, expressed in terms of the Kubler index in millimeters and the Weaver sharpness-ratio.

Reproduced with permission of the copyright owner. Further reproduction prohibited without permission.

The first run consisted of items 2, 3, and 4; the second run consisted of all the five items with a different number of samples.

Reproduced with permission of the copyright owner. Further reproduction prohibited without permission.

VII. RESULTS AND DISCUSSION

VII.1. Mineralogy

Petrologic Description

Sturt Tillite. Under the petrographic microscope, typical samples of fine-grained matrix material are argillites composed mainly of quartz and phyllosilicates (muscovite and chlorite). Preferred orientation by phyllosilicates due to metamorphis cleavage development is common (Fig. 11d). The coarser matrix material shows a "micro-diamictite" texture with a phyllosilicate groundmass and coarser fragments of quartz, quartzite, argillite, carbonate, and igneous rock (Fig. 11e). Development of metamorphic phyllosilicates is indicated by their preferred orientation around coarser grains of, for instance, quartz and feldspar (Fig. 11f).

Tindelpina Shale. Hand specimens of the Tindelpina Shale show a typical varve-like appearance of black, finely laminated silty shale. Veinlets of calcite occasionally occur cutting across these laminations. When weathered, these laminations show the colorful alternation of reddish and greenish bands of less than one millimeter to three millimeters.

Under low magnification, the thin sections show dark and light bands composed of quartz, phyllosilicates (muscovite and chlorite), and organic matter in varying proportions. The darker laminae have more organic matter and phyllosilicates than the lighter ones. Detrital quartz and calcite grains are evenly distributed throughout most thin

Reproduced with permission of the copyright owner. Further reproduction prohibited without permission.

Figure 11. Microphotographs of thin sections of the Tapley Hill Formation, Tindelpina Shale, and Sturt Tillite matrix material.

a. Tapley Hill Formation, showing the varve-like texture with fine laminations of carbonaceous material. Light mineral on right hand corner is calcite veinlet. Plane polarized. Sample collected at type locality, near Darlington, 6 miles south of Adelaide.

b. Tindelpina Shale. No distinctive difference in appearance from the Tapley Hill Formation. Note the opaque grains of iron oxides, derived from oxidized pyrite. Sample No. 89 from drill core.

c. Tindelpina Shale sample. Typical layering and well developed cleavage in Sample No. 38. Plane polarized.

d. Tillite matrix material. Detrital quartz and phyllosilicate groundmass in Sample No. 75T. Plane polarized.

e. Microdiamictite: tillite matrix material with fragments of quartz and carbonate. Note quartz overgrowth. Sample No. 57T. Plane polarized.

f. Tillite matrix of coarser grains. Well developed cleavage shown by the preferred orientation of micaceous minerals around fragments of quartz and feldspar. Sample No. 1T. Crossed polars.

Reproduced with permission of the copyright owner. Further reproduction prohibited without permission.

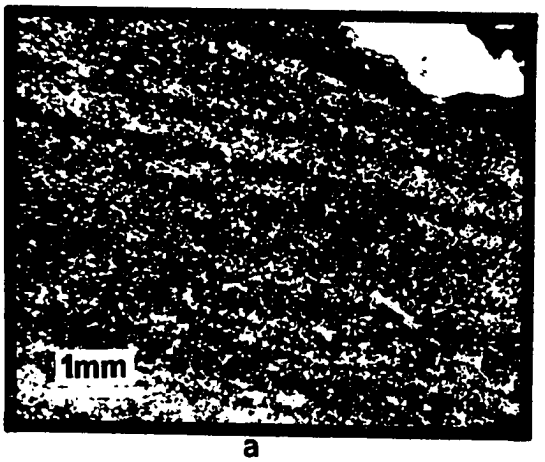

a

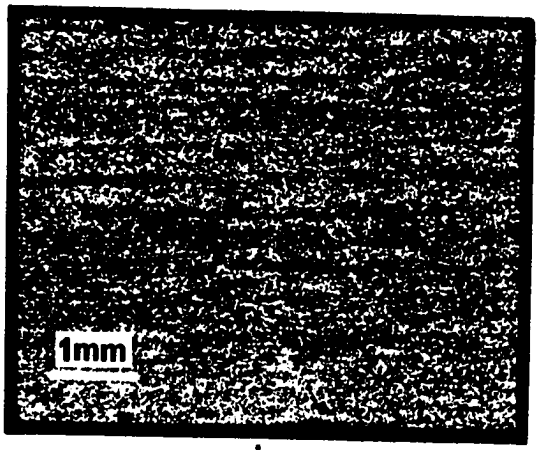

b

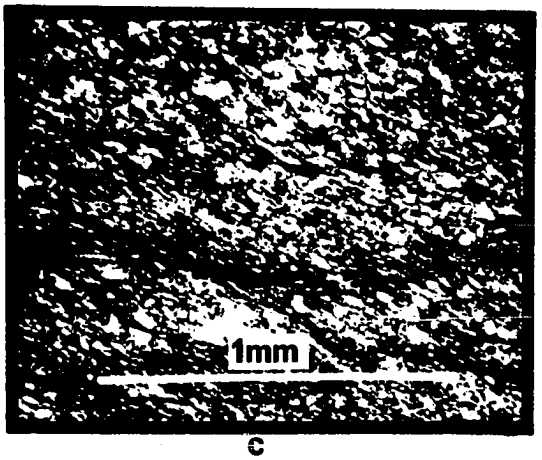

c

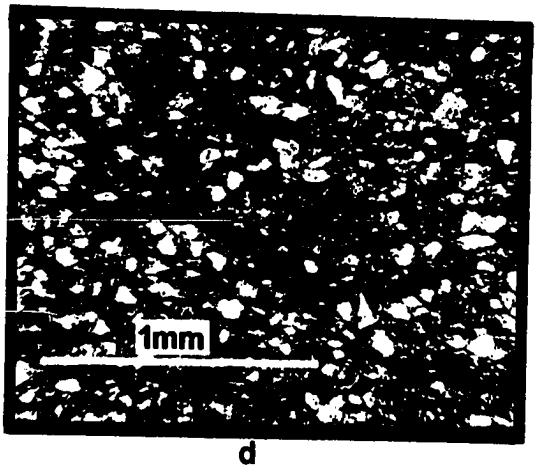

d

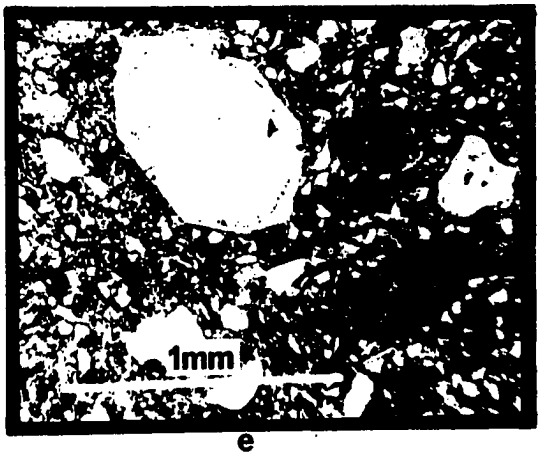

e

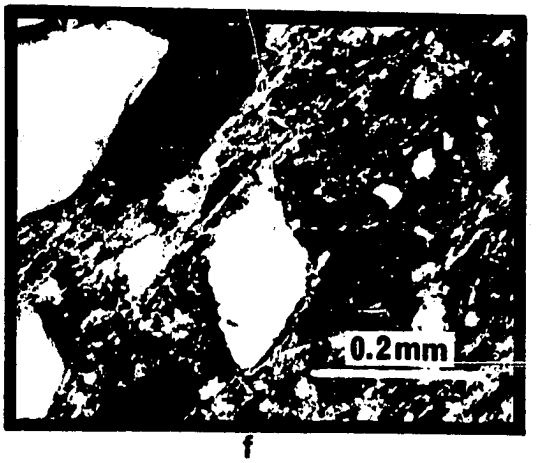

f

Reproduced with permission of the copyright owner. Further reproduction prohibited without permission.

sections. In some specimens, detrital tourmaline, zircon, and rutile have been identified. Pyrite occurs in some samples along the darker laminae; in many cases, this sulfide has altered into iron oxides (Figs. 11a and 11b). Rare detrital muscovite is identified by its unoriented occurrence in the thin sections. Cleavage development is indicated by the orientation of the phyllosilicates at an angle to the sedimentary laminations (Fig. 11c).

Mineralogical Composition

On X-ray diffractograms, there is no significant difference between the mineralogy of the Sturt Tillite material and the mineralogy of the Tindelpina Shale. The mineralogy of these rock units is relatively simple and uniform throughout the area under study. X-ray diffractograms of bulk samples and the minus 2 micron fraction of both units show the presence of chlorite, illite (which is actually muscovite), and quartz; in lesser amounts, feldspars and calcite are also present (Fig. 12). Other constituents recognized under the microscope do not appear on the diffractograms due to their minor amounts.

Estimations of the relative proportions of the principal minerals based on X-ray diffraction of the minus 2 micron fraction of the Tindelpina Shale is shown in figure 13 and Appendix 5. The diagram in figure 13 shows the preponderance of muscovite over chlorite. This quartz-muscovite-chlorite association is the common mineral assemblage for pelitic rocks of extensive areas of low-grade metamorphism (Pitcher and Flinn, 1965; Linke, 1970). Only in two samples was biotite detected

Reproduced with permission of the copyright owner. Further reproduction prohibited without permission.

Figure 12

Typical X-ray diffractograms of bulk samples of the Tapley Hill Formation (TH), Tindelpina Shale, and Sturt Tillite (T).

Reproduced with permission of the copyright owner. Further reproduction prohibited without permission.

Reproduced with permission of the copyright owner. Further reproduction prohibited without permission.

Figure 13

Relative proportions of quartz, chlorite, and muscovite in the Tindelpina Shale, based on X-ray diffraction of the minus 2 micron fraction.

Reproduced with permission of the copyright owner. Further reproduction prohibited without permission.

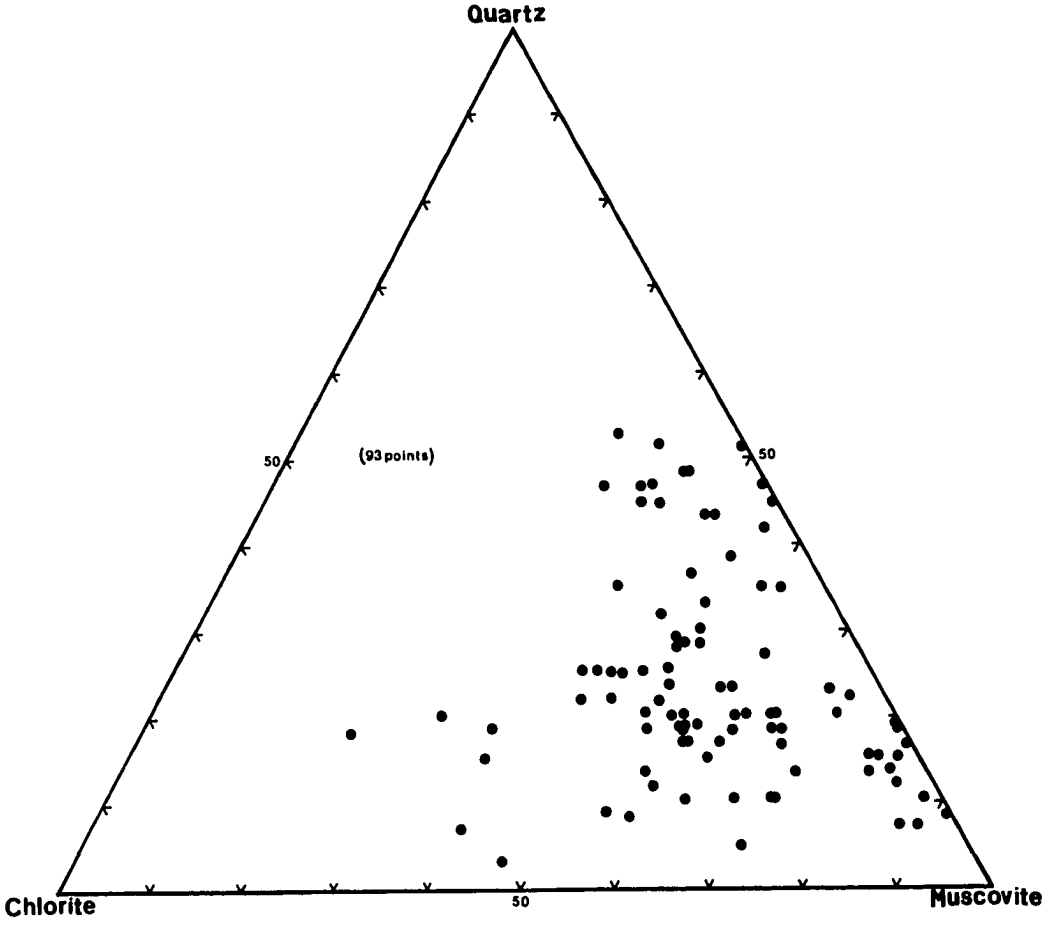

Reproduced with permission of the copyright owner. Further reproduction prohibited without permission.

and these samples are located in the biotite isograd zone of Offler and Fleming (1968).

The absence or presence of chlorite in the samples indicates the different types of clay minerals present and the availability of magnesium before the Tindelpina Shale was metamorphosed into its present state. This metamorphism has simplified the clay mineral assemblage into chlorite and muscovite associations. The uniformity of the mineral assemblage undoubtedly shows the metamorphic character of the Tindelpina Shale.

Basal Spacing of Muscovite

Fifty-three measurements of basal spacings (Appendix 6) give an average value of 9.996 $\mathring{A}$ngstroms with a standard deviation of 0.010 which is about 0.10 per cent. This very low standard deviation indicates the uniformity of the metamorphic muscovite occurring in the Tindelpina Shale.

In his study of the pelitic schists of northwestern Maine, U.S.A., Guidotti (1966) concluded that the basal spacing of the muscovite is sensitive to changes in metamorphic conditions. Yoder and Eugster (1955) reported that muscovite basal spacings vary with the potassium/sodium ratio in the muscovite. In their study of the sillimanite-potash feldspar bearing metamorphic rocks, Evans and Guidotti (1966) found a linear relationship between basal spacing and the paragonite content of muscovite, shown by the following equation:

$$d_{(002)} = 10.006 - 0.27 \text{ Paragonite mole.}$$

Reproduced with permission of the copyright owner. Further reproduction prohibited without permission.

According to this equation, the basal spacing for paragonite-free natural muscovite would be 10.006 Angstroms. Zen and Albee's (1964) value is 10.034 Angstroms, whereas the synthetic muscovite of Yoder and Eugster (1955) is 10.014 Angstroms. The relationship found by Evans and Guidotti (op. cit.) was later modified by Guidotti and Crawford (1968) into a quadratic equation:

$$Y = 28.925 - 1.4728\ X - 0.22855\ X^2$$

where Y = paragonite content of muscovite

X = (Basal spacing -9.920) x 100

Using this equation as an approximation to estimate the paragonite content of the Tindelpina Shale muscovite, it is found that the muscovite has an average paragonite content of 4.5 per cent. It was pointed out by Guidotti (op. cit) that the paragonite content in muscovite depends on various factors, such as temperature, total pressure, water pressure, and in rocks without potash-feldspar, the anorthite content of the coexisting plagioclase.

If the value of 4.5 per cent is accepted as the average paragonite content for the Tindelpina muscovite, then by using the curves constructed by Eugster and Yoder (1955) and their modified version by Evans and Guidotti (1966) for the muscovite-paragonite solvus at 2 kilobar water pressure, the muscovite in the Tindelpina Shale would have been formed at about 300°C. This temperature is indeed the temperature for the greenschist metamorphism (Fyfe, Turner, and Verhoogen, 1958; Velde, 1964).

Reproduced with permission of the copyright owner. Further reproduction prohibited without permission.

$d_{(060)}$-spacing and b_0 parameter of muscovite

Seventy-three measurements of $d_{(060)}$ spacings of muscovite in the Tindelpina Shale give results ranging from 1.500 to 1.509 Angstroms with most being 1.504 Angstroms or over (Appendix 7). This result is similar to that obtained by Maxwell and Hower (1967) in their study in the Belt Series of western Montana and northern Idaho of illite which has undergone high-grade diagenesis or low-grade metamorphism through deep burial. Their illite has $d_{(060)}$ spacings ranging from 1.501 to 1.509 Angstroms with most having values of 1.503 Angstroms or over. Using their curve (Fig. 14a) which was constructed from an earlier work by Hower and Mowatt (1966) it is found that the Tindelpina Shale muscovite has a quarter to a third of its octahedral positions occupied by magnesium and iron.

Yoder and Eugster (1955) also reported that the lower limit of (060) spacing in potassium dioctahedral micas is 1.499 Angstroms for both the 1M and 2M synthetic muscovite. This spacing increases with the introduction of larger cations such as Fe^{2+}, Fe^{3+}, and Mg^{2+} into the octahedral positions replacing Al^{3+}. However, this relationship is not clearly understood (Ernst, 1963).

If the formula of muscovite is $KAl_2Si_3AlO_{10}(OH)_2$, then the iron-magnesium bearing muscovite which is called phengite, has a formula of $K(Mg, Fe^{2+})_{0.5}Al_{1.5}Si_{3.5}Al_{0.5}O_{10}(OH)_2$ (Kanehira and Banno, 1960). It is obvious that the muscovite in the Tindelpina Shale is of phengitic nature.

Reproduced with permission of the copyright owner. Further reproduction prohibited without permission.

Figure 14

a. Magnesium plus iron in dioctahedral illites and montmorillonites as a function of d_{060} (Maxwell and Hower, 1967).

b. Frequency histogram of b_0 values of pre-Alpine (muscovites) and Alpine (phengites) potassic white micas (Sassi, 1972).

c. Frequency histogram of b_0-values ($6 \times d_{060}$) of the Tindelpina Shale muscovite.

Reproduced with permission of the copyright owner. Further reproduction prohibited without permission.

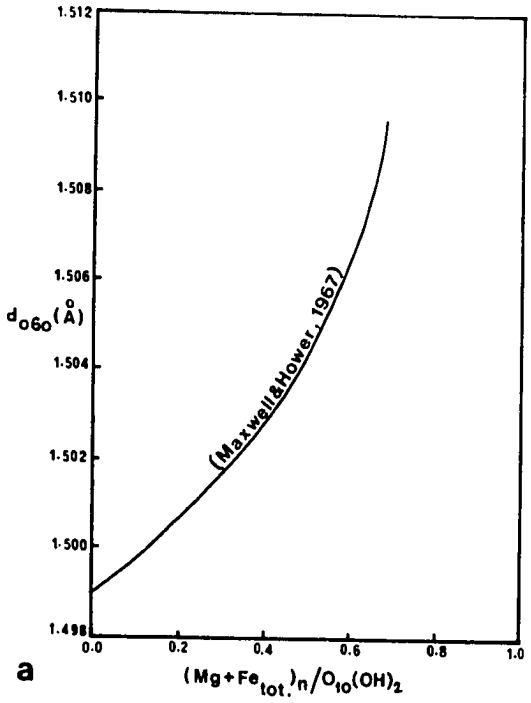

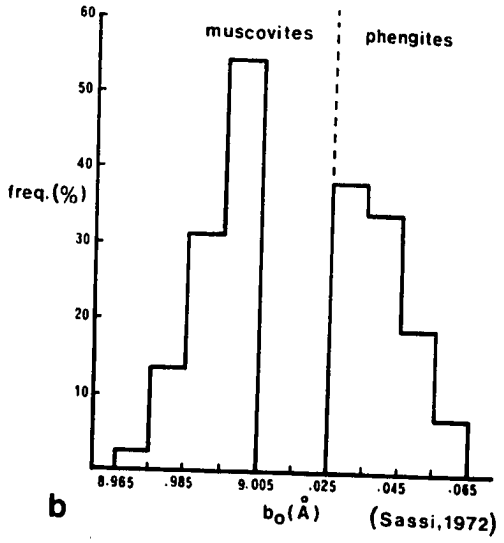

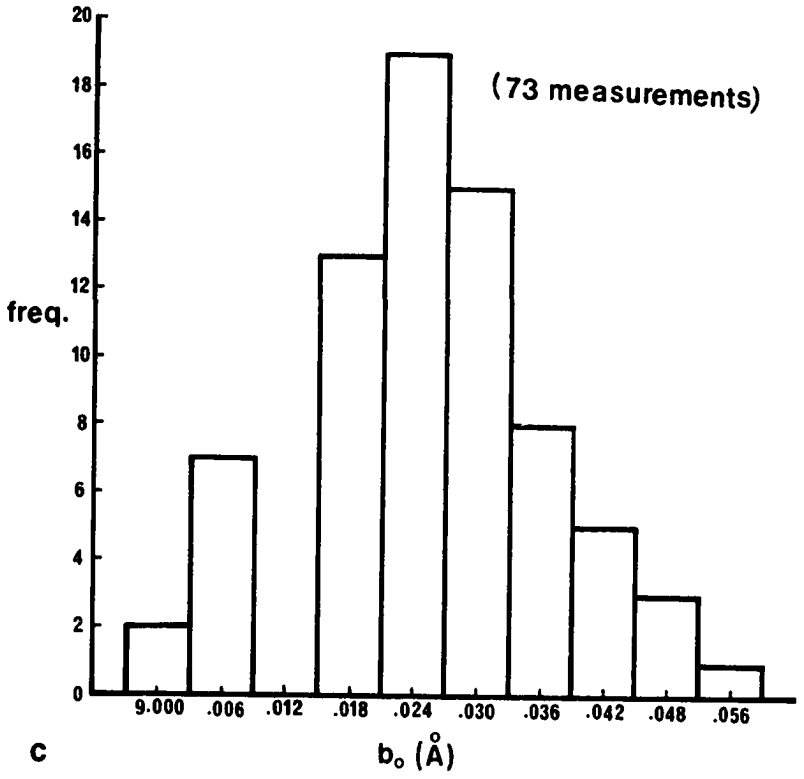

Reproduced with permission of the copyright owner. Further reproduction prohibited without permission.

Beran (1969) pointed out that the formation of phengite is favored by high water pressure and is dependent on the chemical composition of the host rock. He added that the absence of phengite would clearly draw the boundary between the quartz-albite-muscovite (phengite)-chlorite subfacies and the quartz-albite-muscovite-biotite subfacies of the greenschist facies. The occurrence of phengite in low-grade metamorphic rocks is reported to be widespread (Frey, 1969; Mather, 1970). However, petrographic identification of phengite in fine-grained peltic rocks is difficult due to its greenish and pleochroic nature, so that it sometimes resembles biotite.

The b_0-parameter of the muscovite in the Tindelpina Shale was calculated simply by multiplying the $d_{(060)}$-spacing by a factor of six. It has to be emphasized that this calculation is only valid if the muscovite in the samples is of the monoclinic (2M) type. X-ray diffractograms of the Tindelpina Shale and comparison to Yoder and Eugster's (1955) result indicate that the Tindelpina Shale muscovite is indeed of the 2M type.

Results of the seventy-three measurements of $d_{(060)}$ spacings can be converted into values of b_0. The histogram of b_0 parameter distribution (Fig. 14c) looks similar to the one produced by Sassi (1972) for his potassic white micas in the eastern Alps (Fig. 14b). There he distinguished the muscovites, which reflect the low-pressure pre-Permian (Hercynian) metamorphism from the phengites representing the higher pressure of Alpine metamorphism.

Reproduced with permission of the copyright owner. Further reproduction prohibited without permission.

The variability of b_0 for the muscovites and phengites on Sassi's histogram was explained by him to be ovbiously due to the variability of the rock bulk compositions, and the asymmetry of the histogram due to the choice of the class interval. However, he concluded that the absence of b_0 values between 9.005 and 9.025 Angstroms indicates a sharp pressure difference between the Alpine metamorphism and the Hercynian metamorphism. According to Sassi, it is not possible at this stage to construct a graphical representation showing the relationship between b_0 parameter and pressure during metamorphism.

As an approximate analogy to Sassi's results, the b_0 parameters of the Tindelpina Shale muscovite indicate that most of the muscovite is of phengitic nature. Whether this indicates any similarity between the Tindelpina Shale metamorphic condition and the Alpine metamorphism remains questionable.

Intensity ratio of 5 Angstrom-reflection/10 Angstrom-reflection

Sixty-five measurements of intensity ratios of the first two basal reflections of muscovite on the diffractograms are given in Appendix 8 and Table 2.

Table 2

Intensity ratio of 5Å/10Å reflection	
No. of samples:	65
Average:	0.316
Standard Deviation:	0.052
Range:	0.214 - 0.439

Reproduced with permission of the copyright owner. Further reproduction prohibited without permission.

The average intensity ratio falls in the range between 0.3 and 0.4, considered to belong to the phengites by Esquevin (1969). According to him this ratio varies with the types of mica minerals present in the rocks.

Crystallinity of Muscovite

Eighty-five measurements of the Kubler index and the Weaver sharpness ratio normalized to the Hart Ranges muscovite of the minus 2 micron fraction of the Tindelpina Shale give the results shown in Appendix 9 and Table 3.

Table 3

Crystallinity index of muscovite

	Tindelpina Shale (86 samples)		Hart Ranges	
	Kubler index	Weaver ratio	Kubler index	Weaver ratio
Mean	5.68 mm	6.41	5.32mm	5.63
Std. dev.	0.86	2.33	0.28	0.33
Range	4.21 - 7.65	2.89 - 15.37		

It must be pointed out that the muscovite crystallinity index depends to some extent on the chemical composition of the muscovite. In unmetamorphosed sediments the crystallinity of illite depends also on the chemical nature of the water in which this clay mineral occurs and the presence of organic matter (Kubler, 1968).

According to Kubler (1966, 1967) and Weber (1972b) in a common clayshale, the illite crystallinity depends mainly on the temperature during burial. Weber graphically showed the relationship between the

Reproduced with permission of the copyright owner. Further reproduction prohibited without permission.

illite crystallinity and the depth of burial. The effect of tectonic and other thermal events complicates the interpretation of crystallinity index. Factors such as the size of the crystal (not the size of the mineral particle) also affect the crystallinity index (Weber, 1972a). The factors which affect the Kubler index and Weaver sharpness ratio, which can be directly related to the so-called line broadening in X-ray diffraction, have been discussed at length by Henry et al. (1961, pp. 212-218).

Using the conversion graph (Fig. 15) presented by Kubler (1968), the Weaver sharpness ratios of the samples fall into the zone of anchimetamorphism (the beginning of metamorphism) to the beginning of epimetamorphism which is the actual metamorphism. The average Weaver sharpness-ratio of 6.41 falls on the anchimetamorphism zone. An estimate of where the Tindelpina Shale mica falls in the zone of metamorphism may also be indicated by the Kubler index of the muscovite standard which came from a pegmatite body. This muscovite should fall into the epimetamorphism zone. However, the Weaver sharpness ratio of the muscovite standard indicates its anchimetamorphic origin. This mismatch of the Weaver sharpness ratio and the Kubler index illustrates the arbitrarily chosen division of low-grade metamorphic zones, and the fact that comparison of Kubler index measurement from one laboratory to another is not possible without standardization. This conclusion was also made by Weber (1972a and b). Nevertheless, the crystallinity index of the Tindelpina Shale muscovite indicates its metamorphic origin.

Reproduced with permission of the copyright owner. Further reproduction prohibited without permission.

Figure 15

Conversion graph for the Weaver sharpness ratio and the Kubler index, constructed by Kubler (1968, p. 393), based on his 700 measurements of the Kubler indices. Philips diffractometer chart speed 1,600 mm/hour; goniometer 2^{o}/minute.

Reproduced with permission of the copyright owner. Further reproduction prohibited without permission.

Reproduced with permission of the copyright owner. Further reproduction prohibited without permission.

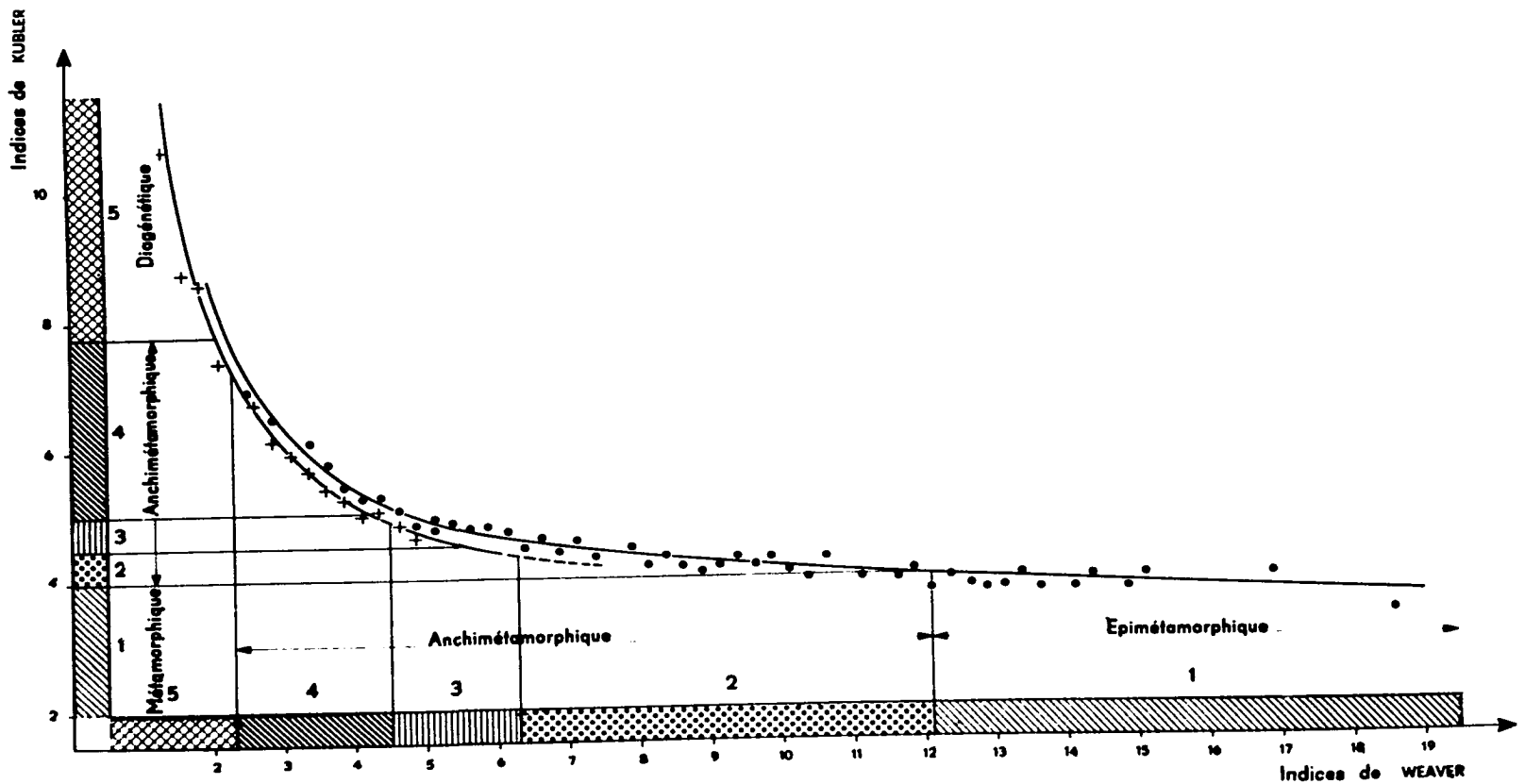

VII.2. Geochemistry

Trace Element Abundance

Table 4 and Appendix 10 shows the results of trace element analyses. The significance of the abundance of each element depends on the lower detection limit of the chosen analytical technique.

Controversy still exists regarding the distribution of trace elements in sediments. In particular, there is no mutual agreement on the statistical distribution of elements whether they are normally or lognormally distributed (Ahrens, 1954a, 1954b, 1963; Chayes, 1954; Shaw, 1961). In the statistical treatment of the trace elements normal distribution statistics were used because some of the trace elements analyzed are normally distributed, and the computer application used in this study requires an assumed normality of the data. A test of normality was done by noting the skewness of each of the element distributions following the method of Preston (1970). The average concentration of each element is its arithmetic mean. The standard deviation of each element should give some indication of the skewness of the distribution of the element.

A selected bibliography of articles published between 1930 and 1965, with annotations, on the minor element contents of marine black shales and related sedimentary rocks has been compiled by Tourtelot (1970). The geochemistry and abundance of elements in rocks have been reviewed in a series of books under the title Handbook of Geochemistry edited by Wedepohl (1969, 1970, 1972). For these reasons, only a very

Reproduced with permission of the copyright owner. Further reproduction prohibited without permission.

TABLE 4

Trace Element Abundances in the Tindelpina Shale in Parts Per Million.

	Sample size	Av.	Std. Dev.	Range	Distribu-tion*	Lower Detection Limit**	Crustal Abundance ***
Ga	152	18.51	4.42	5-33	sk	2	15
Rb	152	146.14	39.41	29-243	n	2	90
Sr	130	160.06	177.84	15-840	sk	2	375
As	126	14.01	10.26	1-76	sk	5	1.8
Ba	135	858.56	191.60	329-1279	n	30	425
B	128	184.47	70.50	36-435	n	10	10
Cr	131	83.18	36.85	26-240	sk	1/30%	100
Cu	129	29.93	18.34	3-139	sk	3	55
Li	132	22.45	8.59	3-54	n	0.5/15%	20
Ni	129	39.91	16.54	2-96	n	3	75
Pb	129	20.68	12.26	.5-59	sk	6	12.5
V	121	191.05	55.27	73-303	n	10/5%	135
Zn	131	62.45	28.17	3-189	n	3	70
Zr	134	224.80	33.29	99-306	n	4	165

*n = normal; sk = skewed

**For Cr, Li, and V, the lower detection limits are in parts per million per absorbance percentage for solutions with dilution factor of 40. For all other trace elements, determined by X-ray fluorescence, the lower detection limits were calculated according to Norrish and Chappell's method (1967, p. 204).

*** (Ahrens, 1965).

Reproduced with permission of the copyright owner. Further reproduction prohibited without permission.

brief discussion on the geochemistry of each element analyzed in this thesis is included.

Gallium. The average gallium concentration of 19 ppm in the 152 samples falls in the typical range of gallium abundance in sediments, particularly in the argillaceous sediments (Table 5).

TABLE 5

Gallium Abundance in Sediments (in ppm)

Concentration	Rock Types	Author
20	Modern marine argillaceous sediments	Potter et al. (1963)
14	Modern fresh-water argillaceous sediments	
20 - 28	Eastern Pacific pelagic sediments	Goldberg and Arrhenius (1958)
4 - 22	Red clays	Burton et al. (1959)
19	Tindelpina Shale	This work

Gallium is a common trace element occurring in argillaceous sediments. Because of the similarity of its crystallochemical properites to aluminum and iron (Ga^{3+} = 0.62Å; Al^{3+} = 0.51Å; Fe^{3+} = 0.64Å), gallium forms an extensive isomorphism with these two elements. The migration of gallium in the sedimentary environment is not clearly understood, however its association with aluminum and iron in sediments is commonly known (Vlasov, 1964; Ataman, 1967). Because of its relatively high ionic polarization, gallium may be adsorbed by clay minerals or hydrous oxides; Vlasov (op. cit.) reported the high concentration of gallium (20 to 100 ppm) in the bauxite deposits.

Reproduced with permission of the copyright owner. Further reproduction prohibited without permission.

Rubidium. The average content of rubidium in the Tindelpina Shale is 146 ppm. Compared to the average values found in other shales, this concentration is close to the rubidium contents of common shales (Table 6).

TABLE 6

Rubidium Concentrations in Argillaceous Sediments (in ppm)

Concentration	Rock Types	Author
281	Marine shales	Degens et al. (1957)
139	Fresh water shales	
160	Pelagic clays	Horstman (1957)
143	Carboniferous shales (Great Britain)	Nicholls and Loring (1962)
120	Atlantic Ocean pelagic clays	Wedepohl (1959)
146	Tindelpina Shale	This work

Heier and Billings (1970) averaged the rubidium content of Recent argillaceous sediments to be 128 ppm.

In the sedimentary environment, rubidium follows potassium closely (Rb^+ = 1.48Å; K^+ = 1.33Å). During the later stages of weathering the potassium/rubidium ratio shows a continuous decrease due to the preferential removal of potassium, while rubidium is more firmly held (Goldschmidt, 1954). Degens et al. (1957) reported that modern argillaceous marine sediments tend to contain more rubidium than their fresh water equivalents. On the basis of Canadian Cretaceous sediments, Campbell and Williams (1965) suggested that the potassium/rubdium ratio in shales may be used as an indicator for their depositional environment. Ratios

Reproduced with permission of the copyright owner. Further reproduction prohibited without permission.

of 250-300 indicate nonmarine to brackish water shales, whereas ratios of 150 to 200 represent marine shales. Out of 117 samples of Tindelpina Shales, 101 samples have potassium/rubidium ratios between 160 to 200; the overall average is 187.

Strontium. One hundred and thirty samples of the Tindelpina Shale give an average strontium concentration of 160 ppm. This figure is much higher than the average strontium content of Precambrian shales (67 ppm) calculated by Reimer (1972). The high concentration of strontium in the Tindelpina Shale is due to the strontium and calcium carbonate association in this sedimentary unit. The content of strontium in shales varies considerably and shows a dependency on calcium (Table 7).

TABLE 7

Concentration of Strontium in Argillaceous Sediments (in ppm)

Concentration	Rock Types	Author
300 (5% Ca)	Shales	Turekian and Kulp (1956)
2075 (35% Ca)	Calcareous deep-sea sediments	
162	Shales	Hirst and Kaye (1971)
86	Clay shales	Schroll (1971)
160	Tindelpina Shale	This work

The dependence of strontium on calcium in shales (Ca^{2+} = 1.06Å; Sr^{2+} = 1.27Å) is complicated by the fact that most shales contain a certain amount of calcium carbonate, and the behavior of strontium in carbonate deposition is not clearly understood. Goldschmidt (1954) stated that in the sedimentary environment, aragonite and anhydrite are the main strontium

Reproduced with permission of the copyright owner. Further reproduction prohibited without permission.

carriers. When aragonite converts into calcite, strontium is set free and may be adsorbed by clay minerals. The dependence of strontium on calcium in shales is also affected by the clay minerals which may bind some of the strontium.

Arsenic. The average arsenic concentration of 14 ppm in the Tindelpina Shale is slightly above the average for shales of 13 ppm quoted by Onishi (1969). He stated that because of the wide variation of arsenic content in shales, it is not easy to obtain a precise average value (Table 8). The geochemical behavior of arsenic in the sedimentary environment is not much known. Onishi (op. cit.) mentioned that the concentration of arsenic in soils tend to be higher than that in igneous rocks.

TABLE 8

Concentration of Arsenic in Argillaceous Sediments (in ppm)

Concentration	Rock Types	Author
4 - 25	Near shore marine shales	Tourtelot (1964)
3 - 53	Offshore marine shales	
100 - 900	Kupferschiefer	Wedepohl (1964)
0.9 - 11.6	Slates	Onishi and Sandell (1955)
14	Tindelpina Shale	This work

Tourtelot (1964) stated that the arsenic content of nonmarine shales is not related to the organic carbon content of the samples. However, in the offshore marine shales, the arsenic content is correlated with the carbon content of such shales. Arsenic may also occur in sedimentary pyrite, in clay minerals and iron hydroxides (or oxides) as an adsorbed

Reproduced with permission of the copyright owner. Further reproduction prohibited without permission.

constituent. As a general rule the occurrence of arsenic in sediments is favored by the reducing condition of the depositional site (Onishi and Sandell, op. cit.). Due to the similarity between the ionic size of arsenic and aluminum and silicon (As^{5+} = 0.47Å; Al^{3+} = 0.50Å; Si^{4+} = 0.41Å) arsenic may substitute the latter elements in feldspars or other aluminosilicates. It is thought that the higher arsenic content in shales produced by weathering process of igneous rocks having low concentration of arsenic may be accounted for by the arsenic contribution from volcanic exhalation. During the regional metamorphism of pelitic rocks, arsenic content may be lowered (Onishi and Sandell, op. cit.).

Barium. The Tindelpina Shale has an average barium content of 858 ppm, which is above the quoted average figure by Puchelt (1972) for shales of 546 ppm with a range of 250 to 800 ppm. Table 9 shows some of the published figures for barium concentration in shales.

TABLE 9

Barium Concentration in Argillaceous Sediments (in ppm)

Concentration	Rock Types	Author
393	Shales (Devonian, New York)	Fenner and Hagner (1967)
499	Carboniferous Shales (Gt. Britain)	Nicholls and Loring (1962)
723	Graptolite Shale	Spencer (1966b)
526	Shales	Degens et al. (1957)
230 - 900	Clay Shales	Schroll (1971)
858	Tindelpina Shale	This work

Reproduced with permission of the copyright owner. Further reproduction prohibited without permission.

Barium does not seem to be an environmental discriminator for non-marine and marine shales (Degens et al., 1957). The association of barium with micas (illites) in shales is not fully understood. Barium in shales is thought to have been associated with organic carbon, or occurring as fine grains of barite.

Turekian and Tausch (1964) reported the high content of barium in the Atlantic deep-sea clays of 1,100 to 2,000 ppm. Wedepohl (1960) reported the higher barium concentration of 6,700 ppm from the Pacific deep-sea clays.

Boron. Analysis of 128 Tindelpina Shale samples gives an average boron content of 184 ppm. Comparison of this average with results of other investigations is shown in Table 10.

TABLE 10

Average Boron Content in Argillaceous Rocks (in ppm)

Concentration	Rock Types	Author
299	Marine clays	Ataman (1967)
117	Esopus Fm. (shale), New York	Fenner and Hagner (1967)
120-130	Shales	Green (1959)
103	Shales	Reynolds (1965)
141	Cambroordovician marine shales (North America)	Shaw and Bugry (1966)
105	Modern marine muds	Shimp et al. (1969)
58	Modern freshwater muds	
184	Tindelpina Shale	This work
224	Sturt Tillite	This work

Reproduced with permission of the copyright owner. Further reproduction prohibited without permission.

The average boron content of the Sturt Tillite (22 samples) is also included in the table as a comparison.

The problems involved in using boron as a paleosalinity indicator have been extensively reviewed by, among others, Harder (1970), Cody (1971), and Couch (1971). In a review of boron contents of shales, Shaw and Bugry (1966) reported that a boron concentration in shales higher than 110 ppm is indicative of marine environment, while less than 50 ppm is indicative of continental origin. The average boron content of the Tindelpina Shale and the Sturt Tillite indicates a marine environment.

It was shown by Frederickson and Reynolds (1960) that a paleosalinity-sensitive value could be computed by adjusting the boron content of a clay so that it corresponds to the boron content of pure illite. The percentage of K_2O in the samples was used as a measure of the amount of illite present. Other investigators have verified the method of Frederickson and Reynolds (*op. cit.*) and found it to be useful in interpreting environmental salinities (Walker and Price, 1963; Reynolds, 1965).

The adjusted boron content of illite (muscovite) in the Tindelpina Shale was calculated from the following equation (Reynolds, 1965):

$$\text{ppm B in muscovite} = \text{total ppm B} \times \frac{\text{Per cent } K_2O \text{ in muscovite}}{\text{Per cent } K_2O \text{ in sample}}$$

This adjusted boron content is meaningful if the following conditions are met:

Reproduced with permission of the copyright owner. Further reproduction prohibited without permission.

1. Illite (in the present case, muscovite) is the only potassium-bearing mineral present.
2. All of the boron is contained in illite.
3. All illite has the same K_2O content.
4. Illite is authigenically formed.

Reynolds pointed out that conditions (1) and (2) generally apply to the clay-size fraction of sediments. Clastic minerals such as micas and feldspars are assumed to be present in insignificant amounts. The presence of small amounts of tourmaline (tourmaline contains up to 10 per cent B_2O_3 or 3 per cent B) would not unduly bias the adjusted boron content of illite-rich rock. However, the adjusted content may increase appreciably in illite-poor materials. The contribution of boron inherent to the clastic muscovite derived from the source material is also assumed to be insignificant. Harder (1961) stated that the low grade metamorphism of the green schist facies of argillaceous rocks may release some of the boron out of illite and form new tourmaline.

Estimation of the boron concentration in the muscovite of the Tindelpina Shale requires that some value be assumed for the K_2O in muscovite. Frederickson and Reynolds (1960) used the value of 7.7 per cent K_2O in illite, whereas Walker and Price (1963) considered 8.5 per cent as a more appropriate figure for their materials. Reynolds (1965) suggested that a value between 7.7 and 10 per cent K_2O would be the appropriate figure (the theoretical content of K_2O in muscovite is 11.8 per cent). He stated that the upper limit should be used for illite

Reproduced with permission of the copyright owner. Further reproduction prohibited without permission.

which produces sharp and high basal peaks on the X-ray diffractograms. The author of this thesis arbitrarily chose 8.5 per cent for the K_2O content of muscovite in the Tindelpina Shale. Reynolds (op. cit.) pointed out that, generally, the same value should be used for all samples of similar lithologic, mineralogic, and stratigraphic character. These conditions are met by the Tindelpina Shale and the Sturt Tillite. The choice of the low value of 8.5 per cent was also meant to compensate for the possible contribution of boron from detrital tourmaline and clastic muscovite. It has been shown that in the mineralogy of the Tindelpina Shale the presence of potash feldspar is insignificant. Furthermore, it is assumed that the muscovite present was originally illite which has adsorbed boron during the Tindelpina Shale deposition. Through later diagenetic and metamorphic processes, this illite was converted into muscovite.

Reynolds (op. cit.) obtained an average value of 422 ppm for the adjusted boron content in his Precambrian (marine) shales. The average value for the adjusted boron content in the Tindelpina Shale is 466 ppm, higher than Reynolds' figure. In comparison with the data obtained by Frederickson and Reynolds (1960, p. 210), the Tindelpina Shale adjusted boron falls well into the normal marine values. If the range of the adjusted boron of 143 to 883 ppm is converted into Walker and Price's (1963, p. 836) "equivalent boron", most values fall between 300 and 400 ppm, also indicating normal marine environment. Using the value of 1.9 per cent for the average K_2O content of sediments

Reproduced with permission of the copyright owner. Further reproduction prohibited without permission.

(Poldervaart, 1955), the average boron content of shales is therefore (1.9/8.5) x 466 ppm = 104 ppm. This value agrees well with Reynolds' figure of 103 ppm. Surprisingly, the Sturt Tillite also has a high adjusted boron content (501 ppm).

Chromium. In the Tindelpina Shale, the average chromium content of 83 ppm is higher than that of pelitic sediments (Table 11). Chromium was one of the elements which Shimp et al. (1969) used to discriminate marine from freshwater muds. However, they pointed out that this element is not a good environmental indicator.

TABLE 11

Average Chromium Concentrations in Argillaceous Rocks (in ppm)

Concentration	Rock Types	Author
70 - 100	Pelitic sediments	Fröhlich (1960)
72	Esopus Fm. (shale), New York	Fenner and Hagner (1967)
80	Shales	Hirst and Kaye (1971)
72	Modern marine muds	Shimp et al. (1969)
72	Freshwater muds	
83	Tindelpina Shale	This work

In sediments, chromium may occur as resistates such as chromite, magnetite, and ilmenite. Relatively high chromium content is found in bauxite and sedimentary iron ores (Fröhlich, 1960). In the weathering environment chromium may be released from the host rocks and remain relatively stable in hydroxides tending to stay behind; this may explain

Reproduced with permission of the copyright owner. Further reproduction prohibited without permission.

the high chromium accmumlation in laterites and bauxite. Evidently chromium behaves in a similar way to iron and aluminum (Fe^{3+} = 0.64 Å; Al^{3+} = 0.57 Å; Cr^{3+} = 0.63 Å) in the sedimentary environment (Gordon and Murata, 1952). In pelitic sediments, illite, as well as iron oxides, seems to be the important chromium carrier.

Copper. The average concentration of copper in the Tindelpina Shale is 30 ppm. This is lower than the range of copper content in argillaceous rocks (Table 12). The occurrence of copper in sedimentary rocks depends on the presence of clay minerals, manganese and iron oxides, plankton, and carbonaceous materials, which act as adsorbers or carriers (De Mumbrum and Jackson, 1956; Heydemann, 1959). In the aqueous environment, copper, like other base metals, may move as cations.

TABLE 12

Average Copper Abundance in Argillaceous Rocks (in ppm)

Concentration	Rock Types	Author
55	Clays and clayshales	Wedepohl (1962)
130	Atlantic clays	
400	Pacific clays	
120	Residual clays from carbonates	
30	Tindelpina Shale	This work

Wedepohl (1962), who has reviewed the geochemistry of copper, stated that copper has great dependence on carbonaceous material, as is shown by the high copper content of black shales such as the Permian Kupferschiefer and the Nonesuch Shale of Michigan. Copper may substitute for

Reproduced with permission of the copyright owner. Further reproduction prohibited without permission.

some iron in sulfides and oxides (Fe^{2+} = 0.83 Å; Cu^{2+} = 0.83 Å). As an adsorber of copper, illite is considered to be next only to montmorillonite. Degens et al. (1957) reported that the organic fraction of freshwater shales tends to have higher copper than the organic fraction of marine shales.

Lithium. The average lithium content in the Tindelpina Shale is much lower than that in shales reported by other authors (Table 13). This is mostly due to the low content of feldspar in the

TABLE 13

Average Lithium Content in Argillaceous Rocks (in ppm)

Concentration	Rock Types	Author
60	Undifferentiated sediments	Ohrdorf (1968)
117	Marine Upper Carvoniferous shales, Germany	
72	Nonmarine Upper Carboniferous shales, Germany	
156	Montmorillonite, Otay, Calif.	
18	Montmorillonite, Upton, Wyo.	
83	Illite	Tardy et al. (1972)
37	Fithian illite, Ill.	
67	Freshwater sediments	Heier and Billings (1970)
55	Littleton Fm., New York	Shaw (1954)
22	Tindelpina Shale	This work

Tindelpina Shale. Ohrdorf (1968) pointed out that micaceous minerals may have relatively high lithium contents. Micas derived from igneous rocks, may contain unusually high lithium concentrations. Consequently,

Reproduced with permission of the copyright owner. Further reproduction prohibited without permission.

detrital micas derived from such rocks may also have high concentrations of lithium. Muscovite may contain 10 ppm to 1 per cent lithium, whereas biotite contains from 70 ppm to 0.8 per cent (Ohrdorf, op. cit.).

Ohrdorf showed that lithium may be used to distinguish marine from freshwater shales, if sample collection is restricted to a single formation or depositional basin. She reported that marine shales tend to have higher concentrations of lithium than freshwater shales. Her conclusion was also found to be true by the earlier work of Keith and Degens (1959).

In the sedimentary environment, lithium, which has been released from the primary minerals, may move around as ionic lithium and then later be adsorbed by clay minerals. Lithium is often accompanied by aluminum and iron, sometimes by potassium and magnesium, and less often by calcium, sodium, and manganese. Lithium is isomorphous with most of these elements in lithium or in non-lithium minerals. Because of its small ionic size (Li^+ = 0.60Å), lithium may easily penetrate phyllosilicate structure and occupy the octahedral site of the clay minerals (Vlasov, 1964).

Nickel. The average content of nickel in the Tindelpina Shale of 40 ppm is similar to the concentration of nickel in shales reported by other workers (Table 14).

During weathering, nickel remains largely in the residual product and is deposited in the hydrolyzates. Unlike divalent iron and manganese, the divalent nickel is very stable in aqueous solution and

Reproduced with permission of the copyright owner. Further reproduction prohibited without permission.

TABLE 14

Average Nickel Concentration in Argillaceous Rocks (in ppm)

Concentration	Rock Types	Author
40	Argillaceous and arenaceous sediments	Hirst and Kaye (1971)
39	Esopus Fm., New York	Fenner and Hagner (1967)
68	Nearshore sediments	Wedepohl (1971)
62	Clays	Ataman and Lucas (1968)
80	Littleton Fm., N.H.	Shaw (1954)
41	Marine Shales	Potter, et al. (1963)
40	Tindelpina Shale	This work

consequently may migrate from a considerable distance. However, only a very small portion of nickel is liberated from the parent material, which is commonly ultrabasic rock, during the weathering process. The bulk of nickel is retained in the solid product of weathering and transported to the sea (Goldschmidt, 1954).

Lead. The lead concentration in shales such as the Tindelpina Shale is expected to be low. The average content in the Tindelpina Shale is 21 ppm, close to the values reported by other investigators (Table 15).

Although the radioactive lead isotopic composition has been extensively studied in relation to rock dating, the nonradiogenic lead geochemistry is less well known. Heide and Lerz (1955) and Wedepohl (1956) have reviewed the geochemistry of lead in various rock types. Wedepohl (op. cit.) found that the highest concentration of lead in

Reproduced with permission of the copyright owner. Further reproduction prohibited without permission.

TABLE 15

Average Lead Abundance in Argillaceous Rocks (in ppm)

Concentration	Rock Types	Authors
126	Clays	Ataman and Lucas (1968)
15	Argillaceous and arenaceous sediments	Hirst and Kaye (1971)
20	Nonpelagic argillaceous clays	Wedepohl (1956)
43	Atlantic deep-sea clays	
140	Pacific deep-sea clays	
13	Marine sediments	Potter et al. (1963)
21	Tindelpina Shale	This work

silicate minerals occurs in potassium feldspar of pegmatitic origin (62-100 ppm). As in the case of other base metals, lead occurs in the sediments adsorbed by clay minerals, manganese hydroxides or oxides, ferric hydroxides, and organisms (forams, radiolaria, plants, etc.). In shales, lead occurs mainly as an adsorbed constituent of clay minerals; however, the mechanism of this adsorption is not clearly understood. The relatively high lead content in pelagic sediments may be due to contribution coming from volcanic exhalation (Wedepohl, op. cit.).

Vanadium. The average concentration of vanadium in the Tindelpina Shale is 191 ppm, higher than that normally found in clays and shales (Table 16). Five analyses of samples collected at the type locality were reported by Coats and Blissett (1971). It is generally known that vanadium is associated with carbonaceous matter. During

Reproduced with permission of the copyright owner. Further reproduction prohibited without permission.

TABLE 16

Average Vanadium Concentration in Argillaceous Rocks (in ppm)

Concentration	Rock Types	Authors
121	Clays and shales	Jost (1932)
118	Marine sediments	Potter et al. (1963)
132	Pacific deep-sea sediments	Landergren and Joensuu (1965)
400	Pierre Shale	Tourtelot et al. (1960)
408	Bituminous sediments (Precambrian)	Cloud Jr. (1965)
greater than 1000	Pennsylvanian black shale, Ky. and Ind.	Vine (1964)
191	Tindelpina Shale	This work
156	Tindelpina Shale	Coats and Blissett (1971)

the decay of organic matter, some vanadium is incorporated as an organo-metallic complex, and some as vanadate which may be fixed by clay minerals (Goldschmidt, 1954; Degens et al., 1957). There is less vanadium in continental clays than in marine clays, probably due to the abundance of planktonic life in the marine environment.

In the sedimentary environment vanadium moves mainly as pentavalent vanadium, which may precipitate as vanadium sulfide in a highly reducing environment. Vanadium may also be associated with sedimentary iron ore deposits (V^{5+} = 0.59Å; V^{3+} = 0.69Å; Fe^{3+} = 0.63Å).

Zinc. The average concentration of zinc in the Tindelpina Shale of 62 ppm is not indicative of any environmental deposition. Two analyses of zinc reported by Coats and Blissett (1971) in the samples collected at the type locality gave values of 20 and 95 ppm.

Reproduced with permission of the copyright owner. Further reproduction prohibited without permission.

Wedepohl (1953, 1972), who has extensively reviewed the geochemistry of zinc in various kinds of rocks, pointed out that in the sedimentary environment, zinc is mainly incorporated in iron or manganese hydroxides and oxides (Fe^{3+} = 0.63Å; Mn^{2+} = 0.80Å; Zn^{2+} = 0.74Å), chlorite, and other clay minerals, and occurs to a lesser degree as a carbonate. He reported that about 70 per cent of shales contain 50 to 130 ppm zinc. Shales having low bituminous matter contain on the average 95 ppm zinc, as compared to 100-200 ppm zinc for shales having higher organic content. Pelagic clays tend to contain more zinc than common shales (Table 17).

TABLE 17

Average Zinc Abundance in Argillaceous Rocks (in ppm)

Concentration	Rock Types	Author
95	Shales	Turekian and Wedepohl (1961)
165	Deep-sea clays	
150	Pierre Shale	Tourtelot *et al.* (1960)
62	Tindelpina Shale	This work

The average content in shales is similar to the crustal abundance as reported by Ahrens (1965).

Zirconium. Analyses of 134 Tindelpina Shale samples give an average zirconium content of 225 ppm, slightly higher than the crustal abundance (165 ppm) or the average zirconium content in shales (Table 18). Although many studies have been done on the occurrence of zirconium as

Reproduced with permission of the copyright owner. Further reproduction prohibited without permission.

TABLE 18

Average Zirconium Concentration in Argillaceous Rocks (in ppm)

Concentration	Rock Types	Author
222	Red clays	Young (1954)
210	Pierre Shale	Tourtelot et al. (1960)
180	Pacific pelagic sediments	Goldberg and Arrhenius (1958)
120	Shales	Rankama and Sahama (1950)
137	Kupferschiefer	Degenhardt (1957)
225	Tindelpina Shale	This work

the heavy mineral zircon in sandstones, the occurrence in shales has not been very thoroughly investigated. Degenhardt (1957) has reviewed the geochemistry of zirconium in various types of rocks, based on 287 analyses. He found that generally the zirconium content of sediments is similar to that of igneous rocks, and that shales have a fairly constant value of 160 ppm. In the coarser detrital sediments such as sandstone, the zirconium concentration varies over a wide range.

The mechanism of zirconium movement during the weathering process is not well understood. However, it may be assumed that zirconium in shales may principally occur as detrital grains of zircon. In addition, zirconium may also move as a complex compound $[ZrO(CO_3)_2]^-$, as hydrated zirconium dioxide, or as adsorbed zirconium in iron and manganese hydroxides. In clay minerals, such as kaolinite, zirconium may possibly substitute some aluminum in the lattice, whereas in illite

Reproduced with permission of the copyright owner. Further reproduction prohibited without permission.

it may inherently occur as zircon microlite in the original mica minerals (Degenhardt, op. cit.).

Depositional Environment of the Sturt Tillite and the Tindelpina Shale - Trace Element Criteria

It was indicated in the previous section on boron abundance in the Sturt Tillite and the Tindelpina Shale that these two stratigraphic units were deposited in a marine environment. To substantiate this finding other trace elements were used following the methods which have been successfully used by other investigators. These methods are empirical, and the explanations are generally related to basic chemistry.

Gallium-boron-rubidium ratio. Degens et al. (1957) showed that the concentrations of gallium, boron, and rubidium in shales, when observed collectively, could indicate the environment of deposition of the shales. They constructed a triangular diagram with the corners representing the concentrations of gallium (multiplied by a factor of ten), boron, and rubidium. Based on the data which they obtained from analyses of the Pennsylvanian sediments of the Appalachian coal basin, it was found that the marine shales could be distinguished from the freshwater shales. In their later paper, Degens et al. (1958) tested their finding on the Pennsylvanian rocks of the Pottsville and Allegheny series in western Pennsylvania. Their result for the identification of the depositional environment agreed with the paleontological evidence. However, they pointed out that the applicability of their method to other sedimentary rocks of other geologic and tectonic settings was not known.

Reproduced with permission of the copyright owner. Further reproduction prohibited without permission.

Plots of data obtained from the Sturt Tillite (Appendix 11) and the Tindelpina Shale (Appendix 10) on the triangle of Degens et al. show the marine nature of the Sturt Tillite and the Tindelpina Shale (Figs. 16 and 17). The central strip on the triangle indicates the zone of Degens et al. data in which the marine environment is not decisively discriminated from the fresh water environment. In a diagram such as shown in Figures 16 and 17, overlapping of data points can occur. Figure 17 suggests that the marine environment of the Tindelpina Shale changes with geographical position, probably becoming more marine towards the center of the Adelaide Geosyncline.

Potassium/rubidium ratio. In a geochemical study of shales of the Manville Group (Lower Cretaceous) of Central Alberta, Canada, Campbell and Williams (1965) reported that the rubidium/potassium ratio of their rocks could be used to identify their depositional environments. If their values are converted into potassium/rubidium ratio, comparison with the average potassium/rubidium ratio of the Sturt Tillite and the Tindelpina Shale (Table 19) suggests the marine environment of these two rock units. Although the potassium/rubidium ratios of the Sturt Tillite and the Tindelpina Shale vary beyond the "normal" upper limit for marine shales, most values are less than 200.

During weathering potassium is more quickly leached away than rubidium, which is held more firmly in the lattice of the micas and feldspars. This leads to a temporary decrease in potassium/rubidium ratio in the weathered material (K/Rb of igneous rocks = 230). Eventually

Reproduced with permission of the copyright owner. Further reproduction prohibited without permission.

Figure 16

Gallium-rubidium-boron ratios of the Sturt Tillite following a method by Degens *et al.* (1957, 1958).

Reproduced with permission of the copyright owner. Further reproduction prohibited without permission.

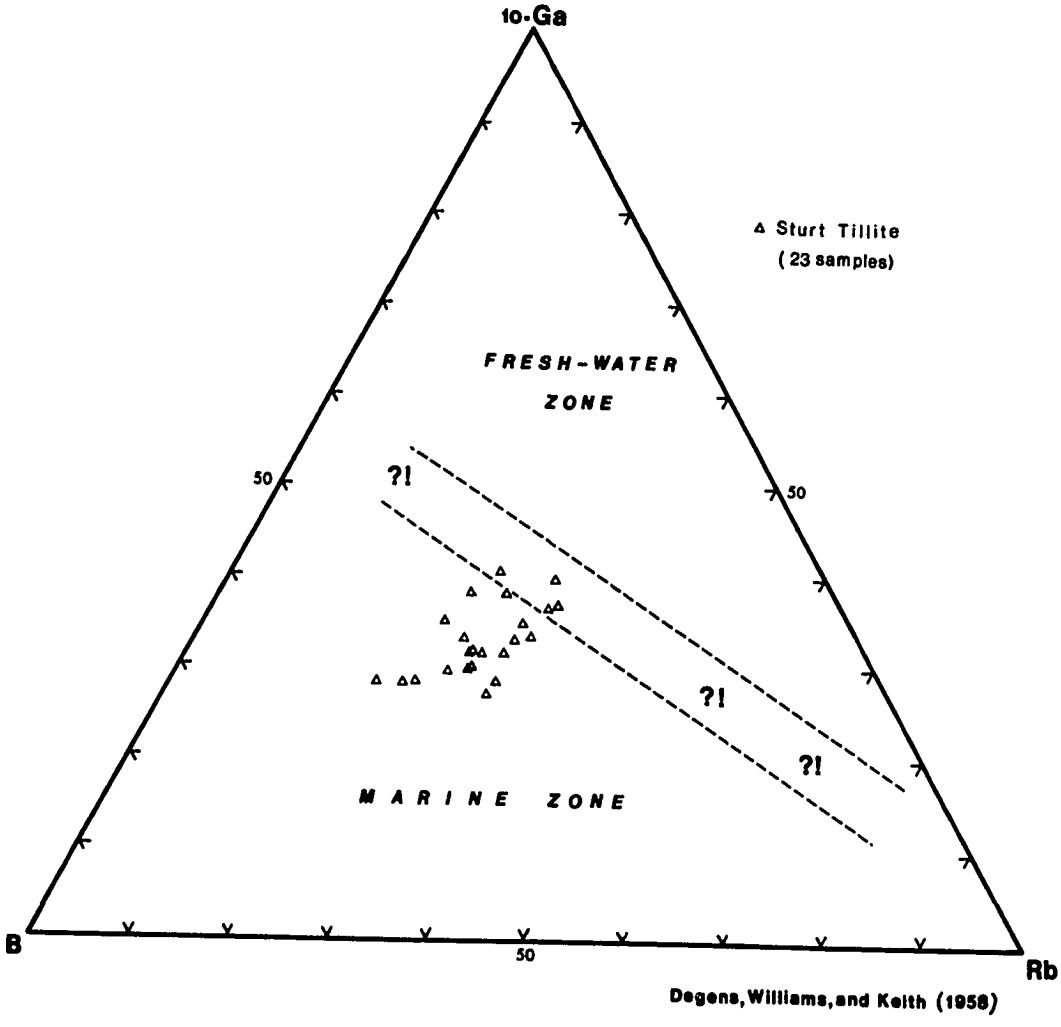

Reproduced with permission of the copyright owner. Further reproduction prohibited without permission.

Figure 17

Gallium-rubidium-boron ratios of the Tindelpina Shale following a method by Degens *et al.* (1957, 1958).

Reproduced with permission of the copyright owner. Further reproduction prohibited without permission.

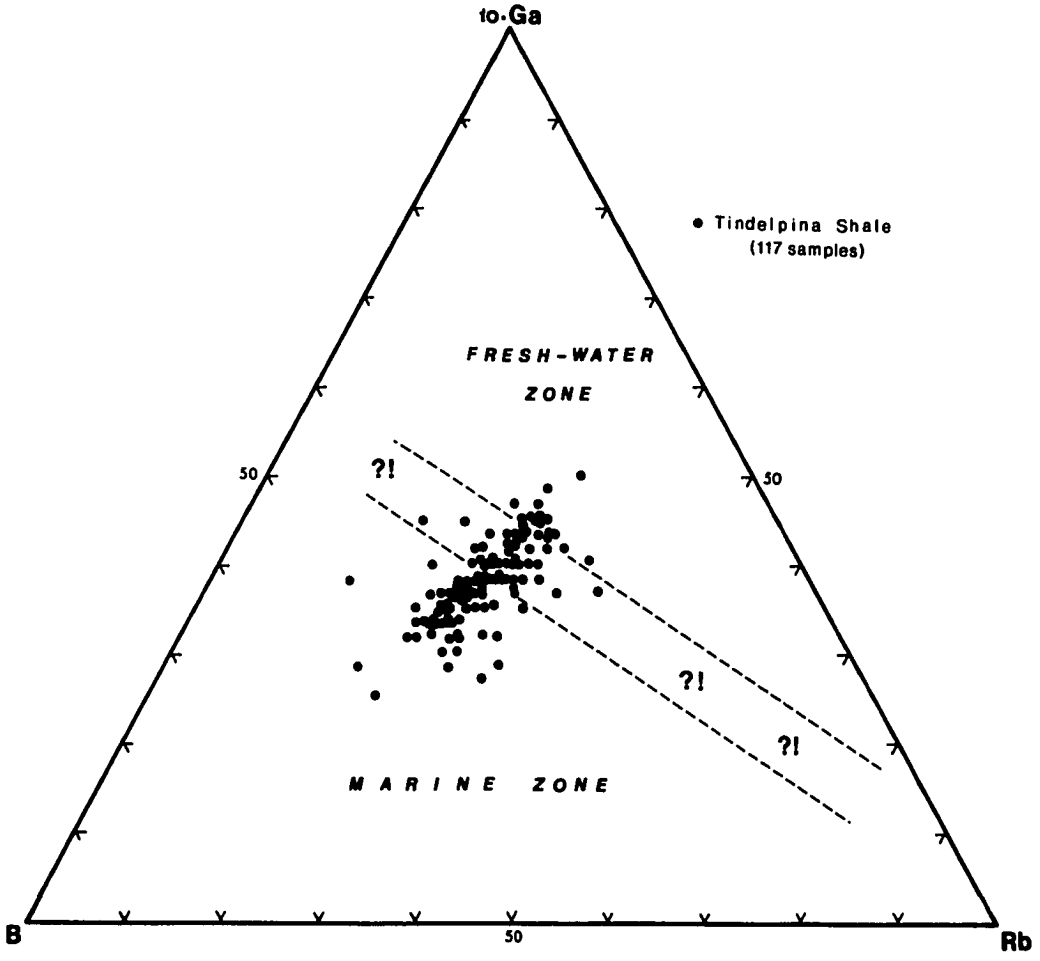

Reproduced with permission of the copyright owner. Further reproduction prohibited without permission.

both rubidium and potassium are removed. The average potassium/rubidium ratio in sediments is about 240.

TABLE 19

Potassium/Rubidium Ratio in Shales

Ratio	Rock Types	Author
150	Shales	Heier and Adams (1964)
3130	Sea water	
150-200	Marine shales	Campbell and Williams (1965)
250-300	Nonmarine to brackish water shales	
181	Gulf of Mexico sediments	Taylor (1960)
188 (range 141-287; std.dev.=28; n=25)	Sturt Tillite	This work
187 (range 140-264; std.dev.=16; n=117)	Tindelpina Shale	This work

In the sedimentary environment, the behavior of rubidium is controlled largely by the extent of adsorption on clay minerals. Illite and montmorillonite which are the common clay minerals occurring in shales may adsorb rubidium more strongly than potassium during diagenesis. This preferential adsorption of rubidium in the marine environment will decrease the potassium/rubidium ratio on shales. Obviously, unweathered clastic debris (micas and potassium feldspars) may partially affect the potassium/rubidium ratios; however, analyses of authigenic illite and glauconite

Reproduced with permission of the copyright owner. Further reproduction prohibited without permission.

indicate that these minerals too have potassium/rubidium ratios near 240 (Heier and Adams, op. cit.).

In a geochemical study of the Gulf of Mexico sediments, Welby (1958) reported that the rubidium content increases slightly with increasing distance from the shore line. This was thought to be due to the rubidium enrichment in marine sediments. Degens et al. (1957, 1958) found similar conclusion with their rocks, in that marine sediments contain more rubidium than freshwater sediments. Taylor (1960) amended Welby's data and found that all of the potassium/rubidium ratios are less than 230.

Rubidium/strontium ratio. Figure 18 plots the rubidium/strontium ratios against the concentrations of rubidium of the Sturt Tillite and its overlying Tindelpina Shale, following Reimer's (1971 and 1972) method. It seems that, in agreement with Reimer's result for marine shales, the tillite shows a strontium depletion relative to the "normal" trend of igneous rocks. He pointed out that there is a general tendency for strontium contents in marine shales to vary with time, and that the Precambrian shales tend to have low strontium content. In his study of an early Precambrian sediment, the Fig Tree Group of South Africa (about 3,300 million years), and other Precambrian shales from other parts of the world, Reimer found that strontium is depleted relative to "normal" igneous rocks. He proposed the possible causes of this depletion:

1. Strontium depleted source rocks of igneous and/or volcanic origin account for most of the material of the specific sediment.

Reproduced with permission of the copyright owner. Further reproduction prohibited without permission.

Figure 18

Plots of the rubidium/strontium ratio against the rubidium concentration of the Sturt Tillite and the Tindelpina Shale, after a method by Reimer (1972). Plots of other shales are from Reimer's compilation.

Reproduced with permission of the copyright owner. Further reproduction prohibited without permission.

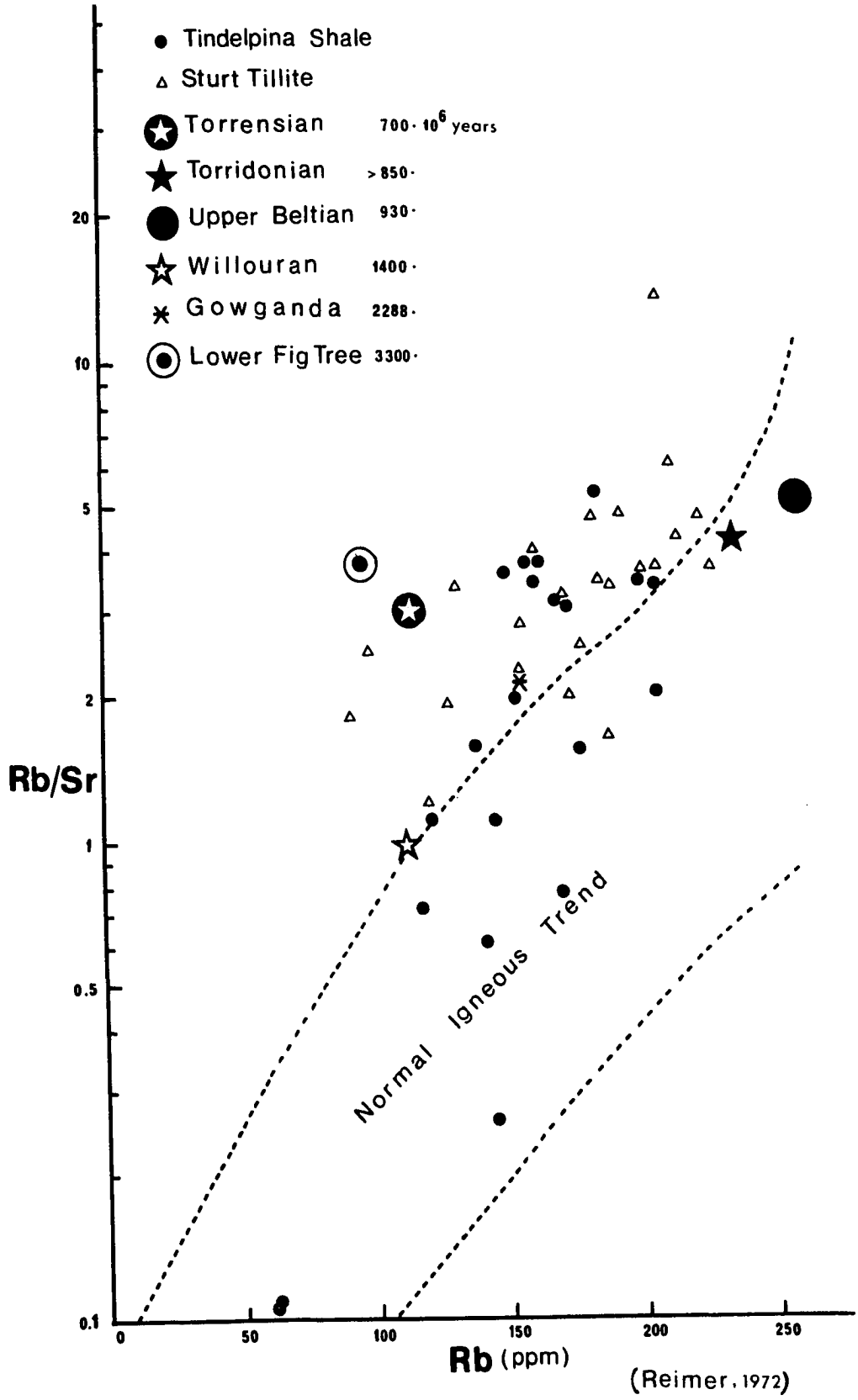

Reproduced with permission of the copyright owner. Further reproduction prohibited without permission.

2. Strontium is preferentially lost during weathering. In marine environments strontium could have been removed from the clays due to the tendency of strontium to be easily taken into solution.
3. Strontium could be lost through the destruction of plagioclase and removed to the surrounding sediments.

Since the tillite represents rock flour of apparently granitic composition, it seems that strontium depletion due to depletion in the source rocks is unlikely. Strontium and calcium which might have been removed from the glacial clays in marine environment as well as during the decay of plagioclase may be reconstituted to form the carbonate lenses which are occasionally present in the Sturt Tillite. As the environment changes into a true marine environment during the deposition of the Tindelpina Shale, strontium was taken from the seawater and incorporated into the carbonate in the Tindelpina Shale whereas rubidium was adsorbed by illite. This process is suggested by the spread of data points in Figure 19.

Major Element Abundance

The results of chemical analyses of the major elements composing the Sturt Tillite and the overlying Tindelpina Shale are shown in Tables 20 and 21. Figure 20 shows the histograms for the Tindelpina Shale. The accuracy of analysis and the chemical composition of each sample are presented in Appendix 12.

Reproduced with permission of the copyright owner. Further reproduction prohibited without permission.

Figure 19

Plots of the rubidium/strontium ratio against the rubidium concentration of the Tindelpina Shale, after a method by Reimer (1972).

Reproduced with permission of the copyright owner. Further reproduction prohibited without permission.

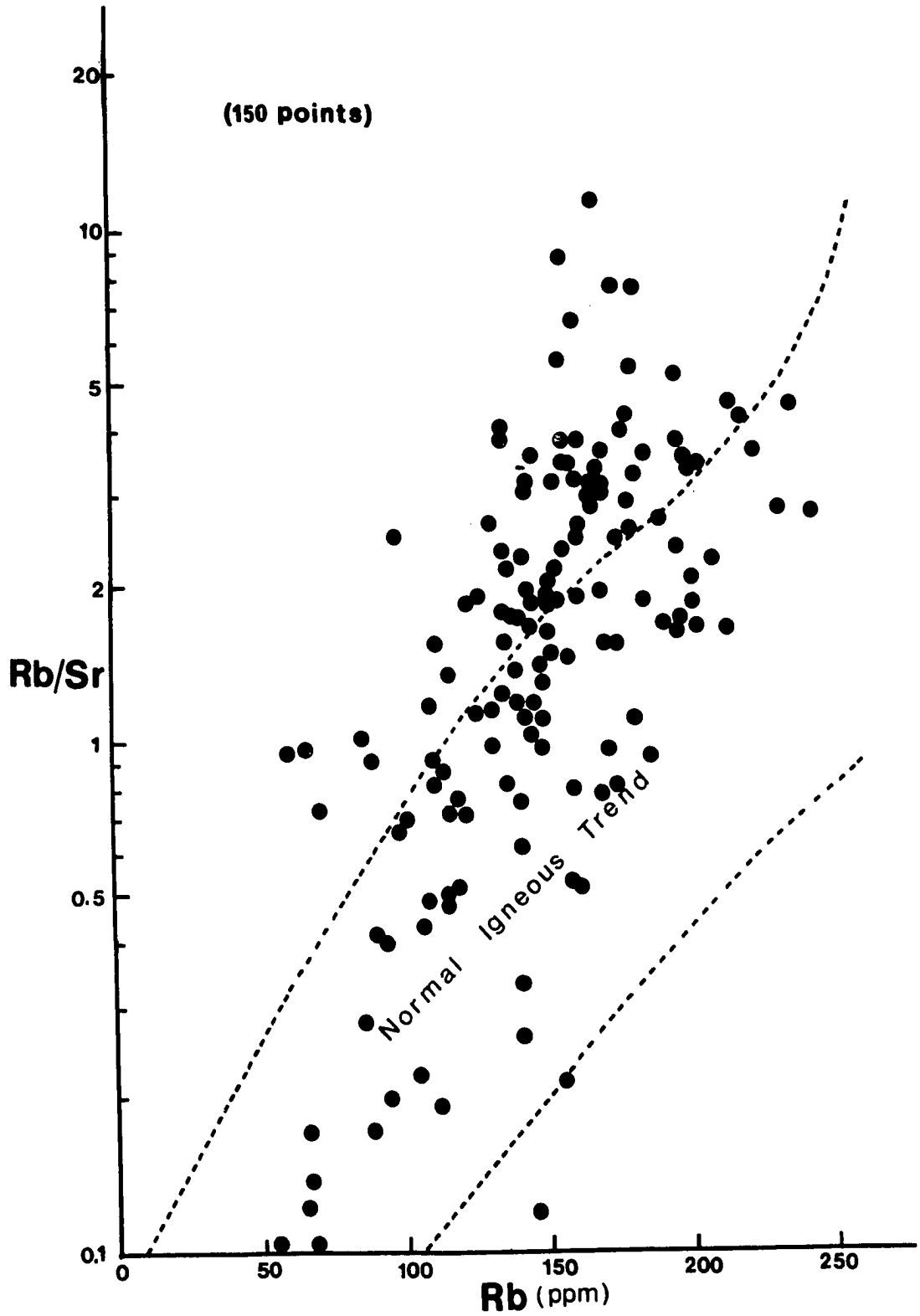

Reproduced with permission of the copyright owner. Further reproduction prohibited without permission.

Reproduced with permission of the copyright owner. Further reproduction prohibited without permission.

TABLE 20

Comparison of chemical compositions (in weight per cent) of the Tindelpina Shale and the underlying Sturt Tillite with other tillites and shales.

	Tindelpina Shale (22 samples)			Sturt Tillite (25 samples)				
	Av.	S.D.	Range	Av.	S.D.	Range	Tillites**	Platform Shales***
SiO_2	59.23	11.21	24.63-70.21	68.79	3.14	60.41-75.43	58.9	50.7
Al_2O_3	13.95	2.72	5.95-16.59	13.54	1.96	7.68-15.90	15.9	15.1
Fe_2O_3	5.89	1.80	1.04-9.61	5.18	0.91	3.14-6.98	7.4	6.7
MgO	4.24	2.84	1.26-13.14	2.60	0.92	1.33-5.64	3.3	3.3
CaO	2.89	5.85	0.10-22.09	0.62	0.93	0.07-3.75	3.2	7.2
Na_2O	1.11	0.45	0.18-1.64	1.23	0.44	0.11-1.93	2.1	0.8
K_2O	3.43	0.78	1.39-4.92	3.76	0.68	2.19-4.90	3.9	3.5
TiO_2	0.95	0.18	0.44-1.17	0.89	0.13	0.51-1.06	0.79	0.78
P_2O_5	0.19	0.07	0.06-0.36	0.13	0.04	0.04-0.26	0.21	0.10
MnO	0.03	0.02	0.00-0.11	0.03	0.03	0.01-0.12	0.10	0.08
Loss on ignition	7.75	7.33	2.79-30.75	3.31	1.04	2.45-6.90	3.77	11.74
Free quartz	38.94	8.69	18.18-49.97	46.08	8.62	30.71-61.77		

** Goldschmidt, 1933 (68 analyses)
*** Vinogradov & Ronov, 1956 (6,800 analyses)

TABLE 21

Chemical Analyses
of Shales

	Tindelpina Shale (158 samples) in weight per cent			Geosynclinal Shales*
	Average	Std. Dev.	Range	
SiO_2	59.77	7.88	24.63-71.27	58.9
Al_2O_3	13.65	2.49	5.95-19.30	16.7
Fe_2O_3	5.45	2.85	0.61-22.55	6.9
MgO	3.75	1.72	0.63-13.14	2.6
CaO	4.01	5.44	0.02-26.68	2.2
Na_2O	1.17	0.65	0.08-5.10	1.6
K_2O	3.35	0.85	0.78-5.62	3.6
TiO_2	0.95	0.19	0.44-1.33	0.78
P_2O_5	0.18	0.07	0.02-0.43	0.16
MnO	0.07	0.10	0.00-1.00	0.09
Loss on ignition	7.31	4.67	0.89-30.75	6.3
Free quartz	40.40	8.64	18.18-88.62	

*Average analysis compiled by Wedepohl (1969), including average composition of shales determined by Clarke (1924).

Reproduced with permission of the copyright owner. Further reproduction prohibited without permission.

Figure 20

Histograms of major oxides and quartz in the Tindelpina Shale.

Reproduced with permission of the copyright owner. Further reproduction prohibited without permission.

Histograms of TINDELPINA SHALE
158 Chemical Analyses
(Frequency vs. Weight Percent)

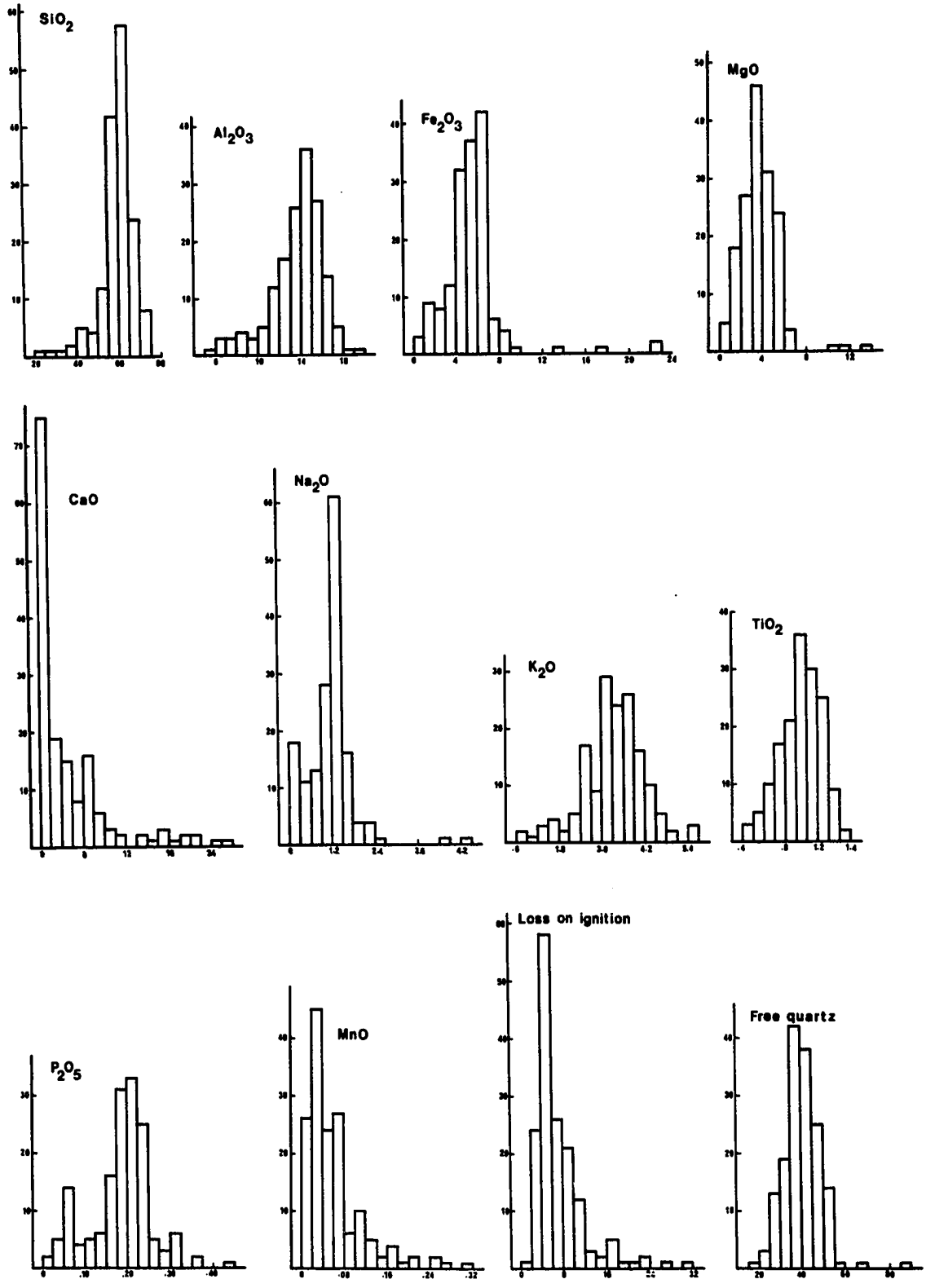

Reproduced with permission of the copyright owner. Further reproduction prohibited without permission.

It seems that there is no significant difference between the chemistry of the Sturt Tillite and the Tindelpina Shale, with the exception of the concentrations of silica, lime, and magnesia. The silica difference is due mainly to the different concentration of quartz in the Sturt Tillite (average 46.08 per cent) and the Tindelpina Shale (average 38.94 per cent). The quartz content of the Tindelpina Shale is much higher than the average quartz content of shales (20 per cent) as quoted by Wedepohl (1969). The Tindelpina Shale quartz content is closer to the average for graywackes which is 37 per cent. The difference in quartz content may be due to the more chemically differentiated Tindelpina Shale compared to the rock flour nature of the tillite matrix and to the difference in their grain sizes. Lime and magnesia are reflections of the increasingly marine environment during the deposition of the Tindelpina Shale, with the introduction of more carbonate.

Comparison of the Sturt Tillite with the continental glacial clays of Norway (Goldschmidt, 1933) shows that they derive from different source material. The higher silica content of the Sturt Tillite is a reflection of the predominantly granitic nature of the source rocks.

Tindelpina Shale (Tables 20 and 21) has similar composition to other shales. The higher lime content of the Tindelpina Shale compared to the geosynclinal shales is due to its calcareous nature. The Russian platform shales have a much higher lime content than the Tindelpina Shale.

Reproduced with permission of the copyright owner. Further reproduction prohibited without permission.

CaO-Na_2O-K_2O triangle. It seems from this diagram (Fig. 21a) that there is no difference between the chemistry of the Sturt Tillite and the Tindelpina Shale, other than the difference in calcium content. It is obvious that there is a marked preponderance of K_2O over Na_2O, indicating there is much more muscovite than plagioclase in those two rock units. The plots of the Sturt Tillite show their similarity of its chemistry to the Torrowangee Series tillite, which is stratigraphically similar, in Broken Hill, New South Wales, which was investigated by Bowes (1970). Bowes pointed out that the higher K_2O content of his tillite matrix is a reflection of the parent material, the Willyama Complex, which is principally composed of various kinds of mica schists, granites, and pegmatites.

Compared to another Precambrian tillite, such as the Gowganda Formation of Ontario, Canada (Young, 1969), the Sturt Tillite differs markedly in its sodium and potassium contents. The Gowganda Formation shows a preponderance of Na_2O over K_2O which reflects the chemistry of the greenstone belts of the Canadian Archean basement (Pettijohn and Bastron, 1953; Young, op. cit.).

Plots of Ca_2O, Na_2O, and K_2O for all Tindelpina Shale samples collected (Fig. 22) indicate the fairly constant Na_2O content with respect to CaO and K_2O. The chemistry of the samples seems to be influenced mainly by the potassium and calcium due to the presence of muscovite and carbonate.

Reproduced with permission of the copyright owner. Further reproduction prohibited without permission.

Figure 21

a. Ca_2O-Na_2O-K_2O triangular diagram for the Sturt Tillite and its overlying Tindelpina Shale.

b. Plots of the major oxides composing the Sturt Tillite and its overlying Tindelpina Shale on the diagram by Ronov and Khlebnikova (1957).

Reproduced with permission of the copyright owner. Further reproduction prohibited without permission.

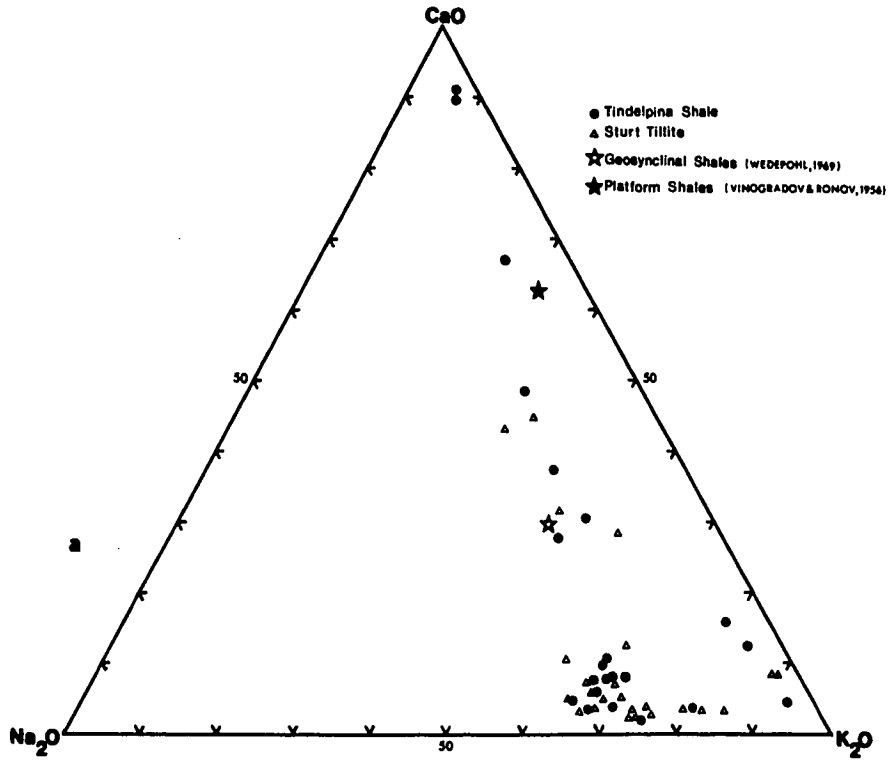

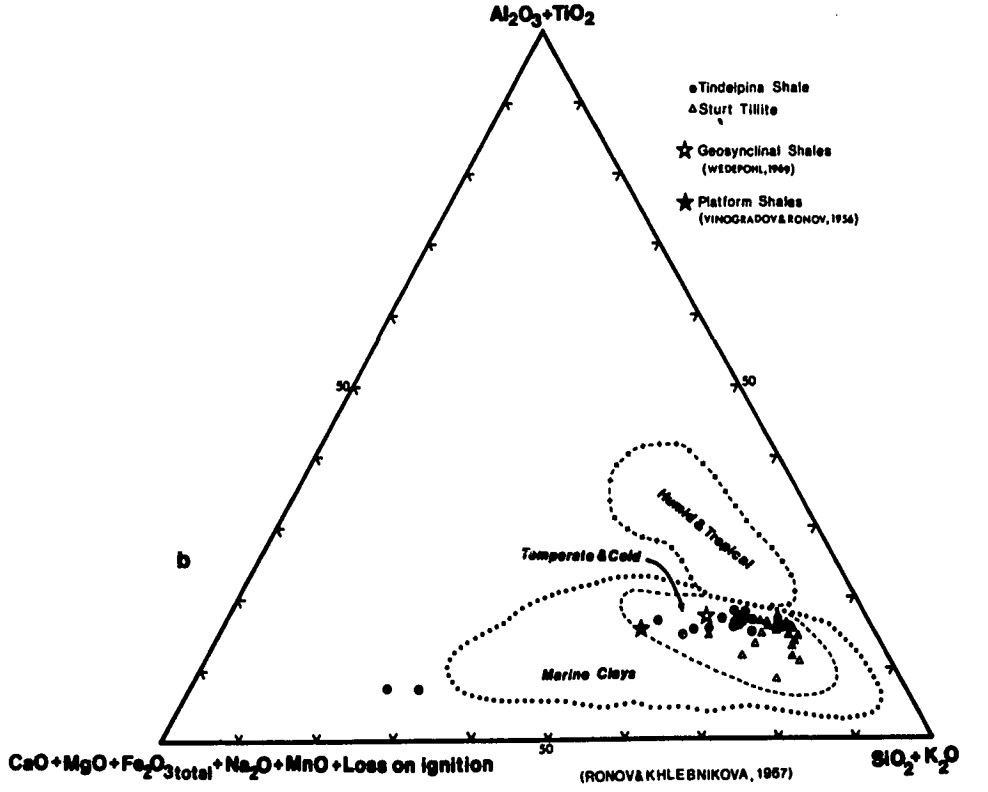

Reproduced with permission of the copyright owner. Further reproduction prohibited without permission.

Figure 22

Ca_2O-Na_2O-K_2O plots of the Tindelpina Shale.

Reproduced with permission of the copyright owner. Further reproduction prohibited without permission.

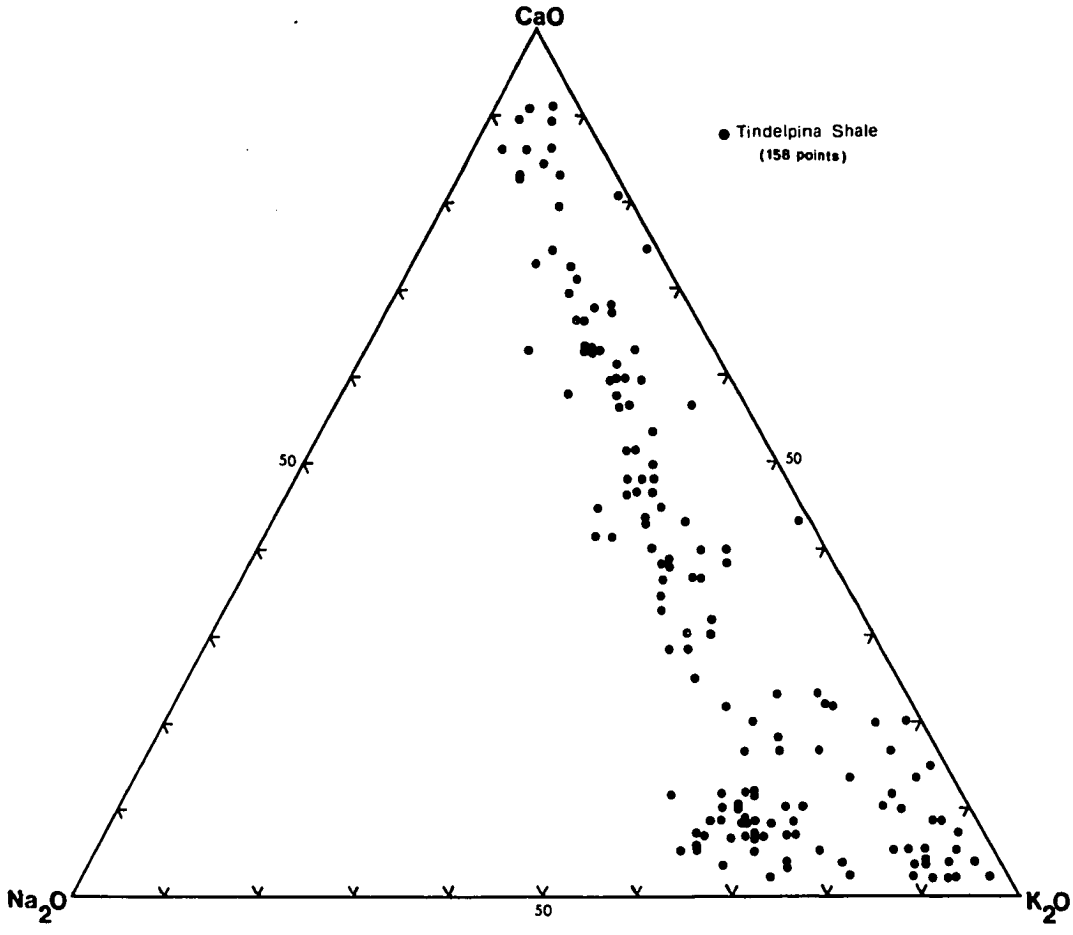

Reproduced with permission of the copyright owner. Further reproduction prohibited without permission.

Environment of Deposition - Major Element Criteria

Diagram by Ronov and Khlebnikova (1957). From the analyses of thousands of clay sediment samples collected in Russia, Ronov and Khlebnikova found that there are definite groupings of clay types, when combination of certain oxides are plotted on a triangular diagram (see p. 25 of this thesis). The continental clays formed in humid and tropical climate tend to have high alumina contents, whereas marine clays and continental clays formed in temperate and cold climates tend to have relatively low alumina contents. Clays of cold climates approach granodiorite in their composition as the initial product of weathering; whereas the humid and tropical clays, as the result of last stages of weathering processes, tend to be enriched in the most stable elements (Al and Ti).

Plots of the Sturt Tillite and the overlying Tindelpina Shale, as well as the overall Tindelpina Shale, are shown in Figures 21b and 23a. It is not possible, however, to tell whether both of these rock units were continental clays deposited in temperate and cold climates or whether they just represent marine sediments. The clustering of the Tindelpina Shale plots (Fig. 23a) suggests the somewhat uniform composition of this shale unit.

Iron and manganese concentrations. Angino (1966) suggested that it is possible to distinguish continental till from glacial marine sediments on the basis of their trace element geochemistry. In a geochemical study of the Antarctic pelagic sediments, he found that it

Reproduced with permission of the copyright owner. Further reproduction prohibited without permission.

Figure 23

a. Plots of the major oxides composing the Tindelpina Shale on a diagram by Ronov and Khlebnikova (1957).

b. Plots of normalized silicon contents (Si=100-Al-Fe) against Al/Fe ratios of the Tindelpina Shale after a method of Dennen and Moore (1971). U.S. Geological Survey reference rocks are indicated by G-2 (granite), GSP-1 (granodiorite), AGV-1 (andesite), and BCR-1 (basalt).

Reproduced with permission of the copyright owner. Further reproduction prohibited without permission.

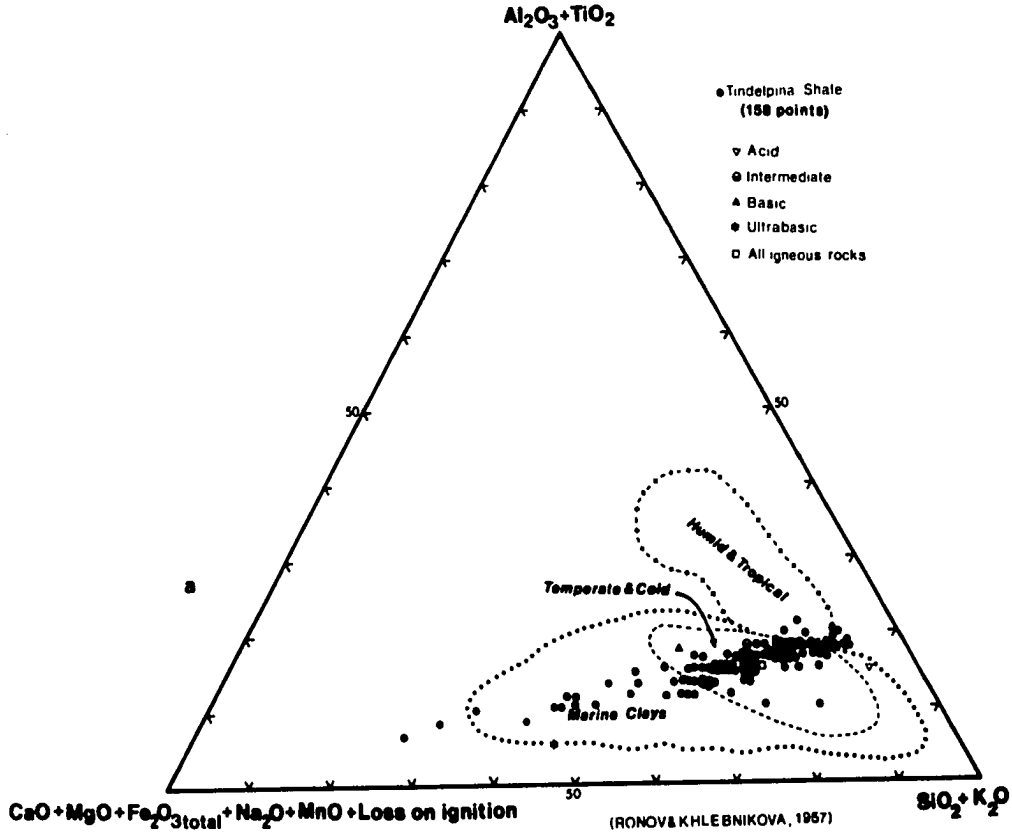

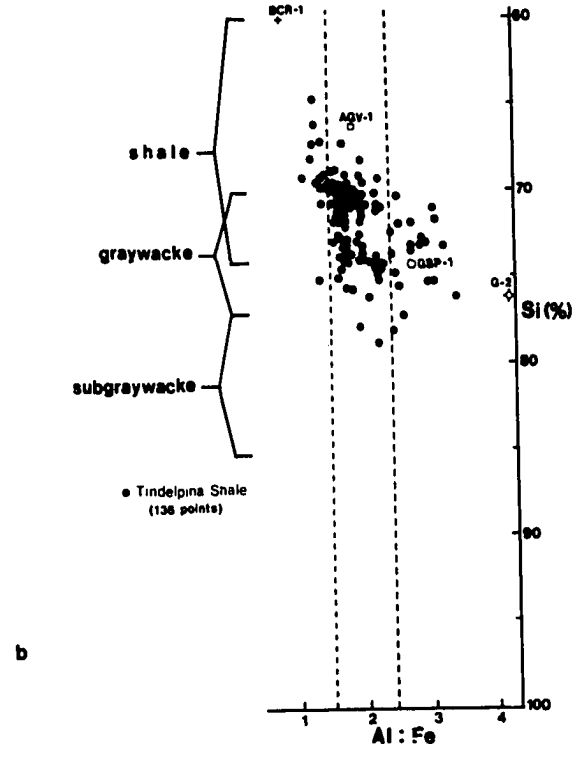

Reproduced with permission of the copyright owner. Further reproduction prohibited without permission.

is possible to distinctly differentiate the glacial marine sediments from the shelf, deep-sea carbonates, and deep-sea clay sediments. He reported that the glacial marine sediments as a type are deficient in chromium, nickel, titanium, iron, and aluminum relative to crustal abundance. On the other hand, the concentrations of elements such as copper, vanadium, and manganese are considerably more than the average crustal abundance. Angino added that trace element criteria could be useful in identifying the presence of glacial marine sediments, presently unrecognized, in the geologic column.

Frakes and Crowell (1973) reported that on the basis of the concentrations of elemental iron and manganese, glacial marine sediments can be distinguished from continental glacial deposits. They found that, in general, the iron content of continental glacial sediments tends to be more concentrated than iron content in the glacial marine deposits and the crustal abundance. This difference in iron concentrations was explained as being mainly due to the relative intensity of the reduction-oxidation process (Frakes, 1973, pers. comm.). The oxidizing condition, which is relatively more prevalent on the continent, will keep iron in its ferric state and will cause iron to precipitate as iron hydroxide. On the other hand, the marine environment is relatively more reducing than the continental environment and keeps iron in its ferrous state making it more mobile. During lithification of the sediments this ferrous iron may be partially removed, thus decreasing the iron content in marine sediments relative to continental sediments. To an extent, the soluble iron in

Reproduced with permission of the copyright owner. Further reproduction prohibited without permission.

seawater may be in the form of hydroxide complex of ferric iron or an uncharged $Fe(OH)_2$.

It is obvious that the abundance of iron is also affected by the provenance. However, the generalization made by Frakes and Crowell (op. cit.) is found to be empirically true. Data obtained from published works substantiated their findings (Fig. 24). Plots of iron and manganese concentrations of the Sturt Tillite and its underlying Tindelpina Shale show that their iron contents are impoverished relative to the crustal abundance. The data point of Goldschmidt (1933) in the same figure is obtained from the average composition of glacial clays of continental origin in Norway, whereas those of Frakes and Crowell (1973) are estimated averages taken from their preprinted paper. The iron-manganese plots for the Sturt Tillite suggest that this tillite unit is of glacial marine origin. The Torrowangee Series tillite studied by Bowes (1970) also has low iron and manganese content (2.81 per cent Fe; 0.04 per cent Mn).

Chemical Maturity

Silicon-aluminum-iron ratio (Dennen and Moore, 1971). When normalized silicon (Si = 100-Al-Fe) is plotted against aluminum/iron ratio of the Sturt Tillite and its overlying Tindelpina Shale (Fig. 25), clustering of data points occur within the zone of Al/Fe = 1.9 ± 0.4 as defined by Dennen and Moore (op. cit.). These data points fall within the compositional range of graywacke and shale. The Tindelpina Shale has lower normalized silicon content than Sturt Tillite. This difference may be explained as being due to the different hydraulic factors affecting

Reproduced with permission of the copyright owner. Further reproduction prohibited without permission.

Figure 24

Iron and manganese concentrations of continental glacial clays and glacial marine sediments (suggested by Frakes, 1973, pers. comm.).

Reproduced with permission of the copyright owner. Further reproduction prohibited without permission.

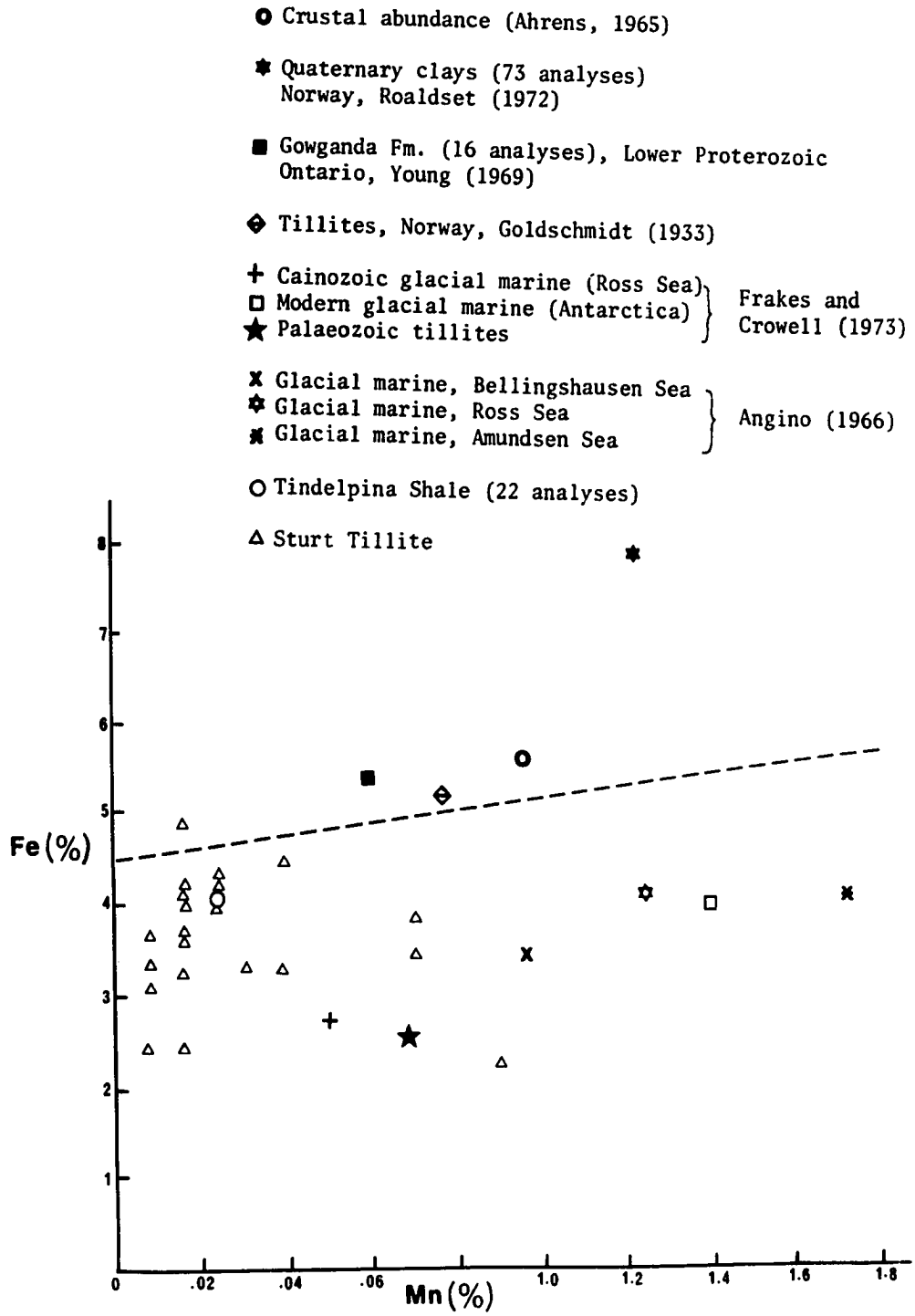

Reproduced with permission of the copyright owner. Further reproduction prohibited without permission.

Figure 25

Plots of normalized silicon content (Si = 100 - Fe - Al) against aluminum/iron ratios after a method of Dennen and Moore (1971). Arrows indicate direction of progressive maturity. Stippled lines show the range of the aluminum/iron ratios of 1.9 ± 0.4.

Reproduced with permission of the copyright owner. Further reproduction prohibited without permission.

Reproduced with permission of the copyright owner. Further reproduction prohibited without permission.

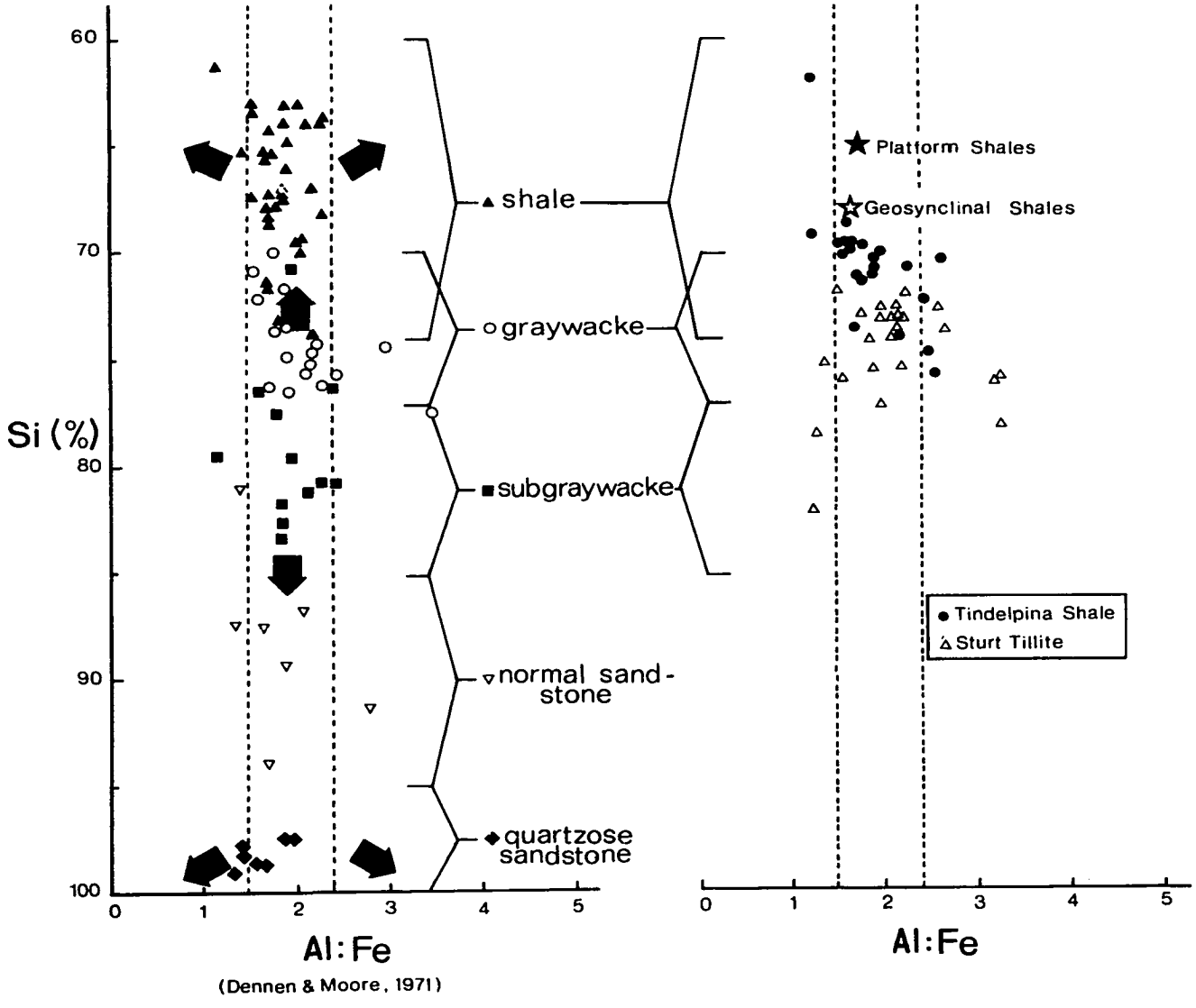

(Dennen & Moore, 1971)

those two rock units during their deposition and also due to their difference in grain size.

In their concept of maturity of sediments Dennen and Moore made several assumptions to interpret the diagram which they constructed:

1. First generation sediments tend to have a composition similar to graywacke and subgraywacke.

2. When $Al/Fe = 1.9 \pm 0.4$, maturity is attained.

3. Initial recycling maintains the aluminum/iron ratio at maturity value but increases or decreases the content of normalized silicon.

4. The aluminum/iron ratio departs significantly from 1.9 ± 0.4 at either high (greater than 90 per cent) or lower (less than 70 per cent) normalizes silicon content.

Thus, rocks such as arkose ($Al/Fe > 2.3$) are considered "immature" due to their contents of feldspars and micas which have not been chemically degraded. Arkose may be considered as the transitional product of the sedimentary process and has a composition between granite ($Al/Fe \approx 4$; $Si \approx 80$ per cent) and subgraywacke ($Al/Fe \approx 1.9$; $Si \approx 80$). Continued cycling, however, will produce either ferruginous sandstones ($Al/Fe < 1.5$; $Si > 90$ per cent) or aluminous shales ($Al/Fe > 2.4$; $Si < 70$ per cent). This progressive course of maturity is shown by the arrows in Figure 25.

On the basis of this principle, plots of the Sturt Tillite and the Tindelpina Shale suggest that their source material is of granitic composition. The Tindelpina Shale generally has aluminum/iron ratios of less than 1.9 whereas the Sturt Tillite has a ratio greater than

Reproduced with permission of the copyright owner. Further reproduction prohibited without permission.

1.9. Plots of most Tindelpina Shale samples (Fig. 23b) fall in the compositional range of graywacke-shale indicating their somewhat mature nature.

Vogt Index. Calculations of Vogt indices (see p. 26) for samples of the Sturt Tillite and its overlying Tindelpina Shale give the following results:

TABLE 22

Vogt Index

	No. of samples	Average Vogt Index	Std. Dev.	Range
Tindelpina Shale	23	1.62	0.92	0.11 - 3.78
Sturt Tillite	25	2.06	0.79	0.73 - 4.20

U.G.S. reference rocks

Peridotite	PCC-1	0.01	Granite	G-2	1.63
Basalt	BCR-1	0.59	Granodiorite	GSP-1	1.96
Andesite	AGV-1	1.01			

At the 95 per cent confidence level t-test, although not very rigorous, shows that there is no significant difference between the Vogt indices of the Sturt Tillite and the Tindelpina Shale. This lack of difference suggests that they either have similar residual character or similar chemistry. It is difficult to interpret the results of calculations of the Vogt indices when the calcium present comes mainly from carbonate rather than from plagioclase.

Reproduced with permission of the copyright owner. Further reproduction prohibited without permission.

VII.3. Statistics

Trend Surface Analysis

Results of trend surface analysis of selected geochemical and mineralogical variables are presented in Figures 27 to 37. The significance of each trend surface is indicated by the percentage of goodness of fit and the F value calculated from analysis of variance. As will be shown, the goodness-of-fit values are generally low, and the F values indicate that the trends generally do not have high significance levels. In spite of this, geologic interpretation may still be made (Harbaugh and Merriam, 1968, p. 68; Tinkler, 1969). The F value only tests whether there is a significant difference between the calculated and the observed values of the variables. If there is no significant difference, it only means that the variation of the data as shown by the trend surfaces is not distinct. In other words, some of the trends shown by the polynomial surfaces are random. This random situation is to be expected from a regional study such as this. Thus, the trends which are shown in the following figures may still be "qualitatively" meaningful.

As previously mentioned (p. 42), no residuals were contoured although they were calculated. The decision whether the trend should be described by a first, second, or higher order equation in a particular problem has not been resolved (Connor and Miesch, 1964). The purpose in this thesis of using trend surface analysis is only to show the

Reproduced with permission of the copyright owner. Further reproduction prohibited without permission.

regional pattern which exists among certain geochemical variables. The choice of surface (up to third degree) is only arbitrarily and conventionally made.

A simple basis is assumed for the interpretation of trend surfaces. The concentrations of elements of high mobility, such as iron, tend to increase, whereas elements of relatively low solubility or in association with detrital constituents, tend to decrease with distance from their source material. Thus, it is to be expected that elements such as silicon, aluminum, and potassium, and detrital minerals such as quartz and zircon, will show decreasing concentrations away from provenance. Admittedly, this simple basis ignores the contribution from the reworking of the underlying rocks on which the composing materials for the Tindelpina Shale were transported and deposited. However, the underlying sediment is the Sturt Tillite which has been shown to have similar chemistry to that of the Tindelpina Shale. Eleven variables were used to construct trend surfaces to represent the different constituents. They are the Niggli parameters (si, al, fm, alk, and k), K_2O/Na_2O Vogt index, quartz, zircon, adjusted boron, and copper.

The Niggli parameters were used in preference to the raw data obtained from the analyses of major oxides to minimize the effect of the built-in correlations existing among the oxides due to their constant sum (100 per cent). The grouping of oxides having similar properties and the use of molecular proportions for the calculation of Niggli parameters are considered to be more elegant and geochemically

Reproduced with permission of the copyright owner. Further reproduction prohibited without permission.

meaningful methods than the use of raw data. It is emphasized, however, that in this thesis the calculation of these parameters does not have any petrogenic implication as it would in igneous petrology (Johannsen, 1931, p. 104; Barth, 1962, p. 63).

The following are the formulas used to calculate the Niggli parameters; all oxides are expressed in molecular proportions (weight per cent divided by molecular weight).

$$si = (SiO_2/TOTAL) \times 100$$

$$al = (Al_2O_3/TOTAL) \times 100$$

$$fm = (2Fe_2O_3+MgO+MnO)/TOTAL \times 100$$

$$mg = MgO/(2Fe_2O_3+MgO+MnO)$$

$$c = (CaO/TOTAL) \times 100$$

$$alk = (Na_2O+K_2O)/TOTAL \times 100$$

$$k = K_2O/(MgO+K_2O)$$

$$TOTAL = Al_2O_3 + 2Fe_2O_3 + MgO + MnO + CaO + Na_2O + K_2O$$

Interpretation of trend surfaces. Only the area indicated in Figure 26 was used to construct the trend surfaces of the Tindelpina Shale.

si. First, second, and third degree surfaces show the trend of si to decrease northward (Fig. 27); si mainly represents detrital quartz, thus decreasing si may be associated with increasing distance from provenance. The second degree surface indicates the northeasterly direction of decreasing si, deflecting towards the northwest and the east. However, second degree surface is not statistically significant. The

Reproduced with permission of the copyright owner. Further reproduction prohibited without permission.

Figure 26

Area covered by trend surface analysis (indicated by stippled lines).

Reproduced with permission of the copyright owner. Further reproduction prohibited without permission.

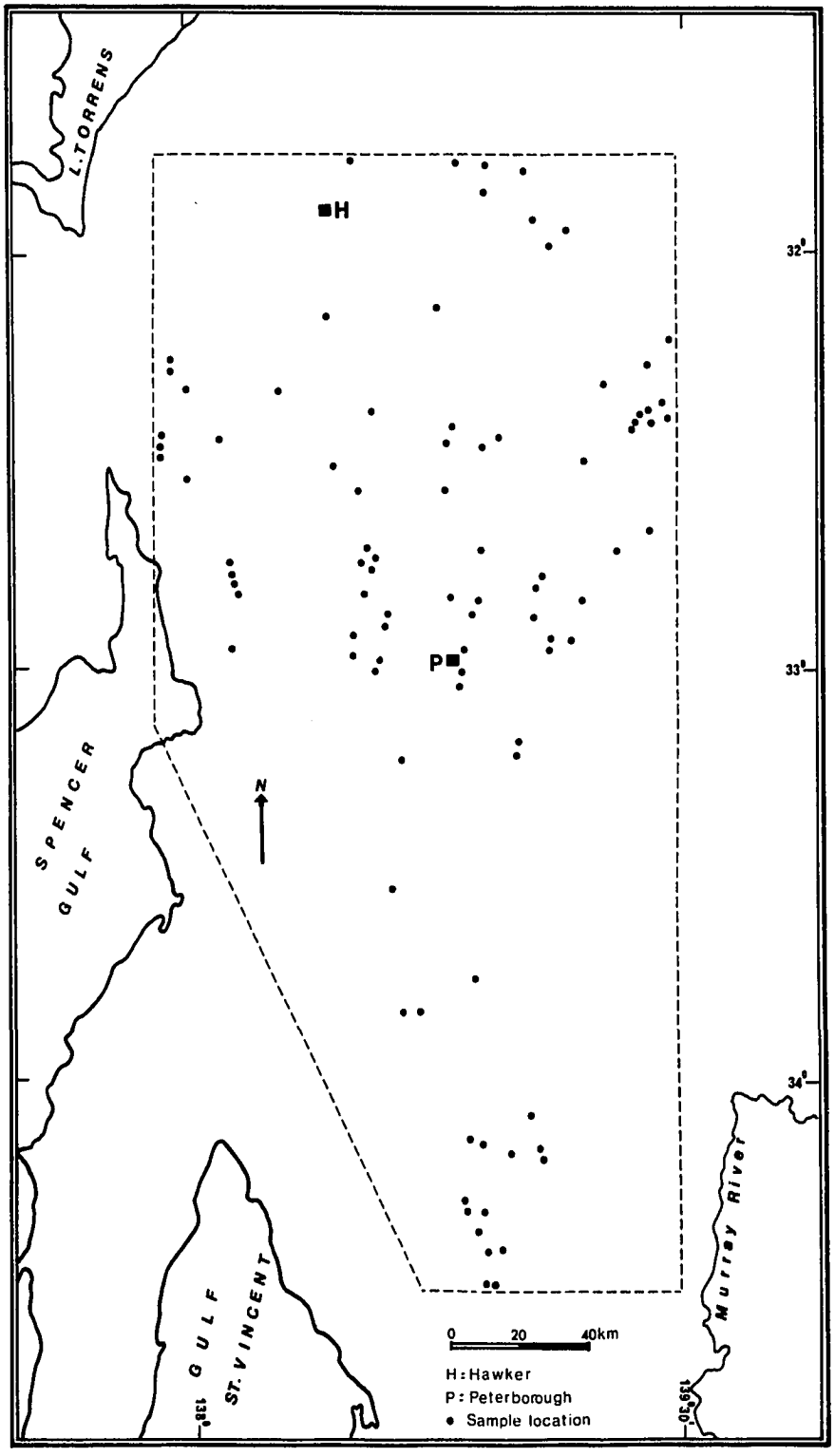

Reproduced with permission of the copyright owner. Further reproduction prohibited without permission.

Reproduced with permission of the copyright owner. Further reproduction prohibited without permission.

Figure 27

Trend surfaces of si (raw data)

Analysis of variance:

	Sum of squares	Degrees of freedom	Mean Square	F	Confidence level
Total	653243.8715	91			
Linear	23904.1034	2	11952.0517	1.69	80%
Residual	629339.7681	89	7071.2334		
Quadratic	10784.1354	3	3594.7118	.50	not significant
Residual	618555.6327	86	7192.5074		
Cubic	44053.9866	4	11013.4967	1.57	80%
Residual	574501.6461	82	7006.1176		

Goodness of fit: Linear 3.66 per cent
Quadratic 5.31 per cent
Cubic 12.05 per cent

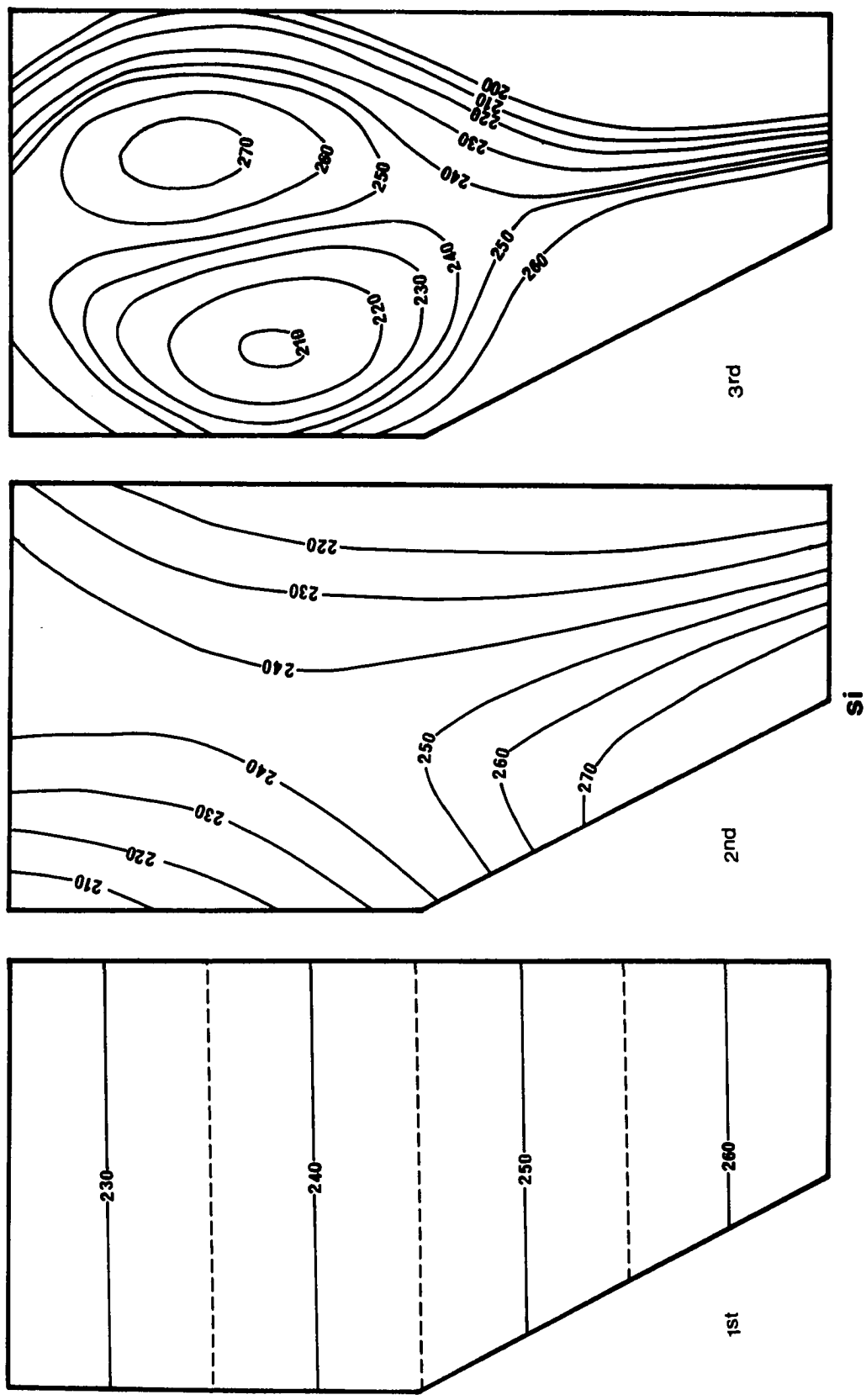

Reproduced with permission of the copyright owner. Further reproduction prohibited without permission.

third degree surface indicates two opposing directions side by side, northerly on the western side and southerly on the eastern side. The southerly trend in the east suggests that the southeastern portion of the area is the deeper part of the geosyncline, and that there was no landmass on this side during the deposition of the Tindelpina Shale.

al. As expected, al shows a very similar trend surface pattern (Fig. 28) to si as indicated by their high correlation coefficient. On the third order surface, there is a depression on the western side of the area and a high on the east. These suggest the possible presence of a source area to the northwest and southwest as well as minor source area in the eastern part of the geosyncline. The decreasing trend toward the southeast suggests the topographically low area in the southeast during the deposition of the Tindelpina Shale.

fm. This Niggli parameter represents combined iron, magnesium, and manganese. In the original usage in igneous petrology, this parameter is associated mainly with the ferromagnesiam minerals which crystallize early during the solidification of igneous rocks. In the case of the Tindelpina Shale, fm mainly represents iron which occurs either as pyrite or as iron oxides. The first order surface shows the southeasterly decrease of fm (Fig. 29). This pattern resolves into a southerly decrease on the western side of the area and a northerly decrease on the eastern side as shown by the second and third order surfaces. As was mentioned earlier, iron tends to be more concentrated in marine than in continental environment. The trends of fm suggest the southwestern location of source material and a minor contribution from the northeastern provenance.

Reproduced with permission of the copyright owner. Further reproduction prohibited without permission.

Reproduced with permission of the copyright owner. Further reproduction prohibited without permission.

Figure 28

Trend surfaces of al (raw data)

Analysis of variance:

	Sum of squares	Degree of freedom	Mean Square	F	Confidence level
Total	13977.7093	91			
Linear	692.4436	2	346.2218	2.32	90.0%
Residual	13285.2657	89	149.2727		
Quadratic	242.1602	3	80.7201	.53	not significant
Residual	13043.1056	86	151.6640		
Cubic	1032.4344	4	258.1086	1.05	not significant
Residual	12010.6712	82	146.4716		

Goodness of fit: Linear 4.95 per cent
Quadratic 6.69 per cent
Cubic 14.07 per cent

Reproduced with permission of the copyright owner. Further reproduction prohibited without permission.

Reproduced with permission of the copyright owner. Further reproduction prohibited without permission.

Figure 29

Trend surfaces of fm (raw data)

Analysis of variance:

	Sum of squares	Degree of freedom	Mean Square	F	Confidence level
Total	2.2648				
Linear	.2600	2	.12999	5.77	99%
Residual	2.0048	89	.02253		
Quadratic	.1244	3	.04145	1.90	85%
Residual	1.8804	86	.02187		
Cubic	.0854	4	.02136	.98	not significant
Residual	1.7950	82	.02189		

Goodness of fit: Linear 11.48 per cent
Quadratic 16.97 per cent
Cubic 20.74 per cent

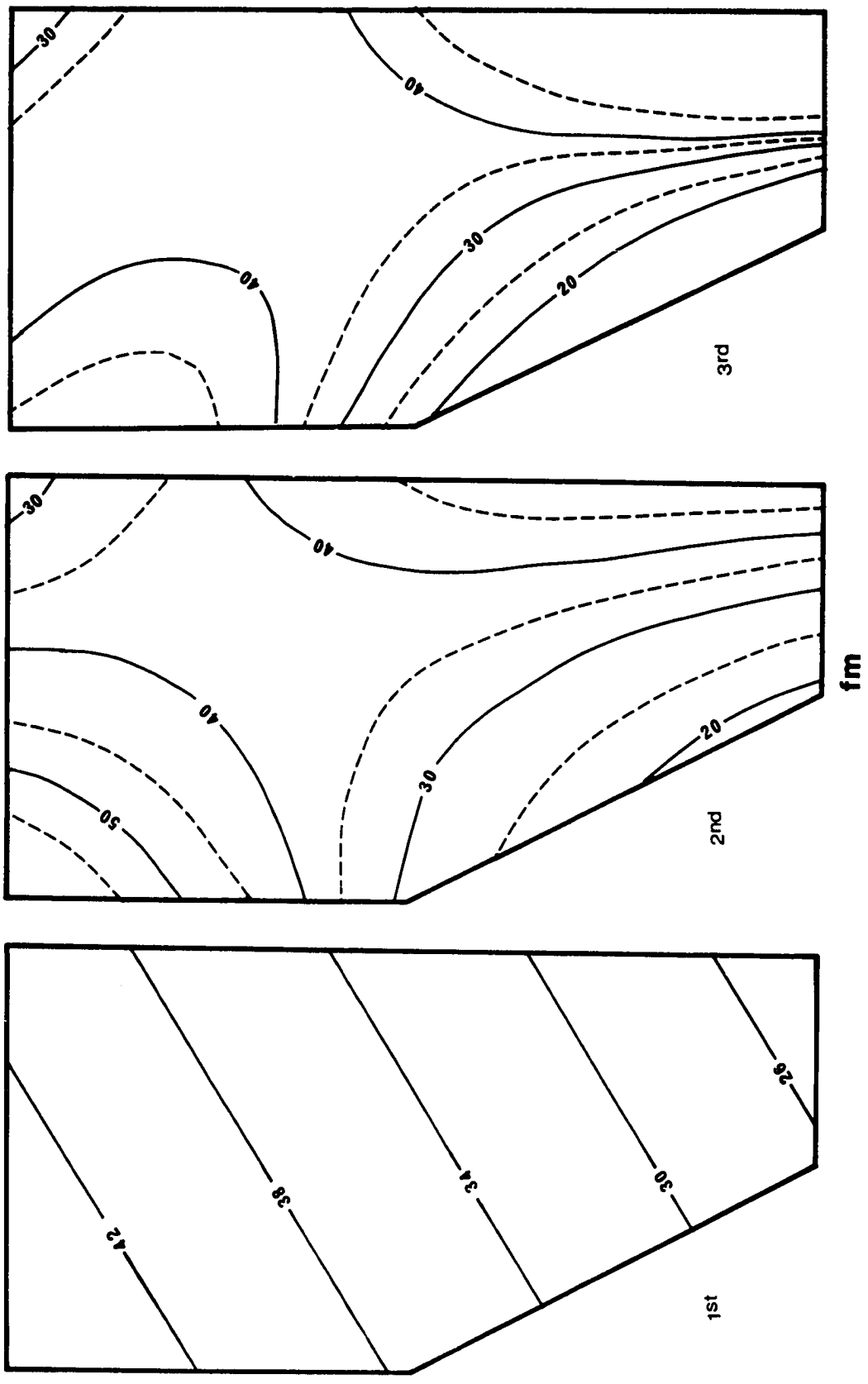

Reproduced with permission of the copyright owner. Further reproduction prohibited without permission.

alk. The parameter alk which represents the relative molecular proportion of the alkalies is dominated by potassium content. The general patterns of the first, second, and third degree surfaces are similar to the trend surfaces of the other parameters (Fig. 30). The interpretation of this parameter is the same as for the others. The northerly decrease on the western side, and southeasterly decrease on the eastern side of the area, suggest the presence of landmasses to the southwest of the geosyncline and in a high contour area on the northeastern section.

k. This parameter shows decreasing magnitude from the southwest towards the northeast deflecting towards the northwest on the second and third order surfaces (Fig. 31). In addition, the third order surface also shows the southeasterly decrease of k on the eastern part of the area. Since k is mainly associated with muscovite (or previously, detrital illite) the decreasing k values towards the center of the geosyncline indicate the southwestern location of the parent material. Second source area appears to occur at this high contour locality in the northeastern section of the area.

Vogt index. The use of the Vogt index (see p. 92) is meant to show any chemical differentiation in the Tindelpina Shale. The resulting trend surfaces indicate that statistically there is not much difference in the chemical maturity of the Tindelpina Shale across the geosyncline. The existing variation is mainly due to the variation of calcium content. The third order surface suggests the northwestern and southwestern provenance with a high on the northeastern section of the geosyncline. Consistent with

Reproduced with permission of the copyright owner. Further reproduction prohibited without permission.

Reproduced with permission of the copyright owner. Further reproduction prohibited without permission.

Figure 30

Trend surfaces of alk (log transformed data)

Analysis of variance:

	Sum of squares	Degree of freedom	Mean Square	F	Confidence level
Total	2.2496	91			
Linear	.0429	2	.0215	.87	not significant
Residual	2.2067	89	.0248		
Quadratic	.0335	3	.0112	.44	not significant
Residual	2.1733	86	.0253		
Cubic	.1783	4	.0446	1.83	80%
Residual	1.9950	82	.0243		

Goodness of fit: Linear 1.91 per cent
Quadratic 3.40 per cent
Cubic 11.32 per cent

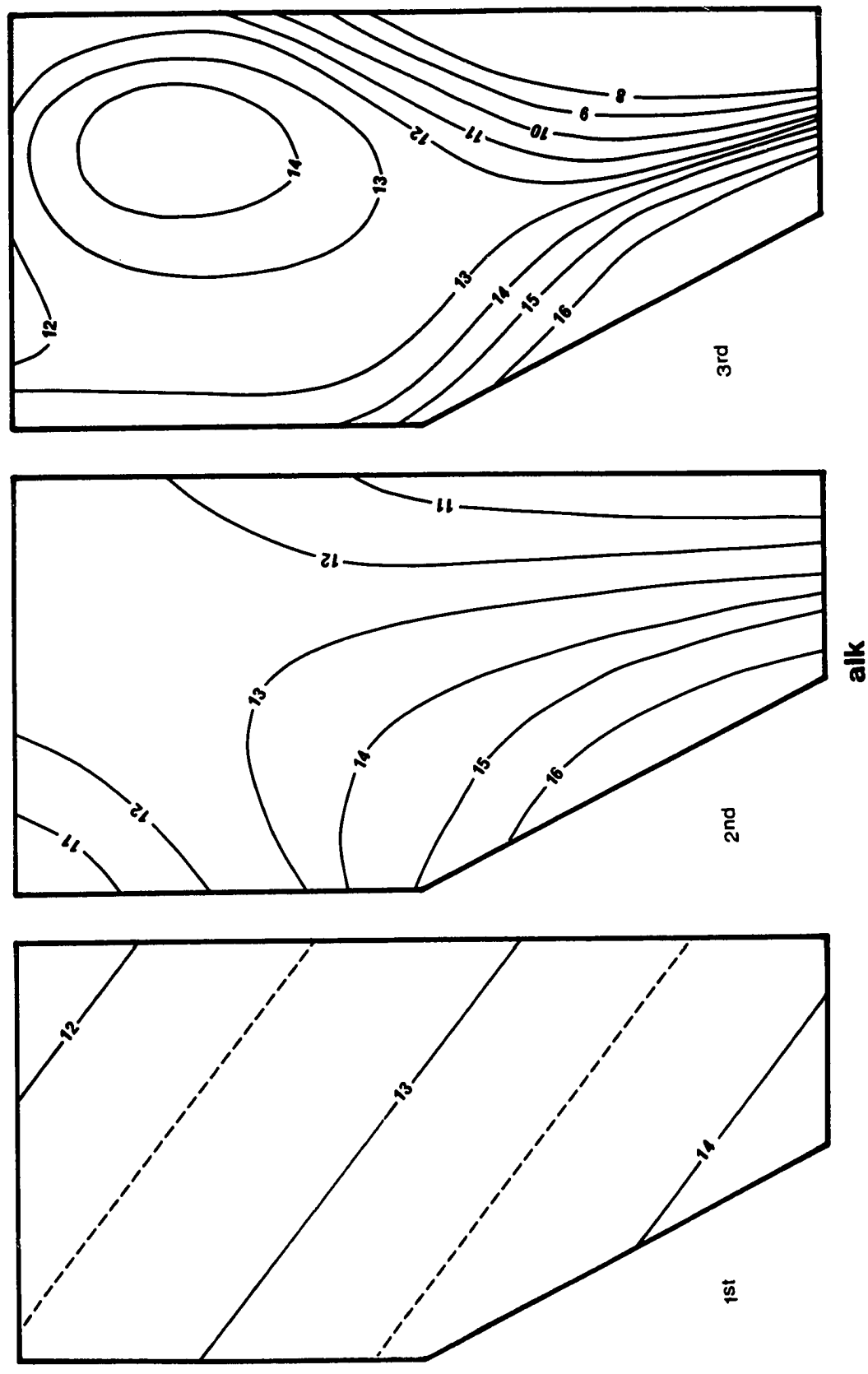

Reproduced with permission of the copyright owner. Further reproduction prohibited without permission.

Reproduced with permission of the copyright owner. Further reproduction prohibited without permission.

Figure 31

Trend surfaces of k (log transformed data)

Analysis of variance:

	Sum of squares	Degree of freedom	Mean Square	F	Confidence level
Total	3.8627	88			
Linear	.1969	2	.0985	2.31	85%
Residual	3.6658	86	.0426		
Quadratic	.1358	3	.0453	1.06	not significant
Residual	3.5299	83	.0425		
Cubic	.2579	4	.0645	1.56	80%
Residual	3.2720	79	.0414		

Goodness of fit: Linear 5.09 per cent
Quadratic 8.62 per cent
Cubic 15.29 per cent

Reproduced with permission of the copyright owner. Further reproduction prohibited without permission.

other trend surfaces, towards the southeast, Vogt indices are decreasing in magnitude, due to increasing carbonate (Fig. 32).

K_2O/Na_2O. Ronov et al. (1966) reported the patterns of K_2O/Na_2O distribution in their study of Russian argillaceous rocks. They found that, in general, the K_2O/Na_2O ratio decreases with increasing distance from the source rock. This was explained as being due to the different mobility of the major elements composing sediments. Thus, sodium, which is more mobile than potassium, will be leached away to a greater extent than potassium, causing a higher K_2O/Na_2O near the provenance.

Trend surfaces of first, second, and third degree suggest the presence of provenance to the west and northwest of the area (Fig. 33).

Quartz. The detrital quartz analyzed in this thesis should show a distribution pattern which indicates decreasing content with increasing distance from the source rock.

The second order surface shows an elongated shape concordant with the pattern of the outcrops of the Tindelpina Shale with a low in the center (Fig. 34). The third order surface resolves the second order surface into a pattern which agrees with the general pattern obtained from other variables. However, F values indicate that these surfaces are due to randomly distributed data. The apparent trends are statistically insignificant.

Zirconium. Only the third degree surface has some significance (Fig. 35). Since zirconium occurs mainly as detrital zircon (see section on factor analysis), then the pattern of the third degree surface suggests

Reproduced with permission of the copyright owner. Further reproduction prohibited without permission.

Reproduced with permission of the copyright owner. Further reproduction prohibited without permission.

Figure 32

Trend surfaces of Vogt Index (raw data)

Analysis of variance:

	Sum of squares	Degree of freedom	Mean Square	F	Confidence level
Total	163.6324	91			
Linear	12.5216	2	6.2608	3.69	95%
Residual	151.1107	89	1.6979		
Quadratic	5.2944	3	1.7648	1.04	not significant
Residual	145.8164	86	1.6955		
Cubic	10.2432	4	2.5608	1.55	80%
Residual	135.5732	82	1.6533		

Goodness of fit: Linear 7.65 per cent
Quadratic 10.89 per cent
Cubic 17.15 per cent

Reproduced with permission of the copyright owner. Further reproduction prohibited without permission.

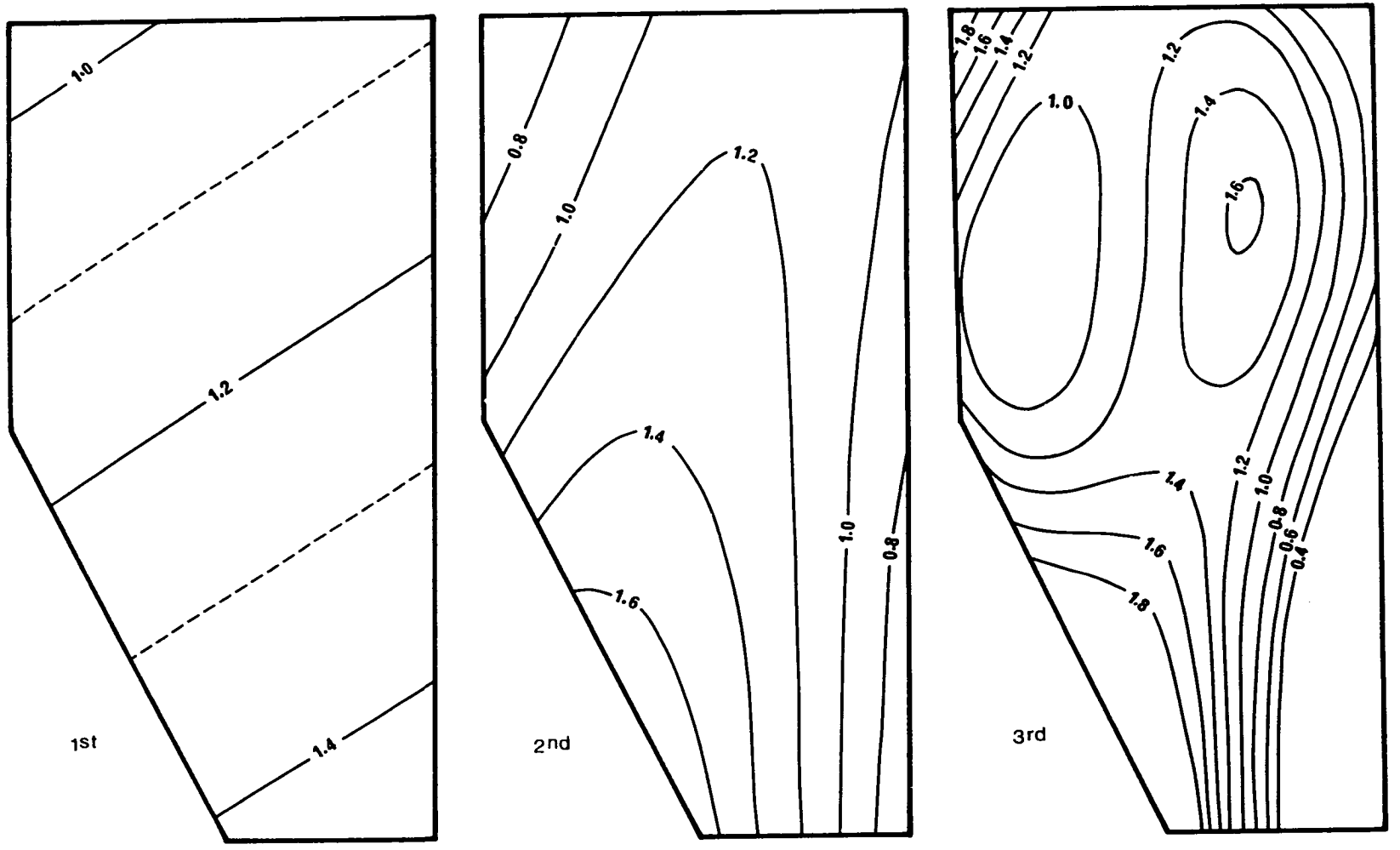

Vogt Index

Reproduced with permission of the copyright owner. Further reproduction prohibited without permission.

Figure 33

Trend surfaces of K_2O/Na_2O (log transformed data)

Analysis of variance:

	Sum of Squares	Degree of freedom	Mean Square	F	Confidence level
Total	14.5238	91			
Linear	.2459	2	.1229	.77	not significant
Residual	14.2780	89	.1604		
Quadratic	.3968	3	.1323	.82	not significant
Residual	13.8812	86	.1614		
Cubic	1.6128	4	.4032	2.69	95%
Residual	12.2684	82	.1496		

Goodness of fit: Linear 1.69 per cent
Quadratic 4.42 per cent
Cubic 15.53 per cent

Reproduced with permission of the copyright owner. Further reproduction prohibited without permission.

Reproduced with permission of the copyright owner. Further reproduction prohibited without permission.

Figure 34

Trend surfaces of quartz (log transformed data)

Analysis of variance:

	Sum of squares	Degree of freedom	Mean Square	F	Confidence level
Total	.9821	91			
Linear	.0112	2	.0056	.51	not significant
Residual	.9709	89	.0109		
Quadratic	.0227	3	.0076	.69	not significant
Residual	.9482	86	.0110		
Cubic	.0584	4	.0146	1.35	75%
Residual	.8898	82	.0109		

Goodness of fit: Linear 1.14 per cent
Quadratic 3.45 per cent
Cubic 9.34 per cent

Reproduced with permission of the copyright owner. Further reproduction prohibited without permission.

Reproduced with permission of the copyright owner. Further reproduction prohibited without permission.

Figure 35

Trend surfaces of Zr (log transformed data)

Analysis of variance:

	Sum of squares	Degree of freedom	Mean Square	F	Confidence level
Total	.8118	91			
Linear	.0017	2	.0008	.09	not significant
Residual	.8101	89	.0091		
Quadratic	.0217	3	.0072	.79	not significant
Residual	.7884	86	.0092		
Cubic	.0610	4	.0152	1.72	80%
Residual	.7275	82	.0089		

Goodness of fit: Linear .21 per cent
Quadratic 2.88 per cent
Cubic 10.39 per cent

Reproduced with permission of the copyright owner. Further reproduction prohibited without permission.

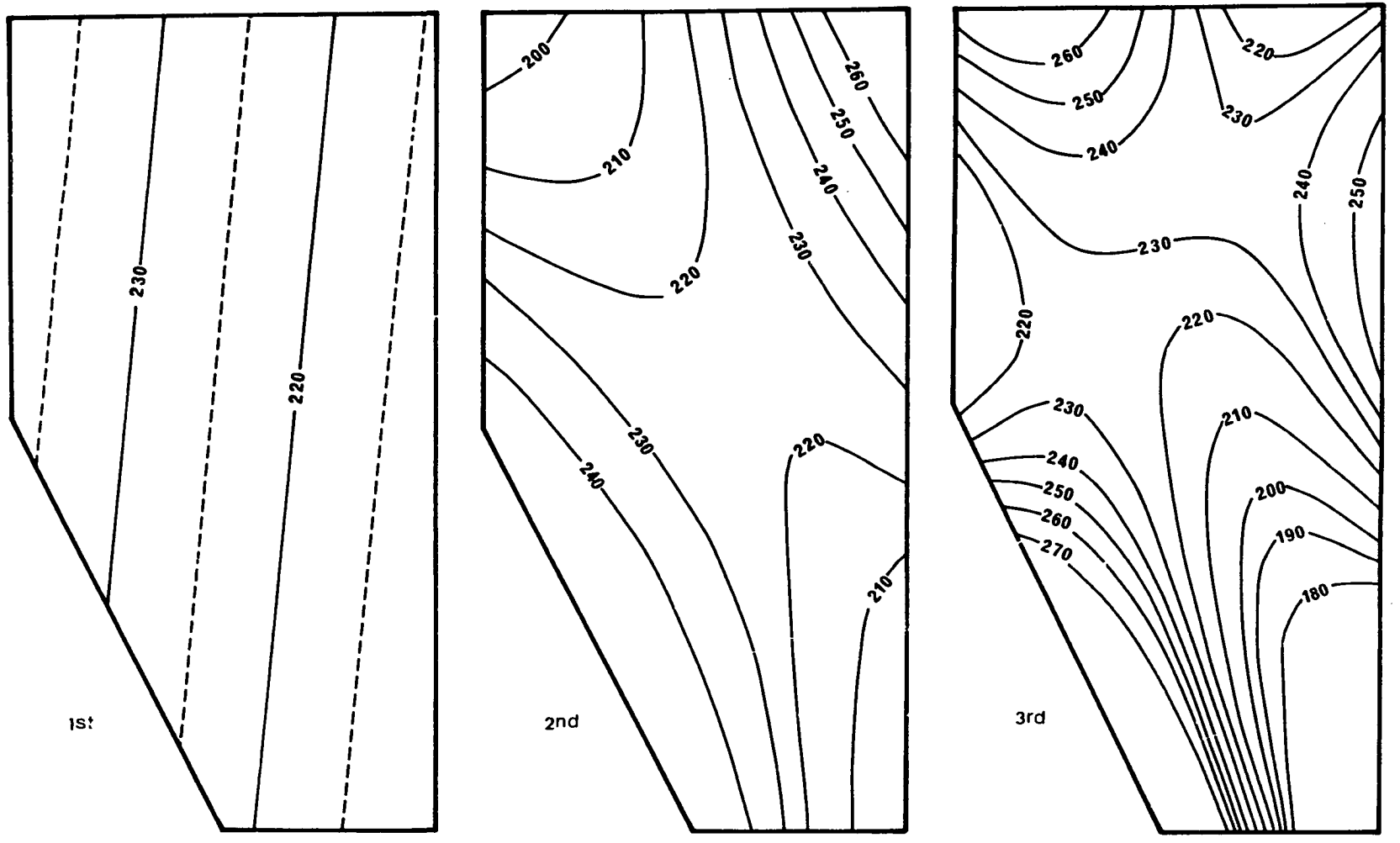

Zirconium

the presence of provenance to the west of the area under study. Decreasing zirconium concentrations to the southeast indicates increasing distance away from the western provenance. The interpretation of zirconium trend surfaces agrees with that of other variables. The contribution of zirconium from the reworking of the underlying sediments is, however, ignored.

Adjusted boron. It should be emphasized that the adjusted boron values calculated for the Tindelpina Shale only indicate the approximate measure of paleosalinity of the seawater in which the Tindelpina Shale was deposited (see p. 67). All surfaces (Fig. 36) show increasing boron contents towards the east, although only the first degree surface is statistically meaningful. The overall patterns suggest the increasing marine condition towards the east, implying the presence of shore line to the west. This means that the main source material for the Tindelpina Shale came from the west, namely, the Gawler Block.

Copper. All trend surfaces for copper statistically have great significance (Fig. 37). However, it is not possible to relate the copper distribution to a single geologic process. The first, second, and third degree surfaces indicate that the high copper contents in the Tindelpina Shale is towards the north in the area of the Parachilna map sheet and towards the south in the Burra and Adelaide sheet areas. It is interesting to note that much of the exploration work in search for stratiform copper deposits has been carried out in the Orroroo-map area, where the trend surfaces indicate the lowest copper concentration.

Reproduced with permission of the copyright owner. Further reproduction prohibited without permission.

Reproduced with permission of the copyright owner. Further reproduction prohibited without permission.

Figure 36

Trend surfaces of boron (raw data)

Analysis of variance:

	Sum of squares	Degree of freedom	Mean Square	F	Confidence level
Total	2118072.0930	85			
Linear	112676.3726	2	56338.1863	2.33	90%
Residual	2005395.7204	83	24161.3942		
Quadratic	24115.9384	3	8038.6461	.32	not significant
Residual	1981279.7821	80	24765.9973		
Cubic	124063.0523	4	31015.7631	1.27	not significant
Residual	1857216.7298	76	24437.0622		

Goodness of fit: Linear 5.32 per cent
Quadratic 6.46 per cent
Cubic 12.32 per cent

Reproduced with permission of the copyright owner. Further reproduction prohibited without permission.

Reproduced with permission of the copyright owner. Further reproduction prohibited without permission.

Figure 37

Trend surfaces of copper (raw data)

Analysis of variance:

	Sum of squares	Degree of freedom	Mean square	F	Confidence level
Total	553588.9886	87			
Linear	35573.1150	2	17786.5575	2.92	90%
Residual	518015.8736	85	6094.3044		
Quadratic	102529.4650	3	34176.4883	6.75	97.5%
Residual	415486.4087	82	5066.9074		
Cubic	157070.9902	4	39267.7475	11.85	99.5%
Residual	258415.4185	78	3313.0182		

Goodness of fit: Linear 6.43 per cent
Quadratic 24.95 per cent
Cubic 53.32 per cent

Reproduced with permission of the copyright owner. Further reproduction prohibited without permission.

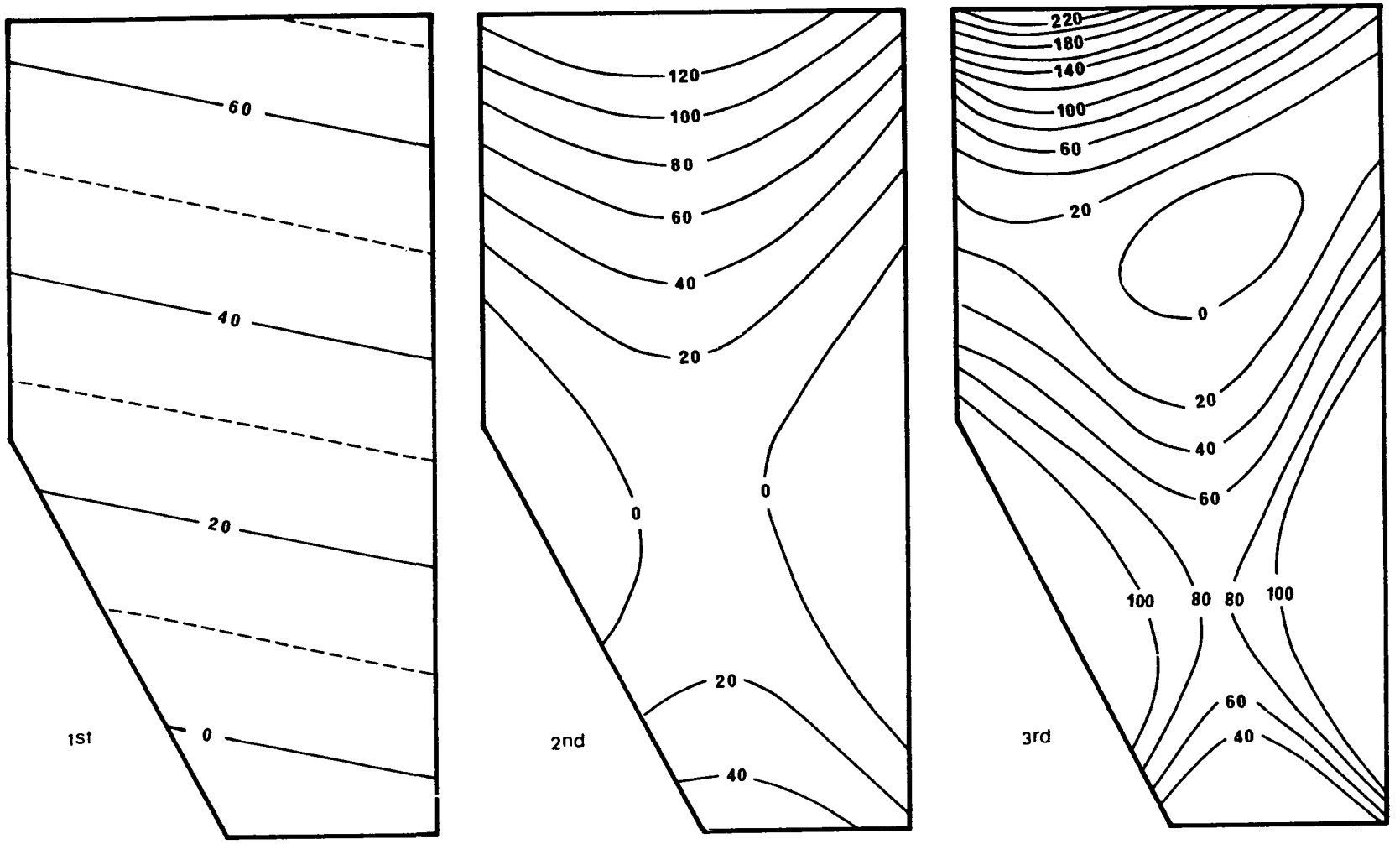

Copper

Factor Analysis

Initially all options of computer output as given in the SPSS program were taken. Later on, only the relevant tables and matrices were required. For clarity, the decimal points of the correlation coefficients and factor loadings are omitted and only up to two significant figures are shown.

It should be emphasized that the interpretation of correlation and factor matrices should be made in conjunction with the knowledge of the distribution of the data, as indicated by their standard deviations. For instance, variables such as titanium, phosphorous, and manganese do not have much variability in their concentrations, and yet in the calculation of the correlation and factor matrices they are given the same weights as the rest of the variables. In other words, the magnitudes of their correlation coefficients and factor loadings should be interpreted as minor in importance to the other variables. The same criteria should also be used for muscovite and chlorite because their percentages are only semi-quantitative estimates.

Coefficients of correlation. Table 23 shows the correlation matrix of 25 variables of raw data obtained from a total of 117 samples. Because of the large number of samples used, the correlation coefficients still have significance even when they are low. The level of significance was determined from a table in Child (1970, p. 95). The correlations among the variables at the 99 per cent significance level are summarized in the following paragraphs.

Reproduced with permission of the copyright owner. Further reproduction prohibited without permission.

Reproduced with permission of the copyright owner. Further reproduction prohibited without permission.

TABLE 23

Correlation Coefficients Among Elements (117 Samples; 25 Variables)

	Si	Al	Fe	Mg	Ca	Na	K	Ti	P	Mn	Ga	Rb	Sr	As	Ba	B	Cr	Cu	Li	Ni	Pb	V	Zn	Zr	Quartz
Si	1.00																								
Al	(0.81)	1.00																							
Fe	-0.04	-0.04	1.00																						
Mg	(-0.50)	(-0.38)	0.10	1.00																					
Ca	(-0.88)	(-0.87)	(-0.24)	(0.23)	1.00																				
Na	(-0.32)	(-0.40)	-0.10	0.10	(0.41)	1.00																			
K	(0.72)	(0.84)	0.02	(-0.32)	(-0.79)	(-0.45)	1.00																		
Ti	(0.70)	(0.88)	-0.03	(-0.30)	(-0.77)	(-0.41)	(0.76)	1.00																	
P	(-0.33)	(-0.30)	(0.36)	(0.26)	(0.21)	(0.26)	-0.19	(-0.22)	1.00																
Mn	(-0.33)	(-0.31)	0.18	0.12	(0.29)	0.13	(-0.28)	(-0.25)	(0.29)	1.00															
Ga	(0.76)	(0.85)	0.05	(-0.29)	(-0.84)	(-0.43)	(0.73)	(0.77)	(-0.32)	(-0.28)	1.00														
Rb	(0.65)	(0.73)	0.17	(-0.29)	(-0.75)	(-0.43)	(0.84)	(0.72)	-0.16	(-0.27)	(0.78)	1.00													
Sr	(-0.68)	(-0.64)	(-0.27)	0.13	(0.79)	(0.37)	(-0.64)	(-0.56)	0.03	(0.22)	(-0.60)	(-0.60)	1.00												
As	0.03	-0.06	0.03	0	-0.04	(-0.23)	0.01	-0.05	0.12	0.03	-0.12	-0.10	-0.13	1.00											
Ba	(0.62)	(0.73)	0.14	(-0.31)	(-0.71)	(-0.26)	(0.60)	(0.73)	(-0.29)	(-0.29)	(0.66)	(0.61)	(-0.51)	(-0.23)	1.00										
B	(0.48)	(0.62)	0.16	(-0.26)	(-0.59)	(-0.35)	(0.60)	(0.62)	-0.05	(-0.27)	(0.56)	(0.64)	(-0.46)	-0.15	(0.54)	1.00									
Cr	0.17	-0.06	(0.33)	-0.09	-0.14	0.01	0.02	-0.14	0.11	0.02	-0.02	0.03	-0.11	-0.05	0.03	0.05	1.00								
Cu	0.11	0.01	-0.12	-0.08	-0.04	(-0.25)	0.10	-0.02	0.01	-0.01	-0.04	-0.08	-0.11	(0.88)	(-0.22)	-0.17	-0.01	1.00							
Li	(0.34)	(0.53)	(0.21)	0.09	(-0.53)	-0.14	(0.35)	(0.50)	-0.01	-0.15	(0.56)	(0.44)	(-0.38)	(-0.25)	(0.47)	(0.43)	0	(-0.30)	1.00						
Ni	0.08	0.16	(0.39)	0.05	(-0.23)	-0.19	(0.24)	0.06	0.18	0.15	0.19	(0.19)	(-0.33)	0.02	-0.01	-0.01	-0.08	0.02	0.17	1.00					
Pb	-0.05	0.10	0.14	0.04	-0.05	-0.05	0.16	(0.21)	0.08	-0.10	0.01	(0.20)	0.04	0.14	0.18	0.16	-0.17	0.03	(0.20)	0	1.00				
V	(0.25)	(0.50)	0.14	-0.15	(-0.40)	-0.19	(0.32)	(0.48)	-0.09	-0.02	(0.45)	(0.36)	(-0.27)	-0.01	(0.42)	(0.38)	-0.18	-0.03	(0.42)	0.13	(0.24)	1.00			
Zn	-0.12	0	(0.62)	0.07	-0.09	-0.05	-0.10	-0.03	0.07	0.12	0.02	-0.01	-0.09	-0.03	0.12	0.06	-0.09	-0.11	(0.25)	(0.36)	0.12	(0.24)	1.00		
Zr	(0.58)	(0.36)	-0.07	(-0.29)	(-0.46)	(-0.23)	(0.27)	(0.37)	(-0.32)	(-0.23)	(0.51)	(0.45)	(-0.35)	0.10	(0.33)	(0.32)	0.14	0.13	0.07	-0.15	-0.07	0.02	-0.15	1.00	
Quartz	(0.55)	(0.26)	0.04	(-0.31)	(-0.42)	(-0.28)	(0.20)	0.13	-0.15	-0.09	(0.40)	(0.26)	(-0.39)	(0.20)	0.15	0.08	(0.21)	(0.22)	-0.01	0.09	(-0.26)	-0.07	-0.10	(0.54)	1.00

Coefficients having values of |0.19| and over are shown in brackets.

$r_{95\%} = 0.19$; $r_{99\%} = 0.26$

Silicon and aluminum. The positive correlations of Si with Al, K, Ti, Ga, Rb, Ba, B, Li, Zr, and quartz are to be expected in the silicate components of the Tindelpina Shale, especially the phyllosilicates. Trace elements Ga, Rb, Ba, B, Li, and V associations with Al and Si indicate their affinity with illite (muscovite). Ti and Zr may occur as inclusions in muscovite and also as detrital components respectively as ilmenite and zircon. It is obvious that detrital quartz is the main dilutent of the Tindelpina Shale. The negative correlations with Mg, Ca, Na, P, Mn, and Sr indicate the presence of carbonate, phosphate, and plagioclase.

Iron. Fe shows weak positive correlations with P, Cr, Ni, and a somewhat stronger correlation with Zn. The presence of iron in sediments is normally covariable with Cr, Ni, and Zn, especially in oxides and pyrite which are the main iron minerals occurring in the Tindelpina Shale. The presence of iron in phosphate (probably apatite) is not an unusual condition in sediments. Weak negative correlation with Sr (and weaker still with Ca) indicate the antipathetic presence of iron minerals with the carbonate.

Magnesium. The very weak positive correlation with P indicates the weak affinity of magnesium with phosphate. The still weaker affinity with Ca indicates the presence of dolomite. Mg has very weak negative correlations with K, Ti, Ga, Rb, Ba, B, Zr, and quartz indicating that the magnesium occurrence is not associated with the silicate components; this implies the Mg-carbonate association.

Reproduced with permission of the copyright owner. Further reproduction prohibited without permission.

Calcium. Ca occurring mainly as a carbonate has positive correlations with Sr and Mn. Its positive correlation with Na indicates a Sr-Na association in plagioclase. The strong negative correlations with the silicate fractions, namely K, Ti, Ga, Rb, Ba, B, Li, Ni, Zr, and quartz is easily understood.

Sodium. This element has weak positive correlations with P and Sr. The presence of Na replacing some of the Ca in phosphate is common, the Na-Sr association in plagioclase is obvious. Moderate negative correlations with the main silicate fraction, namely muscovite (K, Ti, Ga, Rb, Ba, B, and quartz) indicate that Na does not have affinity with muscovite. This was also indicated by the very low paragonite content of muscovite (see p. 53).

Phosphorous. This element has a very weak correlation with Mn. The presence of Mn in phosphate is common. The very weak negative correlations with Ga, Ba, and Zr indicates the antipathetic presence of phosphate with silicate, and the relatively imprecise determination of P in silicate analysis.

Manganese. This element shows only very weak negative associations with Ga, Rb, Ba, and B, indicating that Mn is mainly present not in silicates.

Arsenic and copper. Cu shows a strong positive correlation with one element, namely As. Leaching the samples which contain sulfide mineral (sample numbers 20, 59, 60, 61, 62, and 89) with a cold mixture of H_2O_2 and ascorbic acid did not bring out the presence of Cu and Zn in

Reproduced with permission of the copyright owner. Further reproduction prohibited without permission.

the samples. This leaching is supposed to preferentially dissolve sulphides (Lynch, 1971). This implies that Cu does not occur in the sulphide mineral (pyrite); it should occur in another fraction namely the carbonaceous matter in the Tindelpina Shale.

Lead. This element has a very weak negative correlation with quartz. Probably Pb is associated with the carbonate.

Zirconium. The association of Zr with quartz indicates the detrital nature of these two variables.

Table 24 shows a correlation matrix similar to that in Table 23. The additional variables X, Y, Chlorite, Muscovite, the Kubler Index, and the Weaver sharpness ratio are included, and fewer samples were used. The additional variables which are mineralogical are included with the purpose of correlating them with the geochemical variables.

X-Y coordinates. Moving in an eastwardly direction in the area under study, the concentration of lead and Ni in the Tindelpina Shale seems to decrease, whereas the muscovite content increases. The negative correlation between X-coordinate and the Kubler index indicates the increasing crystallinity of muscovite towards the east. Y correlates weakly and positively with Fe, P, and Ni, indicating the increasing content of iron minerals towards the north. The weak negative correlations of Y with muscovite and the Weaver index indicates the decreasing crystallinity of muscovite toward the north. In other words, the southeastern section of the area under study has muscovite of better crystallinity than the rest of the area. This agrees well with the metamorphic

Reproduced with permission of the copyright owner. Further reproduction prohibited without permission.

Reproduced with permission of the copyright owner. Further reproduction prohibited without permission.

TABLE 24

Correlation Coefficients Among Coordinates, Major Elements, Trace Elements, Principal Minerals, and Metamorphic Index.
(55 Samples; 31 Variables)

	X	Y	Si	Al	Fe	Mg	Ca	Na	K	Ti	P	Mn	Ga	Rb	Sr	As	Ba	B	Cr	Cu	Li	Ni	Pb	V	Zn	Zr	Qtz.	Chl.	Mus.	Kub.	Wea.
X	1.00																														
Y	-0.15	1.00																													
Si	0	-0.03	1.00																												
Al	-0.05	-0.08	(0.79)	1.00																											
Fe	(-0.26)	(0.36)	0.03	0.13	1.00																										
Mg	(-0.29)	0.09	(-0.43)	(-0.32)	(0.52)	1.00																									
Ca	0.13	0.01	(-0.90)	(-0.89)	(-0.31)	0.12	1.00																								
Na	-0.01	-0.08	-0.22	(-0.35)	(-0.30)	-0.05	(0.34)	1.00																							
K	-0.16	0.18	(0.69)	(0.86)	(0.26)	-0.21	(-0.82)	(-0.32)	1.00																						
Ti	-0.15	0.08	(0.70)	(0.89)	0.22	-0.23	(-0.81)	(-0.42)	(0.85)	1.00																					
P	-0.07	(0.46)	(-0.41)	(-0.37)	(0.31)	(0.34)	(0.33)	0.20	-0.21	-0.23	1.00																				
Mn	-0.08	(0.30)	(-0.60)	(-0.65)	-0.10	0.22	(0.69)	0.23	(-0.52)	(-0.45)	(0.44)	1.00																			
Ga	0.05	-0.08	(0.76)	(0.84)	(0.27)	(-0.25)	(-0.85)	(-0.38)	(0.72)	(0.77)	(-0.45)	(-0.65)	1.00																		
Rb	-0.07	0.21	(0.61)	(0.69)	(0.40)	-0.19	(-0.73)	(-0.36)	(0.80)	(0.74)	(-0.25)	(-0.52)	(0.83)	1.00																	
Sr	0.13	-0.20	(-0.61)	(-0.57)	(-0.40)	-0.10	(0.73)	(0.31)	(-0.61)	(-0.52)	0.01	(0.43)	(-0.51)	(-0.54)	1.00																
As	-0.04	0.10	-0.09	(-0.25)	0.06	(0.27)	0.05	-0.21	-0.16	-0.22	(0.33)	0.11	(-0.28)	-0.23	-0.11	1.00															
Ba	-0.02	-0.23	(0.68)	(0.79)	0	(-0.30)	(-0.74)	-0.18	(0.72)	(0.74)	(-0.46)	(-0.68)	(0.72)	(0.61)	(-0.47)	(-0.36)	1.00														
B	-0.11	0.14	(0.54)	(0.72)	0.17	-0.24	(-0.64)	(-0.33)	(0.70)	(0.76)	-0.21	(-0.47)	(0.66)	(0.69)	(-0.43)	-0.21	(0.56)	1.00													
Cr	-0.09	0.11	(0.29)	0.21	-0.13	-0.13	(-0.25)	0.16	(0.25)	0.10	0	-0.03	0.14	0.12	-0.17	0.06	0.12	0.07	1.00												
Cu	-0.01	0.11	-0.04	-0.20	0.04	0.17	0.04	-0.18	-0.13	-0.19	(0.34)	0.08	-0.24	-0.22	-0.08	(0.91)	(-0.28)	-0.19	0.14	1.00											
Li	-0.22	-0.11	(0.38)	(0.61)	(0.52)	0.10	(-0.61)	-0.24	(0.52)	(0.54)	(-0.25)	(-0.51)	(0.64)	(0.59)	(-0.36)	(-0.34)	(0.49)	(0.54)	0.10	(-0.29)	1.00										
Ni	(-0.39)	(0.37)	0.02	0.10	(0.74)	(0.43)	-0.22	(-0.29)	0.20	0.07	(0.33)	0	0.06	0.18	(-0.39)	0.11	-0.12	0	0.01	0.07	(0.30)	1.00									
Pb	(-0.60)	-0.01	-0.06	0.04	(0.34)	(0.25)	-0.10	-0.21	0.13	0.14	0.04	-0.07	-0.02	0.07	0	0.24	-0.03	0.14	-0.08	(0.25)	(0.27)	(0.26)	1.00								
V	-0.13	-0.01	(0.43)	(0.72)	(0.35)	-0.10	(-0.62)	(-0.37)	(0.68)	(0.68)	-0.16	(-0.50)	(0.64)	(0.57)	(-0.36)	-0.11	(0.53)	(0.63)	0	-0.13	(0.66)	0.20	(0.32)	1.00							
Zn	-0.21	-0.15	0.04	0.19	(0.54)	(0.26)	-0.21	-0.18	0.06	0.12	-0.05	(-0.28)	0.22	0.22	-0.18	-0.17	0.15	0.09	-0.16	-0.10	(0.56)	(0.43)	(0.34)	0.21	1.00						
Zr	0.15	0.02	(0.65)	(0.36)	-0.05	(-0.37)	(-0.49)	-0.20	(0.28)	(0.34)	(-0.33)	(-0.28)	(0.60)	(0.51)	(-0.36)	0.08	(0.28)	(0.35)	0.24	0.14	0.06	-0.07	-0.19	0.08	-0.07	1.00					
Qtz.	0.20	-0.05	(0.50)	0.14	-0.05	-0.20	(-0.35)	-0.19	0.03	0.02	-0.18	(-0.29)	(0.37)	0.20	(-0.29)	0.19	0.08	0.05	0.21	0.19	-0.06	-0.07	(-0.27)	-0.11	-0.12	(0.65)	1.00				
Chl.	(-0.29)	0.24	-0.01	-0.17	(0.42)	(0.44)	-0.05	-0.24	-0.13	-0.10	(0.26)	0.10	-0.10	-0.06	-0.15	(0.41)	-0.22	-0.19	0.02	(0.47)	0.04	(0.41)	(0.41)	-0.03	0.24	0.07	0.09	1.00			
Mus.	(0.37)	(-0.42)	0.10	0.24	(-0.40)	(-0.33)	-0.03	-0.16	0.11	(0.25)	(-0.41)	-0.11	0.20	0.08	0.15	-0.23	(0.27)	0.17	-0.24	(-0.28)	-0.08	(-0.43)	-0.23	0.07	-0.12	0.07	-0.09	(-0.57)	1.00		
Kub.	(-0.50)	(0.26)	-0.19	(-0.25)	0.21	0.11	0.21	0.24	-0.14	-0.17	0.14	(0.33)	-0.23	-0.15	0.06	-0.21	-0.16	-0.20	0.01	-0.16	0.03	(0.25)	0.04	(-0.28)	0.18	-0.15	-0.16	0.13	(-0.28)	1.00	
Wea.	0.22	(-0.35)	(0.28)	(0.33)	(-0.35)	-0.19	(-0.29)	-0.15	0.18	(0.28)	(-0.39)	(-0.35)	(0.31)	0.16	-0.12	0.01	(0.26)	(0.31)	-0.02	-0.21	-0.01	(-0.37)	-0.12	(0.25)	(-0.35)	0.19	0.23	(-0.32)	(0.40)	(-0.68)	1.00

Coefficients having values of |0.25| and over are shown in brackets.

$r_{95\%} = 0.25$; $r_{99\%} = 0.33$

Qtz. = quartz, Chl. = chlorite, Mus. = muscovite, Kub. = Kubler index, Wea. = Weaver sharpness-ratio.

grade of this area which borders the area of high grade metamorphism (Offler and Fleming, 1968).

Chlorite. The chlorite correlation with Fe, Mg, As, Cu, Ni, and Pb is due to the common association of this phyllosilicate with those elements (Goldschmidt, 1954).

Muscovite. Muscovite correlates negatively with Fe, P, Ni, and chlorite.

The matrices of correlation coefficients presented previously only show the coherence of the mineralogical and geochemical variables. With a high number of variables, the interpretation of correlation matrices may not be easy. In addition, it is difficult to relate the correlation matrix to physical processes. Because of these difficulties, the simplification of the correlation matrix into a factor matrix is imperative.

Factor loadings. R-mode factor analysis of the 25 variables produced statistically six meaningful factors which account for 72 per cent of the total variance of the data (Table 25). Factors are considered meaningful on the basis of the magnitude of the eigen value with a cut-off point of greater than 1.0000 (in the present case it is 1.0881). Thus, factors which produce eigen values less than 1.0000 are ignored (see Rummel, 1970, p. 359). Table 26 shows the recalculation of the variances using these chosen six factors.

The communality of each variable accounted for by each of the six factors is shown in Table 27. The magnitude of the communalities

Reproduced with permission of the copyright owner. Further reproduction prohibited without permission.

TABLE 25

Factor	Eigen Value	Variance per cent	Cumulative per cent
1	8.7999	35.2	35.2
2	2.7964	11.2	46.4
3	2.3011	9.2	55.6
4	1.8179	7.3	62.9
5	1.1962	4.8	67.6
6	1.0881	4.4	72.0

TABLE 26

Factor	Eigen Value	Variance per cent	Cumulative per cent
1	8.5481	53.8	53.8
2	2.4783	15.6	69.3
3	2.0558	12.9	82.3
4	1.4317	9.0	91.3
5	0.7130	4.5	95.8
6	0.6742	4.2	100.0

Reproduced with permission of the copyright owner. Further reproduction prohibited without permission.

TABLE 27

Variables	Communality
Si	0.8940
Al	0.9281
Fe	0.9971
Mg	0.2348
Ca	0.9289
Na	0.2942
K	0.8462
Ti	0.8410
P	0.4397
Mn	0.1863
Ga	0.8526
Rb	0.7453
Sr	0.6748
As	0.9239
Ba	0.7032
B	0.5624
Cr	0.3911
Cu	0.8706
Li	0.4771
Ni	0.5328
Pb	0.3222
V	0.4154
Zn	0.6631
Zr	0.5278
Quartz	0.6488

Reproduced with permission of the copyright owner. Further reproduction prohibited without permission.

indicates to some extent the strength of the relationships between variables and factors. For example, Mg, Na, Mn, Cr, and Pb do not have factor loadings as high as those of other variables.

The initial factor loadings accounted for by the six orthogonal factors are shown in Table 28. Orthogonal (varimax) rotation produced Table 29 showing "cleaner" loadings. Some loadings are maximized, others are reduced. However, with the orthogonal rotation, the six factors are still uncorrelated. For this reason, further oblique rotation was necessary (Spencer and Degens, 1968). The result is shown in Table 30, on which the geologic interpretation of each factor is based. Table 31 is the correlation matrix showing the relationship between variables and factors.

Factor 1

Statistically this factor is the most dominant one. Strong associations occur among Si, Al, K, Ti, Ga, Rb, Ba, B, Li, Ni, V, and Zr, with their coherence shown by the magnitudes and sign of their factor loadings. The loadings of these elements indicate the influence of their silicate source materials. Strong loadings of K, Al, and Si suggest the abundance of mica clay minerals which have been converted into muscovite, and less frequently, feldspar. The association of Ga, Rb, Ba, B, Li, Ni, and V with clay minerals has been pointed out by various authors. Feldspar may incorporate a portion of Ga, Rb, Ba, and Li, whereas Zr may occur as discrete particles of the mineral zircon and Ti as either rutile or incorporated into clay minerals.

Reproduced with permission of the copyright owner. Further reproduction prohibited without permission.

TABLE 28

Factor Matrix Using Principal Factor with Iterations
(117 Samples; 25 Variables)

Factors / Variables	1	2	3	4	5	6
Si	(87)	(-30)	-03	(-22)	-02	01
Al	(94)	00	-10	16	-09	-06
Fe	11	(59)	(67)	(-34)	(20)	19
Mg	(-36)	(24)	11	10	00	-16
Ca	(-94)	-01	-15	11	00	05
Na	(-46)	13	(-21)	-10	09	-02
K	(85)	-05	02	16	11	(-29)
Ti	(87)	05	-13	(27)	06	00
P	(-28)	(27)	(35)	-02	(29)	(-29)
Mn	(-33)	15	(20)	-06	-08	-09
Ga	(90)	01	-06	-04	-18	-01
Rb	(84)	08	00	02	14	-10
Sr	(-73)	01	(-30)	13	02	19
As	-04	(-55)	(68)	(36)	11	11
Ba	(76)	19	-18	01	07	(21)
B	(67)	18	-08	05	(25)	05
Cr	04	-05	13	(-50)	(34)	00
Cu	00	(-66)	(57)	(34)	01	04
Li	(52)	(44)	-04	07	-02	00
Ni	17	(29)	(44)	-04	(-35)	(-32)
Pb	11	(22)	07	(42)	(24)	15
V	(45)	(28)	05	(31)	-09	16
Zn	04	(54)	(40)	-01	(-29)	(34)
Zr	(49)	(-39)	-05	(-27)	04	(24)
Quartz	(37)	(-45)	(20)	(-48)	-17	05

For clarity, decimal points are omitted.

Loadings at 95% and 99% significance level are respectively $|0.20|$ and $|0.28|$

Loadings at $|0.20|$ and over are shown in brackets.

Reproduced with permission of the copyright owner. Further reproduction prohibited without permission.

TABLE 29

Varimax Rotated Factor Matrix

Factors / Variables	1	2	3	4	5	6
Si	(79)	09	-08	(-29)	(39)	14
Al	(93)	-01	00	00	(20)	-17
Fe	13	00	(76)	09	(-31)	(55)
Mg	(-28)	-05	07	11	(-37)	-06
Ca	(-92)	-06	-15	14	-14	-13
Na	(-44)	(-26)	-10	07	-09	07
K	(90)	09	-15	02	-03	-01
Ti	(86)	-01	-03	(20)	(20)	-14
P	-16	05	07	13	(-56)	(28)
Mn	(-28)	01	16	-07	(-27)	02
Ga	(86)	-06	10	-16	(25)	-10
Rb	(85)	-04	00	05	09	10
Sr	(-74)	-15	-14	(22)	06	-15
As	-04	(96)	02	07	-02	03
Ba	(70)	(-21)	14	17	(34)	04
B	(67)	-13	03	(24)	14	15
Cr	01	-04	-01	-16	03	(60)
Cu	-01	(93)	-09	-05	03	-06
Li	(55)	(-28)	(26)	16	-05	-06
Ni	(26)	07	(38)	(-28)	(-47)	-13
Pb	15	09	10	(53)	-05	-07
V	(45)	-02	(28)	(27)	-06	(-23)
Zn	01	-05	(80)	09	-09	-08
Zr	(37)	13	-06	(-23)	(52)	(22)
Quartz	(27)	(25)	04	(-59)	(32)	(25)

Reproduced with permission of the copyright owner. Further reproduction prohibited without permission.

TABLE 30

Oblique Factor Pattern Matrix

Factors / Variables	1	2	3	4	5	6
Si	(73)	-07	06	(-22)	15	(32)
Al	(90)	-04	-03	-01	-17	14
Fe	05	(77)	02	10	(53)	(-26)
Mg	-19	04	-05	05	-08	(-36)
Ca	(-88)	-12	-04	11	-13	-08
Na	(-40)	-10	(-26)	05	07	-08
K	(99)	(-23)	-07	02	-03	-16
Ti	(84)	-06	-01	(20)	-13	13
P	-01	00	05	11	(24)	(-62)
Mn	(-25)	14	01	-10	00	(-24)
Ga	(80)	08	-08	-16	-09	(23)
Rb	(86)	-04	-05	06	10	-01
Sr	(-77)	-09	-12	(21)	-13	12
As	-07	05	(97)	16	01	-03
Ba	(59)	16	(-20)	19	06	(31)
B	(64)	02	-12	(26)	16	06
Cr	01	00	-05	-07	(61)	-03
Cu	-03	-07	(93)	03	-07	02
Li	(53)	(23)	(-27)	12	-06	-06
Ni	(34)	(30)	04	(-37)	-19	(-44)
Pb	13	10	13	(52)	-06	-07
V	(38)	(28)	00	(24)	(-23)	08
Zn	-16	(84)	-03	03	-08	07
Zr	(23)	00	12	-13	(25)	(51)
Quartz	17	08	(21)	(-51)	(26)	(33)

Reproduced with permission of the copyright owner. Further reproduction prohibited without permission.

TABLE 31

Oblique Factor Structure Matrix

Factors / Variables	1	2	3	4	5	6
Si	(82)	-02	14	(-25)	(23)	(60)
Al	(94)	12	01	04	-13	(45)
Fe	14	(82)	-01	04	(47)	(-41)
Mg	(-30)	09	-08	08	-12	(-44)
Ca	(-94)	(-27)	-10	12	-18	(-36)
Na	(-46)	-15	(-28)	07	04	(-20)
K	(89)	01	11	04	01	(23)
Ti	(87)	10	-01	(24)	-13	(41)
P	(-20)	14	03	08	20	(-61)
Mn	(-30)	15	00	-10	-01	(-35)
Ga	(88)	20	-03	-12	-03	(48)
Rb	(85)	14	-02	08	12	(29)
Sr	(-75)	(-26)	19	(22)	(-20)	-13
As	-03	00	(94)	00	02	-06
Ba	(73)	(22)	(-20)	(21)	05	(47)
B	(68)	14	-13	(27)	13	(27)
Cr	02	-01	-01	-17	(62)	00
Cu	00	-12	(93)	-11	-03	04
Li	(55)	(37)	(-28)	19	-09	05
Ni	(24)	(47)	08	(-31)	-14	(-39)
Pb	14	16	04	(52)	-15	-07
V	(46)	(35)	-04	(29)	(-27)	12
Zn	04	(80)	-08	06	-13	-19
Zr	(41)	-10	17	(-21)	(31)	(60)
Quartz	(31)	00	(31)	(-59)	(37)	(41)

Reproduced with permission of the copyright owner. Further reproduction prohibited without permission.

Negative loadings shown by Ca, Na, Mn, and Sr indicate the presence of another phase, namely carbonate. The association of Na and Ca suggests the presence of plagioclase (albite).

A dominant factor containing loadings for a large number of variates has been assumed to indicate the effect of sorting during transport and deposition, as well as provenance (Spencer and Degens, 1968). In the present case, it is evident that provenance is the main factor, although sorting during transport and deposition has separated the constituents into predominantly phyllosilicate and detrital quartz fractions. This is also indicated by factor 6 and the correlation coefficient between factors 1 and 6 (Table 32).

Factor 2

Strong positive loadings occur for Fe and Zn with weaker loading for Ni and V. It seems reasonable to associate this factor with the influence of Eh and pH from the depositional environment. Iron in the Tindelpina Shale occurs mainly as authigenic pyrite and iron oxides, and to a lesser extent as chlorite. The occurrence of pyrite and iron oxides in sediments is predominantly controlled by Eh and pH (Krumbein and Garrels, 1952). Ni and V may occur as adsorbed cations in the iron oxides.

The weak positive loading of Li is not clearly understood at this stage. The antipathetic relationship with K may cause K to have a negative sign. These elements are diadochic and may occur in potash feldspar. The formation of iron oxides and sulfide may also be affected by diagenesis processes, as will be indicated by factor 5.

Reproduced with permission of the copyright owner. Further reproduction prohibited without permission.

TABLE 32

Factor Pattern Correlations

Factor	1	2	3	4	5	6
1	1.00					
2	0.21	1.00				
3	0.04	-0.04	1.00			
4	0.02	0.02	-0.16	1.00		
5	0.03	-0.04	0.04	-0.17	1.00	
6	0.34	-0.24	0.02	-0.04	0.05	1.00

Reproduced with permission of the copyright owner. Further reproduction prohibited without permission.

Factor 3

This factor is dominated by positive loadings of As and Cu. In the Tindelpina Shale, many occurrences of copper mineralization have been observed which are generally associated with minor tectonic shearing or formation of small faults. No examples were collected from such occurrences. This disturbance might cause the remobilization of copper accompanied by arsenic forming copper mineralization which as seen today shows secondary alteration of copper carbonates and oxides.

This mineralization is also associated with the presence of quartz veins as shown by the weak positive loadings of quartz. However, the presence of arsenic and copper do not have any significant relation to other variables. These two elements are probably associated with the organic fraction of the Tindelpina Shale, which was not analyzed. If this association does exist, as is generally thought by other investigators (Tourtelot, 1964), then factor 3 can be called a biogenic activity factor because the organic matter may have come from decaying algae.

Negative loadings of Na, Ba, and Li indicates the presence of albite, which is common feldspar in rocks of low green schist facies.

Factor 4

All significant loadings in this factor are weak, with the exception of Ni, Pb, and quartz. This bipolar factor includes negative loadings of quartz, Ni, and Si, which are in opposition to the

Reproduced with permission of the copyright owner. Further reproduction prohibited without permission.

positive loadings of Ti, Sr, B, Pb, and V. The association of B and Sr may suggest the influence of a marine condition during the deposition of the Tindelpina Shale. The association of V, Ti, and P has been reported to occur in a reducing marine environment where black, bituminous shale may be deposited (Baumann, 1964). Pb and Sr may be easily incorporated into the carbonate fraction. The loading of detrital quartz opposing the carbonate fraction may be explained as being due to the fact that quartz is the more important constituent closer to provenance. The importance of quartz decreases away from provenance, as marine influence becomes more important. The weak negative loading of Ni is not understood at this stage.

Factor 4 which accounts for 9.0 per cent of the total data variance may be called the salinity factor because of the loading of boron.

Factor 5

Moderately strong positive loadings of Fe and Cr are to be expected because of their covariability in the sedimentary environment. Fe, which occur in the Tindelpina Shale as pyrite and oxides, may be formed authigenically as a result of diagenetic processes and, at the same time, Cr may be adsorbed. The association of P with Fe may occur in iron phosphate minerals which can be diagenetically formed. Zr and quartz, which show weak positive loadings, may also contribute to this factor by forming authigenic zircon and quartz. For these reasons, factor 5 which accounts for only 4.8 per cent of the total variance (Table 25) is called the diagenetic factor.

Reproduced with permission of the copyright owner. Further reproduction prohibited without permission.

Factor 6

The moderately strong loadings of Si, Zr, and quartz may be best related to the detrital nature of these variables. In turn, this detrital factor may be related to the proximity of the sediments to their provenance, and to sorting during the deposition and transport of the sediments. The occurrence of detrital zircon in fine grained sediments has been reported by Hirst and Kaye (1971). The association of Ga and B may be related to the detrital clay minerals. The choice of factor 6 as the proximity-to-provenance factor is supported by the positive correlations of this factor to the variables Si, Al, K, Ti, Ga, Rb, Ba, B, Zr, and Quartz shown in the factor structure matrix (Table 31). This choice is also supported by the correlation coefficient (0.34) of factor 1 (provenance/sorting) to factor 6 in Table 32.

Tables 33 to 39 are similar to Tables 25 to 32 with the difference that the former are for 31 variables instead of 25. The varimax rotated factors for the 31 variables are not present.

Out of these 31 variables, seven factors were extracted using the same criteria as in the extraction of the six factors for the 25 variables. It is to be expected that by introducing more variables, the number of factors extracted will also change (Tables 33 and 37). In Table 37, it is interesting to note that the first four factors may be interpreted in the same way as those of Table 30 (factors 1, 2, 3, and 6). In other words, these four factors represent

Reproduced with permission of the copyright owner. Further reproduction prohibited without permission.

TABLE 33

Factor	Eigen Value	Variance per cent	Cumulative per cent
1	9.9668	32.2	32.2
2	4.9538	16.0	48.1
3	3.0162	9.7	57.9
4	2.1187	6.8	64.7
5	1.6791	5.4	70.1
6	1.4870	4.8	74.9
7	1.1209	3.6	78.5

TABLE 34

Factor	Eigen Value	Variance per cent	Cumulative per cent
1	9.7753	43.9	43.9
2	4.6343	20.8	64.7
3	2.7566	12.4	77.1
4	1.7893	8.0	85.1
5	1.3923	6.3	91.4
6	1.1648	5.2	96.6
7	0.7557	3.4	100.0

Reproduced with permission of the copyright owner. Further reproduction prohibited without permission.

TABLE 35

Variables	Communality
X	0.6358
Y	0.7280
Si	0.8917
Al	0.9178
Fe	0.9329
Mg	0.5143
Ca	0.9813
Na	0.5439
K	0.9046
Ti	0.8879
P	0.6273
Mn	0.6668
Ga	0.9220
Rb	0.7965
Sr	0.6102
As	0.8791
Ba	0.7460
B	0.6718
Cr	0.3042
Cu	0.7691
Li	0.7562
Ni	0.6325
Pb	0.7273
V	0.7025
Zn	0.6104
Zr	0.7900
Qtz.	0.6664
Chl.	0.5816
Mus.	0.5933
Kub.	0.7182
Wea.	0.5588

Reproduced with permission of the copyright owner. Further reproduction prohibited without permission.

TABLE 36

Factor Matrix Using Principal Factor With Iterations
(55 Samples; 31 Variables)

Factors / Variables	1	2	3	4	5	6	7
X	-05	(-54)	20	-05	-05	(53)	-12
Y	-05	(46)	15	(48)	(46)	20	13
Si	(83)	-11	(30)	22	-12	-18	-03
Al	(94)	-05	-05	-02	11	-08	-09
Fe	25	(83)	-12	-02	-11	(39)	-01
Mg	-27	(57)	-05	-24	-08	14	-18
Ca	(-94)	-14	-18	-03	07	10	17
Na	(-40)	-21	-20	(33)	-03	-24	(-36)
K	(87)	13	-03	11	(34)	-08	-07
Ti	(88)	05	-08	-01	(30)	-05	13
P	(-42)	(46)	13	13	(35)	18	-22
Mn	(-71)	10	-04	21	26	04	20
Ga	(93)	-05	03	05	-17	13	10
Rb	(83)	13	-01	15	06	20	15
Sr	(-62)	(-31)	-26	-13	0	-09	20
As	-24	(29)	(76)	(-36)	14	-09	-02
Ba	(80)	-18	-16	01	-04	-16	-13
B	(76)	01	-08	-01	(28)	01	13
Cr	16	01	24	(31)	05	(-28)	-21
Cu	-21	(31)	(73)	-26	08	-17	01
Li	(66)	(33)	(-38)	-10	-21	0	-10
Ni	11	(76)	-04	08	-06	18	-05
Pb	07	(53)	-10	(-45)	06	(-41)	23
V	(71)	18	-17	(-29)	22	01	-04
Zn	21	(46)	(-34)	-17	(-45)	07	03
Zr	(49)	-17	(53)	(30)	-24	03	(31)
Qtz.	25	-16	(61)	21	(-39)	09	03
Chl.	-11	(64)	(33)	-10	-19	-09	08
Mus.	19	(-62)	-19	-24	09	14	22
Kub.	-25	(37)	(-33)	(53)	-16	-26	19
Wea.	(34)	(-52)	16	(-34)	12	06	-10

For clarity, decimal points are omitted.

Loadings at 95% and 99% significance level are respectively $|0.28|$ and $|0.37|$.

Loadings of $|0.28|$ or over are shown in brackets.

Reproduced with permission of the copyright owner. Further reproduction prohibited without permission.

TABLE 37

Oblique Factor Pattern Matrix
(55 Samples; 31 Variables)

Factors / Variables	1	2	3	4	5	6	7
X	-17	-02	-06	13	-01	(74)	14
Y	20	08	01	04	(84)	-03	-03
Si	(61)	-08	03	(49)	-14	-02	-23
Al	(90)	-02	-08	06	-13	01	-06
Fe	20	(86)	-03	-01	24	0	18
Mg	-17	(56)	20	(-28)	0	-01	02
Ca	(-80)	-19	-09	-24	17	-01	20
Na	(-28)	-14	-27	-24	-06	02	(-53)
K	(98)	-05	-03	-03	16	-05	-10
Ti	(92)	-13	-06	-04	11	-12	13
P	-07	25	22	(-34)	(51)	13	-17
Mn	(-49)	-19	-02	-14	(49)	-12	08
Ga	(64)	15	-17	(41)	-13	08	13
Rb	(70)	15	-17	(29)	18	04	17
Sr	(-57)	(-34)	-13	-18	-08	-13	20
As	-11	-02	(92)	05	05	-01	0
Ba	(70)	-06	-20	06	(-29)	-02	-13
B	(79)	-12	-07	04	12	-06	16
Cr	20	-11	09	12	05	-07	(-46)
Cu	-13	-03	(83)	14	04	-10	-06
Li	(53)	(47)	-26	-05	-26	-14	02
Ni	13	(66)	04	-02	24	-11	0
Pb	19	04	(37)	-21	-18	(-67)	21
V	(80)	11	06	-22	-08	-04	15
Zn	-02	(63)	-20	05	(-30)	-21	16
Zr	11	-14	08	(84)	06	02	06
Qtz.	-12	06	18	(73)	-10	22	-12
Chl.	-17	(39)	(42)	19	-04	(-29)	0
Mus.	12	(-41)	-19	-02	-17	20	(39)
Kub.	(-30)	10	(-43)	14	25	(-54)	-18
Wea.	(33)	(-31)	18	-06	(-29)	(35)	10

Reproduced with permission of the copyright owner. Further reproduction prohibited without permission.

TABLE 38

Oblique Factor Structure Matrix

Factors / Variables	1	2	3	4	5	6	7
X	-11	(-29)	-05	14	-12	(77)	15
Y	06	22	10	04	(82)	-16	-15
Si	(76)	-04	-03	(72)	-26	07	-21
Al	(94)	03	-17	(37)	(-31)	04	04
Fe	26	(91)	08	01	(28)	(-31)	19
Mg	-22	(57)	(28)	(-33)	15	-23	05
Ca	(-91)	-24	-03	(-54)	(28)	01	12
Na	(-39)	-23	-26	-26	04	02	(-52)
K	(93)	08	-10	(28)	-01	-06	-02
Ti	(92)	01	-14	(29)	-10	-08	19
P	(-29)	(29)	(32)	(-36)	(62)	-07	-21
Mn	(-63)	-13	05	(-36)	(56)	-14	-04
Ga	(84)	14	-22	(62)	(-32)	11	17
Rb	(80)	22	-19	(48)	-01	01	18
Sr	(-61)	(-37)	-15	(-41)	-04	-02	17
As	-18	09	(93)	04	17	-01	-05
Ba	(77)	-05	(-30)	(31)	(-43)	05	-02
B	(79)	-01	-14	25	-08	-02	21
Cr	17	-07	08	24	08	-04	(-48)
Cu	-17	10	(85)	11	18	-09	-12
Li	(63)	(50)	(-28)	11	(-31)	-26	14
Ni	14	(74)	14	-01	(33)	(-36)	-01
Pb	15	(31)	(33)	-23	-10	(-67)	25
V	(77)	21	-02	02	-22	-09	(28)
Zn	14	(64)	-16	01	-24	(-37)	21
Zr	(35)	-12	08	(87)	-05	16	-06
Qtz.	11	-02	21	(74)	-11	(30)	-20
Chl.	-12	(53)	(50)	11	20	(-41)	-06
Mus.	16	(-50)	(-28)	0	(-36)	(38)	(44)
Kub.	-27	23	(-35)	-03	(36)	(-60)	(-28)
Wea.	(33)	(-41)	08	10	(-43)	(49)	20

Reproduced with permission of the copyright owner. Further reproduction prohibited without permission.

TABLE 39

Factor Pattern Correlations

Factors	1	2	3	4	5	6	7
1	1.00						
2	0.10	1.00					
3	-0.09	0.12	1.00				
4	0.32	0	0.03	1.00			
5	-0.19	0.14	0.12	-0.07	1.00		
6	0	-0.33	-0.01	0.12	-0.13	1.00	
7	0.10	0.03	-0.03	-0.13	-0.17	0.05	1.00

Reproduced with permission of the copyright owner. Further reproduction prohibited without permission.

respectively provenance/sorting, Eh-pH, biogenic activity, and proximity to source rocks. The effectively unchanged status of these four factors indicates that they are statistically meaningful (Rummel, 1970, p. 359). The meaningful correlation of factors 1 and 4 also still exists (Table 39).

The appearance of weak factor loadings belonging to the variable Chl. (chlorite) and Mus. (muscovite) in factors 2, 3, 6, and 7 should be interpreted with different emphasis from the loadings of the other variables. The association of chlorite with Fe, Mg, Li, and Ni shown in factor 2 is common. However, the association of As, Cu, and Pb with chlorite in factor 3 is not easily understood.

Factors 5 and 6

The appearance of a strong Y-coordinate loading in factor 5 indicates its regional effect on the variance of the data. Thus, positive loadings of Y, P, and Mn indicate the increasing contents of these elements probably occurring as phosphates towards the north. The presence of a negative loading of the metamorphic indicator (Wea.) indicates that the metamorphism affecting the Tindelpina Shale increases towards the south. This has also been indicated by the correlation matrix shown in Table 24.

In factor 6, the association of variables X, Kub. and Wea. indicates the increasing metamorphic effect on the crystallinity of muscovite towards the east. This eastward progressive low-grade metamorphism has also been reported in a joint work by Sumartojo *et al.*

Reproduced with permission of the copyright owner. Further reproduction prohibited without permission.

(1973). It is interesting to note that Pb concentration decreases with increasing metamorphism. Shaw (1954) reported the opposite case where, in the Littleton Formation of New York, Pb increases with increasing metamorphism. He explained this as being due to a metasomatic process on a small scale. This factor also indicates the weak negative loading of Chl. relative to X.

Factor 7

The positive loadings of Na and Cr which oppose muscovite in factor 7, accounting 3.6 per cent (Table 33) of the total data variance is not understood. Statistically, it may be ignored (Rummel, 1970, p. 356).

Reproduced with permission of the copyright owner. Further reproduction prohibited without permission.

VIII. SUMMARY AND CONCLUSION

The Tindelpina Shale is a laminated black shale resembling varve under both megascopic and microscopic examination. The laminations appear as red and green ribbons on weathered surfaces; on fresh surfaces they are alternately dark and light, due to different concentrations of phyllosilicates (muscovite and chlorite) and carbonaceous matter. In the case of the Tindelpina Shale these laminations are thought to be due to seasonal changes during the deposition in a quiet, shallow, marine environment near shore. Cyclic deposition of organic matter was responsible for the carbonaceous laminae.

The mineralogy of the Tindelpina Shale as revealed by X-ray diffraction on the minus two-micron fraction, is simple. The mineral assemblage is composed mainly of quartz, muscovite, and chlorite. This assemblage is typical of the metamorphic grade of the low greenschist facies. In lesser amounts, potash feldspar, plagioclase (albite), and calcite are also present. The basal spacing of muscovite suggests its low paragonite content, and this is indicative of very low stage regional metamorphism. The d_{060} spacing (as well as the b_0 parameter) indicates the phengitic nature of muscovite, and is also characteristic of low grade metamorphism. On the basis of the muscovite crystallinity, the effect of this regional metamorphism has statistically been shown to increase towards the east and towards the south. That is, the highest metamorphic grade of the area under study is in the southeastern section. This conclusion is in general agreement with the findings of Offler and Fleming (1968) whose area of high metamorphic grade (staurolite-andalusite schist) borders the

Reproduced with permission of the copyright owner. Further reproduction prohibited without permission.

southeastern section of the present study. In general, the metamorphism taking place in the Adelaide Geosyncline is related to orogenic events during Late Cambrian to Ordovician times (Thomson, 1969, p. 81). In the case of the Tindelpina Shale, the metamorphic effect is presumably due in part to the depth of burial.

There has been no conclusive evidence of the glacial marine origin of the Sturt Tillite, although one of the pioneer geologists in South Australia, the late Sir Douglas Mawson, suggested the glacial marine nature of this tillite (Dr. A.W. Kleeman, 1973, pers. comm.). On the basis of the boron content, gallium-boron-rubidium ratios, potassium/rubidium ratios, and the iron-manganese contents, it is empirically shown that the Sturt Tillite is a glacial-marine sediment, and that the Tindelpina Shale is a marine shale. The spread of gallium-boron-rubidium ratios towards the non-marine zone in the diagram of Degens et al. (1958) suggests a near-shore depositional environment for the Tindelpina Shale.

Results of major element analyses show that there is essentially no difference between the chemistry of the Tindelpina Shale and the Sturt Tillite with the exception of their contents of lime, magnesia, and silica. The Tindelpina Shale has higher lime and magnesia, and lower silica contents than the Sturt Tillite. This chemical similarity suggests one of the three possible relationships between the Sturt Tillite and the Tindelpina Shale:

1. The source material for the two rock units is the same.

2. The Tindelpina Shale was derived from the Sturt Tillite without undergoing extensive chemical differentiation.

3. The Tindelpina Shale and the Sturt Tillite are time-equivalent units, implying that the Tindelpina Shale is a facies of the

Reproduced with permission of the copyright owner. Further reproduction prohibited without permission.

tillite.

Present-day exposures of the Tindelpina Shale do not allow distinction between cases (1) and (2). The absence of ice-rafted pebbles in the Tindelpina Shale is a strong argument against case (3).

Up to third-order trend surfaces of selected geochemical variables (Niggli parameters si, al, fm, alk,and k, K_2O/Na_2O, Vogt index, quartz, zircon, adjusted boron, and copper) result in similar patterns, consistent with the geometry of the elongated north-south trough of the Adelaide Geosyncline. The degree of significance of each trend surface is indicated by the percentage of goodness-of-fit and the confidence level of the F-test. For those variables which show significant trends, the confidence level is usually better than 80 per cent. Trend surface of copper show north-south distribution in contrast to the other variables which show west-to-east trends. The trend surfaces show that the main contributor to the chemistry of the Tindelpina Shale came from source rocks to the west of the Adelaide Geosyncline, namely the Gawler Block. An eastern provenance, the Williyama Block, acts as a minor contributor. The dispersal pattern of the chemical variables (Fig. 38) suggests the presence of the main shore line in the west with an increasing marine condition towards the east. This pattern agrees well with the general conclusions made by Preiss (1973) who did a paleogeographic study of the Late Precambrian sediments in the Adelaide Geosyncline based on stromatolites.

Factor analysis applied on the 25 variables (Si, Al, Fe, Mg, Ca, Na, K, Ti, P, Mn, Ga, Rb, Sr, As, Ba, B, Cr, Cu, Li, Ni, Pb, V, Zn, Zr, and quartz) reduced the number of these variables into six

Reproduced with permission of the copyright owner. Further reproduction prohibited without permission.

Figure 38

Dispersal pattern of selected geochemical variables during the Tindelpina Shale sedimentation.

H = Hawker

P = Peterborough

Reproduced with permission of the copyright owner. Further reproduction prohibited without permission.

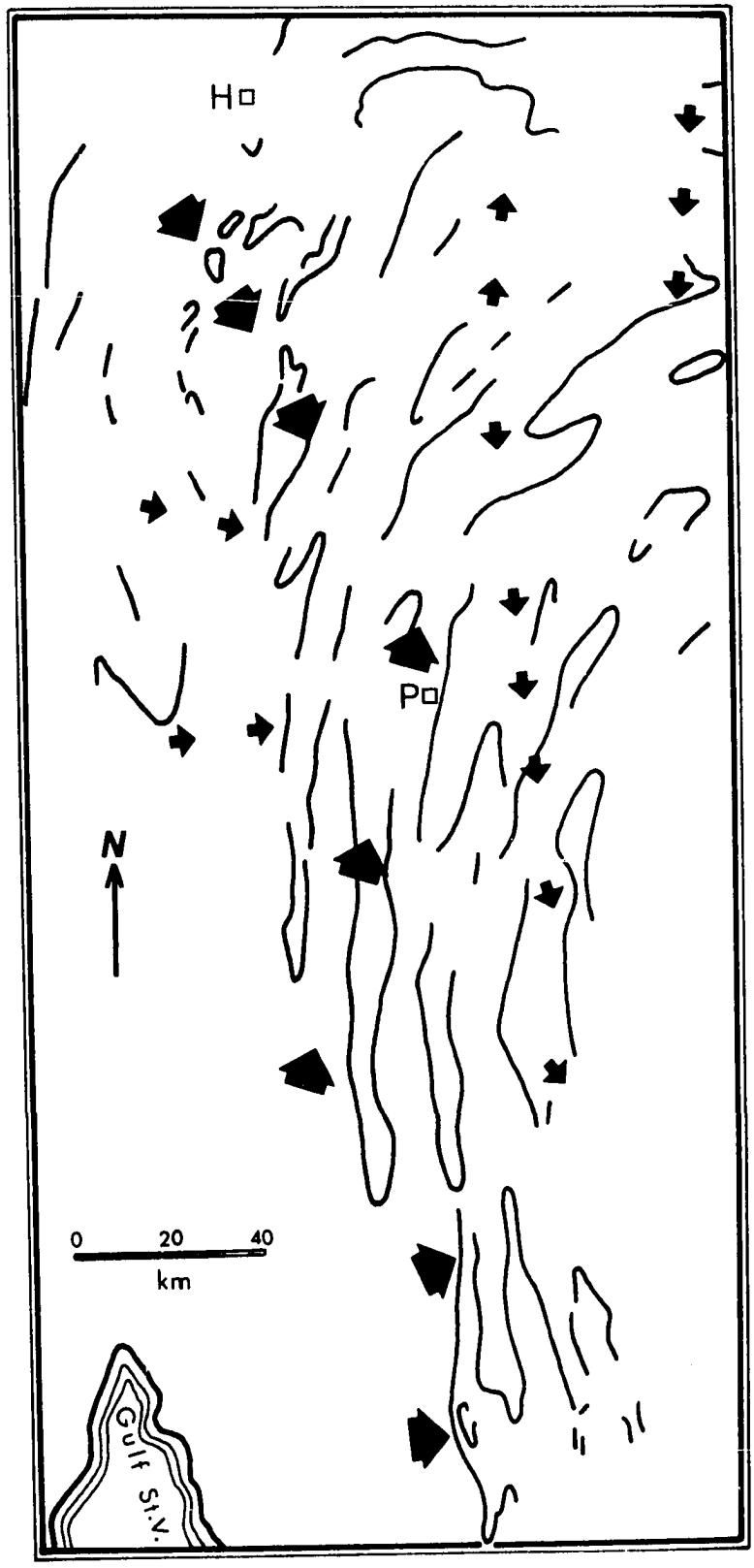

Reproduced with permission of the copyright owner. Further reproduction prohibited without permission.

factors which account for most of the variance among the variables. These six factors are related to provenance/sorting, Eh-pH, biogenic activity, diagenesis, salinity, and proximity to source rocks.

The results of this regional mineralogical and geochemical study provide a basic framework within which more specific studies may be carried out. This framework is therefore both original and useful to South Australian geology. Understanding of the geochemistry and mineralogy of the Adelaide Geosyncline rocks could be expanded by applying the methods used in this study to other stratigraphic horizons.

Reproduced with permission of the copyright owner. Further reproduction prohibited without permission.

REFERENCES

ABBEY, S., 1967, Analysis of rocks and minerals by atomic absorption spectroscopy: Part I, Determination of magnesium, lithium, zinc, and iron. Geol. Survey Canada, Paper 67-37.

ADLER, I., 1966, X-ray Emission Spectrography in Geology: Amsterdam, Elsevier, 258 pp.

AGTERBERG, F.P., 1964, Methods of trend surface analysis: Colo. School Mines Quart., 59, 111-130.

AHRENS, L.H., 1954a, The lognormal distribution of the elements: Geochim. Cosmachim. Acta, 5, 49-73.

_____, 1954b, The lognormal distribution of the elements. II: Geochim. Cosmochim. Acta, 6, 121-131.

_____, 1963, Lognormal-type distribution in igneous rocks IV: Geochim. Cosmochim. Acta, 27, 233-343.

_____, 1965, Distribution of the Elements in our Planet: New York, McGraw Hill.

ANGINO, E.E., 1966, Geochemistry of Antarctic pelagic sediments: Geochim. Cosmochim. Acta, 30, 939-961.

_____, and BILLINGS, G.K., 1967, Atomic Absorption Spectrometry in Geology: Amsterdam, Elsevier Publ. Co., 144 pp.

ARMOUR-BROWN, A. and NICHOL, I., 1970, Regional geochemical reconnaissance and the location of metallogenic provinces: Econ. Geol., 65, 312-330.

Reproduced with permission of the copyright owner. Further reproduction prohibited without permission.

ATAMAN, G., 1967, La géochimie du bore et du gallium dans les minéraux argileux: Chem. Geol., 2, 297-309.

_____ and LUCAS, J., 1968, Relation entre la répartition des éléments dans les minéraux argileux et la paleogeographie Triasique du Jura, in: L.H. AHRENS, Ed., Origin and Distribution of the Elements: New York, Pergamon Press, 1023-1038.

BANNO, S. and CHAPPELL, B.W., 1969, X-ray fluorescent analysis of Rb, Sr, Y, Pb and Th in Japanese Paleozoic slates: Geochem. Jour., 3, 127-134.

BAUMANN, I., 1964, Patronit, VS_4 und die Mineralparagenese von Minasragra, Peru: N. Jb. Miner. Abh., 101, 97-108.

BAYLISS, P. and LEVINSON, A.A., 1970, Clay mineralogy and boron determinations of the shales from the Reindeer Well, Mackenzie River delta, N.W.T., Canada: Bull. Canad. Petrol. Geol., 18, 80-83.

BERAN, A., 1969, Beiträge zur Verbreitung und Genesis phengitführender Gesteine in den Ostalpen: Tschermaks Min. Petr. Mitt., 13, 115-130.

BERNER, R.A., 1967, Thermodynamic stability of sedimentary iron sulfides: Am. Jour. Sci., 265, 773-785.

BINKS, P.J., 1971, The geology of the Orroroo 1:250,000 map area: Rept. Invest., Geol. Survey S. Aust., no. 36, 114 pp.

Reproduced with permission of the copyright owner. Further reproduction prohibited without permission.

BISCAYE, P.E., 1965, Mineralogy and sedimentation of Recent deep-sea clay in the Atlantic Ocean and adjacent seas and oceans: Bull. Geol. Soc. America, 76, 803-832.

BJØRLYKKE, K., 1965, The Middle Ordovician of the Oslo region, Norway: 20. The geochemistry and mineralogy of some shales from the Oslo region: Norsk Geol. Tidsskr., 45, 435-456.

BLATT, H., MIDDLETON, G., and MURRAY, R., 1972, Origin of Sedimentary Rocks: New Jersey, Prentice-Hall, Inc., 634 pp.

BOWES, D.R., 1970, Petrochemistry of Upper Proterozoic Glacigene rocks of the Torrowangee Series at Poolamacca, Broken Hill, New South Wales: Proc. Geologists' Assoc. London, 81, 473-482.

BROWN, G., 1961, The X-ray Identification and Crystal Structures of Clay Minerals: London, Mineral Soc., 544pp.

BRISTOL, C.C., 1968, The quantitative determination of minerals in some metamorphosed volcanic rocks by X-ray diffraction: Canad. Jour. Earth Sci., 5, 235-242.

BURST, J.F., 1959, Postdiagenetic clay-mineral environmental relationship in the Gulf Coast Eocene: Clays and Clay Min., 6, 327-341.

_____, 1969, Diagenesis of Gulf Coast clayey sediments, and its possible relation to petroleum migration: Am. Assoc. Petroleum Geologists Bull., 53, 73-93.

BURTON, C.D., CULKIN, F. and RILEY, J.P., 1959, The abundance of gallium and germanium in terrestrial materials: Geochim. Cosmochim. Acta, 16, 151-180.

Reproduced with permission of the copyright owner. Further reproduction prohibited without permission.

BUTLER, B.C.M., 1965, Compositions of micas in metamorphic rocks, in: W.S. PITCHER and G.W. FLINN, Eds., Control of Metamorphism: London, Oliver and Boyd, 368 pp.

CAMERON, E.M., 1967, A computer program for factor analysis of geochemical and other data. Geol. Survey Canad., Paper 67-39, 42 pp.

CAMPANA, B., 1958, The Mt. Lofty-Olary Region and the Flinders Range Region, in: M.F. GLAESSNER and L.W. PARKIN, Eds., The Geology of South Australia: Jour. Geol. Soc. Australia, 5, 1-163.

CAMPBELL, F.A. and WILLIAMS, G.D., 1965, Chemical composition of shales of Mannville Group (Lower Cretaceous) of Central Alberta, Canada: Am. Assoc. Petroleum Geologists Bull., 49, 81-87.

CARMICHAEL, I.S.E., HAMPEL, J., and JACK, R.N., 1968, Analytical data on the U.S.G.S. standard rocks: Chem. Geol., 3, 59-64.

CARROLL, D., 1970, Clay minerals: A guide to their X-ray identification: Geol. Soc. America Spec. Paper, 126, 80 pp.

CATTELL, R.B., 1965, Factor analysis: An introduction to essentials: Biometrics, 21, 190-210 and 405-435.

CHAMPION, K.P., HURST, H.J., and WHITTEM, R.N., 1968, Tables of mass absorption coefficients for use in X-ray spectrochemical analysis: Sydney, Austr. Atomic Energy Comm. AAEC/TM 454.

CHAYES, F., 1954, The lognormal distribution of the elements: a discussion: Geochim. Cosmochim. Acta, 6, 119-120.

Reproduced with permission of the copyright owner. Further reproduction prohibited without permission.

CHAYES, F. and SUSUKI, Y., 1963, Geological contours and trend surfaces: a discussion: Jour. Petrol., 4, 307-312.

CHILD, D., 1970, The Essentials of Factor Analysis: New York, Holt, Rinehart & Winston, 107 pp.

CIPRIANI, C. and SCOLARI, A., 1971, Metamorphic white micas: definition of paragenetic fields: Schweiz. Min. Petr. Mitt., 51, 259-302.

CLARKE, F.W., 1924, Data of geochemistry: U.S. Geol. Survey Bull., 770, 1-841.

CLOUD, P.E., Jr., GRUNER, J.W., and HAGEN, H., 1965, Carbonaceous rocks of the Soudan Iron Formation (Early Precambrian): Science, 148, 1713-1716.

COATS, R.P., 1964, Umberatana Group: Quart. Geol. Notes, Geol. Survey S. Aust., no. 9, p. 7-12.

COATS, R.P. and BLISSETT, A.H., 1971, Regional and Economic Geology of the Mount Painter Province: Geol. Survey S. Aust. Bull. 43, 426 pp.

CODY, R.D., 1970, Anomalous boron content of two continental shales in eastern Colorado: Jour. Sed. Petrol., 40, 750-754.

_____, 1971, Adsorption and the reliability of trace elements as environmental indicators for shales: Jour. Sed. Petrol., 41, 461-471.

COLE, A.J., 1969, An iterative approach to the fitting of trend surfaces: Computer Contr., 37, 27 pp.

Reproduced with permission of the copyright owner. Further reproduction prohibited without permission.

CONNOR, J.J. and MIESCH, A.T., 1964, Analysis of geochemical prospecting data from the Rocky Range, Beaver County, Utah: U.S. Geol. Survey Prof. Paper, 475-D, D79-D83.

COOLEY, W.W. and LOHNES, P.R., 1971, Multivariate Data Analysis: New York, J. Wiley & Sons, Inc., 364 pp.

COOMBS, D.S., 1954, The nature and alteration of some Triassic sediments from southland, New Zealand: Trans. Roy. Soc. New Zealand, 82, 65-109.

COSGROVE, M.E., 1973, The geochemistry and mineralogy of the Permian red beds of Southwest England: Chem. Geol., 11, 31-47.

COUCH, E.L., 1971, Calculation of paleosalinities from boron and clay mineral data: Am. Assoc. Petroleum Geologists Bull., 55, 1829-1837.

CRONAN, D.S., 1969, Inter-element associations in some pelagic deposits: Chem. Geol., 5, 99-106.

DEGENHARDT, H., 1957, Untersuchungen zur geochemischen Verteilung des Zirkoniums in der Lithosphäre: Geochim. Cosmochim. Acta, 11, 279-309.

DEGENS, E.T., WILLIAMS, E.G., and KEITH, M.L., 1957, Environmental studies of Carboniferous sediments. Part I: Geochemical criteria for differentiating marine from freshwater shales: Am. Assoc. Petroleum Geologists Bull., 41, 2427-2455.

_____, _____, and _____, 1958, Environmental Studies of Carboniferous sediments. Part II: Application of geochemical criteria: Am. Assoc. Petroleum Geologists Bull., 42, 981-997.

Reproduced with permission of the copyright owner. Further reproduction prohibited without permission.

DE MUMBRUM, L.W. and JACKSON, M.L., 1956, Copper and zinc exchange from dilute neutral solutions by soil colloidal electrolytes: Soil Sci., 81, 353.

DENNEN, W.H. and MOORE, B.R., 1971, Chemical definition of mature detrital sedimentary rocks: Nature (Phys. Sci.), 234, 127-128.

DE SEGONZAC, G.D., 1970, The transformation of clay minerals during diagenesis and low-grade metamorphism: A review: Sedimentology, 15, 281-346.

DIXON, W.J., Ed., 1970, BMD Biomedical Computer Programs X-series Supplement: Berkeley, Univ. Calif. Press, 260 pp.

DOVETON, J.R., 1970, Trend analysis of a thin sedimentary sequence within the Upper Carboniferous of Ayrshire, Scotland: Math. Geol., 2, 47-62.

ENGEL, A.E.J., 1958, Progressive metamorphism and granitization of the major paragneiss, northwest Adirondack Mountains, New York, Part I, Total rock: Geol. Soc. America Bull., 69, 1369-1414.

ERNST, W.G., 1963, Significance of phengitic micas from low-grade schists: Amer. Mineral. 48, 1357-1373.

ERNST, W., 1970, Geochemical Facies Analysis: New York, Elsevier Publ. Co., 152 pp.

ESQUEVIN, J., 1969, Influence de la composition chimique des illites sur leur cristallinité: Bull. Centre Rech. Pau-SNPA, 3, 147-153.

Reproduced with permission of the copyright owner. Further reproduction prohibited without permission.

EVANS, B.W. and GUIDOTTI, C.V., 1966, The sillimanite-potash feldspar isograd in western Maine, U.S.A.: Contr. Mineral. and Petrol., 12, 25-62.

FABBI, B.P. and ESPOS, L.F., 1972, X-ray fluorescence determination of arsenic, antimony, nickel, rubidium, scandium, vanadium, and zinc in rock standards and other rock samples: U.S. Geol. Survey Prof. Paper, 800-B, B 147-B152.

FENNER, P. and HAGNER, A.F., 1967, Correlation of variations in trace elements and mineralogy of the Esopus Formation, Kingston, New York: Geochim. Cosmochim. Acta, 31, 237-261.

FLANAGAN, F.J., 1969, U.S. Geological Survey standards--II. First compilation of data for the new U.S.G.S. rocks: Geochim. Cosmochim. Acta, 33, 81-120.

FLEET, M.E.L., 1965, Preliminary investigations into the sorption of boron by clay minerals: Clay Minerals. Bull. 6, 3-17.

FLEISCHER, M., 1969, U.S. Geological Survey standards--I. Additional data on rocks G-1 and W-1, 1965-1967: Geochim. Cosmochim. Acta, 33, 65-79.

FRAKES, L.A. and CROWELL, J.C., 1973, Characteristics of modern glacial marine sediments--Application to Gondwana Glacials: Canberra, Proc. and papers 3rd Gondwana Symposium (in press).

FREDERICKSON, A.F. and REYNOLDS, R.C., 1960, Geochemical method for determining paleosalinity Clays and Clay Min., 8, 203-213.

Reproduced with permission of the copyright owner. Further reproduction prohibited without permission.

FREY, M., 1969, Die Metamorphose des Keupers vom Tafeljura bis zum Lukmanier-Gebiet (Veranderungen tonig-mergeliger Gesteine vom Bereich der Diagenese bis zur Staurolith-Zone): Beitr. Geol. Karte Schweiz., N.F., 137.

FRÖHLICH, F., 1960, Beitrag zur Geochemie des Chroms: Geochim. Cosmochim. Acta, 20, 215-240.

FYFE, W.S., TURNER, F.J. and VERHOOGEN, J., 1958, Metamorphic reactions and metamorphic facies: Geol. Soc. America Mem. 73.

GABIS, Victor and SICHÈRE, Marie-Claude, 1970, Analyses des éléments majeurs des roches silicatées par spectrometrie de fluorescence X: Bull. Soc. fr. Minéral. Cristallogr., 93, 386-393.

GARRELS, R.M. and MACKENZIE, F.T., 1971, Evolution of Sedimentary Rocks: New York, W.W. Norton & Co., Inc., 397 pp.

GLAESSNER, M.F. and PARKIN, L.W., Eds., 1958, The geology of South Australia: Jour. Geol. Soc. Australia, 5(2), 1-163.

GOLDBERG, E.D. and ARRHENIUS, G., 1958, Chemistry of Pacific pelagic sediments: Geochim. Cosmochim. Acta, 13, 153-212.

GOLDSCHMIDT, V.M. and PETERS, C., 1932, Zur Geochemie des Bors: Nachr. Ges. Wiss. Göttingen (Math. Kl.), 402-407, 528-545.

_____, 1933, Grundlagen der quantitativen Geochemie: Fortschr. Mineral, 17, 112-156.

_____, 1954, Geochemistry: Oxford, Clarendon Press, 730 pp.

GOOD, D.I., 1964, FORTRAN II trend-surface program for the IBM 1620: Kansas Geol. Survey Spec. Distr. Publ. 14, 54 pp.

Reproduced with permission of the copyright owner. Further reproduction prohibited without permission.

GORDON, J., Jr. and MURATA, K.J., 1952, Minor elements in Arkansas bauxite: Econ. Geol., 47, 169-179.

GRANT, F., 1957, A problem in the analysis of geophysical data: Geophysics, 22, 309-344.

GREEN, J., 1959, Geochemical table of the elements for 1959: Bull. Geol. Soc. America, 70, 1127-1184.

GREEN, J. and POLDERVAART, A., 1958, Petrochemical fields and trends: Geochim. Cosmochim. Acta, 13, 87-122.

GUIDOTTI, C.V., 1963, Metamorphism of the pelitic schists in the Bryant Pond Quadrangle, Maine: Amer. Mineral., 48, 772-791.

_____, 1966, Variations of the basal spacings of muscovite in sillimanite-bearing pelitic schists of Northwestern Maine: Amer. Mineral., 51, 1778-1786.

_____, and CRAWFORD, K.E., 1968, Determination of Na/Na+K in muscovite by X-ray diffraction and its use in the study of pelitic schists in northwest Maine Abstract: Geol. Soc. America Spec. Paper, 115, 86.

HARBAUGH, J.W., 1963, BALGOL program for trend-surface mapping using an IBM 7090 computer: Kansas Geol. Survey Spec. Distr. Publ., 3, 17 pp.

_____, and MERRIAM, D.F., 1968, Computer Applications in Stratigraphic Analysis: New York, John Wiley & Sons, Inc., 282 pp.

HARDER, H., 1959, Beitrag zur Geochemie des Bors 1, 2. Nachr. Akad. Wiss. Göttingen (II. math.-phys. Kl.) 67-183.

Reproduced with permission of the copyright owner. Further reproduction prohibited without permission.

_____, 1961, Einbau von Bor in detritische Tonminerale. Experimente zur Erklärung des Borgehaltes toniger Sedimente: Geochim. Cosmochim. Acta, 21, 284-294.

_____, 1963, In wie weit ist Bor ein marines Leitelement?: Fortschr. Geol. Rheinl. Westf., 10, 239-252.

_____, 1970, Boron content of sediments as a tool in facies analysis: Sediment Geol., 4, 153-175.

HARMAN, H.N., 1967, Modern Factor Analysis, 2nd ed. Chicago, Univ. Chicago Press, 469 pp.

HEIDE, F. and LERZ, H., 1955, Zur Geochemie des Bleies: Chem. Erde, 17, 217-222.

HEIER, K.S. and ADAMS, J.A.S., 1964, The geochemistry of the alkali metals, in: L.H. AHRENS, F. PRESS, and S.K. RUNCORN, Eds.: Phys. Chem. Earth, 5, 253-381.

_____, and BILLINGS, G.K., 1971, Lithium, in: K.H. WEDEPOHL, Handbook of Geochemistry, II/2: New York, Springer-Verlag.

HENRY, N.F.M., LIPSON, H., and WOOSTER, W.A., 1961, The Interpretation of X-ray Diffraction Photographs: London, McMillan & Co., 282 pp.

HEYDEMANN, A., 1959, Adsorption aus sehr verdünnten Kupferlösungen an reinen Tonmineralen: Geochem. Cosmochim. Acta, 15, 305-329.

HIRST, D.M. and KAYE, M.J., 1971, Factors controlling the mineralogy and chemistry of an Upper Visean sedimentary sequence from Rockhope, County Durham: Chem. Geol., 8, 37-59.

Reproduced with permission of the copyright owner. Further reproduction prohibited without permission.

HORSTMAN, E.L., 1957, The distribution of lithium, rubidium, and caesium in igneous and sedimentary rocks: Geochim. Cosmochim. Acta, 12, 1-28.

HOWARTH, R.J., 1967, Trend-surface fitting to random data - an experimental test: Am. Jour. Sci., 265, 619-625.

HOWCHIN, W., 1904, Geology of the Mount Lofty Ranges, pt. 1: The coastal district: Trans. Roy. Soc. S. Austr., 28, 253-280.

_____,1918, The Geology of South Australia (in two divisions) Adelaide, Govt. Print, 543 pp.

_____, 1929, The Geology of South Australia, with notes on the chief geological systems and occurrences in the other Australian states: 2nd Ed., Adelaide, 320 pp.

HOWER, J., 1959, Matrix corrections in the X-ray spectrographic trace element analysis of rocks and minerals: Amer. Mineral., 44, 19-32.

_____, and MOWATT, T.C., 1966, The mineralogy of illites and mixed-layer illite/montmorillonites: Amer. Mineral., 51, 825-854.

HUBER-SCHAUSBERGER, I., JANDA, I., DOLEZEL, P., and SCHROLL, E., 1970, Chemische und spektrochemische Analyse internationaler Referenz gesteinsproben: Tschermaks Miner. Petr. Mitt., 14, 195-211.

IMBRIE, J. and VAN ANDEL, TJ. H., 1964, Vector analysis of heavy mineral data: Bull. Geol. Soc. America, 75, 1131-1156.

Reproduced with permission of the copyright owner. Further reproduction prohibited without permission.

JAMES, H.L., 1972, Note 40-Subdivision of Precambrian: An interim scheme to be used by U.S. Geological Survey: Am. Assoc. Petroleum Geologists Bull., 56, 1128-1133.

JENKINS, R. and DE VRIES, J.L., 1967, Practical X-Ray Spectrometry: New York, Springer-Verlag, 184 pp.

JOHNS, R.K., 1961, Geology and mineral resources of southern Eyre Peninsula: Geol. Survey S. Aust. Bull., 37, 102 pp.

JOHNS, W.D., 1963, Die Verteilung von Chlor in rezenten marinen und nichtmarinen Sedimenten: Fortschr. Geol. Rheinland Westfalen, 10, 215-230.

JOHNS, W.D., GRIM, R.E. and BRADLEY, W.F., 1954, Quantitative estimates of clay minerals by diffraction methods: Jour. Sed. Petrol., 24, 242-251.

JOST, K., 1932, Über den Vanadiumgehalt der Sedimentgesteine und sedimentaren Lagerstätten: Chem. Erde, 7, 177-190.

KANEHIRA, K. and BANNO, S., 1960, Ferriphengite and aegirinjadeite in a crystalline schist of the Iimori District, Kii Peninsula: Jour. Geol. Soc. Japan, 66, 654-659.

KEITH, M.L. and DEGENS, E.T., 1959, Geochemical indicators of marine and fresh-water sediments, in: P.H. ABELSON, Ed., Researches in Geochemistry: New York, J. Wiley & Sons, Inc., 38-61.

KELLER, W.D., 1963, Diagenesis in clay minerals - A review: Clays and Clay Min., 10, 136-157.

Reproduced with permission of the copyright owner. Further reproduction prohibited without permission.

KENNEDY, W.Q., 1951, Sedimentary differentiation as a factor in the Moine-Torridonian correlation: Geol. Mag., 88, 257-267.

KLUG, H.P. and ALEXANDER, L.E., 1954, X-ray Diffraction Procedures: New York, John Wiley & Sons, Inc., 716 pp.

KOCH, G.S., Jr., and LINK, R.F., 1970, Statistical Analysis of Geological Data: New York, John Wiley & Sons, Inc., 375 pp.

KODAMA, H., BRYDON, J.E. and STONE, B.C., 1967, X-ray spectrochemical analysis of silicates using synthetic standards with a correction for inter-element affects by a computer method: Geochim. Cosmochim. Acta, 31, 649-659.

KOSSOVSKAYA, A.G. and SHUTOV, V.D., 1970, Main aspects of the epigenesis problem: Sedimentology, 15, 11-40.

KREJCI-GRAF, K., 1964, Geochemical diagnosis of facies: Proc. Yorkshire Geol. Soc., 34 (23), 469-521.

KRUMBEIN, W.C., 1956, Regional and local components in facies maps: Am. Assoc. Petroleum Geologists Bull., 40, 2163-2194.

_____, 1959, Trend surface analysis of contour-type maps with irregular control-point spacing: Jour. Geophys. Res., 64, 823-834.

_____, 1963, Confidence intervals on low-order polynomial trend surfaces: Jour. Geophys. Res., 68, 5869-5878.

_____, and GARRELS, R.M., 1952, Origin and classification of chemical sediments in terms of pH and oxidation-reduction potentials: Jour. Geol., 60, 1-33.

Reproduced with permission of the copyright owner. Further reproduction prohibited without permission.

_____, and GRAYBILL, F.A., 1965, An introduction to statistical models in geology: New York, McGraw-Hill Book Co., 475 pp.

KUBLER, B., 1964, Les argiles, indicateurs de métamorphisme: Rev. Inst. franc. Pétrole, 19, 1093-1113.

_____, 1966, La cristallinité de l'illite et les zones tout à fait supérieurs du métamorphisme, in: Colloque sur les etages tectoniques: A la Baconnière, Neuchâtel, 105-122.

_____, 1967, Anchimétamorphisme et schistosité: Bull Centre Rech. Pau-SNPA, 1, 259-278.

_____, 1968, Évaluation quantitative du métamorphisme par la cristallinité de l'illite: Bull. Centre Rech. Pau-SNPA, 2, 385-397.

LANDERGREN, S., 1945, Contribution to the geochemistry of boron: 2. Ark. Kemi. Miner. Geol., 19A, 31 pp.

_____, and JOENSUU, O., 1965, Studies on trace element distribution in a sediment core from the Pacific Ocean: Progr. in Oceanogr., 3, 179-189.

LEVINSON, A.A. and LUDWICK, J.C., 1966, Speculation on the incorporation of boron into argillaceous sediments: Geochim. Cosmochim. Acta, 30, 855-861.

LIEBHAFSKY, H., PFEIFFER, H.G., WINSLOW, E.H., ZEMANY, P.D., 1960, X-ray Absorption and Emission in Analytical Chemistry--Spectrochemical Analysis with X-rays: New York, John Wiley & Sons, 357 pp.

Reproduced with permission of the copyright owner. Further reproduction prohibited without permission.

LINKE, W., 1970, Mineralogie und Petrologie ostalpiner Tonschiefer: Tschermaks Miner. Petr. Mitt., 14, 7-25.

LUDBROOK, N.H. and JOHNS, R.K., 1970, Geology of South Australia: Extract from "South Australian Year Book, 1970": S. Austr. Dept. Mines, 16 pp.

LYNCH, J.J., 1971, The determination of copper, nickel, and cobalt in rocks by atomic absorption spectrometry using a cold leach, in: R.W. BOYLE, Ed., Geochemical Exploration: Proc. 3rd. Internatl. Geochem. Expl. Symp., Canadian Inst. Min. Metall. Spec., 11, 313-314.

MASTINS, H., JONES, J.B., and NESBITT, R.W., 1972, X-ray mass absorption applied to mineral and rock analysis: Jour. Geol. Soc. Australia, 19, 217-224.

MATALAS, N.C. and REIHER, B.J., 1967, Some comments on the use of factor analysis: Water Resources Res., 3, 213-223.

MATHER, J.D., 1970, The biotite isograd and the lower green schist facies in the Dalradian rocks of Scotland: Jour. Petrol., 11, 253-275.

MATHER, P.M., 1972, Study of factors influencing variation in size characteristics of fluvioglacial sediments: Math. Geol., 4, 219-234.

MAXWELL, D.T. and HOWER, J., 1967, High-grade diagenesis and low-grade metamorphism of illite in the Precambrian Belt Series: Amer. Mineral., 52, 843-857.

Reproduced with permission of the copyright owner. Further reproduction prohibited without permission.

MIDDLETON, G.V., 1960, Chemical composition of sandstones: Bull. Geol. Soc. America, 71, 1011-1026.

MILLER, R.L., 1956, Trend surfaces: their application to analysis and description of environments of sedimentation: Jour. Geol., 64, 425-446.

_____, and KAHN, J.S., 1962, Statistical analysis in the geological sciences: New York, John Wiley & Sons, Inc.

_____, and WELLER, J.M., 1952, Significant comparisons in paleontology: Jour. Paleont., 26, 993-996.

MIRAMS, R.C., 1964, BURRA sheet - Geological Atlas of South Australia, 1:250,000 series, Geol. Survey S. Australia.

MOORE, A.C., 1969, A method for determining mineral compositions by measurement of the mass absorption coefficients: Amer. Mineral., 54, 1180-1189.

MOORE, B.R., and DENNEN, W.H., 1970, A geochemical trend in silicon-aluminum-iron ratios and the classification of clastic sediments: Jour. Sed. Petrol., 40, 1147-1152.

MUFFLER, L.J.P. and WHITE, D.E., 1969, Active metamorphism of Upper Cenozoic sediments in the Salton Sea-geothermal Field and the Salton trough, southeastern California: Bull. Geol. Soc. America, 80, 157-182.

NACKOWSKI, M.P., MARDIROSIAN, C.A., and BOTBOL, J.M., 1967, Trend surface analysis of trace chemical data, Park City District, Utah: Econ. Geol., 62, 1072-1087.

Reproduced with permission of the copyright owner. Further reproduction prohibited without permission.

NICHOLLS, G.D. and LORING, D.H., 1962, The geochemistry of some British Carboniferous sediments: Geochim. Cosmochim. Acta, 26, 181-223.

NIE, N.H., BENT, D.H., and HULL, C.H., 1970, SPSS (Statistical Package for the Social Sciences): New York, McGraw-Hill, Inc., 343 pp.

NORRISH, K., and CHAPPELL, B.W., 1967, X-ray fluorescent spectroscopy, in: J. ZUSSMAN, Ed., Physical methods in determinative mineralogy: London, Academic Press, 161-214.

_____, and HUTTON, J.T., 1969, An accurate X-ray spectrographic method for the analysis of a wide range of geological samples: Geochim. Cosmochim. Acta, 33, 431-453.

_____, and TAYLOR, R.M., 1962, Quantitative analysis by X-ray diffraction: Clay Min. Bull., 5, 98-109.

OERTEL, A.C., 1961, Spectrographic Analysis of Mineral Powders: Adelaide, S. Australia, Div. Soils, CSIRO.

OFFLER, R. and FLEMING, P.D., 1968, A synthesis of folding and metamorphism in the Mt. Lofty Ranges, South Australia: Jour. Geol. Soc. Australia, 15, 245-266.

OHRDORF, R., 1968, Ein Beitrag zur Geochemie des Lithiums in Sedimentgesteinen: Geochim. Cosmochim. Acta, 32, 191-208.

OLDHAM, C.H.G., and SUTHERLAND, D.G., 1955, Orthogonal polynomials: their use in estimating the regional effect: Geophysics, 20, 295-306.

Reproduced with permission of the copyright owner. Further reproduction prohibited without permission.

O'LEARY, M., LIPPERT, R.H., and SPITZ, O.T., 1966, FORTRAN IV and Map program for computation and plotting of trend surfaces for degrees 1 through 6: Kansas Geol. Survey Computer Contr. 3, 48 pp.

ONDRICK, C.W., and GRIFFITHS, J.C., 1969, Trend surface analysis applied to the Rensselaer Graywacke and its implications to the Taconics: Jour. Sed. Petrol., 39, 176-186.

_____, and SRIVASTAVA, G.S., 1970, CORFAN-FORTRAN IV Computer program for correlation, factor analysis (R- and Q-mode) and varimax rotation: Kansas Geol. Survey Computer Contr., 42, 92 pp.

ONISHI, H., 1969, Arsenic, in: K.H. WEDEPOHL, Handbook of Geochemistry, Vol. II/1: New York, Springer-Verlag.

_____, and SANDELL, E.B., 1955, Geochemistry of arsenic: Geochim. Cosmochim. Acta, 7, 1-33.

PARKER, A., 1969, Some trace element determinations on the new USGS silicate rock standards: Chem. Geol., 4, 445-449.

PARKIN, L.W., Ed., 1969, Handbook of South Australian Geology: Geol. Survey S. Aust., 268 pp.

PERRY, E. and HOWER, J., 1970, Burial diagenesis in Gulf Coast pelitic sediments: Clays and Clay Minerals, 18, 165-177.

PETTIJOHN, F.J., and BASTRON, A., 1959, Chemical composition of argillites of the Cobalt Series (Precambrian) and the problem of soda-rich sediments: Bull. Geol. Soc. America, 70, 593-600.

Reproduced with permission of the copyright owner. Further reproduction prohibited without permission.

PITCHER, W.S. and FLINN, G.S., Eds. 1965, Controls of Metamorphism: Edinburgh, Oliver and Boyd, 368pp.

POLDERVAART, A., 1955, Chemistry of the earth's crust, in: Crust of the earth: Geol. Soc. America Spec. Paper, 62, 119-144.

POTTER, P.E., SHIMP, N.F., and WITTERS, J., 1963, Trace elements in marine and fresh-water argillaceous sediments: Geochim. Cosmochim. Acta, 27, 669-694.

PREISS, W.V., 1973, Paleoecological interpretations of South Australian Precambrian stromatolites: Jour. Geol. Soc. Australia, 19, 501-532.

PRESTON, D.A., 1970, FORTRAN IV program for sample normality tests: Kansas Geol. Survey Computer Contr., 41, 28 pp.

PUCHELT, H., 1972, Barium, in: K.H. WEDEPOHL, Ed., Handbook of Geochemistry Vol. II/3: New York, Springer-Verlag.

RANKAMA, K., and SAHAMA, T.G., 1950, Geochemistry: Chicago, Univ. Chicago Press, 911 pp.

READ, W.A., and MERRIAM, D.F., 1966, Trend-surface analysis of stratigraphic thickness data from some Namurian rock east of Stirling, Scotland: Scottish Jour. Geol., 2, 96-100.

REIMER, T., 1971, Strontium depletion in Early Precambrian sediments: N. Jb. Miner. Mh., 12, 527-541.

_____, 1972, The evolution of the rubidium and strontium content of shales: N. Jb. Miner. Abh., 116, 167-195.

Reproduced with permission of the copyright owner. Further reproduction prohibited without permission.

REYNOLDS, R.C., 1963, Matrix corrections in trace element analysis by X-ray fluorescence: Estimation of the mass absorption coefficient by Compton scattering: Amer. Mineral., 48, 1133-1143.

_____, 1965, The concentration of boron in Precambrian sea: Geochim. Cosmochim. Acta, 29, 1-16.

_____, 1967, Estimation of mass absorption coefficients by Compton scattering: improvements and extensions of the method: Amer. Mineral., 52, 1493-1502.

ROALDSET, E., 1972, Mineralogy and geochemistry of Quaternary clays in the Numedal area, southern Norway: Norsk Geol. Tidsskr., 52, 335-369.

RONOV, A.B., GIRIN, Yu.P., KAZAKOV, G.A., and ILYUKHIN, M.N., 1966, Sedimentary differentiation in platform and geosynclinal basins: Geochem. Internatl., 3, 595-608.

_____, and KHLEBNIKOVA, Z.V., 1957, Chemical composition of the main genetic clay types: Geochemistry, 6, 527-552.

_____, and MIGDISOV, A.A., 1971, Geochemical history of the crystalline basement and the sedimentary cover of the Russian and North American platforms: Sedimentology, 16, 137-185.

RUMMEL, R.J., 1970, Applied Factor Analysis: Evanston, Northwestern Univ. Press, 617 pp.

Reproduced with permission of the copyright owner. Further reproduction prohibited without permission.

SAMPSON, R.J., 1968, R-mode factor analysis program in FORTRAN II for the IBM 1620 computer, in: D.F. MERRIAM, Ed., Computer programs for multivariate analysis in geology: Kansas Geol. Survey Computer Contr. 20, 58 pp.

SASSI, F.P., 1972, The petrological and geological significance of the b_0 values of potassic white micas in low-grade metamorphis rocks. An application to the eastern Alps: Tschermaks Min. Petr. Mitt., 18, 105-113.

SCHROLL, E., 1971, Beitrag zur Geochemie des Bariums in Carbonatgesteinen und Klastischen Sedimenten der ostalpinen Trias: Tschermaks Min. Petr. Mitt., 15, 258-278.

_____, and STEPAN, E., 1969, Zur Rontgenfluoreszenzanalyse geologischen Materials: Taschermaks Miner. Petrogr. Mitt., 13, 131-147.

SCHULTZ, L.G., 1964, Quantitative interpretation of mineralogical composition from X-ray and chemical data for the Pierre Shale: U.S. Geol. Survey Prof. Paper 391-C, 31 pp.

SEGNIT, R.W., 1939, The Precambrian-Cambrian succession -- The general and economic geology of these systems, in portions of South Australia: Geol. Survey S. Aust. Bull., 18, 191 pp.

SHAW, D.M., 1954, Trace elements in pelitic rocks. Part I Variation during metamorphism Part II Geochemical relations: Geol. Soc. America Bull., 65, 1151-1182.

Reproduced with permission of the copyright owner. Further reproduction prohibited without permission.

_____, 1961, Element distribution laws in geochemistry: Geochim. Cosmochim. Acta, 23, 116-134.

_____, and BUGRY, R., 1966, A review of boron sedimentary geochemistry in relation to new analyses of some North American shales: Canad. Jour. Earth Sci., 3, 49-63.

SHIMP, N.F., WITTERS, J., POTTER, P.E., and SCHLEICHER, J.A., 1969, Distinguishing marine and freshwater muds: Jour. Geol., 77, 566-580.

SPEARMAN, C., 1904, General intelligence, objectively determined and measured: Amer. Jour. Psychol., 15, 201-293.

SPENCER, D.W., 1966a, Factor Analysis: Woods Hole Oceanogr. Inst., Unpubl. Manuscr. Ref. No. 66-39, 101 pp.

_____, 1966b, Factors affecting element distribution in a Silurian graptolite band: Chem. Geol., 1, 221-249.

_____, and DEGENS, E.T., 1968, Factors affecting element distribution in sediments, in: L.H. AHRENS, Ed., Origin and Distribution of the Elements: New York, Pergamon Press, 981-998.

SPRIGG, R.C., 1946, Reconnaissance geological survey of portion of the western escarpment of the Mount Lofty Ranges: Trans. Roy. Soc. S. Austr., 70, 313-347.

_____, 1952, Sedimentation in the Adelaide Geosyncline and the formation of the continental terrace, in: M.R. Glaessner and E.A. Rudd, Eds., Sir Douglas Mawson Annivers. Vol.: Adelaide, Univ. Adelaide, 153-159.

Reproduced with permission of the copyright owner. Further reproduction prohibited without permission.

STERN, W.B., 1972, Zur röntgenspektrometrischen Analyse von silikatischen Gesteinen und Mineralien: Schweiz. Min. Petr. Mitt., 52, (1), 1-25.

SUMARTOJO, J., McKIRDY, D., TUCKER, D.H., and GOSTIN, V.A., 1973, Organic, mineralogic, and magnetic indications of metamorphism in the Late Precambrian Tapley Hill Formation of the Adelaide Geosyncline: Abstract, 45th Austr. New Zeal. Assoc. Adv. Sci. Congr., Sect. 3, Perth.

SUMMERHAYES, C.P., 1972, Geochemistry of continental margin sediments from northwest Africa: Chem. Geol., 10, 137-156.

TALBOT, J.L. and NESBITT, R.W., 1968, Geological Excursions in the Mount Lofty Ranges and the Fleurieu Peninsula: Sydney, Angus and Robertson, 60 pp.

TARDY, Y., KREMPP, G., and TRAUTH, N., 1972, Le lithium dans les minéraux argileaux des sédiments et des sols: Geochim. Cosmochim. Acta, 36, 397-412.

TAYLOR, S.R., 1960, Occurrence of alkali metals in some Gulf of Mexico sediments; amended Rb values and K/Rb ratios: Jour. Sed. Petrol., 30, 317-323.

THOMSON, B.P., 1969, Precambrian Basement Cover. The Adelaide System, in: L.W. PARKIN, Ed., Handbook of South Australian Geology: Geol. Survey S. Aust., 49-83.

Reproduced with permission of the copyright owner. Further reproduction prohibited without permission.

TILL, R. and SPEARS, D.A., 1969, The determination of quartz in sedimentary rocks using an X-ray diffraction method: Clays and Clay Min., 17, 323-327.

TINKLER, K.J., 1969, Trend surfaces with low explanations, the assessment of their significance: Amer. Jour. Sci., 267, 114-123.

TOURTELOT, E.B., 1970, Selected annotated bibliography of minor-element content of marine black shales and related sedimentary rocks, 1930-1965: U.S. Geol. Survey Bull. 1293, 118 pp.

TOURTELOT, H.A., 1964, Minor-element composition and the organic carbon content of marine and nonmarine shales of Late Cretaceous age in the western interior of the United States: Geochim. Cosmochim. Acta, 28, 1579-1604.

_____, SCHULTZ, L.G., and GILL, J.R., 1960, Stratigraphic variations in mineralogy and chemical composition of the Pierre Shale in South Dakota and adjacent parts of North Dakota, Nebraska, Wyoming, and Montana, in: Short papers in the geological sciences: U.S. Geol. Survey Prof. Paper, 400-B, B 447-452.

TROSTEL, L.J. and WYNNE, D.J., 1940, Determination of quartz (free silica) in refractory clays: Jour. Amer. Ceram. Soc., 23, 18-22.

TUCKER, D.H., 1972, Magnetic and Gravity Interpretation of an Area of Precambrian Sediments in Australia: Univ. Adelaide, Unpubl. Ph.D. thesis.

TUREKIAN, K.K. and KULP, J.L., 1956, The geochemistry of strontium: Geochim. Cosmochim. Acta, 10, 245-296.

_____, and TAUSCH, E.H., 1964, Barium in deep-sea sediments of the Atlantic Ocean: Nature, 201, 696-697.

Reproduced with permission of the copyright owner. Further reproduction prohibited without permission.

_____, and WEDEPOHL, K.H., 1961, Distribution of the elements in some major units of the earth's crust: Bull. Geol. Soc. America, 72, 175-191.

van BILJON, W.J. and BENSCH, J.J., 1970, The "crystallinity" of illite as a measure of contact metamorphism in mudstone of the Karroo System, South Africa: Johannesburg, Proc. and Papers, 2nd Gondwana Symposium, 451-454.

Van der MAREL, H.W., 1966, Quantitative analysis of clay minerals and their admixtures: Contr. Mineral. Petrol., 12, 96-138.

VELDE, B., 1964, Low grade metamorphism of micas in pelitic rocks: Washington Carnegie Inst. Yearbook, 63, 142-147.

VINE, J.D., 1964, Metals in Pennsylvanian black shale from Kentucky and Indiana (abs.): Geol. Soc. America Spec. Paper, 82, 212.

VINOGRADOV, A.P. and RONOV, A.B., 1956, Composition of the sedimentary rocks of the Russian Platform in relation to the history of its tectonic movements: Geochemistry, 6, 533-559.

VLASOV, K.A., Ed., 1964, Geochemistry of rare elements and Genetic Types of Their Deposits: Vol. I: Geochemistry of rare elements: Z. LERMAN, transl. (1966), Jerusalem: Israel Program for Scient. Transl.

VOGT, T., 1927, Sulitjelmafeltets geologi og petrografi: Norges Geol. Undersøkelse, 121, 540 pp.

Reproduced with permission of the copyright owner. Further reproduction prohibited without permission.

WALKER, C.T., and PRICE, N.B., 1963, Departure curves for computing paleosalinity from boron in illites and shales: Am. Assoc. Petroleum Geologists Bull., 47, 833-841.

WALLIS, J.R., 1968, Factor analysis in hydrology - an agnostic view: Water Resources Res., 4, 521-527.

WARNER, J. and AL-MISHWT, A., 1968, Variations of the basal spacing of muscovite with metamorphic grade in southeastern Pennsylvania: Proc. Pennsylvania Acad. Sci., 42, 193-202.

WARSHAW, C.M. and ROY, R., 1961, Classification and a scheme for the identification of layer silicates: Bull. Geol. Soc. America, 72, 1455-1492.

WEAVER, C.E., 1958, Geologic interpretation of argillaceous sediments: Am. Assoc. Petroleum Geologists Bull., 42, 254-309.

_____, 1960, Possible uses of clay minerals in the search for oil: Clays and Clay Min., 8, 214-227.

_____, and BECK, K.C., 1971, Clay water diagenesis during burial--How mud becomes gneiss: Geol. Soc. America Spec. Paper, 134, 96 pp.

WEBER, K., 1972a, Notes on determination of illite crystallinity: N. Jb. Miner. Mh., 6, 267-276.

_____, 1972b, Kristallinität des Illits in Tonschiefern und andere Kriterien schwacher Metamorphose im nordöstlichen Rheinischen Schiefergebirge: N. Jb. Geol. Palaönt. Abh., 141, 333-363.

Reproduced with permission of the copyright owner. Further reproduction prohibited without permission.

WEDEPOHL, K.H., 1953, Untersuchungen zur Geochemic des Zinks: Geochim. Cosmochim. Acta, 3, 93-142.

_____, 1956, Untersuchungen zur Geochemie des Bleis: Geochim. Cosmochim. Acta, 10, 69-148.

_____, 1960, Spurenanalytische Untersuchungen an Tiefseetonen aus dem Atlantik. Ein Beitrag zur Deutung der geochemischen Sonderstellung von pelagischen Tonen: Geochim. Cosmochim. Acta, 18, 200-231.

_____, 1962, Beiträge zur Geochemie des Kupfers: Geol. Rundsch., 52, 492-504.

_____, 1964, Untersuchungen am Kupferschiefer in Nordwestdeutschland: Ein Beitrag zur Deutung der Genese bituminöser Sedimente: Geochim. Cosmochim. Acta, 28, 305-364.

_____, Ed., 1969, Handbook of Geochemistry Vol. I: New York, Springer-Verlag, 442 pp.

_____, Ed., 1970, Handbook of Geochemistry, Vol. II/2: New York, Springer-Verlag.

_____, 1971, Environmental influences on the chemical composition of shales and clays, in: L.H. AHRENS, Phys. Chem. Earth, 8, 305-333.

_____, 1972, Zinc, in: K.H. WEDEPOHL, Ed., Handbook of Geochemistry, Handbook of Geochemistry, Vol. II/3: New York, Springer-Verlag.

WELBY, C.W., 1958, Occurrence of alkali metals in some Gulf of Mexico sediments: Jour. Sed. Petrol., 28, 431-452.

Reproduced with permission of the copyright owner. Further reproduction prohibited without permission.

WHITTEN, E.H.T., 1959, Composition trends in a granite: modal variation and ghost stratigraphy in part of the Donegal Granite, Eire: Jour. Geophys. Res., 64, 835-848.

_____, 1973, The practical use of trend-surface analyses in the geological sciences: NATO Adv. Study Inst. - Display and Analysis of Spatial Data: Univ. Nottingham, United Kingdom.

YODER, H.S., EUGSTER, H.P., 1955, Synthetic and natural muscovites: Geochim. Cosmochim. Acta, 8, 225-280.

YOUNG, E.J., 1954, Trace elements in Recent marine sediments (abs.): Bull. Geol. Soc. America, 65, 1329.

YOUNG, G.M., 1969, Geochemistry of Early Proterozoic tillites and argillites of the Gowganda Formation, Ontario, Canada: Geochim. Cosmochim. Acta, 33, 483-492.

ZACHARIASEN, W.H., 1934, The crystal lattice of boric acid, H_3BO_3: Z. Kristall., 88, 150.

ZEN, E-AN, and ALBEE, A.L., 1964, Coexistent muscovite and paragonite in pelitic schists: Amer. Mineral., 49, 904-925.

Reproduced with permission of the copyright owner. Further reproduction prohibited without permission.

APPENDICES

Reproduced with permission of the copyright owner. Further reproduction prohibited without permission.

APPENDIX 1

Instrumentation and Operating Conditions for X-ray Diffraction

Generator:	Philips PW 1010
X-ray tube:	Copper target (40 KV, 25 mA)
	Nickel filter, $\frac{1}{2}^{o}$ - $\frac{1}{2}^{o}$ collimator slits
Goniometer:	Philips PW 1050/30
	Speeds: 1^{o}, $\frac{1}{2}^{o}$, $\frac{1}{4}^{o}$ 2θ-angle per minute
Detector:	Proportional counter operated at about 1560 Volts with an attachment of a curved-crystal monochromator AMR E-202-60 (Advanced Metals Research Corp.) Peak calibration was done by using silicon-powder (111-plane) set at 2θ-angle of 28.425^{o}.
Linear amplifier:	Philips PW 4072/01
	Differential Time Constant = 1 micro second
	Attenuation = 1x
	Internal Time Constant = 2 micro second
Rate Meter:	Ecko Electronics Type N 600A
	Pulse Height Analyser - Thresdhold: 10 Volts
	Gate width: 5 Volts
	Pulse Rate: 300 and 1,000 counts per second
	Mean Probable Error: 3 per cent
	Amplifier Gain: 25
Chart Recorder:	Honeywell Controls Ltd. 63 B/220
	Speed: 1 cm per minute

Reproduced with permission of the copyright owner. Further reproduction prohibited without permission.

Reproduced with permission of the copyright owner. Further reproduction prohibited without permission.

Appendix 2

Operational Condition
(Modified PHILIPS All-vacuum X-ray Spectrograph PW/1540)

Element	As	Ba	Cu	Ga	Rb	Sr	Pb	Ni	Zn	Zr
Line	$K\alpha$	$L\beta_1$	$K\alpha$	$K\alpha$	$K\alpha$	$K\alpha$	$L\beta$	$K\alpha$	$K\alpha$	$K\alpha$
2θ-position	48.82°	79.19°	65.56°	56.18°	37.99°	35.87°	40.36°	71.26°	60.60°	32.12°
Background position*	46.94°	80.39°	64.56°	57.18°	39.05°	36.93°	41.02°	70.00°	59.62°	32.80°
Tube anode (kV/mA)	Mo 60/40	Cr 60/40	Au 55/35	Mo 60/40	Mo 60/40	Mo 60/40	Mo 60/40	Au 55/35	Au 55/35	Au 55/35
Collimator**	Fine	Fine	Coarse	Fine	Fine	Coarse	Fine	Coarse	Coarse	Fine
Path	Air	Vacuum	Air	Air	Air	Air	Air	Air	Air	Air
Crystal (LiF)	220	200	220	220	220	220	220	220	220	220
Detector (Volts)	Sci. 660	F.P. 1,380	Sci. 655	Sci. 670	Sci. 675	Sci. 650	Sci. 610	Sci. 690	Sci. 660	Sci. 575
Counting time (Secs.)	100	40	40	100	40	40	40	40	40	40

*Two background positions are generally preferable; in the one background position, the slope of the background was determined on silica blank.

**Coarse collimator: 480 micrometers; fine collimator: 160 micrometers.

Pulse-height analyser setting for scintillation counter (Sci.): 150/300, and for flow-proportional counter (F.P.): 150/150 (lower level/window).

Note: As and Zr should be respectively corrected by Pb $L\alpha$ and Sr$K\beta$ interference.

APPENDIX 3

Determination of Mass-Absorption Coefficient

Methods of determining mass-absorption coefficients have been described by various authors. There are two principal techniques:

1. If the chemical composition of the material is known, the coefficient can be calculated (Klug and Alexander, 1954).

2. Empirical methods; by direct measurement (Norrish and Chappell, 1967; Moore, 1969, and Mastins, et al., 1972), and indirect measurement. There are two methods of indirect measurement; the measurement of the Compton scattering-radiation intensity (Reynolds, 1963, 1967), and of the intensity of the primary-beam (tube radiation) scatter (Schroll and Stepán, 1969).

In this thesis, the calculation method was used to determine the barium mass-absorption coefficient with loss on ignition assumed to be mainly due to carbonate. The mass-absorption coefficients of the other elements were indirectly determined by measuring the Compton scattering-radiation intensity.

Compton scattering method. The method as described by Reynolds (1967) was adopted with a slight modification. Instead of an yttrium-oxide filter and a lithium-fluoride (200) crystal, the fine collimator (160 microns) of the x-ray spectrometer and a lithium-fluoride (220) crystal were used to resolve the molybdenum Compton-scatter of the primary radiation (Fig. A. 1c).

Reproduced with permission of the copyright owner. Further reproduction prohibited without permission.

Figure A. 1 Compton-scatter method

a. Relationship between the mass-absorption coefficient and the Compton-scatter intensity, after Reynolds (1963).

b. Relationship between the mass-absorption coefficient for various wave-lengths and the Compton-scatter intensity, this work.

c. Tracing of diffractogram of the Compton-scatter peak and the Mo-Kα radiation of the tube.

Reproduced with permission of the copyright owner. Further reproduction prohibited without permission.

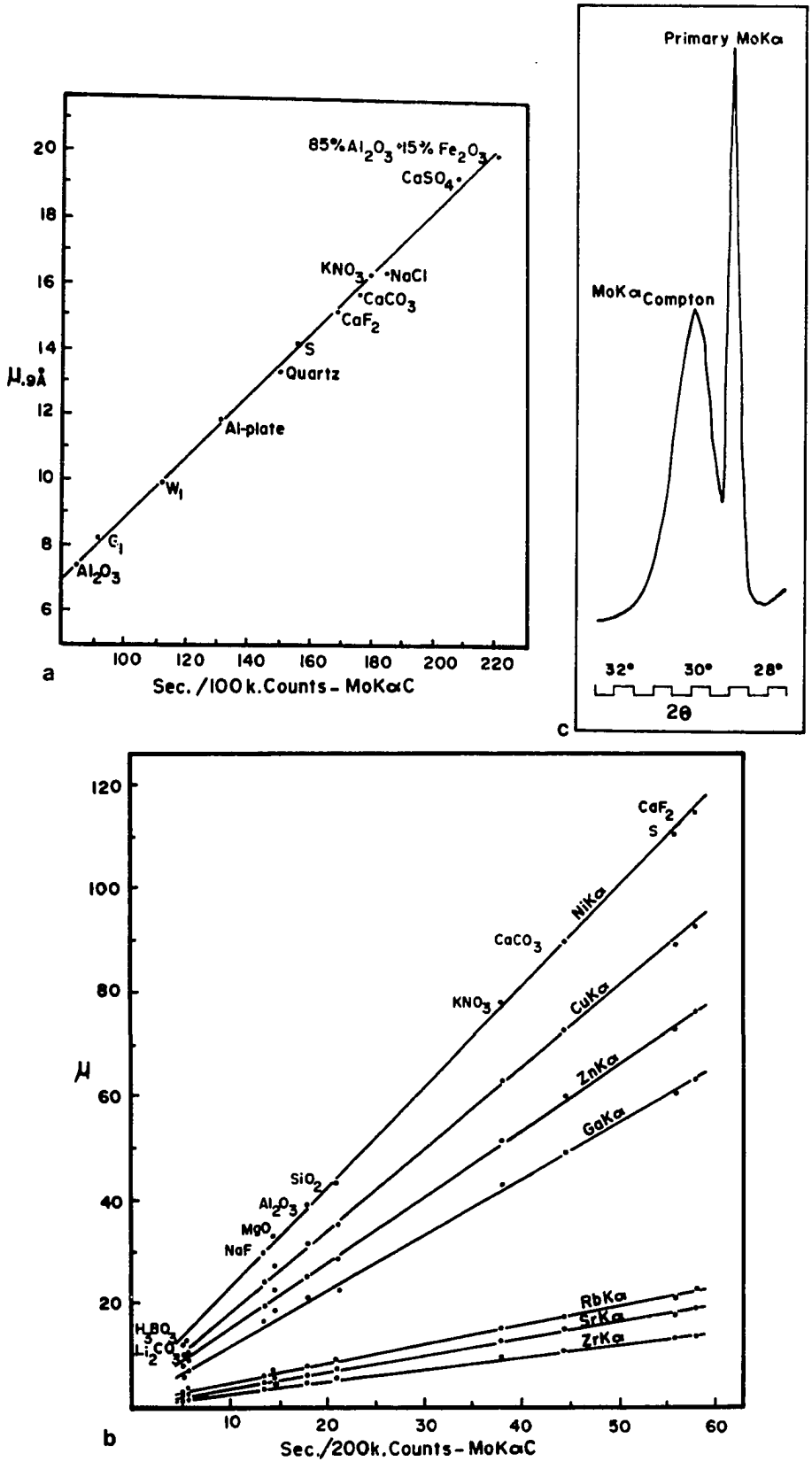

Reproduced with permission of the copyright owner. Further reproduction prohibited without permission.

The mass-absorption coefficients of several materials with known chemical composition were calculated at different wave lengths using a published table by the Australian Atomic Energy Commission (Champion, et al., 1968). These coefficients were plotted against their respective measured Compton-scatter intensities. Calibration lines were constructed from these plots. The intensity of the Compton-scatter of each rock sample was measured, then each mass-absorption coefficient was determined using the constructed calibration lines. To facilitate the reading of each calibration line, the following linear relationships were used:

$$U_{ZrKa}\ (\lambda = 0.788\ \text{Å}) = 0.2342\ MoK\alpha_C + 0.3770$$

$$U_{SrKa}\ (\lambda = 0.877\ \text{Å}) = 0.3179\ " + 0.4511$$

$$U_{RbKa}\ (\lambda = 0.927\ \text{Å}) = 0.3720\ " + 0.5187$$

$$U_{GaKa}\ (\lambda = 1.341\ \text{Å}) = 1.0609\ " + 1.2769$$

$$U_{ZnKa}\ (\lambda = 1.437\ \text{Å}) = 1.2872\ " + 1.8304$$

$$U_{CuKa}\ (\lambda = 1.542\ \text{Å}) = 1.5713\ " + 2.2557$$

$$U_{NiKa}\ (\lambda = 1.659\ \text{Å}) = 1.9328\ " + 2.7497$$

These equations were derived from the following instrumental conditions:

Mo-tube: 60 kV, 40 mA

Detector: Scintillation Counter (at 685 V)

Preset counts: 20,000

Counting time (uncorrected for dead-time) normalized to 21.40 seconds for pure silica glass scanned at $2\theta = 29.80^{\circ}$.

Reproduced with permission of the copyright owner. Further reproduction prohibited without permission.

Gallium mass-absorption coefficient was used to correct PbLβ and AsKα ; this method is legitimate as pointed out by Hower (op. cit.) and Mastins et al. (op. cit. p. 224).

Reproduced with permission of the copyright owner. Further reproduction prohibited without permission.

APPENDIX 4

X-ray fluorescence operating condition for silicate analysis (PHILIPS All-Vacuum X-ray Spectrograph PW/1540)

Element	X-ray tube	kV	mA	2Θ*	Crystal**	Crystal Position	Counting time (in seconds)
Si	Cr	60	40	79.50	PET	2	40
Al	Cr	60	40	115.50	PET	2	40
Fe	Cr	50	20	57.78	LiF_{200}	1	20
Mg	Cr	60	40	106.60	ADP	2	100
Ca	Cr	40	20	113.45	LiF_{200}	1	20
K	Cr	50	40	20.96	PET	2	20
Ti	Cr	50	20	86.42	LiF_{200}	1	20
P	Cr	60	40	111.40	Ge	2	40
Mn	Mo	50	40	63.25	LiF_{200}	1	20

*2Θ values vary slightly from machine to machine, depending on the mechanical accuracy. A table should be consulted to find the theoretical values.

**PET = Pentaerythrite

ADP = Ammoniumdihydrogenphosphate

Proportional flow counter (gas: 10 per cent argon in methane) was used throughout the analysis. The e.h.t. (extra high tension) of the counter varied from 1380 to 1440 Volts, depending on the element sought.

Reproduced with permission of the copyright owner. Further reproduction prohibited without permission.

Reproduced with permission of the copyright owner. Further reproduction prohibited without permission.

APPENDIX 5

Estimated mineral percentages based on the diffractograms of the minus 2 micron fraction of the Tindelpina Shale.

Reproduced with permission of the copyright owner. Further reproduction prohibited without permission.

ESTIMATED MINERAL PERCENTAGES

SAMPLE	CHLORITE	MUSCOVITE	QUARTZ	FELDSPAR	CALCITE
TH1	13.04	47.83	26.09	8.70	4.35
1	20.00	52.57	13.71	6.86	6.86
1002	15.87	48.41	25.40	7.94	2.38
3	6.15	55.38	30.77	7.69	0.00
4	25.00	58.75	8.13	5.00	3.13
5	22.00	57.00	17.00	4.00	0.00
6	0.00	88.63	7.36	4.01	0.00
7	41.96	28.57	16.96	12.50	0.00
8	0.00	82.08	17.92	0.00	0.00
9	12.63	50.53	30.53	6.32	0.00
11	19.48	53.25	16.23	6.49	4.55
12	5.24	75.52	12.59	6.64	0.00
14	5.90	87.82	6.27	0.00	0.00
16	2.52	75.71	11.36	2.52	7.89
17	0.00	78.53	16.67	4.81	0.00
18	4.56	87.45	4.94	3.04	0.00
19	0.00	38.75	33.13	4.38	23.75
20	12.18	65.99	18.27	3.55	0.00
21	.92	82.95	9.22	6.91	0.00
22	13.25	70.86	11.26	4.64	0.00
23	9.72	52.78	12.50	8.33	16.67
24	33.00	55.17	7.88	3.94	0.00
26	12.50	43.75	43.75	0.00	0.00
28	21.09	58.59	12.89	7.42	0.00
32	4.05	82.43	13.51	0.00	0.00
33	19.90	63.35	8.90	6.28	1.57
351	15.79	52.63	25.00	6.58	0.00
352	13.78	69.39	16.84	0.00	0.00
37	30.00	48.00	25.00	21.00	3.00
40	23.62	37.80	19.69	16.54	2.36
46	7.01	44.59	38.85	9.55	0.00
47	23.87	52.90	20.00	3.23	0.00
48	53.13	40.63	6.25	0.00	0.00
51	0.00	76.92	14.84	8.24	0.00
53	7.69	48.08	32.69	11.54	0.00
53	6.25	38.13	40.00	12.50	3.13
54	1.87	37.38	28.04	32.71	0.00
55	5.44	68.71	18.37	7.48	0.00
57	21.65	55.15	17.53	5.67	0.00
59	11.54	35.38	40.00	13.08	0.00
590	16.67	67.78	8.33	7.22	0.00
60	6.96	32.17	40.87	14.78	5.22
61	14.49	28.99	36.23	12.32	7.97
62	22.90	47.33	22.14	7.63	0.00
63	21.13	54.93	16.90	7.04	0.00
65	3.55	72.78	20.12	3.55	0.00
66	0.00	30.23	31.40	10.47	27.91
67	5.70	75.95	12.03	6.33	0.00
68	9.40	57.05	23.49	8.06	2.01
69	5.26	72.63	22.11	0.00	0.00

Reproduced with permission of the copyright owner. Further reproduction prohibited without permission.

ESTIMATED MINERAL PERCENTAGES

SAMPLE	CHLORITE	MUSCOVITE	QUARTZ	FELDSPAR	CALCITE
71	40.00	35.20	15.20	9.60	0.00
74	25.45	44.55	21.82	5.45	2.73
75	5.49	39.56	34.07	9.89	10.99
77	11.95	38.99	42.77	6.29	0.00
78	16.57	40.24	16.57	5.92	20.71
79	22.62	69.44	3.97	3.97	0.00
80	21.47	38.65	19.02	7.98	12.88
81	15.51	56.15	20.86	5.88	1.60
83	58.82	23.53	17.65	0.00	0.00
85D	12.34	64.94	14.29	8.44	0.00
86	25.64	43.59	18.80	11.97	0.00
89	13.51	52.70	18.92	11.49	3.38
90	3.70	55.56	30.86	9.88	0.00
91	7.14	39.29	42.86	10.71	0.00
93	0.00	55.07	44.93	0.00	0.00
94	34.25	51.93	6.63	7.18	0.00
95	24.65	47.18	10.56	9.15	8.45
96	11.72	46.88	32.81	8.59	0.00
97	8.82	27.21	6.62	2.21	55.15
98	19.23	53.85	26.92	0.00	0.00
99	16.74	68.28	9.26	5.73	0.00
101B	26.32	52.63	17.11	3.95	0.00
102	12.50	36.46	39.58	11.46	0.00
103	31.47	44.76	20.28	3.50	0.00
107	28.92	42.17	21.69	7.23	0.00
109	21.05	52.63	17.54	8.77	0.00
1121	2.31	70.77	9.23	2.31	15.38
1122	11.91	45.45	13.64	2.73	27.27
1124	17.00	44.00	20.00	5.00	14.00
113TH	13.51	51.35	14.86	3.38	16.89
114	37.91	32.23	12.32	8.06	9.48
115	22.90	56.49	15.27	5.34	0.00
1161	22.22	59.03	15.28	3.47	0.00
117	26.09	51.45	18.12	4.35	0.00
118	10.62	28.32	44.25	16.81	0.00
119	28.48	56.29	9.60	5.63	0.00
123	17.95	50.43	26.50	5.13	0.00
124	1.40	83.92	14.69	0.00	0.00

APPENDIX 6

Basal spacings of muscovite in the Tindelpina Shale (in Å Angstroms).

Reproduced with permission of the copyright owner. Further reproduction prohibited without permission.

SAMPLE	(002) SPACING OF ILLITE		
	DELTA	2-THETA	(002) SPACING
MISC.	124.470000	17.750014	9.993434
1	124.900000	17.739300	9.999421
5	124.450000	17.750513	9.993155
8	125.100000	17.734317	10.002208
10	125.100000	17.734317	10.002208
16	125.150000	17.733071	10.002906
17	124.200000	17.756742	9.989678
18	124.300000	17.754250	9.991069
20	125.050000	17.735563	10.001511
21	124.350000	17.753004	9.991764
23	123.900000	17.764217	9.985508
24	123.900000	17.764217	9.985508
25	124.650000	17.745529	9.995939
27	124.050000	17.760479	9.987592
28	125.050000	17.735563	10.001511
29	124.450000	17.750513	9.993155
31	124.050000	17.760479	9.987592
32	123.750000	17.767954	9.983424
33	124.300000	17.754250	9.991069
35?	125.550000	17.723104	10.008486
37	124.600000	17.746775	9.995243
38	124.300000	17.754250	9.991069
40	124.500000	17.749267	9.993851
47	124.570000	17.747523	9.994825
48	124.800000	17.741792	9.998028
51	124.600000	17.746775	9.995243
54	125.300000	17.729333	10.004997
55	125.470000	17.725098	10.007369
63	124.650000	17.745529	9.995939
65	124.850000	17.740546	9.998725
67	124.300000	17.754250	9.991069
68	125.500000	17.724350	10.007788
69	124.250000	17.755496	9.990373
71	123.600000	17.771692	9.981342
74	125.400000	17.726842	10.006392
79	124.350000	17.753004	9.991764
81	125.850000	17.715629	10.012675
86	125.200000	17.731825	10.003603
89	124.070000	17.759981	9.987870
90	123.650000	17.770446	9.982036
93	124.250000	17.755496	9.990373
95	124.150000	17.757987	9.988983
97	124.650000	17.745529	9.995939
98	125.220000	17.731327	10.003882
99	124.350000	17.753004	9.991764
101H	124.200000	17.756742	9.989678
107	125.450000	17.725596	10.007090
109	125.750000	17.718121	10.011278
114	124.550000	17.748021	9.994547
115	125.250000	17.730579	10.004300
117	124.450000	17.750513	9.993155
119	125.000000	17.736808	10.000815
121	124.450000	17.750513	9.993155
123	125.050000	17.735563	10.001511

Reproduced with permission of the copyright owner. Further reproduction prohibited without permission.

APPENDIX 7

$d_{(060)}$ spacings and b_0 parameters of the Tindelpina Shale muscovite (in Angstroms).

Reproduced with permission of the copyright owner. Further reproduction prohibited without permission.

SPACING OF ILLITE

SAMPLE	DELTA	2-THETA	(060) SPACING	bo
MUSCO	1.550000	61.583490	1.505883	9.035301
1	1.700000	61.733490	1.502584	9.015505
1002	1.650000	61.683490	1.503682	9.022092
3	1.600000	61.633490	1.504782	9.028691
4	1.550000	61.583490	1.505883	9.035301
5	1.650000	61.683490	1.503682	9.022092
6	1.650000	61.683490	1.503682	9.022092
7	1.700000	61.733490	1.502584	9.015505
8	1.750000	61.783490	1.501488	9.008929
9	1.600000	61.633490	1.504782	9.028691
10	1.700000	61.733490	1.502584	9.015505
12	1.600000	61.633490	1.504782	9.028691
14	1.850000	61.883490	1.499302	8.995811
16	1.600000	61.633490	1.504782	9.028691
18	1.700000	61.733490	1.502584	9.015505
19	1.700000	61.733490	1.502584	9.015505
20	1.600000	61.633490	1.504782	9.028691
21	1.650000	61.683490	1.503682	9.022092
22	1.600000	61.633490	1.504782	9.028691
23	1.600000	61.633490	1.504782	9.028691
24	1.650000	61.683490	1.503682	9.022092
25	1.500000	61.533490	1.506987	9.041922
26	1.550000	61.583490	1.505883	9.035301
27	1.650000	61.683490	1.503682	9.022092
32	1.400000	61.433490	1.509200	9.055199
33	1.500000	61.533490	1.506987	9.041922
35	1.500000	61.533490	1.506987	9.041922
37	1.550000	61.583490	1.505883	9.035301
38	1.750000	61.783490	1.501488	9.008929
40	1.550000	61.583490	1.505883	9.035301
47	1.500000	61.533490	1.506987	9.041922
48	1.550000	61.583490	1.505883	9.035301
51	1.700000	61.733490	1.502584	9.015505
53	1.500000	61.533490	1.506987	9.041922
54	1.650000	61.683490	1.503682	9.022092
55	1.650000	61.683490	1.503682	9.022092
59	1.550000	61.583490	1.505883	9.035301
60	1.600000	61.633490	1.504782	9.028691
61	1.550000	61.583490	1.505883	9.035301
62	1.600000	61.633490	1.504782	9.028691
65	1.650000	61.683490	1.503682	9.022092
67	1.650000	61.683490	1.503682	9.022092
68	1.700000	61.733490	1.502584	9.015505
69	1.800000	61.833490	1.500394	9.002365
71	1.600000	61.633490	1.504782	9.028691
74	1.600000	61.633490	1.504782	9.028691
78	1.650000	61.683490	1.503682	9.022092
80	1.650000	61.683490	1.503682	9.022092
84	1.700000	61.733490	1.502584	9.015505
89	1.750000	61.783490	1.501488	9.008929
90	1.600000	61.633490	1.504782	9.028691
91	1.650000	61.683490	1.503682	9.022092
93	1.750000	61.783490	1.501488	9.008929
94	1.450000	61.483490	1.509092	9.048555
95	1.550000	61.583490	1.505883	9.035301
96	1.600000	61.633490	1.504782	9.028691
97	1.750000	61.783490	1.501488	9.008929
98	1.700000	61.733490	1.502584	9.015505
99	1.650000	61.683490	1.503682	9.022092
100H	1.650000	61.683490	1.503682	9.022092
101H	1.600000	61.633490	1.504782	9.028691
102	1.750000	61.783490	1.501488	9.008929
106	1.650000	61.683490	1.503682	9.022092
107	1.700000	61.733490	1.502584	9.015505
1121	1.750000	61.783490	1.501488	9.008929
1122	1.700000	61.733490	1.502584	9.015505
113TH	1.700000	61.733490	1.502584	9.015505
114	1.650000	61.683490	1.503682	9.022092
115	1.650000	61.683490	1.503682	9.022092
1161	1.600000	61.633490	1.504782	9.028691
117	1.700000	61.733490	1.502584	9.015505
118	1.650000	61.683490	1.503682	9.022092
123	1.550000	61.583490	1.505883	9.035301
124	1.450000	61.483490	1.509092	9.048555

Reproduced with permission of the copyright owner. Further reproduction prohibited without permission.

APPENDIX 8

Intensity ratio of the 5 Å-reflection/10 Å-reflection of muscovite.

Sample No.	Ratio	Sample No.	Ratio
1	0.283	57	0.280
1002	0.328	59	0.348
3	0.389	60	0.405
4	0.277	61	0.300
5	0.333	62	0.290
7	0.375	63	0.324
8	0.352	65	0.236
9	0.292	66	0.385
10	0.317	67	0.258
12	0.306	68	0.376
14	0.277	69	0.376
16	0.325	71	0.372
17	0.347	75	0.375
20	0.323	77	0.323
21	0.250	78	0.279
22	0.439	79	0.371
23	0.263	80	0.270
24	0.311	81	0.248
25	0.267	83	0.400
26	0.238	85D	0.250
27	0.397	86	0.294
28	0.340	89	0.282
33	0.240	90	0.286
352	0.309	93	0.296
37	0.367	95	0.298
40	0.333	97	0.274
46	0.386	98	0.214
48	0.369	99	0.226
51	0.328	101B	0.368
53	0.344	106	0.394
54	0.300	107	0.286
55	0.317	1121	0.326

Reproduced with permission of the copyright owner. Further reproduction prohibited without permission.

APPENDIX 9

Crystallinity of muscovite expressed in terms of the Kubler Index (Kub.) in millimeters and the Weaver sharpness-ration (Wea.).

Sample	Kub.	Wea.	Sample	Kub.	Wea.
1	5.34	6.23	61	6.53	6.05
1002	5.64	8.19	62	5.20	5.96
3	5.64	5.97	63	6.62	5.52
4	6.44	4.73	65	5.20	5.96
5	4.58	7.06	67	4.33	13.53
6	4.23	11.01	68	5.09	6.12
7	6.68	4.17	69	5.09	6.25
8	4.23	15.37	74	5.20	7.87
9	4.46	5.81	78	4.26	6.61
10	5.50	5.80	80	5.68	6.21
11	5.35	9.98	81	5.20	4.75
12	4.78	8.47	83	4.58	3.74
13	5.86	5.75	86	6.15	4.96
14	4.83	10.04	89	5.09	8.70
16	4.59	11.55	90	4.58	9.71
17	4.30	12.96	91	4.84	8.60
18	6.44	5.83	93	6.37	6.50
19	4.83	10.06	94	5.87	7.25
21	6.11	5.57	95	4.84	7.49
22	7.43	3.09	964	5.40	5.89
23	5.44	4.53	97	6.81	4.23
25	6.45	6.91	98	6.57	3.35
26	7.65	4.22	99	7.04	5.55
27	6.44	2.89	100B	6.88	3.92
32	7.13	3.06	101B	6.19	5.75
33	5.94	5.82	102	6.57	4.28
35	4.78	7.73	106	7.64	3.78
37	5.61	5.06	107	6.44	5.44
38	5.68	6.15	108	4.93	6.75
40	5.69	5.05	109	6.19	4.47
47	5.61	6.43	110	5.16	6.03
48	4.58	9.10	111	5.09	6.60
51	4.95	6.32	1121	5.35	5.79
53	4.97	7.37	1122	6.37	5.12
54	5.68	5.56	1124	5.59	6.35
55	4.21	10.19	114	6.93	5.24
57	6.11	6.59	115	6.44	4.94
59	6.24	5.84	1161	4.33	7.94
591	6.38	4.16	117	6.61	4.49
60	6.37	6.06	118	6.44	6.22
			123	5.85	4.23
			124	5.59	6.56

Reproduced with permission of the copyright owner. Further reproduction prohibited without permission.

Reproduced with permission of the copyright owner. Further reproduction prohibited without permission.

APPENDIX 10

Result of trace element (in ppm) and quartz (in per cent) analyses of the Tindelpina Shale. 0 = not analyzed.

Fourth and fifth figures of sample number refer to additional samples collected at 25-foot intervals. For example, 1121 means first example collected at point 112; 1122 collected at 25 feet above 1121. Samples 1202 and 1203 are from the Tapley Hill Formation, collected at type locality.

Accuracy of analytical method is indicated by the analyses of several U.S. Geological Survey reference rocks.

Reproduced with permission of the copyright owner. Further reproduction prohibited without permission.

TRACE ELEMENTS AND QUARTZ CONTENT

SAMPLE	X	Y	GA	RB	SR	A#	BA	B	CR	CU	LI	NI	PB	V	ZN	ZR	QUARTZ
1	19.20	11.30	19	144	131	20	1229	187	52	38	25	45	22	220	87	204	32.51
1002	19.18	11.26	20	158	46	23	1006	181	137	43	17	57	0	273	91	222	27.41
2	19.10	11.34	18	231	82	34	1057	249	68	49	16	47	55	262	29	254	33.75
3	32.96	55.46	10	66	378	2	612	58	64	12	10	22	14	92	35	178	33.63
4	26.74	26.28	18	132	15	9	772	117	58	22	23	37	12	188	105	187	42.30
5	26.12	27.92	12	88	498	12	558	125	58	19	19	29	24	129	66	102	27.92
6	23.40	26.70	25	178	0	7	1116	277	82	16	21	7	24	290	15	271	42.89
7	23.96	26.56	19	60	0	0	1112	852	80	19	18	10	4	0	0	273	48.54
8	25.38	26.48	12	91	221	76	644	101	57	12	10	16	15	128	30	188	44.22
9	20.56	32.52	13	100	453	3	729	98	75	97	15	39	29	158	57	223	29.45
10	26.72	26.26	17	101	144	14	870	94	44	23	18	32	10	120	69	245	42.81
11	24.34	22.28	17	160	312	5	767	131	147	26	18	47	16	120	87	234	39.10
12	23.44	24.12	22	167	98	4	1022	242	73	32	24	43	17	253	69	246	27.49
13	24.26	21.04	15	106	0	3	929	0	72	32	12	35	8	147	62	284	38.95
14	24.14	21.14	22	71	0	1	741	291	74	4	3	2	26	80	0	248	52.30
16	23.38	24.42	26	180	0	7	1097	228	68	9	26	11	21	276	24	253	40.55
17	23.98	23.94	21	85	80	3	1096	272	82	8	11	9	6	157	3	304	66.06
18	24.80	23.10	22	97	224	8	974	182	76	19	17	34	4	215	45	240	49.27
19	23.12	46.42	18	143	0	17	820	175	61	34	26	45	36	0	48	183	43.52
20	25.80	43.20	21	145	0	14	745	136	98	40	29	44	12	263	86	203	38.43
21	23.64	33.72	23	184	97	5	1156	159	118	29	25	28	10	128	108	251	49.63
22	21.36	32.72	22	235	52	0	1103	202	70	35	14	34	14	120	20	238	51.38
23	25.74	43.64	5	64	525	12	433	76	56	35	9	20	14	103	52	117	38.89
24	20.38	43.32	22	169	85	3	1036	191	83	14	27	34	27	255	120	247	36.73
25	20.38	37.94	14	94	448	7	661	81	48	15	17	33	17	127	69	187	30.05
26	12.34	47.90	6	68	805	16	486	37	78	27	6	20	19	85	24	190	30.30
28	22.60	54.78	23	190	70	14	1060	182	71	22	26	35	45	279	71	249	44.03
29	18.94	50.10	25	179	61	6	1262	248	60	3	19	6	29	257	23	306	48.39
30	20.10	49.36	20	201	97	14	801	297	192	56	21	36	39	170	102	256	34.20
31	20.06	48.86	20	156	41	15	973	158	88	19	32	54	19	242	95	219	40.72
32	19.70	47.44	6	47	840	9	351	45	56	10	7	19	14	73	26	207	21.79
33	18.30	47.44	18	126	67	11	948	116	72	33	23	55	25	188	94	214	35.44
34	18.38	47.94	21	137	34	18	946	166	119	50	32	73	13	162	141	238	43.80
351	22.74	49.92	24	156	738	6	914	198	96	21	30	22	25	273	39	180	48.35
352	22.74	49.91	24	175	114	7	1063	186	111	18	34	34	36	231	50	228	44.30
36	24.24	49.80	23	181	34	9	873	293	99	26	53	44	14	206	62	247	38.07
37	27.64	48.10	20	143	0	5	815	133	78	21	32	59	10	196	68	207	40.00
381	18.90	54.68	23	147	41	19	922	104	88	34	35	77	14	191	105	216	41.45
39	17.58	55.76	9	61	637	3	421	52	31	13	15	24	7	103	46	221	20.16
40	12.86	51.42	18	136	0	14	795	102	105	23	26	47	24	224	71	207	40.41
41	28.60	48.32	30	162	42	18	963	218	108	37	42	76	7	257	90	223	46.24
42	23.50	47.86	22	175	71	18	1034	184	91	26	37	51	14	267	56	254	47.87
43	27.70	48.24	23	168	54	0	1023	181	95	29	35	91	10	261	73	260	48.92
44	26.66	49.04	19	137	87	7	1184	345	223	29	19	20	3	158	22	295	49.97
45	26.92	50.56	22	196	115	0	1037	321	96	61	27	47	5	235	24	240	51.10
46	18.98	51.56	23	169	216	22	1074	172	66	49	37	52	54	189	93	242	39.47
47	19.30	51.32	15	115	237	10	774	86	80	37	24	48	17	206	75	210	37.03
48	19.40	51.56	23	175	221	5	1155	214	82	8	24	24	34	254	80	271	33.70
49	19.10	52.06	19	151	79	24	899	162	66	22	26	39	59	132	76	234	35.91
50	26.78	50.24	19	136	107	10	811	161	68	27	18	35	4	202	57	192	39.01
51	24.30	51.16	24	159	305	7	1034	267	79	18	27	48	22	241	88	254	31.33

Reproduced with permission of the copyright owner. Further reproduction prohibited without permission.

TRACE ELEMENTS AND QUARTZ CONTENT

SAMPLE	X	Y	GA	RB	SR	AS	BA	B	CR	CU	LI	NI	PB	V	ZN	ZR	QUARTZ
52	23.22	46.98	20	162	42	0	827	300	45	31	26	182	26	185	312	211	51.02
53	19.22	57.74	19	142	232	40	875	165	205	36	43	39	19	0	57	222	32.89
54	22.48	62.46	16	117	87	2	1124	144	145	77	13	4	7	120	4	242	35.17
55	29.04	49.62	18	149	0	33	814	193	104	14	18	31	6	221	18	207	29.40
56A	15.30	58.74	19	143	83	18	769	242	70	38	28	38	25	231	64	206	35.60
56B	15.31	58.73	19	152	64	16	835	251	70	38	32	42	26	207	54	212	25.72
56C	15.30	58.74	21	138	82	18	757	252	79	30	26	46	17	202	94	195	34.70
56D	15.29	58.73	20	154	64	17	865	235	80	26	28	35	22	207	64	208	39.95
57	11.20	54.16	22	185	51	15	998	192	88	33	26	35	38	202	33	229	42.77
57B	11.04	54.18	20	189	32	23	946	268	79	38	29	36	32	212	48	230	54.11
58	11.14	59.14	21	223	61	16	1133	319	75	20	30	31	62	162	35	239	35.00
59	13.14	50.64	21	166	52	18	992	262	78	11	26	37	23	254	66	238	42.57
590	13.14	50.64	21	166	52	18	760	271	83	18	24	51	26	171	70	193	40.49
591	13.14	50.63	21	165	55	18	1005	253	94	14	36	40	23	250	70	238	36.66
592	13.15	50.62	21	162	65	15	982	243	81	27	32	45	24	254	77	231	38.41
593	13.13	50.63	22	158	46	15	971	176	77	17	34	60	20	228	81	231	42.15
594	13.14	50.62	22	161	50	17	966	216	59	24	26	113	25	162	78	232	36.82
60	12.90	51.40	21	151	76	18	899	213	70	19	29	37	22	236	69	202	46.72
60A1	12.91	51.39	17	138	182	16	827	0	71	23	20	46	16	236	64	224	38.23
602	12.94	51.37	20	136	74	14	849	108	79	22	27	51	20	231	76	237	37.75
61	12.92	51.04	19	147	80	15	936	225	77	22	27	54	25	267	73	219	44.41
62	12.96	51.54	20	153	0	18	921	211	85	22	27	78	27	248	86	224	40.18
63	12.84	51.28	18	144	73	19	866	187	82	24	26	49	31	215	72	208	29.44
64	17.20	61.76	22	158	197	21	859	180	74	16	24	26	30	215	41	238	29.91
65	32.62	57.50	19	203	59	3	1020	275	70	19	22	21	10	152	66	298	45.33
66	32.62	57.86	7	63	800	7	419	139	44	13	13	9	8	0	27	99	18.18
67	29.98	58.80	19	146	125	3	761	331	80	13	18	0	14	188	24	203	38.18
69	33.10	60.48	24	202	122	3	1164	238	130	41	25	32	15	261	55	269	38.81
70	29.06	55.76	20	153	0	19	1107	148	98	64	30	35	44	267	109	241	42.09
71	31.80	52.62	21	155	28	11	725	233	64	11	23	35	4	119	36	248	48.28
72	30.40	51.70	20	157	45	37	847	279	53	28	23	51	23	205	189	244	43.74
73	22.70	56.44	22	158	110	7	935	139	26	25	33	35	9	119	57	247	46.11
74	31.58	57.40	33	243	87	12	758	190	93	30	20	34	2	127	65	560	88.62
75	31.45	57.32	21	171	56	8	977	155	79	33	54	36	11	0	47	231	47.32
76	31.33	57.32	6	29	0	9	329	36	39	11	10	19	9	0	38	203	28.18
77	28.50	65.60	20	199	56	18	929	115	71	42	29	51	27	267	69	237	46.93
78	27.60	64.82	13	115	231	10	702	79	68	24	14	45	21	165	74	159	53.37
79	26.60	68.10	20	171	178	19	1016	248	66	30	28	46	30	271	92	220	37.26
80	24.36	68.20	16	119	162	11	730	217	48	14	27	32	14	231	60	201	31.49
81	24.30	67.14	25	201	109	18	950	214	61	42	29	41	23	303	85	213	28.01
82	26.76	66.00	21	152	93	25	950	146	64	34	28	136	23	273	69	201	49.42
83	22.50	74.46	9	66	68	229	389	62	102	761	5	44	33	138	30	288	56.85
84	22.30	74.70	20	160	0	112	568	292	0	0	0	0	42	0	0	223	45.32
85	22.90	67.30	14	153	81	19	619	0	67	85	4	34	0	175	9	229	37.47
850	22.90	67.30	14	153	0	0	619	178	0	0	0	0	0	0	0	229	47.91
859	22.90	67.30	20	152	83	47	941	187	43	38	29	35	57	229	49	233	37.82
85D	22.89	67.29	21	197	52	21	1014	273	76	43	31	35	25	238	42	223	40.38
86	21.82	74.50	16	124	0	9	621	182	113	14	20	48	10	119	19	280	45.07
87	19.04	90.22	22	157	18	199	683	122	70	980	5	15	16	194	7	278	52.69
88	18.00	89.24	25	169	15	18	506	95	84	310	4	129	1	174	37	173	53.04
89	18.80	90.18	18	183	0	48	654	134	73	14	10	72	18	210	9	235	43.44

Reproduced with permission of the copyright owner. Further reproduction prohibited without permission.

TRACE ELEMENTS AND QUARTZ CONTENT

SAMPLE	X	Y	GA	RB	SR	AS	BA	B	CR	CU	LI	NI	PB	V	ZN	ZR	QUARTZ
90	21.36	92.72	18	145	0	11	517	187	106	0	10	7	2	221	0	306	40.47
91	18.80	90.18	16	149	0	21	790	209	106	20	19	46	0	188	24	205	33.70
92	19.60	95.44	21	175	23	126	632	112	65	999	16	18	5	239	1	289	48.22
93	20.18	95.84	26	171	56	21	617	681	76	999	16	5	10	800	2	222	52.98
94	10.00	99.58	20	200	58	18	873	435	68	56	25	46	34	239	60	260	37.13
95	5.34	103.70	15	111	0	13	651	115	60	21	0	31	14	138	64	232	42.71
96	5.32	104.30	16	55	572	13	482	96	61	39	9	28	37	128	45	233	24.01
961	5.31	104.30	19	162	85	18	857	128	78	44	21	40	20	195	75	228	35.42
962	5.32	104.30	16	140	0	13	802	197	113	42	20	18	20	182	51	202	36.83
963	5.31	104.30	15	127	113	0	809	162	48	33	24	28	27	128	111	216	38.01
964	5.32	104.30	16	135	111	4	767	171	59	29	24	30	20	145	71	261	33.54
965	5.33	104.30	15	113	130	8	692	159	240	16	24	36	17	184	71	214	36.29
966	5.32	104.30	10	66	466	15	498	107	56	58	11	34	27	466	133	169	26.67
97	11.60	101.60	11	90	232	0	520	113	61	54	23	36	23	129	75	246	46.95
98	7.60	98.98	18	156	0	14	726	222	88	39	18	53	31	208	88	225	33.42
1004	5.48	101.10	22	197	83	17	1065	226	60	45	17	41	26	285	82	250	38.90
1008	5.49	101.80	23	181	70	19	981	212	49	51	17	44	25	154	66	249	30.94
101A	5.78	100.70	19	172	112	22	1057	205	68	37	18	96	39	163	64	225	34.14
101B	5.78	100.70	17	132	0	12	686	156	60	41	20	43	22	184	61	193	36.23
102	7.62	98.98	18	162	64	17	777	253	74	41	26	52	32	195	90	226	28.43
103	8.62	98.52	14	110	94	45	1048	211	76	66	21	97	19	253	430	176	38.57
104	8.31	98.52	15	111	0	9	683	165	75	34	17	50	11	158	75	263	53.33
106	5.82	100.60	19	152	74	18	838	180	70	41	33	47	24	230	74	223	40.07
107	18.74	68.68	17	107	220	8	668	119	97	25	21	48	7	142	57	199	39.18
108	29.08	95.14	15	118	230	33	816	82	164	33	18	41	20	147	77	257	42.35
109	30.98	97.34	11	85	294	8	688	107	106	6	14	31	10	161	28	181	40.09
110	18.32	3.92	20	148	137	5	1101	164	77	139	21	44	47	266	53	252	40.27
111	39.34	52.48	15	145	87	5	787	134	520	1	15	24	4	69	16	244	53.39
1121	31.10	97.54	20	213	0	8	1098	252	41	28	16	28	3	162	21	230	34.75
1122	31.10	97.54	18	149	107	5	775	125	43	31	18	51	7	163	34	195	46.91
1123	31.10	97.54	17	153	0	4	787	147	43	6	12	34	5	145	39	207	38.82
1124	31.11	97.55	20	145	79	10	892	173	89	6	12	41	8	219	44	247	40.58
113	30.98	97.28	17	152	0	13	760	0	41	24	13	43	12	145	61	210	41.05
114	10.24	59.76	16	134	85	11	883	103	108	22	14	55	22	124	43	205	39.82
115	10.00	56.86	16	142	83	19	950	128	65	37	21	43	30	162	46	226	41.97
1161	23.78	49.46	15	110	334	18	676	113	45	36	17	40	28	112	88	162	29.48
1162	27.70	48.24	20	177	44	9	1098	255	78	28	23	32	0	136	55	212	51.96
1163	23.74	49.44	12	112	581	21	613	108	67	17	17	28	70	121	92	139	33.67
117	10.04	59.86	19	141	103	11	1279	107	64	31	17	40	11	156	61	220	41.83
118	12.72	56.70	17	142	119	16	769	202	153	36	29	47	21	133	74	199	45.82
1181	9.80	55.96	20	139	147	18	747	0	156	35	27	50	47	0	74	188	41.82
1182	9.80	56.14	19	176	125	0	749	229	150	37	29	44	0	0	75	185	41.79
11821	9.80	56.14	19	176	125	0	740	220	0	0	0	0	0	0	0	0	39.87
119	9.80	56.15	20	196	118	22	1215	0	212	37	18	42	52	118	80	231	46.15
1202	-0.00	-0.00	17	122	0	9	732	124	0	34	19	51	18	0	74	208	36.17
1203	-0.00	-0.00	19	135	0	8	685	0	0	12	18	49	20	0	62	213	44.81
121	14.10	3.10	19	213	47	2	750	230	77	11	10	95	13	127	69	214	50.82
122	24.00	56.06	21	167	98	6	923	286	59	0	23	0	10	0	60	228	38.37
123	22.94	57.10	18	156	50	0	926	253	69	0	21	0	8	0	96	240	53.30
124	19.40	46.98	19	195	38	4	941	274	48	0	18	0	12	0	53	267	45.83

Analyses of some U.S. Geological Survey reference rocks.

Gallium

	(1)	(2)	(3)	(4)	(5)
BCR-1	19	22	-	18	15
G-1	17	-	18	20	18
G-2	18	20	-	23	26
GSP-1	19	19	-	23	16

Rubidium

	(1)	(2)	(3)	(4)	(5)	(6)
AGV-1	70	89	-	Not	69	73
G-1	-	-	220	determined	202	
G-2	175	234	-		174	171
GSP-1	260	343	-		202	270
PCC-1	5	.5	-		<1.l.d.	<5
W-1	25	-	22		24	-

Strontium

	(1)	(2)	(3)	(4)	(5)	(6)
AGV-1	640	657	-	Not	682	751
G-1	-	-	250	determined	236	-
G-2	465	463	-		481	598
GSP-1	230	247	-		183	265
PCC-1	<3	.3	-		<1.l.d.	5
W-1	195	-	180		205	-

Copper

	(1)	(2)	(3)	(4)	(5)
G-1	17	-	13	11	12
G-2	10	11	-	10	10
GSP-1	30	35	-	49	26
SY-1	-	-	-	15	7
T-1	-	-	-	66	49
W-1	-	-	110	116	109

Reproduced with permission of the copyright owner. Further reproduction prohibited without permission.

Nickel

	(1)	(2)	(3)	(4)	(5)
BCR-1	15	15	-	10	11
G-1	3	-	1.2	1.2	4
PCC-1	2450	2430	-	2650	2662
SY-1	-	-	-	41	44

Lead

	(1)	(2)	(3)	(4)	(5)
BCR-1	5	18	-	17	13
DTS-1	<5	15	-	13	11
G-1	-	-	49	48	49
GSP-1	60	52	-	55	48
PCC-1	5	13	-	14	5
W-1	10	-	8	8	6

Zinc

	(1)	(2)	(3)	(4)	(5)
G-1	40	-	45	46	43
G-2	80	75	-	76	78
SY-1	-	-	-	280	215
T-1	-	-	-	123	168
W-1	-	-	82	82	80

Zirconium

	(1)	(2)	(3)	(4)	(5)
BCR-1	180	185	-	228	198
G-1	-	-	210	206	201
GSP-1	585	544	-	385	426
SY-1	-	-	-	3300	2591
T-1	-	-	-	250	180
W-1	85	-	100	103	93

(1) Carmichael, Hampel and Jack (1968)
(2) Flanagan (1969)
(3) Fleischer (1969)
(4) Huber-Schausberger (1970)
(5) This thesis
(6) Parker (1969)

Reproduced with permission of the copyright owner. Further reproduction prohibited without permission.

APPENDIX 11

Gallium, Rubidium, Strontium, and Boron Contents of the Sturt Tillite (in ppm). 0 = not analyzed.

Sample	Ga	Rb	Sr	B
$1T_1$	20	190	39	246
$1T_2$	22	158	39	0
19T	19	186	55	189
30T	21	204	15	175
31T	10	119	98	136
$35T_1$	18	198	54	216
$35T_2$	18	198	55	0
36T	26	209	34	237
38T	18	172	86	234
$39T_1$	16	125	38	181
$39T_2$	15	126	38	0
41T	21	153	32	249
44T	21	211	49	175
46T	21	218	45	295
53T	20	181	52	250
$59T_1$	13	126	65	136
$59T_2$	17	168	52	259
60T	7	90	50	110
65T	20	186	111	363
66T	21	176	69	365
73AT	22	224	60	300
75T	19	153	67	369
77T	20	204	55	201
95T	18	155	55	125
105T	14	98	39	119

Reproduced with permission of the copyright owner. Further reproduction prohibited without permission.

Reproduced with permission of the copyright owner. Further reproduction prohibited without permission.

APPENDIX 12

Results of chemical analyses of the major oxides (in per cent) composing the Sturt Tillite and the Tindelpina Shale. Letter T after sample number indicates tillite. Accuracy of analytical method is shown by the results of analysis of four U.S. Geological Survey reference rocks.

Reproduced with permission of the copyright owner. Further reproduction prohibited without permission.

WEIGHT PERCENTS OF OXIDES

	SIO2	AL2O3	FE2O3	MGO	CAO	NA2O	K2O	TIO2	P2O5	MNO	LOSS	TOTAL
1	57.51	13.58	6.51	4.71	4.15	1.31	3.16	.90	.19	.05	7.98	100.05
1002	61.10	14.55	6.72	3.69	1.84	1.44	3.47	.99	.21	.05	6.07	100.13
19	51.68	15.52	9.61	1.51	.20	.99	4.92	.89	.36	.05	12.81	98.54
30	64.86	13.69	8.71	2.28	.21	.18	4.57	.82	.24	.02	4.36	99.94
31	64.45	15.14	6.12	3.98	.42	1.45	3.53	1.03	.10	.01	3.85	100.08
351	65.19	15.45	4.85	3.43	.16	1.60	3.56	1.04	.17	.01	4.43	99.89
36	62.00	16.59	4.85	3.99	.33	1.64	3.92	1.14	.29	.02	3.85	98.62
381	64.36	15.19	6.94	3.59	.40	1.09	3.40	1.02	.19	.01	4.45	100.64
39	29.01	6.50	2.84	13.14	18.11	.73	1.39	.44	.10	.02	27.71	99.99
41	64.02	16.11	5.35	3.32	.55	.19	3.62	1.11	.22	.02	5.27	99.78
44	69.70	14.51	5.18	1.26	.70	.20	3.33	.98	.11	0.00	4.68	100.65
46	62.79	15.69	6.06	3.80	.20	1.37	3.68	1.17	.23	.01	4.10	99.10
53	63.36	14.16	6.32	2.25	.24	1.62	3.33	.98	.25	.03	6.54	99.08
59	63.01	15.26	6.10	3.40	.45	1.39	3.84	1.06	.23	.03	4.87	99.64
590	62.30	14.85	5.95	3.63	.45	1.39	3.78	1.02	.22	.03	4.99	98.61
60	58.03	14.05	6.07	4.48	2.82	1.34	3.45	.96	.21	.04	8.11	99.56
65	70.21	14.32	4.31	2.19	.10	1.25	3.93	1.02	.07	.01	2.79	100.20
66	24.63	5.95	1.04	11.71	22.09	.71	1.60	.53	.06	.04	30.75	99.11
75	63.28	15.57	7.38	3.08	.57	1.31	3.64	1.06	.23	.03	3.59	99.74
77	63.37	14.71	6.99	3.89	.50	1.24	3.36	1.04	.20	.01	3.91	99.22
95	56.70	11.31	4.89	5.16	7.29	.96	2.62	.75	.16	.11	7.56	97.51
106	60.40	14.21	6.84	4.81	1.91	1.03	3.32	.97	.23	.03	5.97	99.72
1T1	65.87	15.62	5.29	2.69	.18	1.93	4.04	.99	.12	.02	2.89	99.64
1T2	67.00	13.80	6.98	4.25	.36	1.48	3.40	.81	.16	.02	2.75	101.01
19T	68.12	14.88	5.32	2.12	.14	1.20	4.09	.97	.13	.02	2.97	99.96
30T	67.16	14.59	5.27	3.17	.17	.70	4.90	.85	.13	.02	2.99	99.95
31T	68.59	14.70	5.77	1.77	.07	1.41	4.13	1.02	.09	.02	2.45	100.02
35T1	68.42	14.20	5.93	2.30	.18	1.65	3.83	.95	.14	.02	2.75	100.37
35T2	68.35	14.16	6.20	2.12	.18	1.65	3.84	.96	.14	.03	2.75	100.38
36T	70.05	14.79	3.46	1.79	.19	1.49	4.45	.84	.12	.01	2.55	99.74
38T	65.86	12.30	4.95	3.38	2.02	1.10	4.44	.86	.15	.09	5.26	100.41
39T1	72.01	12.19	5.97	2.64	.28	1.38	3.25	.81	.13	.03	2.66	101.35
39T2	73.81	10.58	5.47	2.18	.20	1.39	2.79	.72	.13	.09	2.67	100.03
41T	67.01	15.04	5.41	2.64	.31	.15	3.66	1.04	.17	.01	4.12	99.56
44T	71.58	13.47	3.14	1.33	.37	.11	3.91	.74	.04	.12	3.54	98.35
46T	67.92	14.71	5.21	1.74	.17	1.03	4.58	.98	.14	.02	3.30	99.80
53T	68.52	14.29	5.24	2.32	.36	1.37	3.84	.94	.15	.02	3.15	100.20
59T1	66.92	11.01	6.31	3.80	1.90	1.21	3.00	.79	.13	.05	4.63	99.75
59T2	69.95	13.71	4.79	1.93	.13	.80	4.21	.90	.12	.01	2.83	99.38
60T	73.55	7.68	4.77	2.49	2.61	1.25	2.19	.51	.09	.04	4.49	99.67
65T	72.29	12.50	4.84	1.70	.07	1.17	3.31	.85	.12	.01	2.93	99.79
66T	67.59	15.44	4.44	2.86	.27	1.65	4.11	1.06	.12	.01	2.56	100.11
73AT	66.60	15.90	4.68	2.19	.23	1.42	4.73	.99	.11	.02	2.85	99.72
75T	69.65	14.65	3.50	2.82	.60	1.71	3.55	.96	.15	.02	2.70	100.31
77T	67.09	14.85	5.66	2.46	.26	1.36	3.84	.98	.15	.03	3.25	99.93
95T	60.41	13.45	4.74	5.64	3.75	1.36	3.36	.98	.26	.05	6.90	100.90
105T	75.43	10.17	6.05	2.75	.44	.74	2.45	.67	.15	.02	2.77	101.64

Reproduced with permission of the copyright owner. Further reproduction prohibited without permission.

WEIGHT PERCENTS OF OXIDES

	SIO2	AL2O3	FE2O3	MGO	CAO	NA2O	K2O	TIO2	P2O5	MNO	LOSS	TOTAL
2	63.84	16.67	6.07	1.63	.20	.62	4.74	1.18	.11	.01	4.00	99.07
3	46.67	8.56	3.44	2.91	17.61	1.49	1.70	.55	.24	.15	15.65	98.97
4	56.43	13.28	5.51	5.39	5.39	1.22	2.89	.81	.19	.06	8.77	99.94
5	32.00	8.79	5.06	10.38	16.47	1.10	1.73	.59	.24	.15	23.19	99.70
6	66.82	14.69	3.43	2.22	.06	.44	3.89	1.16	.06	.04	5.08	98.09
7	70.89	14.94	.54	.89	.13	5.10	3.17	.70	.06	.04	2.09	98.65
8	56.87	10.70	3.05	5.14	7.00	2.32	2.01	.77	.18	.06	11.40	99.50
9	53.27	11.14	4.96	3.84	10.11	1.53	2.62	.74	.19	.06	10.55	99.01
10	62.11	12.87	5.16	4.35	3.15	1.76	2.68	.98	.19	.06	6.02	99.33
11	60.88	14.17	6.94	4.83	4.55	1.75	3.54	.94	.19	.09	2.34	100.22
12	64.37	19.30	2.72	1.92	.08	1.34	3.87	1.16	.13	.01	5.08	99.98
13	58.53	11.31	4.84	3.64	9.57	1.40	2.29	.92	.18	.16	6.05	98.89
14	70.83	16.36	1.62	.75	.50	1.50	2.80	1.03	.02	.05	3.62	99.08
16	63.08	17.05	4.16	1.73	.05	.85	4.15	1.19	.13	.02	6.87	99.28
17	71.11	17.79	.61	.63	.06	.32	2.92	1.11	.02	.01	5.51	100.09
1701	69.72	18.81	.87	.72	.07	.29	3.07	1.13	.06	0.00	5.13	99.87
18	64.23	16.01	4.67	3.92	.30	1.42	3.89	1.00	.12	.01	4.32	99.89
20	56.49	13.95	5.27	5.53	3.49	1.17	3.23	.94	.21	1.00	8.29	99.57
21	66.61	16.40	4.21	1.88	.09	.40	4.04	1.07	.05	.01	4.72	99.48
22	69.10	15.95	3.01	1.61	.03	.43	4.57	1.03	.03	.04	3.40	99.20
23	42.70	8.03	2.88	1.85	21.17	2.17	1.43	.46	.43	.11	18.39	99.62
24	67.28	16.35	4.23	1.82	.18	.39	3.66	1.11	.06	0.00	5.54	100.62
25	54.34	10.26	4.57	3.73	10.74	1.68	2.20	.68	.19	.08	11.34	99.81
26	44.50	7.87	2.42	2.11	19.67	2.35	1.62	.63	.16	.26	17.61	99.20
28	62.23	15.59	6.43	3.44	.51	1.10	4.06	1.21	.23	.08	4.04	98.92
29	70.76	15.20	3.33	1.97	.39	.39	3.55	1.23	.07	.03	4.04	100.96
32	39.30	6.46	2.17	2.14	24.80	1.92	1.03	.46	.14	.26	20.46	99.14
33	57.98	13.30	6.10	5.42	3.99	1.41	2.96	.88	.19	.07	7.63	99.93
34	63.86	14.53	7.65	4.01	.42	1.21	3.21	1.02	.17	.01	4.25	100.34
352	65.42	16.25	3.78	3.84	.57	1.63	3.90	1.10	.08	.01	4.40	100.98
37	63.24	14.34	6.36	4.50	.49	.48	3.16	.91	.22	.06	4.25	98.01
381	64.36	15.19	6.94	3.60	.40	1.09	3.41	1.02	.19	.02	4.45	100.67
40	56.31	13.41	5.82	5.10	3.89	1.39	3.10	.88	.17	.09	8.89	99.05
42	67.36	16.76	2.83	3.11	.33	.16	3.81	1.12	.04	.03	4.88	100.43
43	65.74	17.33	4.19	2.21	.02	.22	3.75	1.14	.05	.01	5.28	99.94
45	62.85	15.66	6.07	2.44	1.46	.61	4.33	1.10	.23	.03	5.09	99.87
47	56.03	12.41	5.73	5.05	6.83	1.41	2.67	.79	.18	.07	9.23	100.40
48	66.43	16.38	4.20	2.88	.33	.21	4.02	1.27	.08	.01	5.26	101.07
49	60.89	14.08	5.95	6.04	1.51	1.34	3.43	1.00	.13	.03	5.93	100.33
50	58.36	14.14	5.95	5.77	3.38	1.38	3.13	.85	.23	.07	7.71	100.97
51	64.89	16.61	4.56	2.44	.47	.35	3.69	1.15	.13	.02	5.10	99.41
52	50.65	13.05	22.55	2.32	.15	.27	3.29	.93	.25	.04	5.82	99.32
54	65.58	14.16	1.11	2.00	2.76	4.32	4.09	.81	.26	.06	4.76	99.85
55	53.77	13.47	4.65	4.64	6.35	1.52	3.39	.94	.22	.11	11.01	100.07
56A	58.06	13.59	6.24	5.00	3.35	1.36	3.07	.94	.27	.02	7.40	99.30
56B	61.33	14.18	6.17	4.43	1.99	1.29	3.40	.97	.22	.02	5.99	99.99
56C	56.88	13.27	6.07	6.01	3.88	1.19	3.09	.92	.23	.04	8.39	99.97
56D	59.51	14.21	6.07	4.67	2.48	1.13	3.47	.97	.21	.05	6.75	99.52
57	66.28	14.96	4.56	2.66	.18	1.01	4.13	1.07	.06	.01	4.20	99.12
57B	63.38	15.21	6.65	3.73	.49	.38	4.28	1.04	.21	.01	4.18	99.56

Reproduced with permission of the copyright owner. Further reproduction prohibited without permission.

WEIGHT PERCENTS OF OXIDES

	SIO2	AL2O3	FE2O3	MGO	CAO	NA2O	K2O	TIO2	P2O5	MNO	LOSS	TOTAL
58	58.96	14.83	7.98	3.95	1.22	.31	4.67	1.20	.23	.02	5.84	99.21
591	63.34	15.07	6.05	3.74	.46	1.39	3.85	1.04	.22	.02	4.65	99.83
592	63.35	15.03	6.53	3.70	.32	1.37	3.80	1.04	.23	.02	4.33	99.72
593	63.02	15.18	6.31	3.90	.36	1.29	3.70	1.03	.21	.02	4.32	99.34
594	63.63	15.18	6.34	4.13	.33	1.40	3.71	1.04	.24	.03	4.13	100.16
60A1	54.30	14.99	5.58	4.97	6.32	1.23	3.20	.88	.21	.06	8.68	100.42
602	61.52	13.54	6.74	5.03	2.19	1.42	3.14	.97	.21	.03	5.70	100.49
6002	69.75	17.15	1.07	1.40	.02	.27	4.03	1.19	.05	0.00	5.06	99.99
61	58.97	14.71	6.07	4.21	2.88	1.40	3.45	.97	.20	.03	6.69	99.58
62	61.52	15.29	6.62	3.77	1.29	1.18	3.60	1.01	.24	.05	5.29	99.86
63	58.30	13.70	6.09	4.82	3.10	1.45	3.28	.93	.19	.04	7.48	99.38
64	65.61	14.52	5.55	3.65	.25	1.67	3.42	1.01	.19	.02	3.86	99.75
67	59.47	13.02	3.11	4.62	4.79	1.34	3.19	.89	.20	.04	9.08	99.75
69	62.26	17.20	5.44	2.65	.71	1.43	4.37	1.31	.32	.03	3.82	99.54
70	63.54	14.46	8.02	4.36	.42	1.49	3.42	1.06	.25	.06	3.36	100.44
71	65.77	14.90	6.27	3.91	.50	1.07	3.17	1.18	.19	.02	3.79	100.77
72	62.82	14.67	8.48	2.87	.86	.87	3.49	1.01	.20	.02	4.36	99.65
73	69.82	15.92	1.51	1.80	.14	.26	4.14	1.33	.03	.02	4.51	99.48
74	70.77	12.85	5.49	2.66	.20	1.35	2.53	.79	.08	.01	2.67	99.40
76	37.39	6.19	2.41	2.29	26.68	1.73	.87	.65	.19	.16	22.01	100.57
78	59.04	11.55	4.87	3.43	7.07	1.52	2.67	.67	.19	.05	8.47	99.53
79	62.73	15.26	6.54	3.69	.94	1.22	3.74	1.04	.19	.03	4.44	99.82
80	55.07	12.17	5.25	5.27	6.71	1.38	2.73	.85	.17	.05	10.21	99.86
81	60.55	16.58	7.24	3.29	.44	1.05	4.00	1.09	.14	.02	5.04	99.44
82	57.76	13.69	13.11	2.76	.95	.89	3.14	.94	.31	.55	5.38	99.48
83	56.26	9.59	5.25	5.87	6.71	.11	2.26	.63	.36	.13	12.03	99.20
84	63.34	14.86	7.63	1.71	.72	.08	4.26	1.07	.24	.11	4.33	98.35
85	57.10	11.84	3.86	1.95	8.87	1.16	4.05	.78	.18	.07	10.22	100.08
850	57.35	11.94	3.85	1.98	8.87	1.16	4.05	.78	.18	.07	10.22	100.45
85B	60.43	15.69	8.87	3.44	.36	1.32	3.85	1.10	.16	.01	4.70	99.93
85D	64.63	15.15	5.97	3.12	.36	1.28	4.43	.97	.18	.02	4.26	100.37
86	67.60	13.04	5.53	4.90	3.47	1.81	3.13	.96	.29	.27	6.50	107.50
87	71.27	16.27	2.07	.86	.07	.10	4.43	1.13	.06	.01	3.47	99.74
88	67.66	15.93	1.62	2.20	1.33	.16	5.62	.85	.07	.02	4.43	99.89
89	58.03	13.87	5.68	4.35	3.77	.08	4.87	.93	.23	.12	7.45	99.38
90	47.20	12.20	1.30	1.85	14.90	.21	3.27	1.24	.07	.02	17.27	99.53
91	55.23	13.76	4.77	4.77	4.71	1.28	3.52	.89	.20	.07	10.06	99.26
92	70.73	15.65	1.89	1.60	.14	.17	5.56	1.15	.04	.01	3.33	100.27
93	69.49	16.21	1.03	1.75	.36	.16	5.49	.76	.03	.01	3.82	99.11
94	62.81	15.00	6.69	3.47	.55	1.06	4.26	1.16	.26	.03	4.63	99.92
95	56.70	11.31	4.89	5.16	7.29	.96	2.62	.75	.16	.11	9.50	99.45
96	41.77	8.86	3.45	2.99	19.53	2.53	1.43	.65	.17	.13	17.87	99.58
961	58.45	13.48	5.99	5.02	3.44	1.07	3.59	.94	.20	.03	7.97	100.18
962	58.77	13.59	3.77	5.67	5.06	1.10	3.47	1.07	.31	.19	7.05	100.05
963	56.22	12.22	4.45	4.43	7.07	1.34	2.93	.91	.21	.06	9.33	99.17
964	56.19	12.34	4.11	5.29	6.41	1.40	3.00	.88	.19	.04	9.46	99.31
965	56.35	11.73	4.84	4.44	8.18	1.57	2.60	.86	.19	.06	10.15	100.97
966	43.27	9.26	4.94	2.94	17.95	2.31	.78	.66	.17	.12	16.64	99.04
97	56.13	10.19	4.60	3.20	10.52	1.96	1.90	.71	.16	.07	10.26	99.70
98	59.06	14.30	6.49	5.19	3.06	1.01	3.49	1.18	.32	.21	6.16	100.67
100A	63.19	14.72	5.87	2.74	.91	.75	4.26	1.24	.17	.02	5.21	99.08

Reproduced with permission of the copyright owner. Further reproduction prohibited without permission.

WEIGHT PERCENTS OF OXIDES

	SIO2	AL2O3	FE2O3	MGO	CAO	NA2O	K2O	TIO2	P2O5	MNO	LOSS	TOTAL
100B	60.74	15.18	6.66	4.02	1.10	1.02	4.13	1.13	.22	.02	5.23	99.45
101A	54.82	13.47	6.33	3.06	6.82	1.11	3.66	1.17	.17	.02	9.08	99.71
101B	55.71	13.36	6.09	5.33	5.61	1.34	3.21	1.12	.30	.21	7.56	99.84
1002	61.10	14.55	6.72	3.69	1.84	1.44	3.47	.99	.21	.05	6.07	100.13
102	58.12	13.92	6.33	5.12	2.61	1.16	3.67	.99	.22	.04	7.52	99.70
103	46.40	11.18	22.53	3.60	3.15	.82	2.38	.74	.23	.31	8.60	99.94
104	62.84	12.45	6.20	3.74	3.24	1.67	2.49	.83	.21	.04	6.39	100.10
107	54.83	11.80	5.38	4.32	7.61	1.47	2.54	.76	.23	.07	10.57	99.58
107	54.83	11.91	5.37	4.28	7.59	1.47	2.54	.76	.26	.07	10.57	99.66
108	62.05	12.20	5.43	4.38	6.02	1.84	2.61	.76	.18	.12	3.87	99.46
109	50.25	10.51	3.91	3.30	13.96	1.30	2.29	.61	.19	.17	14.08	100.57
110	62.75	14.99	4.05	6.28	1.76	1.03	3.17	1.08	.19	.04	4.19	99.53
111	61.51	9.49	17.43	3.57	1.52	1.20	2.66	.58	.27	.10	.89	99.22
1121	54.32	14.14	5.44	3.89	6.14	.62	4.09	1.26	.25	.11	9.92	100.18
1122	55.82	12.36	6.69	3.06	6.81	1.22	3.12	.81	.25	.06	8.85	99.05
1123	55.22	12.23	5.51	2.59	8.95	1.29	2.91	.85	.21	.09	9.85	99.70
1124	63.87	14.26	5.86	2.47	2.34	1.38	3.17	1.02	.24	.06	5.00	99.67
113	58.07	12.47	4.87	4.09	7.00	1.52	2.64	.78	.22	.07	9.40	101.13
114	60.63	12.63	5.78	5.57	2.62	1.37	3.14	.91	.19	.03	6.23	99.10
115	57.68	12.61	5.71	6.08	3.61	1.20	3.17	.91	.19	.04	8.19	99.39
1161	49.15	11.71	6.99	5.27	9.18	1.52	2.42	.73	.19	.09	12.31	99.56
1162	64.06	14.77	7.87	3.69	.25	1.01	3.65	.97	.16	.02	3.64	100.09
1163	42.74	10.18	4.25	3.43	17.92	1.46	2.45	.62	.30	.11	16.87	100.33
117	63.01	12.97	4.37	5.06	2.61	1.36	3.22	.91	.20	.04	6.17	99.92
118	54.68	12.97	6.18	4.98	4.76	1.36	3.11	.84	.19	.06	9.90	99.03
1181	62.81	13.11	4.32	4.68	2.99	.84	3.89	.99	.21	.07	6.96	100.87
1182	62.49	14.41	5.49	4.27	1.24	.56	4.29	1.23	.21	.11	5.08	99.38
119	62.72	14.76	5.50	4.32	1.25	.63	4.32	1.25	.21	.11	5.09	100.16
1202	56.23	12.24	5.24	5.52	5.90	1.27	2.75	.85	.20	.07	9.55	99.82
1203	66.46	13.92	5.20	5.27	.32	1.46	3.06	.98	.29	.18	3.14	100.28
121	66.49	14.19	5.29	2.56	1.62	1.00	4.52	.76	.16	.05	3.12	99.76
122	63.77	15.69	5.33	3.45	.65	1.44	3.61	1.07	.26	.02	3.92	99.21
123	67.34	13.94	5.75	3.13	.28	1.48	3.19	.88	.18	.03	2.95	99.15
124	69.99	14.19	4.77	2.14	.18	1.30	4.16	.97	.15	.02	3.00	100.87
11821	62.28	13.07	4.30	4.63	2.88	.87	3.87	.98	.21	.06	6.96	100.11

Comparison of analyses of four United States Geological Survey reference rocks.

	G_2		GSP-1		AGV-1		PCC-1	
	(1)	(2)	(1)	(2)	(1)	(2)	(1)	(2)
SiO_2	68.80	69.19	67.17	67.27	59.43	58.99	41.48	41.87
Al_2O_3	15.39	15.34	15.01	15.11	17.14	17.01	0.82	0.85
Fe_2O_3*	2.68	2.76	4.23	4.33	6.72	6.80	8.14	8.53
MgO	0.95	0.78	0.92	0.95	1.65	1.49	43.65	43.56
CaO	1.94	1.98	2.04	2.03	4.94	4.98	0.53	0.53
Na_2O	4.10	4.15	2.85	2.88	4.10	4.33	0.06	0.05
K_2O	4.58	4.51	5.76	5.48	2.90	2.89	0.00	0.01
TiO_2	0.47	0.53	0.68	0.69	1.04	1.08	0.01	0.02
P_2O_5	0.14	0.14	0.27	0.28	0.50	0.48	0.00	0.01
MnO	0.05	0.03	0.05	0.04	0.10	0.09	0.09	0.12
L.o.i.	0.57	0.56	0.80	0.79	1.38	1.34	4.85	4.88

(1) This work (2) Recommended values (Flanagan, 1969)

(*) Total iron oxides

L.o.i. = Loss on ignition.

For comparison purpose, only the oxides which were analysed in this thesis were copied from Flanagan's paper.

Reproduced with permission of the copyright owner. Further reproduction prohibited without permission.